

MOL.19980422.0911

~~AD-19970723.0053~~
over
#2

WBS: 1.2.1.10

SCPB: N/A

QA: N/A

PREDECISIONAL DOCUMENT

**Civilian Radioactive Waste Management System
Management & Operating Contractor**

INFORMATION ONLY

**Degraded Mode Criticality Analysis of
Immobilized Plutonium Waste Forms in a Geologic Repository**

A00000000-01717-5705-00014 REV 01

February 7, 1997

Prepared for:

**U.S. Department of Energy
Office of Civilian Radioactive Waste Management
1000 Independence Avenue S.W.
Washington, DC 20585**

Prepared by:

**TRW Environmental Safety Systems Inc.
1180 Town Center Drive
Las Vegas, Nevada 89134**

**Under Contract Number
DE-AC01-91RW00134**

9902240052 990107
PDR WASTE
WM-11 PDR

102-2

WBS: 1.2.1.10
SCPB: N/A
QA: N/A

PREDECISIONAL DOCUMENT

Civilian Radioactive Waste Management System
Management & Operating Contractor

Degraded Mode Criticality Analysis of
Immobilized Plutonium Waste Forms in a Geologic Repository

A00000000-01717-5705-00014 REV 01

February 7, 1997

Prepared by:

P. Gottlieb
P. Gottlieb

2/7/97
Date

J. W. Davis
J. W. Davis

2/7/97
Date

P. Cloke
P. Cloke

2/7/97
Date

J. R. Massari
J. R. Massari

2/7/97
Date

Reviewed by:

A. H. Wells
A. H. Wells

2/7/97
Date

Approved by:

Donald G. Hitti FOR HAB
H. A. Benton, Manager
Waste Package Development

2/7/97
Date

A. M. Segrest
A. M. Segrest, Manager
MGDS Development

02/07/97
Date

fw

PREDECISIONAL DOCUMENT

Intentionally Left Blank

EXECUTIVE SUMMARY

The Office of Fissile Materials Disposition has undertaken evaluations of various plutonium waste forms for final disposition in a geologic repository. It has been determined that one of the principal technical considerations for disposal of these waste forms is their long-term performance in a repository environment. This long-term performance consists of two elements, releases of radioactivity (dose) to the accessible environment (called total system performance assessment), and long-term criticality behavior of the waste forms and packages in the repository. This report addresses only the long-term criticality issues; the total system performance assessment is the subject of a separate report (Reference 1).

Criticality issues for the plutonium waste forms as packaged for disposal in a geologic repository fall into three broad categories:

- Those associated with the as-fabricated (intact) waste packages
- Those associated with the degraded package and waste form in the near-field environment
- Those associated with the flow and transport of the fissile material into the far field with reconcentration (external criticality).

A systematic approach to criticality evaluations was formulated and has been followed. Criticality analyses of intact waste forms were first conducted, and the configurations from these designs used to degrade the waste form and package, to be followed by transport of the fissile material into the far field with reconstitution. This report focuses on the degraded mode criticality analyses, based on the intact configurations evaluated earlier (Reference 2).

This report addresses two primary waste forms associated with the proposed plutonium immobilization concepts, can-in-canister glass and can-in-canister ceramic. Both waste forms consist of cans of either lanthanide borosilicate glass or a ceramic similar to Synroc C. These cans are placed into defense high-level waste pour canisters which are backfilled with defense high-level waste glass. Because these concepts are in a developmental stage, coordination with the formulation team has been maintained. It is the intent of these evaluations to provide feedback to the glass and ceramic formulation teams giving the characteristics and features that must be maintained in their product, such that acceptance of the waste form in a geologic repository can continue to be considered. Because specific data for evaluations of long-term criticality are not readily available for these waste forms, ranges of values have been used to bracket the behavior. The findings of these analyses should assist the waste form producers to tailor their product specifications for repository disposal.

The primary considerations for determining criticality potential in a repository are the fissile material concentration in the waste form, the concentration of the neutron absorber, the waste package configuration, and the resulting configurations of all these parameters as degradation of the waste form and package occurs over time. The waste form dissolution is assumed to be congruent, so that all the species contained in the waste form are released to the solution at a rate that is proportional to the amount of the species contained in the waste form. The dissolution rate and the chemical

PREDECISIONAL DOCUMENT

behavior of these species determine the percent that remains in solution and the percent that is precipitated immediately upon release from the waste form, which in turn determines whether critical masses can be accumulated in precipitated masses within the waste package or in the near-field. The likely range of chemical conditions and species was determined by means of computer code (EQ3/6) to account for many species simultaneously, and by means of hand analytical calculations accounting for only a few species simultaneously. These calculations were used to estimate the solubility of the principal neutronically significant species (i.e., principal fissile or absorber elements) plutonium, uranium, and gadolinium as a function of pH for the range of values likely to be encountered (5.5 to 10).

Because the Nuclear Waste Policy Act (as amended) identifies Yucca Mountain as the only location for repository site characterization studies, the basis of all scenario development and analysis is placement of waste packages into drifts excavated in unsaturated tuff. All scenarios begin with:

- An infiltration of water incident on the waste package followed by water penetration of the waste package barriers
- Water penetration of the stainless steel pour canister containing the waste cans
- Water penetrating the filler glass
- Water penetrating the can directly containing the waste form
- Water contacting the surfaces of the waste form, thereby beginning the waste form alteration process.

The scenarios then proceed along three parallel paths that are characterized by differing locations of holes in the waste package barriers. Any of these types of scenario can lead to three final configurations:

- A. Insoluble waste form alteration products precipitated at the bottom of the waste package in a clayey mass, for which the most likely geometry is a cylinder sector conforming to the bottom of the waste package.
- B. Fissile material (plutonium and uranium) precipitated on metal surfaces.
- C. Fissile material trapped in the invert.

The primary focus of this study is the first configuration. The second configuration would be a very thin geometry, and scoping calculations showed it to require an unrealistically large critical mass. Bounding calculations were performed for the third configuration and the results are discussed in the text.

The analysis is focused on determining the range of concentrations of uranium, plutonium, and gadolinium that can occur in the clayey mass precipitated at the bottom of the package, and to determine whether these concentrations are critical. The principal analysis tool is a program that

PREDECISIONAL DOCUMENT

computes the amounts of plutonium, uranium, gadolinium, and chromium in solution as a function of time with inputs from a range of possible waste form dissolution rates and stainless steel corrosion rates. The program model is sufficiently general that it can represent all three types of scenarios described above. The key parameter in this analysis is the pH of the solution since the chemical analysis has suggested that the gadolinium solubility can be as high as 3,000 parts-per-million for a pH as low as 5.5. A number of cases were identified with concentrations that could produce criticality.

MAJOR FINDINGS

Design Implications

Analysis of a representative set of potentially critical configurations leads to the following findings which directly impact waste form design:

- A critical parameter for determining criticality risk is the Dissolution Product Factor that is defined as the product of the intrinsic material dissolution rate per unit surface area, multiplied by the ratio of total waste form surface area (outer surface area plus the, generally, much larger internal surface area exposed by fracturing) to outer waste form surface area (or inner surface area of the waste form can). Threshold (limiting) Dissolution Product Factor values have been determined for the nominal waste forms for both glass and ceramic, using the principal degradation modes considered in this study. Any waste form that has an actual Dissolution Product Factor less than its corresponding threshold Dissolution Product Factor, cannot go critical.
- The Dissolution Product Factor limit (threshold) for the nominal ceramic waste form is approximately twice the value for the nominal glass waste form (for the nominal environmental conditions and dissolution rates). This is primarily due to the hafnium present in the ceramic, which serves as a backup neutron absorber under those conditions in which the primary absorber, gadolinium, becomes soluble and is removed from the waste package. The hafnium is present in the ceramic because it occurs naturally in small amounts in the same ore as the zirconium, which is a principal component of the ceramic. If a comparable concentration of hafnium is incorporated in the glass form, the Dissolution Product Factor limit of the glass waste form would be comparable to that of the ceramic waste form.
- The results of this study could not distinguish between the long-term performance of the ceramic and the glass waste forms because of a lack of definitive data on the following:
 - Long-term dissolution rates of the waste forms (per unit surface area)
 - Effective surface area (enhanced by internal fracturing)
 - The degree to which hafnium can be incorporated into the glass waste form matrix without limiting the plutonium carrying capability to less than the target 10%.

PREDECISIONAL DOCUMENT

- For the waste forms and degradation modes considered here, it is possible to preclude the possibility of criticality by reducing the plutonium loading from the nominal 205 kg per waste package. For the ceramic waste form this loading should be reduced to 100 kg, and for the glass waste form the value should be 50 kg. This factor of 2 difference arises because of the presence of hafnium in the ceramic form as discussed above. As with the Dissolution Product Factor limit, this difference can be negated by adding hafnium to the glass waste form. The required reduction in plutonium loading can be achieved either by using a co-disposal concept (mixing defense high-level waste canisters with plutonium canisters in a waste package), or by reducing the concentration of plutonium in the waste form.
- The potential for criticality may be reduced by adding depleted uranium as waste package filler between the pour canisters. The addition of 200 kg depleted uranium will, typically, lower the k_{eff} of a nearly critical configuration by 0.05. If the depleted uranium is encapsulated in a matrix chemically similar to that used for the plutonium waste form (either glass or ceramic), it will tend to be mobilized at the same rate as the uranium in the waste form. Once mobilized, the depleted uranium will transport with the chemically identical fissile uranium-235 which is the decay product of the plutonium-239, thereby significantly reducing the potential for external criticality (which will be evaluated in a future report).

Conditions that can lead to criticality

The type and quantity of neutron absorber included in the proposed immobilized plutonium waste forms are sufficient to prevent criticality in intact configurations, even if the waste package is filled with water (highest possible concentration of moderator). For criticality to occur in, or near, a waste package of immobilized plutonium waste form, most of the neutron absorber has to be separated from the fissile material. The following conditions could arise from the interaction of the waste package materials and the environment, which could result in sufficient separation of fissile material and neutron absorber.

- A low pH (less than 6.0) may permit the principal added neutron absorber, gadolinium, to have at least 1000 times the solubility of uranium or plutonium. Under certain (possible) flow conditions, this difference in solubility could result in so much of the gadolinium being removed from the waste package, that there is the potential for a criticality event.
- The corrosion of the waste package stainless steel (specifically the stainless steel of the pour canister) may result in the oxidation of chromium or molybdenum to a high enough valence state that the water becomes acidic. The resulting pH of the water in the waste package depends on the rate at which the acid that is produced is flushed from the system. For the current range of estimated infiltration rate from the environment into the drift (1 to 10 mm/yr) and standing water contained in 10% of the waste package volume, the pH could be lowered to a value of 5. Elimination of most of the stainless steel components of the waste package would obviously limit the potential for acidification.

PREDECISIONAL DOCUMENT

- If the above conditions hold during the period of principal waste form degradation, the relatively insoluble fissile material being released from the degrading waste form may precipitate in a clay mass which could contain sufficient water to moderate a criticality.
- If all of the above conditions hold, the earliest time of criticality occurrence is typically 100,000 years; under certain "worst case" conditions, the earliest time to criticality could be as low as 12,000 years.

Conditions that can preclude the processes which can lead to criticality

The following conditions will tend to prevent the occurrence of the conditions that can lead to criticality (listed above).

- The acidity produced by the corroding stainless steel may be neutralized by the alkalinity of the incoming water (which may be maintained at a high pH by remnants of the concrete drift liner).
- Certain elements present in the waste package may form precipitates of gadolinium that have not yet been identified in the chemical literature. Such precipitates could limit the solubility of gadolinium, even at low pH.
- Even if there are conditions that lead to high gadolinium solubility, there may be sufficient penetration of the package bottom that the fissile material does not precipitate in a compact cylinder sector at the bottom of the waste package.

Sensitivity considerations

- The occurrence of criticality is relatively independent of the infiltration rate, except at rates above 20 mm/yr (four times the present estimated value), which tend to shift the pH toward neutrality, thereby limiting the potential for gadolinium removal and resulting criticality.
- For a given amount of fissile material and neutron absorber collected in the clayey material at the bottom of the waste package, an inhomogeneous distribution of fissile material may result in a k_{eff} significantly larger than the homogeneous distribution. For example, if a cylinder sector of homogeneous distribution has a $k_{eff}=0.96$, a concentration of the fissile material and neutron absorber in the upper half would give a $k_{eff}=0.99$ and concentration in the lower half would give $k_{eff}=1.07$. These represent the optimum inhomogeneity with respect to criticality enhancing horizontal stratification; further concentration to the upper and lower 25% results in $k_{eff}=0.86$ and 1.05, respectively. Major horizontal stratification is relatively unlikely, but there are a few physical mechanisms that could produce such distributions. These possible variations do not effect the basic results of this study, but they do indicate that there could be worse cases.

RECOMMENDATIONS

Data needs. The analyses of this study revealed important information gaps, particularly in the following areas:

- Long-term corrosion rate of stainless steel.
- Oxidation states of chromium resulting from stainless steel corrosion in the expected Yucca Mountain environment.
- Long-term dissolution rates of both the glass and ceramic waste forms under conditions that simulate the repository environment.
- Internal fracturing of the waste form matrix, both in the initial fabrication and after prolonged radiation exposure.
- Gadolinium and hafnium solubility in an aqueous solution containing likely minerals and covering the range of expected pH (to be obtained from both further literature search and experiment); this information is needed to confirm the conclusion of this study regarding the relative persistence of hafnium over gadolinium within the waste package.
- Hafnium carrying capability of the glass waste form, particularly with respect to limiting the plutonium carrying capability.

Computation tools. The following are improvements in computational capability that would significantly enhance the precision of the decision process:

- Improved thermodynamic database for EQ3/6
- Improved calculation models in EQ3/6 and/or AREST-CT, particularly to account for the dilution of confined solutions by incoming water.

Future studies. The following additional studies will be very useful for the waste form selection decision, and will be necessary for the ultimate licensing of the chosen alternative.

- Conduct risk-based analysis, using the most current performance data, to show consequences of those scenarios that exhibit the potential for a criticality event.
- Evaluate the potential for external, far-field criticality.
- Evaluate the effect of incorporating large amounts of depleted uranium in the waste form or waste package, particularly to limit any possibility of external criticality.

PREDECISIONAL DOCUMENT

CONTENTS

	Page
EXECUTIVE SUMMARY	iv
ACRONYMS	xvi
1. INTRODUCTION AND BACKGROUND	1-1
2. WASTE FORM AND WASTE PACKAGE DESCRIPTIONS	2-1
2.1 GLASS WASTE FORM	2-1
2.1.1 Nominal Pu-glass Description	2-1
2.1.2 Additional Glass WF Composition Considerations	2-1
2.2 CERAMIC WASTE FORM DESCRIPTION	2-3
2.2.1 Nominal Pu-ceramic Description	2-3
2.2.2 Future Decisions for Ceramic WF Size and Composition	2-4
2.3 WASTE PACKAGE DESCRIPTION	2-4
3. APPROACH AND METHODOLOGY	3-1
3.1 GENERAL REQUIREMENTS FOR CRITICALITY	3-1
3.1.1 Breach of Barriers	3-1
3.1.2 Separation of Neutron Absorber from Fissile Material	3-2
3.1.3 Sufficient Moderator	3-2
3.1.4 Sufficient k_{eff} (Criticality Threshold)	3-3
3.2 ANALYSIS STRATEGY/METHODOLOGY	3-3
3.2.1 Mass Balance Calculations	3-4
3.2.2 Chemistry Calculations (EQ3/6) in Support of Mass Balance	3-6
3.3 REPOSITORY ENVIRONMENT AND OTHER PARAMETERS	3-6
4. INPUT DATA VALUES	4-1
4.1 DISSOLUTION RATES	4-1
4.2 SOLUBILITY	4-3
4.3 ENVIRONMENTAL PARAMETERS	4-4
5. SCENARIO CONCEPTS FOR WF DEGRADATION AND SUBSEQUENT PROCESSES	5-1
5.1 PHYSICAL SCENARIOS FOR GLASS WF DEGRADATION	5-1
5.1.1 Breached-Top-Only Scenario, Circulation Flushing Only	5-7
5.1.2 Breached-Top-and-Side Scenario, Both Flow-Through and Circulation Flushing	5-9
5.1.3 Breached-Top-and-Bottom Scenario, Flushing by Flow-through	5-10
5.2 PHYSICAL SCENARIOS FOR CERAMIC WASTE FORM DEGRADATION	5-12
5.3 CHEMICAL ANALYSIS METHODOLOGY AND GENERAL RESULTS	5-15
5.3.1 EQ3/6 and Mass Balance Considerations	5-14
5.3.2 Thermodynamic Data and Static Mass Balance Relationships for Gd	5-16

PREDECISIONAL DOCUMENT

CONTENTS (Continued)

	Page
5.3.3 Alkalinity of J-13 Well Water	5-18
5.3.4 Solubilities of Gd, Pu, and U under Acidic Conditions	5-19
5.3.5 Compositions of Solid Phases Resulting from Degradation of WP Components	5-21
5.4 CHEMICAL SCENARIOS FOR GLASS WASTE FORM DEGRADATION ..	5-22
5.4.1 Unlimited Access of Air with Alkali Glass Composition	5-22
5.4.2 Restricted Access of Air with Alkali Glass Composition	5-24
5.4.3 Unlimited CO ₂ and O ₂ with No Alkali in the Glass	5-24
5.4.4 Limited CO ₂ and O ₂ with No Alkali in the Glass	5-24
5.4.5 Composition of Solid Degradation Products From Glass	5-25
5.5 CHEMICAL SCENARIOS FOR CERAMIC WASTE FORM DEGRADATION	5-26
5.5.1 Modeling of Ceramic WF Degradation	5-26
5.5.2 Composition of Solid Degradation Products From Ceramic	5-27
5.6 FISSILE MATERIAL TRAPPED IN THE INVERT	5-28
6. REPRESENTATIVE WASTE FORM DEGRADATION CONFIGURATIONS	6-1
6.1 TYPICAL CONFIGURATIONS FROM GLASS WASTE FORM DEGRADATION	6-1
6.1.1 Altered WF Slumped to Bottom of WP	6-1
6.1.1.1 Undissolved WF separated from the clayey material	6-3
6.1.1.2 Undissolved WF distributed uniformly within the clayey material	6-3
6.1.2 Invert Accumulation	6-5
6.1.3 Other Configurations	6-5
6.2 TYPICAL CONFIGURATIONS FROM CERAMIC WASTE FORM DEGRADATION	6-6
6.2.1 Slumped to Bottom	6-6
6.2.2 Invert Accumulation	6-6
6.2.3 Other Configurations	6-7
7. CRITICALITY CALCULATIONS (k_{eff})	7-1
7.1 BASIS CALCULATIONS WITH MCNP	7-1
7.1.1 Clayey Configuration from Degradation of DHLW Glass and Pu Immobilization Glass	7-1
7.1.2 Clayey Configuration from Degradation of DHLW Glass and Pu Immobilization Ceramic	7-3
7.1.3 Accumulations of ²³⁵ U Outside the WP In or On the Invert	7-4
7.2 MULTI-VARIATE REGRESSIONS FOR DEGRADED GLASS AND CERAMIC WASTE FORMS	7-5
7.3 COUPLED MASS BALANCE/CRITICALITY EVALUATIONS AND RESULTS	7-6
7.3.1 Glass WF Results	7-8
7.3.2 Ceramic WF Results	7-17

PREDECISIONAL DOCUMENT

CONTENTS (Continued)

	Page
7.3.3 Undissolved WF distributed in clay	7-25
7.4 WASTE FORM DESIGN CONSIDERATIONS	7-27
7.4.1 Pu Loading Alternatives	7-27
7.4.2 Gd:Pu Ratio Alternatives	7-27
7.4.3 Glass vs Ceramic	7-30
7.5 ADDITIONAL RELEVANT RESULTS	7-30
7.5.1 Effects of Non-Homogeneous Fissile Distribution	7-30
7.5.2 Evaluation of Sm as Replacement Option for Gd	7-36
7.5.3 Investigation of Dryout in the Degraded Glass Clayey Configuration	7-37
7.5.4 Effects of ²³⁸ U in Degraded Glass Clayey Composition	7-37
7.5.5 Variation of Hf Content in the Degraded Ceramic WF	7-38
8. MAJOR FINDINGS AND RECOMMENDATIONS	8-1
8.1 DESIGN IMPLICATIONS	8-1
8.2 CONDITIONS THAT CAN LEAD TO CRITICALITY	8-2
8.3 CONDITIONS THAT CAN PRECLUDE THE PROCESSES WHICH CAN LEAD TO CRITICALITY	8-2
8.4 SENSITIVITY CONSIDERATIONS	8-3
8.5 RECOMMENDATIONS	8-3
9. REFERENCES	9-1
APPENDIX A MATERIAL PROPERTIES AND REPOSITORY ENVIRONMENT PARAMETERS	A-1
APPENDIX B PROGRAM TO TRACK WASTE PACKAGE DEGRADATION PARAMETERS	B-1
APPENDIX C SUMMARY OF RESULTS OF EQ3/6 CALCULATIONS	C-1
APPENDIX D ACTIVITY COEFFICIENTS	D-1
APPENDIX E JUSTIFICATION OF STATIC MASS BALANCE METHODOLOGY	E-1
APPENDIX F GADOLINIUM THERMODYNAMIC DATA	F-1
APPENDIX G CRITICALITY DATA POINTS	G-1
APPENDIX H ASSUMPTIONS	H-1

FIGURES

	Page
2.1.1-1 Defense High-Level Waste Glass Canister with Plutonium Cans	2-2
2.3-1 DHLW Waste Package	2-5
5-1 System Perspective of Event/Process Sequences for the Degradation of Pu Immobilized in Glass and Subsequent Material Movements	5-2
5-2 Physical Perspective of Event/Process Sequences for the Degradation of Pu Immobilized in Glass and Subsequent Material Movements	5-3
5-3 Chemistry Perspective of Process Sequences for the Degradation of Pu Immobilized in Glass and Subsequent Material Movements	5-4
5.1-1 Degraded Barriers, Degraded Canisters, Glass Fractures	5-5
6.1.1-1 WP Model for Homogenized Clayey Material Slumped to Bottom	6-2
6.1.1-2 WP Model for Concentration of all Pu/U/Gd in Top Layer of Clay	6-4
6.1.1-3 WP Model for Concentration of Pu/U/Gd on One End of WP	6-4
7.3.1-1 k_{eff} vs Time Glass Waste Infiltration Rate = 1 mm/yr, Stainless Steel Corrosion Rate = 0.1 $\mu\text{m}/\text{yr}$	7-9
7.3.1-2 Peak k_{eff} vs Infiltration Rate, DPF Family, Glass WF Stainless Steel Corrosion Rate = 0.1 $\mu\text{m}/\text{yr}$	7-10
7.3.1-3 Glass WF: Peak k_{eff} as a Function of Infiltration Rate for Typical Values of Stainless Steel Corrosion Rate at DPF = 1.5E-3 (g/m ² /day)	7-11
7.3.1-4 Glass WF: Years (1000) to Earliest Criticality Stainless Steel Corrosion Rate = 0.1 $\mu\text{m}/\text{yr}$, pH = 5.5	7-12
7.3.1-5 DPF Limit for k_{eff} = .98, Glass WF	7-13
7.3.1-6 DPF Limit, k_{eff} = .93, Glass WF	7-14
7.3.1-7 DPF Limit, k_{eff} = 0.98 and 0.93, Glass WF Stainless Steel Corrosion Rate = 0.10	7-15
7.3.2-1 k_{eff} vs Time, Ceramic WF Infiltration Rate = 1 mm/yr, Stainless Steel Corrosion Rate = 0.1 $\mu\text{m}/\text{yr}$	7-18
7.3.2-2 Ceramic WF: k_{eff} as a Function of Infiltration Rate for Typical Values of WF Dissolution Rate x Factor (Dissolution Product)	7-19
7.3.2-3 Ceramic WF: Peak k_{eff} as a Function of Infiltration Rate for Typical Values of Stainless Steel Corrosion Rate at DPF = 1.5E-3 (g/m ² /day)	7-20
7.3.2-4 Ceramic WF: Years (1000) to Earliest Criticality for Stainless Steel Corrosion Rate = 0.1 $\mu\text{m}/\text{yr}$	7-21
7.3.2-5 Ceramic WF: DPF Limits for k_{eff} = 0.98	7-22
7.3.2-6 Ceramic WF: Dissolution Product Limit for k_{eff} = 0.93	7-23
7.3.2-7 DPF Limit, k_{eff} = 0.98 and 0.93, Ceramic WF, Stainless Steel Corrosion Rate = 0.1 $\mu\text{m}/\text{yr}$	7-24
7.4.1-1 Glass WF: DPF Limit as a Function of Pu Loading Fraction, for Stainless Steel Corrosion Rate = 0.1 $\mu\text{m}/\text{yr}$	7-28
7.4.1-2 Ceramic WF: DPF Limit as a Function of Pu Loading Fraction, for Stainless Steel Corrosion Rate = 0.1 $\mu\text{m}/\text{yr}$	7-29
7.4.2-1 Reverse Behavior of Time to Earliest Criticality as a Function of DPF for a Family of Gd:Pu Mole Ratios (Infiltration Rate = 0.3 mm/yr, Stainless Steel Corrosion Rate = 0.1 $\mu\text{m}/\text{yr}$)	7-31

PREDECISIONAL DOCUMENT

FIGURES (Continued)

	Page
7.4.3-1 DPF Limit, Glass and Ceramic Compared ($k_{eff} = 0.98$) for Infiltration Rate = 1 mm/yr	7-32
7.4.3-2 DPF Limit vs Infiltration Rate, Glass and Ceramic Compared ($k_{eff} = 0.98$) for Stainless Steel Corrosion Rate = 0.1 $\mu\text{m}/\text{yr}$	7-33
7.5.1-1 Effects on k_{eff} of Pu/U/Gd Distribution Within the Clay for the 25kg/25kg/0.25kg Case	7-35

PREDECISIONAL DOCUMENT

TABLES

	Page
4.1-1	Dissolution Rates 4-1
4.1-2	Surface Area Multiplication Factor for Internal Fracturing 4-2
4.1-3	304L Stainless Steel General Corrosion Rates in J-13 Well Water 4-2
4.2-1	Solubility 4-3
4.3-1	Environmental Parameters 4-4
5.3.4-1	Bounding Values of Gd Solubility from EQ6 Runs 5-20
5.4.5-1	Elemental Components of the Clayey Mass from Degraded Filler Glass and Pu Immobilization Glass 5-25
5.5.2-1	Elemental Components of the Clayey Mass from Degraded Filler Glass and Pu Immobilization Ceramic 5-27
5.6-1	Representative List of Calcium-Rich Zeolites Which Could Result from Concrete Degradation 5-29
7.1.3-1	Accumulations of 1 wt% ²³⁵ U in Chabazite (40%) and Aggregate (60%) from Degraded Concrete in a 75 cm Deep Cylinder Segment 7-5
7.2-1	Coefficients for Glass and Ceramic WF Regressions 7-6
7.3-1	Summary of Input Parameters for Criticality Evaluations 7-7
7.3.3-1	Comparison of DPF thresholds (SS crsn rate = 0.10 μm/yr, Infiltration rate = 1 mm/yr), for indicated Pu loading, in units of 0.001 g/m ² /day 7-26
7.3.3-2	Time to earliest criticality (x1000 yrs*) At DPF=10 (x0.001 g/m ² /day) 7-26
7.5.1-1	Effect on k _{eff} of Pu/U/Gd Concentration in Bottom of Clay 7-34
7.5.1-2	Effect on k _{eff} of Pu/U/Gd Concentration in Top of Clay 7-34
7.5.1-3	Effect on k _{eff} of Concentrating Pu/U/Gd on One End of WP 7-34
7.5.1-4	Effect on k _{eff} of Half Volume on One End of WP (Same Concentration) 7-36
7.5.2-1	Comparison of Gd and Sm in Degraded DHLW Glass/Pu Immobilization Glass 7-36
7.5.3-1	Investigation of Dryout of Degraded Glass Configuration 7-37
7.5.4-1	Comparison of ²³⁸ U in Degraded DHLW Glass/Pu Immobilization Glass 7-38
7.5.5-1	Variation of Hf Wt% in Zr for the Degraded Ceramic WF 7-38
7.5.5-2	Calculations to Determine Equivalent Hf Wt% in Zr to Replace 0.5 kg Gd for the Degraded Ceramic WF 7-39

PREDECISIONAL DOCUMENT

ACRONYMS

ATS	Alkali-tin-silicate
Cr	Chromium
DHLW	Defense High-Level Waste
DPF	Dissolution Product Factor
Gd	Gadolinium
Hf	Hafnium
La-BS	Lanthanide Borosilicate
Mo	Molybdenum
MTU	Metric Ton Uranium
NRC	U.S. Nuclear Regulatory Commission
Pu	Plutonium
REE	Rare Earth Elements
SS	Stainless Steel
TSPA	Total System Performance Assessment
U	Uranium
WF	Waste Form
WP	Waste Package

PREDECISIONAL DOCUMENT

Intentionally Left Blank

1. INTRODUCTION AND BACKGROUND

The Office of Fissile Materials Disposition has undertaken an evaluation of numerous waste forms (WFs) containing plutonium (Pu) for ultimate disposal in a geologic repository. It has been determined that one of the principal technical considerations for disposal of these WFs is their long-term performance in a repository environment. This long-term performance consists of two elements: total system performance of the WF and package (i.e., releases to the accessible environment) in the repository, and long-term criticality behavior of these WFs and packages in the repository. The total system performance assessment is the subject of a separate report (Reference 1).

The objectives of this report are to evaluate alternative glass and ceramic WFs with respect to the major criticality issues and to suggest design criteria which are likely to satisfy the criticality regulatory requirements. These evaluations should reflect the range of environmental parameters which are likely to occur in the repository.

Criticality issues for the Pu WFs as packaged for disposal in a geologic repository, fall into three broad categories:

- Those associated with the as-fabricated (intact) waste packages (WPs)
- Those associated with the degraded package and WF in the near-field environment
- Those associated with the flow and transport of the fissile material into the far-field with reconcentration (external criticality).

Earlier studies (Reference 2) have shown that the as-fabricated or intact configuration is well within the U.S. Nuclear Regulatory Commission (NRC) promulgated requirements for criticality control for geologic disposal as indicated in 10 CFR 60, *Disposal of High-Level Radioactive Wastes in Geologic Repositories*. These analyses considered several different WFs, MOX spent fuels (both boiling water reactors and pressurized water reactors) and WFs immobilized in glass; and ceramic matrices produced by different processes. This report focuses on only the degraded mode criticality considerations for two specific WF configurations, can-in-canister glass and can-in-canister ceramic. Accumulations of fissile material and possible criticalities inside the WP and in the near-field are addressed.

Degradation scenarios that span the range of potential criticality occurrences have been developed. These scenarios can be used to screen Pu disposition alternatives and to rank them with respect to criticality risk. The possibility for the occurrence of these scenarios has been ascertained from simple mass balance models using currently available data on a range of parameter values pertaining to the alteration of typical glass and ceramic WFs, and the solubility of the principal isotopic species of interest.

Section 2 of the report describes the WFs and the WP. Section 3 gives information concerning the physical conditions and configurations which can lead to criticality, and describes the analysis methodology. Section 4 describes the conceptual processes and events which can lead to potentially

PREDECISIONAL DOCUMENT

critical configurations. Section 5 gives the input data values to be used in the evaluation calculations. Section 6 describes the configurations of material (in the WP or in the near field) that could occur and that have the potential for criticality. Section 7 gives the results of the calculations and identifies those configurations that have some potential for criticality. Section 8 gives the conclusions that can be drawn from this study, including recommendations for WF design, and recommendations of materials tests that could provide data/information to improve behavior/process models.

2. WASTE FORM AND WASTE PACKAGE DESCRIPTIONS

2.1 GLASS WASTE FORM

2.1.1 Nominal Pu-glass Description

The can-in-canister glass WF nominally consists of Pu dissolved in a Lanthanide Borosilicate (La-BS) glass with an equi-molar ratio of a neutron absorber (gadolinium). Based on the latest data, the La-BS glass appears to be the most suitable, but other alternatives are still being investigated, particularly the alkali-tin-silicate (ATS) glass. The Pu bearing glass is poured into cans which are, in turn, supported on a rack/basket, and embedded in a defense high-level waste (DHLW) glass filler within a DHLW-type canister as shown in Figure 2.1.1-1. The compositions of the La-BS and DHLW filler glass are presented in Appendix A, Tables A-1 and A-2.

The primary unit of this WF is a glass cylinder inside a stainless steel can with the outside dimensions as 12.035 cm diameter x 57.535 cm long and 0.3175 cm thick. The interior volume of this can (5808 cm³) is 85% filled with a La-BS glass doped with approximately 10 wt% Pu and 6.6 wt% gadolinium (Gd) (1:1 mole ratio with the Pu), as described in Table A-1. The Gd serves as the principal neutron absorber which prevents criticality, even when the WP is filled with water. The density of the doped glass is approximately 5.5 gm/cm³, so that each can has approximately 2.56 kg of Pu.

Different glass WFs are being investigated that provide high solubility of Pu and Gd within the glass, and high resistance to dissolution in water having chemical composition similar to that expected in a Yucca Mountain repository environment. The ranges of dissolution rates for these glasses are summarized, together with the range of dissolution rates for the most likely ceramic WF, in Section 4.1, Table 4.1-1.

It is assumed that the dissolution of the glass WF is congruent, which means that each component of the glass will be released from the solid form at a rate which is equal to the glass dissolution rate multiplied by the weight fraction of that component. It is further assumed that the individual ionic breakdown products (components) of the glass dissolution will go into solution as the glass is dissolved. However, those ions which are insoluble will immediately precipitate, generally at the point of dissolution. These low solubility components will generally be incorporated into the altered layer (which is similar to the initial glass, but without all the soluble components of the initial glass).

2.1.2 Additional Glass WF Composition Considerations

Optimum Neutron Absorber

Gd has been the nominal choice for neutron absorber because, of all the elements, it has the largest absorption cross section (most efficient) for thermal neutrons. However, other elements have better features with respect to other requirements. Samarium (Sm) has been suggested as a lower cost alternative and may be almost as efficient as Gd for an epi-thermal to fast neutron. The effectiveness

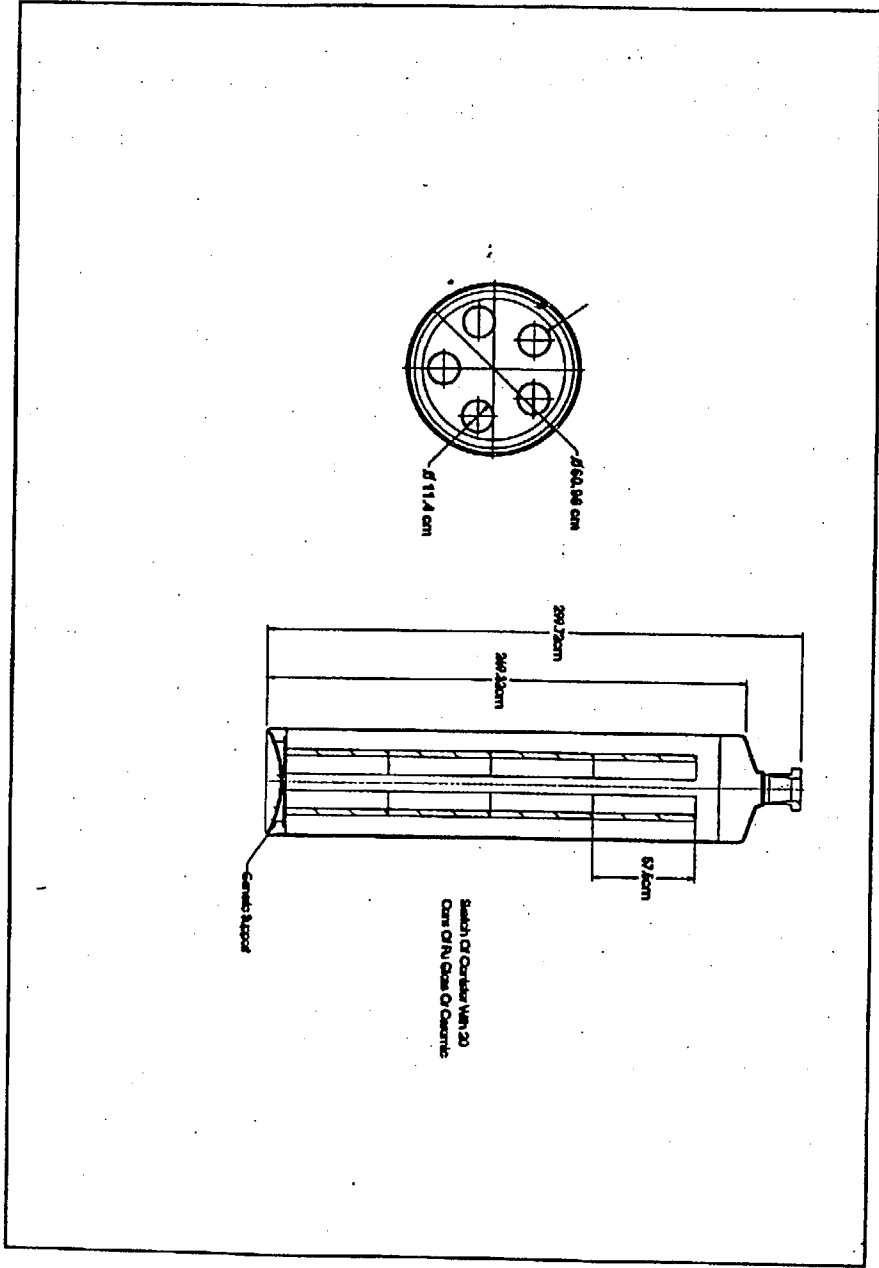


Figure 2.1.1-1: Defense High-Level Waste Glass Canister with Plutonium Canes

of Sm for a probable degraded composition is investigated in Section 7.5.2. Hafnium (Hf) is the least soluble (which is important in preventing removal of the neutron absorber over tens of thousands of years), but is also the most expensive. The effectiveness of Hf is investigated in Section 7.5.5.

Phase Separation Considerations for Pu and Gd

Tests on formulations of ATS and Loeffler glass showed that, while most of the Pu dissolved in the glass, some sub-stoichiometric PuO_2 particles were present. This suggests that the solubility limit for Pu plus Gd was probably reached for this glass chemistry. It is expected that the La-BS glass should be able to minimize such phase separation by slow processing or cooling.

If a Pu or Gd phase separation does occur, it is likely to cause non-congruent dissolution of the glass. Furthermore, inclusions could weaken the glass and make it more susceptible to both mechanical fracture and the chemical dissolution processes.

2.2 CERAMIC WASTE FORM DESCRIPTION

As with glass, the ceramic WF is contained in cans, supported on a rack/basket, embedded in a DHLW filler glass, within a DHLW type canister, as shown in Figure 2.1.1-1. The size and number of the cans will be such that the amount of Pu per canister is the same as with the glass WF. The precise size and content of the individual WF units are being determined by some experimental optimization. For this analysis, the following parameters have been chosen, and closely approximate the glass WF in can size.

2.2.1 Nominal Pu-ceramic Description

For the ceramic can-in-canister concept, each can is assumed to contain 5 ceramic cylinders. There are 20 cans per canister, just as for the glass WF. The ceramic cylinders are assumed to be cold pressed and sintered, so there is no metal bellows or top and bottom plate.

Dimensions—Each disk (or cylinder) is 11 cm diameter by 11 cm high; they are stacked 5 deep in each can. As with the glass can-in-can, the total can length is 57.535 cm, the can shell thickness is 0.3175 cm, and the can outer diameter is 12.035 cm (Reference 10).

Composition—The ultimate formulation of the ceramic has not yet been decided, but the preliminary composition is a variant of Synroc-C with the following mineral compositions (wt%): zirconolite (66%), pyrochlore (15%), hollandite (8%), and rutile (11%) (Reference 11). For convenience, the ceramic will be referred to as Synroc-C, which is to be understood as a generic name. The zirconolite incorporates 0.336 kg Gd per cylinder, and 0.512 kg Pu per cylinder. Therefore, each can contains just 2.56 kg of Pu and a 20 can canister has 51.2 kg of Pu, just as in the glass can-in-can alternative. It should be noted that naturally occurring zirconium contains approximately 2 wt% Hf which is a strong neutron absorber, although not nearly as strong as Gd. This Hf can have a significant effect on criticality because it is insoluble, even in the low range of pH (6.5 to 5.5) where Gd is very soluble. The effect of this amount of Hf remaining in any

precipitate in the WP is incorporated into the analysis of ceramic WF criticality potential in Section 7.3.2, and the effect of variations in the Hf concentration are described in Section 7.5.5.

Mass—The total mass in each 11 cm high cylinder is 5.12 kg.

As with the glass WF, it is assumed that any ceramic dissolution is congruent, which means that each component of the ceramic will be released from the initial solid WF at a rate which is equal to the ceramic dissolution rate multiplied by the weight fraction of that component.

2.2.2 Future Decisions for Ceramic WF Size and Composition

Experimental efforts are underway to develop a ceramic formulation with a minimum amount of pyrochlore. The pyrochlore phase suffers the primary radiation damage resulting in high fracture factors (surface areas); however, the pyrochlore phase also acts as the "overflow" for the Pu when the zirconolite is fully loaded. The removal of pyrochlore and any effect on Pu loading in the ceramic form are still under investigation.

WF Dimensions—The WF diameter will be as large as is practical within the constraints of the hot press process, but it is expected that it will be less than 9 cm. The length of the individual WF cylinders is expected to remain approximately 11 cm.

Can Size—The can length will be adjusted to accommodate an integral number of WF cylinders, or vice-versa, within the constraint of being close to an integral number of cans in the useable length of the DHLW size canister.

2.3 WASTE PACKAGE DESCRIPTION

The WP for immobilized Pu is the same for both glass and ceramic WFs, since both WFs will be fit into the same DHLW size canister. For this reason the WP will be similar to the CRWMS current design for DHLW. The WP is nominally loaded with four canisters. The WP design may be enlarged somewhat to accommodate five canister in the interest of greater efficiency, but such a design is not considered as part of this study. The cross section of a four canister package is given in Figure 2.3-1. The nominal Pu loading per WP is specified by 4 Pu loaded canisters per WP. To minimize the potential for criticality, it may be desirable to reduce this loading by replacing one or more of the Pu loaded canisters with ordinary DHLW canisters. The reduction in criticality potential from such a strategy is evaluated in Section 7.4.1.

The WP for the immobilized Pu WFs consists primarily of a corrosion allowance outer barrier and a corrosion-resistant inner barrier. The corrosion-allowance outer barrier will likely be Cu-Ni 5 cm thick or carbon steel 10 cm thick as is used in the CRWMS current design for the commercial spent nuclear fuel WP. The former will minimize the availability of iron (which could significantly enhance the glass dissolution/alteration rate by forming Fe_2SiO_4), but the extent of the benefit is uncertain, and the latter is much cheaper. The inner barrier will be corrosion resistant, high nickel, Alloy 825 or Alloy 625, 2 cm thick. The performance, with respect to corrosion and penetration by water, of this two barrier system is discussed in Section 3.1.

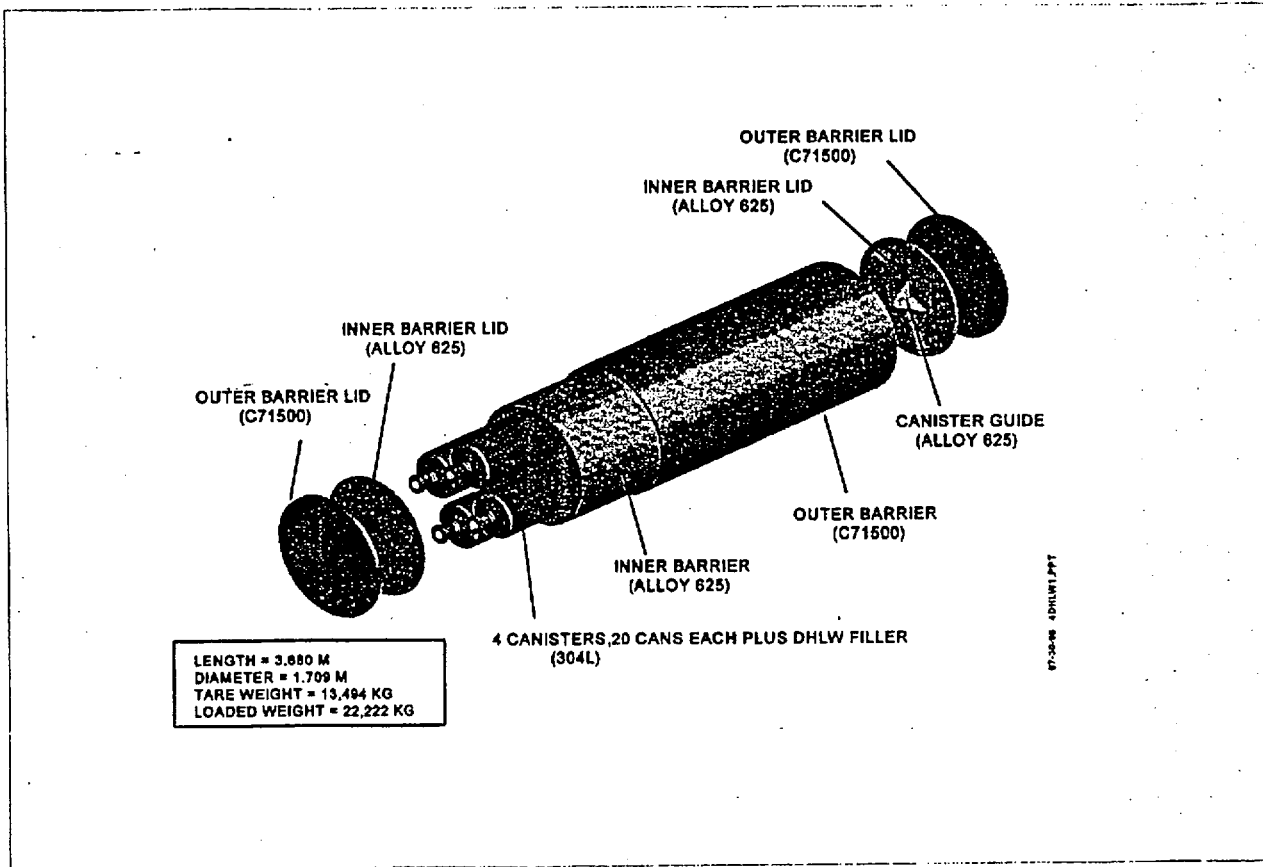


Figure 2.3-1. DHLW Waste Package

PREDECISIONAL DOCUMENT

The WFs are contained within the WPs in stainless steel canisters approximately 3 meters overall length, 61 cm outer diameter and 1 cm thick. The WP size to accommodate these canisters is approximately 3.4 meters overall length. The WP contains at least 4 of these canisters and therefore has an inner diameter of at least 150 cm. Alternatively, for more assured criticality control, the immobilized Pu canisters might be emplaced one to a WP, with the other canisters being ordinary DHLW.

3. APPROACH AND METHODOLOGY

The approach and methodology described here apply generally to both internal and external criticality and to both glass and ceramic WFs. However, most of the illustrations are for internal scenarios and the glass WF. This approach is necessary because the internal scenarios are the precursors to any external criticality, and because the glass WF has more variations in resulting configurations. These distinctions are further explained with the discussion of specific scenarios (including processes following complete WF degradation) in Section 4 and with the discussion of specific configurations (resulting from the specific scenarios, and including configurations with the possibility of near-field external criticality) in Section 6.

3.1 GENERAL REQUIREMENTS FOR CRITICALITY

The requirements identified in this section refer to the events and processes that must be present for a criticality event; however, they do not assure that a criticality will occur. The occurrence of criticality is determined/verified by calculation of k_{eff} as a function of the principal neutronic significant species (i.e. principal fissile and absorber elements as determined by the product of their cross section and their atom density in the mixture) U, Pu, and Gd.

3.1.1 Breach of Barriers

The barriers surrounding the Pu containing WF must be breached before water can begin the dissolution process. These barriers are the inner and outer barriers of the WP, the stainless steel canister, the filler glass, and the stainless steel can containing the Pu WF (glass or ceramic).

First penetration of the WP barriers is expected to result from pitting corrosion, but the rate of this corrosion is subject to some uncertainty. In the most recent repository Total System Performance Assessment (TSPA-95, Reference 3), the time to first pit penetration, averaged over all WPs for the 83 MTU/acre case (within the current design thermal loading range), was approximately 3500 years. This mean time was relatively insensitive to infiltration rate (approximately the same mean failure time for both high- and low-infiltration scenarios) and is based on what is considered to be a conservative inner barrier corrosion model. For this study, the additional conservative assumption will be made that pits can provide a sufficient aperture for water entry, thus allowing water penetration to begin at the time of first pit penetration.

It is assumed that water penetration of the pour canister by 25% of the initial pour canister surface pits will be sufficient to permit significant aqueous attack of the WF. An 1100 year time for 25% of the pits to penetrate the pour canister was calculated using a stainless steel bulk corrosion rate of 0.1 $\mu\text{m}/\text{yr}$ together with a pitting rate enhancement factor of 4, and an estimate of the standard deviation of the distribution of pitting rates equal to 50% of the mean pitting rate. This estimate is somewhat arbitrary, but most of the cases considered in this study involve earliest time to criticality of more than 40,000 years, which will be fairly insensitive to uncertainty in start times of a few thousand years.

Making the conservative assumption that the filler glass provides no protection, based on the fact that it will be highly fractured (by a factor of 30), the mean time for first water penetration to the WF

is $3500+1100 = 4600$ years. It should be noted that although the filler glass may not provide direct protection for the WF, the presence of the degrading filler glass is likely to keep the solution alkali so that the solubility of Gd is low and Gd will precipitate as fast as it can be released, thereby delaying the time to the start of Gd-free buildup of fissile material in the clayey precipitate. This is discussed further in Sections 7.3 and 7.3.1 (in connection with the discussion of Figure 7.3.1-4).

3.1.2 Separation of Neutron Absorber from Fissile Material

For criticality to occur, nearly all the primary criticality control material, Gd, must be removed from the vicinity of the fissile material. Even if all this primary absorber is removed, there could still be enough of the secondary absorbers (particularly iron) to prevent criticality. For this reason, calculations of k_{eff} will include reasonably conservative estimates of the amounts of all insoluble neutron absorbers. There will be no credit taken for the boron in the filler borosilicate glass, because boron is very soluble and would be one of the first species removed from the WP.

It is also possible to have a criticality by separating the fissile species (Pu and/or uranium (U)) from the Gd while both remain in the WP. The potential for such segregation is unknown at this time; however, EQ3/6 calculations suggest it may be possible to have selective precipitation (adsorption) of a significant fraction of the Pu or U oxide on a metal surface, while virtually all Gd goes into the clay which has resulted from the filler glass dissolution. This would require essentially complete depletion of O_2 by reaction with the metal and the maintenance of such a micro environment on and adjacent to the metal surface. The criticality potential of such selective precipitation is limited by two considerations:

- The precipitated layer of fissile oxide on a metal surface will be very thin (unfavorable criticality geometry)
- Any layer of fissile oxide on a metal surface will be likely to re-dissolve with exposure to water with higher oxygen content.

Both Pu and Gd can precipitate as oxides or hydroxides. Other phases are possible, depending on the water chemistry. EQ3/6 modeling indicates that Gd will most likely precipitate as the hydroxy carbonate, phosphate, and/or fluoride. These EQ3/6 studies also indicate that the largest amounts of the 3 species of primary interest will be associated with specific minerals as follows: Pu in PuO_2 ; U in haiweeite ($Na_4UO_2(CO_3)_3$) or soddyite $[(UO_2)_3Si_2O_9 \cdot 6H_2O]$; and Gd in $GdOHCO_3$ or $GdPO_4 \cdot H_2O$.

3.1.3 Sufficient Moderator

There are three possible materials available in the repository that could be moderators for criticality of ^{239}Pu or ^{235}U if present in sufficient quantity: water, carbonates, or silica. Preliminary evaluations of the configurations which can arise from the fissile material of a single WP, have indicated that water has the dominant moderating effect. For this reason all the configurations likely to become critical must have a mechanism for retaining water in the package, or absorbing fissile material into highly saturated clay (which is one possible configuration of the altered glass WF as explained in

Section 5.1) or similar mineral. Insufficient amounts of carbonates are present to provide significant moderation on their own. Silica is a less efficient moderator than hydrogen or carbon, and thus requires greater masses of fissile material spread over a larger volume with a low amount of neutron absorbers. This tends to make silica more of a concern for external far-field criticality, which will be the subject of a future evaluation. In addition, for internal criticality to occur, water must be present in any case to remove the neutron absorber. However, both silica and carbonates will be considered in the sense that they are part of the clay mixture for internal criticality.

3.1.4 Sufficient k_{eff} (Criticality Threshold)

Results are presented in terms of a calculated k_{eff} and in terms of WF design parameters relating the possibility of occurrence of configurations having k_{eff} above some threshold value defining criticality. The physical definition of criticality is $k_{\text{eff}} \geq 1.0$. However, the present NRC licensing requirement applicable to repository criticality is that the calculated k_{eff} be < 1.0 minus a 5% administrative (safety) margin and a further decrement for uncertainty and bias. For commercial spent nuclear fuel, this translates into $k_{\text{eff}} < 0.91$ including a bias and uncertainty associated with applicable criticality safety benchmark calculations, and uncertainty associated with the spent fuel isotopic compositions. However, for immobilized weapons-grade Pu in which all of the Pu is assumed to be ^{239}Pu (or ^{235}U with time), no burnup credit (or associated uncertainty) is used, leading to an approximate limit of $k_{\text{eff}} < 0.93$. This is based on an assumed 2% bias and uncertainty inferred from applicable criticality safety benchmark evaluations (approximately twice the worst case as calculated using MCNP) primarily composed of U and Pu nitrate solutions (Evaluated Benchmark Experiment Descriptions from Reference 42).

There is some possibility that the NRC will permit a risk-based criticality evaluation methodology, for which the 5% margin is not relevant. For this reason, this study presents results for two thresholds, $k_{\text{eff}} \geq 0.93$ and $k_{\text{eff}} \geq 0.98$ (1 minus bias and uncertainty). Most of the comparisons are presented with respect to the higher threshold based on the anticipated NRC rule-change.

3.2 ANALYSIS STRATEGY/METHODOLOGY

The following are the principal components of the strategy to achieve the objective of this evaluation:

- A. Generate scenarios from the possible environmental input parameters and the possible WP and WF performance parameters with respect to various environmentally initiated degradation processes; this modeling predicts pH increase and decrease accompanied by a large increase in total dissolved species in a closed system;
- B. Verification of solubilities of solids containing fissile isotopes and those with neutron absorbers at pH values predicted in a., but with dilute water (unaltered J13); these calculations also confirm what solids are most stable;
- C. Screen configurations of fissile and absorber material resulting from these processes according to threshold values relating to separation of absorber and fissile and relating to the amount of moderator;

- D. Use MCNP to compute k_{eff} for those configurations for which the screening offers some possibility of criticality.

The first component of this strategy, generation of scenarios and resulting configurations is accomplished by the solution of a set of mass balance equations, which are described in Section 3.2.1. The solubility inputs for these calculations are found from experimental data and from theoretical calculations of chemical equilibria using the program EQ3/6, as described in Section 3.2.2.

The analysis considers internal criticality only within one WP at a time. It also considers the possibility of external criticality in the near field, but with fissile mass no more than is available from a single WP. To achieve an 80-100 MTU/acre repository thermal loading, and not exceed other repository thermal goals such as peak spent nuclear fuel cladding and drift wall temperature limits, the WPs will be placed far enough apart (at least 16 m) that neutronic coupling between fissile material in, or from, different packages is virtually impossible.

3.2.1 Mass Balance Calculations

The configurations of WP contents are determined by the use of a simple mass balance computer code for the simultaneous evaluation of the dissolution of the WF and separation of fissile material from the neutron absorbers. The WF is assumed to dissolve congruently, which means that each component goes into solution at a rate which is proportional to its initial percentage in the WF. As the WF is dissolved, the species go into solution, but any excess concentrations (above the solubility limit) are immediately precipitated. In the case of the glass WF, these species will typically be incorporated directly into the altered phase which is formed from the immediate precipitation of most of the non-soluble components of the glass.

The intention is ultimately to model the potential for separation of neutron absorber from fissile material in the WP. However, the present simple model bookkeeping lumps all the dissolution products remaining in the WP (at any given time) together into what is called the dissolution product mixture. This dissolution product mixture also includes a relatively small fraction which is actually in solution and thereby available for removal from the WP by water transport. Except for the relatively small fraction which is actually in solution, the dissolution product mixture serves as a surrogate for the several precipitated phases, and is considered to be available for inclusion in these precipitated phases as part of the sample configurations described in Section 6. The amount of each dissolution product species actually in solution is approximated by the solubility limit of that species. This approximation is accurate to within 10%, since, for the WFs used in this study, the dissolution rate is more than 10 times faster than the removal rate.

The mass balance equations model the following processes:

- Decay of ^{239}Pu to ^{235}U
- Dissolution of the WF, permitting the fissile and neutron absorbing species to go into solution

PREDECISIONAL DOCUMENT

- Dissolution of stainless steel (SS), releasing chromium (Cr) oxidized to chromate which lowers the pH and increases the Gd solubility
- Removal of the solution containing (at various concentrations) the species of interest.

The governing mass balance equations are listed below. In the following equations, the WF is designated as glass, but the equations can be applied equally to the ceramic WF. The dissolution product mixture remaining in the WP is designated by dpm. This dpm is described as a clayey material in Section 5.3, and the specific compositions assumed for this study are given in Sections 5.4.5 and 5.5.2, Tables 5.4.5-1 and 5.5.2-1 for the glass and ceramic WFs, respectively. The quantities max U, max Pu, and max Gd are the solubility limit maximums which approximate the amounts actually in solution as described in the previous paragraph.

$$d(\text{U in dpm})/(dt) = + (\text{U fraction in glass}) \times (\text{glass dissolution rate}) + .693 (\text{Pu in dpm})/24100 - (\text{volumetric flow rate}) \times (\text{max U})$$

$$d(\text{U in glass})/(dt) = + .693 (\text{Pu in glass})/24100 - (\text{U fraction in glass}) \times (\text{glass dissolution rate})$$

$$d(\text{Pu in dpm})/(dt) = + (\text{Pu fraction in glass}) \times (\text{glass dissolution rate}) - .693 (\text{Pu in dpm})/24100 - (\text{volumetric flow rate}) \times (\text{max Pu})$$

$$d(\text{Pu in glass})/(dt) = - .693 (\text{Pu in glass})/24100 - (\text{Pu fraction in glass}) \times (\text{glass dissolution rate})$$

$$d(\text{Gd in dpm})/(dt) = (\text{Gd fraction in glass}) \times (\text{glass dissolution rate}) - (\text{volumetric flow rate}) \times (\text{max Gd}),$$

$$d(\text{Gd in glass})/(dt) = - (\text{Gd fraction in glass}) \times (\text{glass dissolution rate})$$

$$d(\text{Cr in SS})/(dt) = - (\text{Exposed SS surface area}) \times (\text{SS corrosion rate per unit area})$$

$$d(\text{Cr in solution})/(dt) = -d(\text{Cr in SS})/(dt) - (\text{volumetric flow rate}) \times (\text{Cr in solution})$$

The computer code to implement these differential equations in finite difference algorithms is given in Appendix B. In the present approximation the dissolution rate is adjusted for the decreasing surface area as the initial WF is degraded.

The initial quantity of ²³⁵U is taken to be zero, and the initial quantity of ²³⁹Pu is taken to be 93% of the total weapons grade Pu contained in the WF. However, the program does set a time for the start of WF dissolution which is at least several thousand years to account for the time required to breach the WP and the stainless steel canister and can containing the WF. During this time a significant fraction of the ²³⁹Pu will decay into U, and this conversion is counted in the calculation.

3.2.2 Chemistry Calculations (EQ3/6) in Support of Mass Balance

The following types of analyses are used in support of the scenario generation mass balance calculations:

- A succession of quasi-equilibrium states, or reaction path modeling, using EQ3/6, tracing the degradation/dissolution of the WF and other components of the WP
- Verification of solubilities by EQ3/6 equilibrium calculations focused on a limited number of species that scoping computations indicate to be present in significant quantity over a range of pH conditions.

To overcome various limitations of the computer code and its associated database, simple theoretical plots of solubility against pH were made and compared to EQ3/6 computer calculations at selected pH values. These calculations were performed where possible for low total concentrations of total dissolved species from the point of view that, after an initial period of high concentrations resulting from the relatively rapid degradation of DHLW filler glass, the WP and its contents will be largely flushed of highly soluble salts. This is because most of the filler glass degrades before the WP can be completely flushed by the slow groundwater infiltration.

The primary purpose of the chemistry calculations is to determine whether conditions for high Gd solubility and low U and Pu solubility can exist for a sufficient amount of time, while the WF glass or ceramic is degrading, to permit the precipitation of U and Pu (presumably in a clayey mass at the bottom of the WP) while the Gd is flushed away. Such a clayey mass without significant neutron absorber would be the most likely configuration to cause criticality. The results of the chemical analyses described in Section 5, indicate that such conditions can occur if the WF degrades faster than the stainless steel, and the infiltration rate is within the likely range of 0.1 to 10 mm/yr.

3.3 REPOSITORY ENVIRONMENT AND OTHER PARAMETERS

It is assumed that the geologic repository is an unsaturated site, in an arid climate, exposed to an oxidizing atmosphere. The available repository environmental parameters from the site characterization efforts at Yucca Mountain are used. The principal parameters are given in Appendix A. Values of parameters of repository environment and WF performance used to generate the specific scenarios of this document are given in Section 5.

4. INPUT DATA VALUES

The tables in this section provide a possible range of input parameter values. This range is based on data available in the literature and the results of some experimental efforts currently underway. Because specific data for Pu loaded glass and ceramic matrices under repository environmental conditions is not available, this range represents a basis for sensitivity analysis. The dissolution rates are applicable to the either glass or ceramic WFs, as indicated. The other parameters are applicable to both the glass and ceramic WFs.

A more detailed description of all the environmental parameters is given in Appendix A.

4.1 DISSOLUTION RATES

The WF glass dissolution rates are based on limited Performance Confirmation Testing performed by Bates, primarily on ATS glass (Reference 13). Preliminary test results on Loeffler glass, which is representative of three possible glass dissolution stages, indicate that the glass remains in the stage with the slowest dissolution rate for at least a year, which leads to the low end of the range of dissolution rates in Table 4.1-1. The Pu and Gd appear to remain in the reacted (altered) glass layer, without apparent segregation. Only a thin clay layer is expected to form during the test. However, the layer may thicken with time.

Table 4.1-1. Dissolution Rates

Material	Max (g/m ² /day)	Min (g/m ² /day)
DHLW glass (filler)*	3.7x10 ⁻³ (at 66°C)	1.5x10 ⁻⁴ (at 26°C)
ATS **	1.3x10 ⁻³	8x10 ⁻⁴
Ceramic (Synroc-C)†	10 ⁻⁴	10 ⁻⁷

* From formula developed by Bourcier and reported in TSPA-95 (Reference 3), evaluated at pH=7. Review of experimental data by M.J. Plodinec has suggested a range of 0.1 to 0.0001 (Reference 14). However, this reference suggests that the high end of this range may be too conservative because it is based on a 28 day test which included a significant amount of the high dissolution rate stage I (which typically lasts only 7 days).

** Inferred from Bates (Reference 13); the range of values is expected to cover the La-BS glass, for which the actual experimental data should be available by 8/97.

† Reference 4, reviewed by R. Van Konynenburg

The actual dissolution rates, in mass per unit time, are determined by multiplying the appropriate dissolution rate per unit area, from the above table, by the WF surface area. For this purpose, it should be noted that both ceramic and glass have their surface area enhanced by extensive internal fracturing. In glass this fracturing arises directly from differential stresses acquired during the cooling from the melt. In ceramic the fracturing arises over 1000 years from the differential radiation induced expansion, principally between the major crystal type, zirconolite, and the minor types pyrochlore and hollandite. The present ceramic optimization effort on behalf of this program will include the minimization of the amount of pyrochlore and/or minimizing the grain size to minimize this effect. The range of values used are given in Table 4.1-2.

Table 4.1-2. Surface Area Multiplication Factor for Internal Fracturing

Material type	Max	Min
DHLW glass (filler)	100	30
ATS, La-borosilicate	30	6
Ceramic (Synroc-C)	15,000*	1

*Represents extreme metamictization.

The outer glass surface area for each can is approximately 0.194 m² (a cylinder with length equal to 85% of the can inside length, and diameter equal to the inner diameter of the can). For the WF sizes and WP loading specified in this document, the external surface area is approximately 15.5 m² per WP, so the total surface area exposed to dissolution is 1550 m².

It should be noted that need for the dissolving water to traverse the filler glass may have some retarding effect on the dissolution rate of the Pu glass. However, it is expected that the filler glass will dissolve at least 10 times faster than the Pu-glass so any such protection could only delay the Pu-glass dissolution by less than 10%. Furthermore, the internal fracturing of the DHLW glass permits rapid penetration by water. For these reasons, and for conservatism, the relatively minor delay due to the protection provided by filler glass is neglected.

Information on the dissolution rate of 304L stainless steel and Alloy 625 is also necessary for purposes of later estimating the amount of Cr in solution as a result of the corrosion of the canisters and the WP inner barrier. Several researchers have investigated the general corrosion rates of 304L stainless steel in a J-13 well water environment at various temperatures and test durations. Table 4.1-3 below summarizes the results of these corrosion tests covering the expected temperature range at the time of WP breach. Considering the fact that these are very short term tests compared with the time scales considered in this analysis, and that the general corrosion rate of stainless steel typically decreases with time due to formation of a protective passive film, a general corrosion rate of 0.1-0.2 μm/yr should provide conservative results for the dissolution of the stainless steel canisters.

Table 4.1-3. 304L Stainless Steel General Corrosion Rates in J-13 Well Water

Test Duration (hours)	Test Temp(s) (°C)	Corrosion Rate (μm/yr)	Reference
10-11k	50-100	0.07-0.13	16, p. 24
3.5-5k	50-100	0.03-0.23	15, p. 64
8.8k	28	0.08-0.28	15, p. 28
1k	100	0.25	15, p. 28
0-1k	90	0.08-0.37	17, p. 108
1-2k	90	0.04-0.07	17, p. 108
0-2k	90	0.02-0.14	18, p. 35

As Alloy 625 has only recently been adopted as the inner barrier material for the WP, corrosion data in repository representative environments is not yet available. However, data is available for corrosion of Alloy 625 in sea water, which is a more corrosive environment than J-13 well water. Reference 19 (p.12) indicates that a sample with a surface area of 671 cm² lost only 20 mg during a 365 day immersion in quiet sea water. Using the Alloy 625 density of 8.44 g/cm³ this translates to a corrosion rate of only 0.0035 $\mu\text{m}/\text{yr}$. In comparison, Reference 20 indicates that 304L stainless steel had a corrosion rate of 13.5 $\mu\text{m}/\text{yr}$ during a comparable exposure to sea water, which is at least 2 orders of magnitude higher than its corrosion rate in J-13 well water. Assuming that this difference applies equally to Alloy 625, and considering the fact that the inner barrier surface area exposed is much less than that of the stainless steel, it appears that Alloy 625 corrosion will supply a negligible amount of Cr compared to the stainless steel.

4.2 SOLUBILITY

The following solubility limits (see Table 4.2-1) have been derived from a number of sources, as indicated in the notes. In particular, some of them have been inferred from the extrapolation of time dependent experimental data, as indicated in the notes.

Table 4.2-1. Solubility

Species	Max (ppm, or g/m ³)	Min (ppm, or g/m ³)
Pu ⁽¹⁾	2.4 ⁽⁵⁾	2.4x10 ⁻³
U ⁽¹⁾	2400 ⁽⁶⁾	2.4x10 ⁻³
Gd ⁽²⁾	16 ⁽⁴⁾	0.01
Eu ⁽²⁾	15 ⁽⁷⁾	.015
B	10 ⁴	unknown
Fe ⁽⁴⁾	450	4.5

(1) References 3 and 10.

(2) Inferred from Bates' reports of experimental observations, at neutral pH (Reference 13). It should be noted that recent, but limited, data from ASTO (Reference 3) indicates that Gd appears to dissolve about two orders of magnitude faster than Pu, although these rates are very low. This may be related to the locations of the Gd and Pu within the ceramic phases. This should be studied as part of the ceramic evaluation effort at ANL.

(3) Reference 10.

(4) Literature review.

(5) For pH<5, very low oxygen, and assuming that the precipitation of Pu is kinetically inhibited; a more representative maximum would be 0.024 ppm.

(6) For very low silica only; a more representative maximum would be 2.4 ppm.

(7) For pH<5 only, a more representative maximum would be 0.15 ppm.

(8) Since this value is for neutral pH, it is much smaller than the upper limit of the range of values estimated for pH=5.5 discussed in Section 5.3.4, and indicated in Table 5.3.4-1.

4.3 ENVIRONMENTAL PARAMETERS

Table 4.3-1 is a summary of the range of the environmental parameters which are directly used in the EQ3/6 calculations and the mass balance calculations. These ranges are typical of those which would be expected in a nuclear repository containing 63,000 MTU of commercial spent nuclear fuel situated in an environment like Yucca Mountain. The numbers are consistent with those used in TSPA-95 (Reference 3). Details are given in Appendix A, and in TSPA-95.

Table 4.3-1. Environmental Parameters

Parameter	Max	Min
Temperature (°C)	68 (5,000 yrs)	26 (100,000 yrs)
Infiltration (mm/yr)	10	0.1
pH	7.4	6.9
Partial Pressure CO ₂	10 ^{-2.8} bar	10 ^{-4.8} bar
Dissolved O ₂ (mg/liter)	5.7	2 (uncertain)
Silica (mg/liter)	64.3	57

5. SCENARIO CONCEPTS FOR WF DEGRADATION AND SUBSEQUENT PROCESSES

A systemic view of the processes that can lead to potentially critical configurations for Pu immobilized in glass is given in Figure 5-1. The individual processes are represented by boxes, which also represent yes/no points with respect to the outcomes of the processes. The processes and outcomes are arranged in horizontal layers by process type, with a brief identification of each type at the left side of the chart. This horizontal layering roughly corresponds to the flow of time from top to bottom of the chart. Each box is numbered, to serve as reference for the individual scenarios described below. The paths leading to the bottom of the chart represent scenarios which have the potential for criticality, while paths leading to the right of the chart represent scenarios which can not produce any criticality. It should be noted that boxes 13, 15, and 17 deal with the possibility of unmoderated criticality. These possibilities have not yet been analyzed; it is expected that the probability of collecting the necessary critical mass will be very small, and the risk of unmoderated criticality will be much smaller than the risk of moderated criticality.

The system perspective of Figure 5-1 is used to ensure that all credible possibilities have been considered and to identify the most likely of these to be characterized by the sequence of physical and chemical processes. These perspectives are shown in Figures 5-2 and 5-3 for the physical and chemical processes, respectively. The details of these processes are described below.

5.1 PHYSICAL SCENARIOS FOR GLASS WF DEGRADATION

The physical processes involved in the degradation of glass WFs and subsequent material movements are shown in Figure 5-2. In this chart time flow is generally from the top down. All scenarios begin with infiltration of water incident on the WP followed by water penetration of the barriers, water penetration of the stainless steel canister containing the waste cans, water penetrating the filler glass, water penetrating the can directly containing the WF, and water contacting the surfaces of the WF beginning the WF alteration process. This wetting of the interior surfaces immediately following the breach of the surrounding barrier is a conservative assumption, because the fractures defining many of these surfaces will have such narrow apertures that fresh water cannot access them sufficiently fast to maintain the dissolution rate.

These processes are indicated by the first five blocks on Figure 5-2. Following these initial degradation processes the WP and its contents can be represented by the sketch in Figure 5.1-1. The short line segments in the filler glass represent fractures which can provide rapid penetration paths to the interior of the WF.

Following these initial degradation steps, any wetted surfaces of the glass will continue to degrade. The scenarios then proceed along three parallel paths, as shown in Figure 5-3. These scenarios are characterized by differing locations of holes in the WP and resulting differing flow regimes within the WP. Glass degradation proceeds through two alteration layers:

- A thin inner "gel" layer containing insoluble species from the degraded glass waste
- An outer, "altered," layer containing precipitated clays and similar minerals.

The altered layer may serve as a focus for re-precipitation, particularly at the bottom of the package.

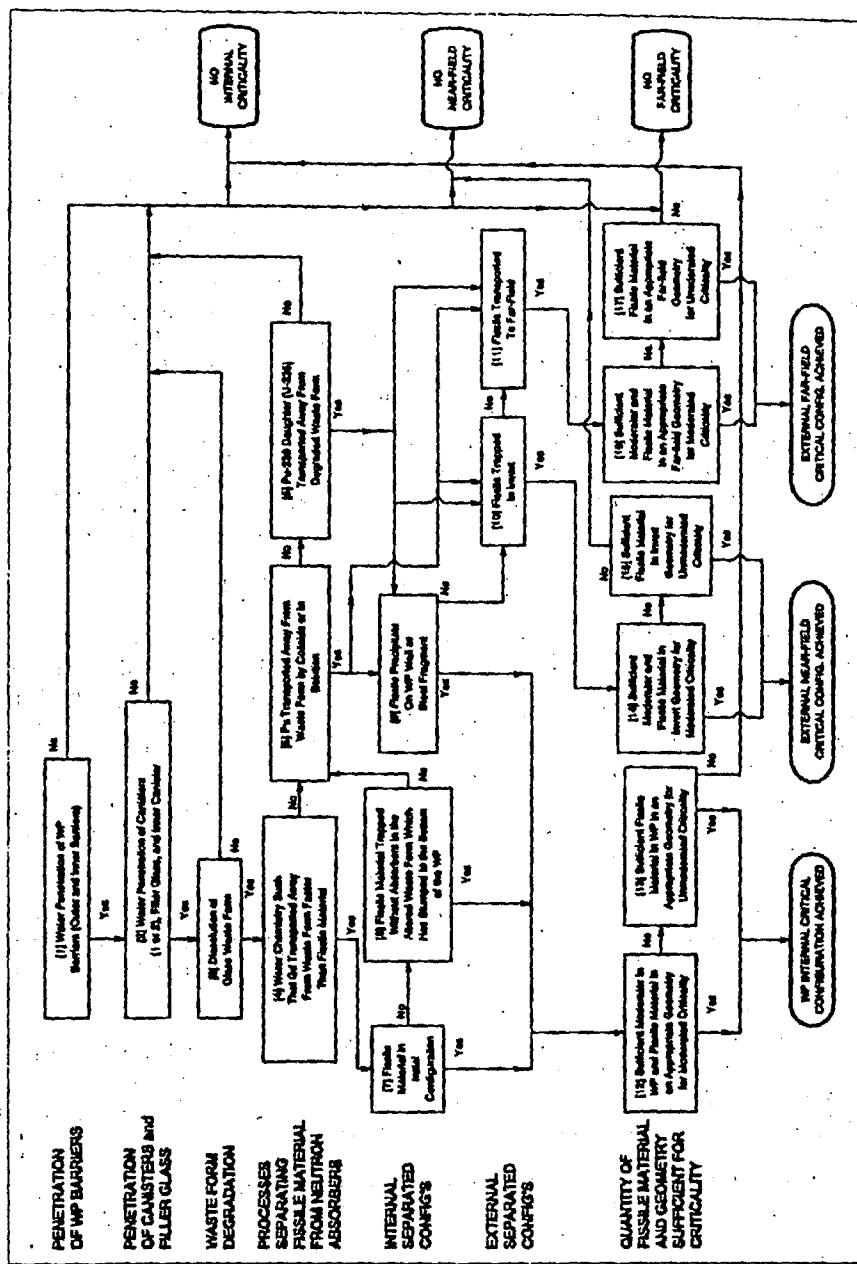


Figure 5-1. System Perspective of Event/Process Sequences for the Degradation of Pu Immobilized in Glass and Subsequent Material Movements

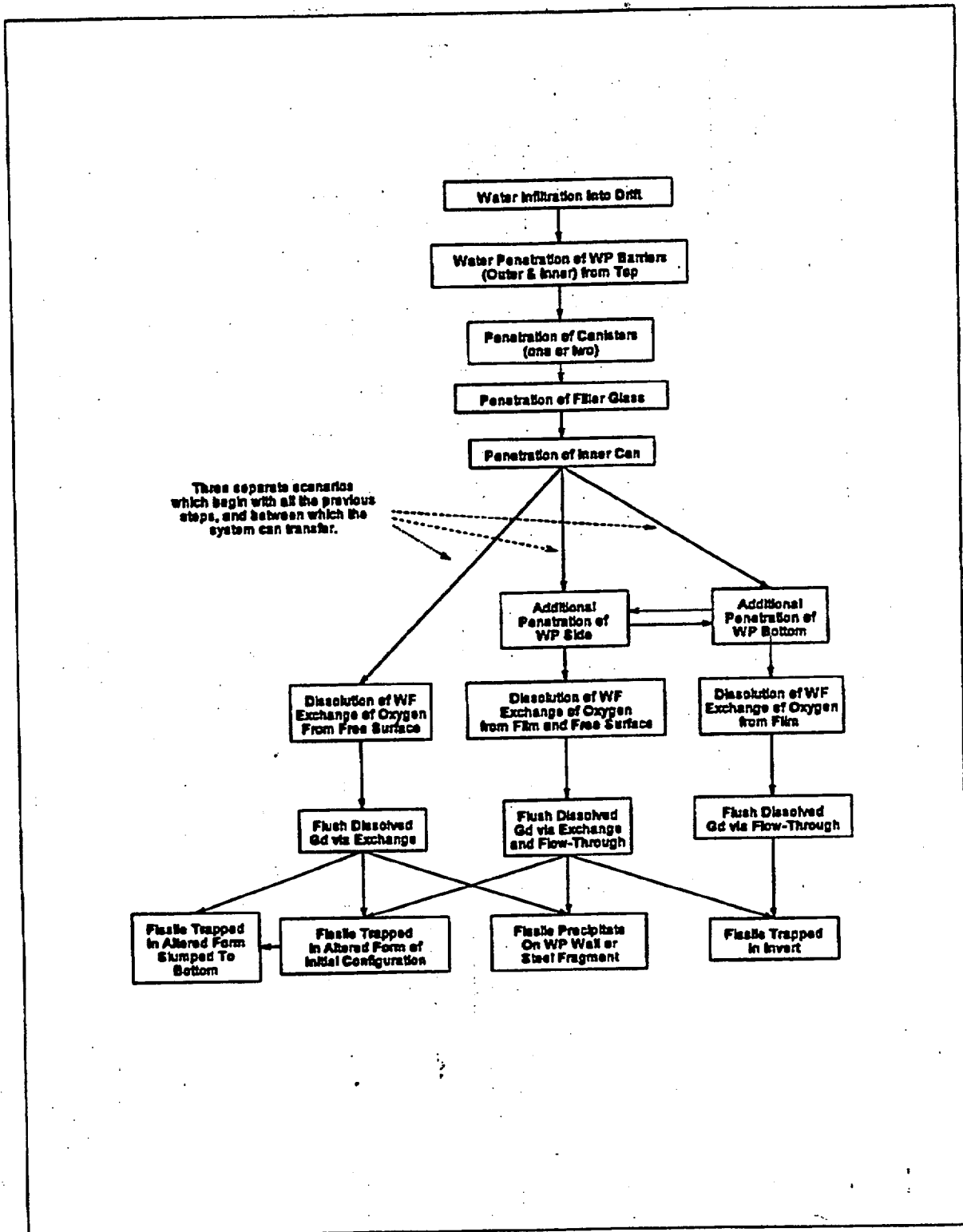


Figure 5-2. Physical Perspective of Event/Process Sequences for the Degradation of Pu Immobilized in Glass and Subsequent Material Movements

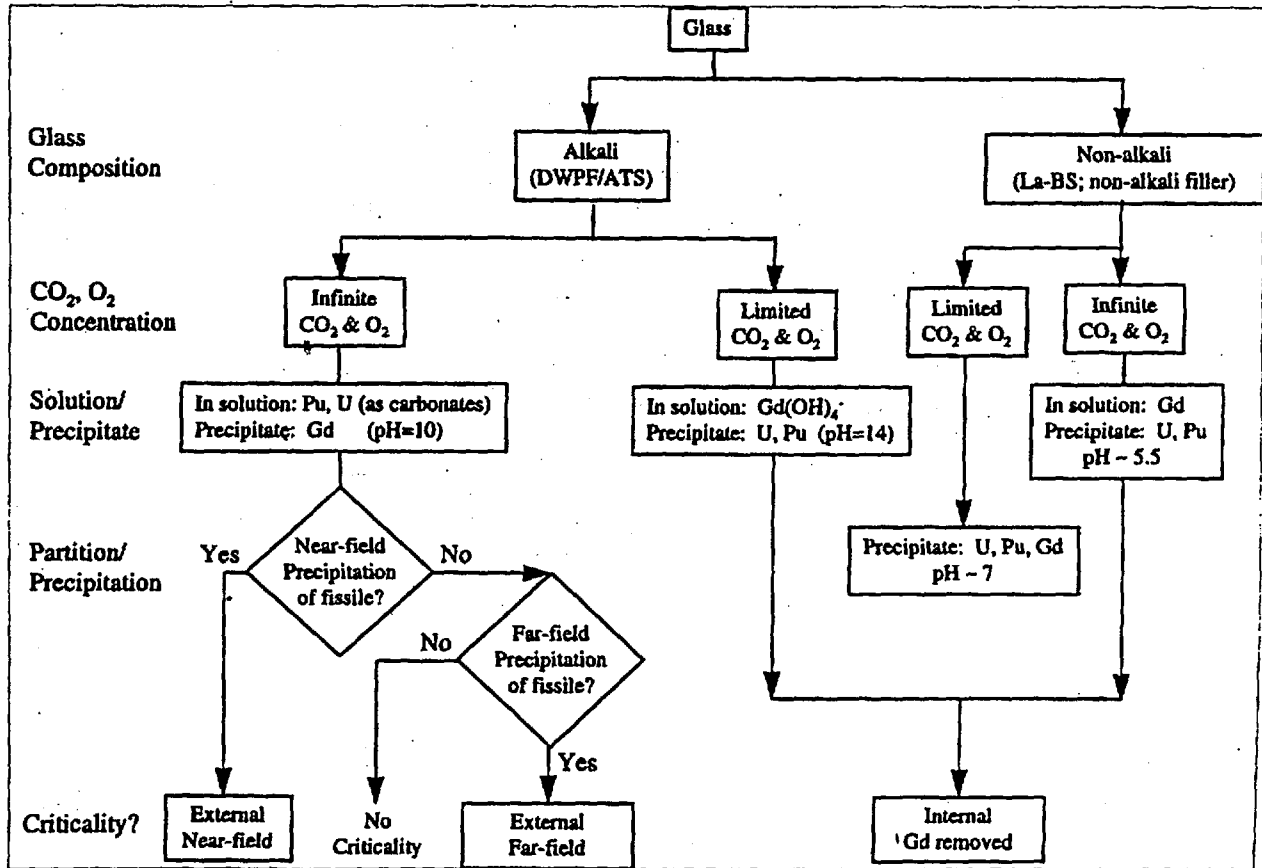


Figure 5-3. Chemistry Perspective of Process Sequences for the Degradation of Pu Immobilized in Glass and Subsequent Material Movements

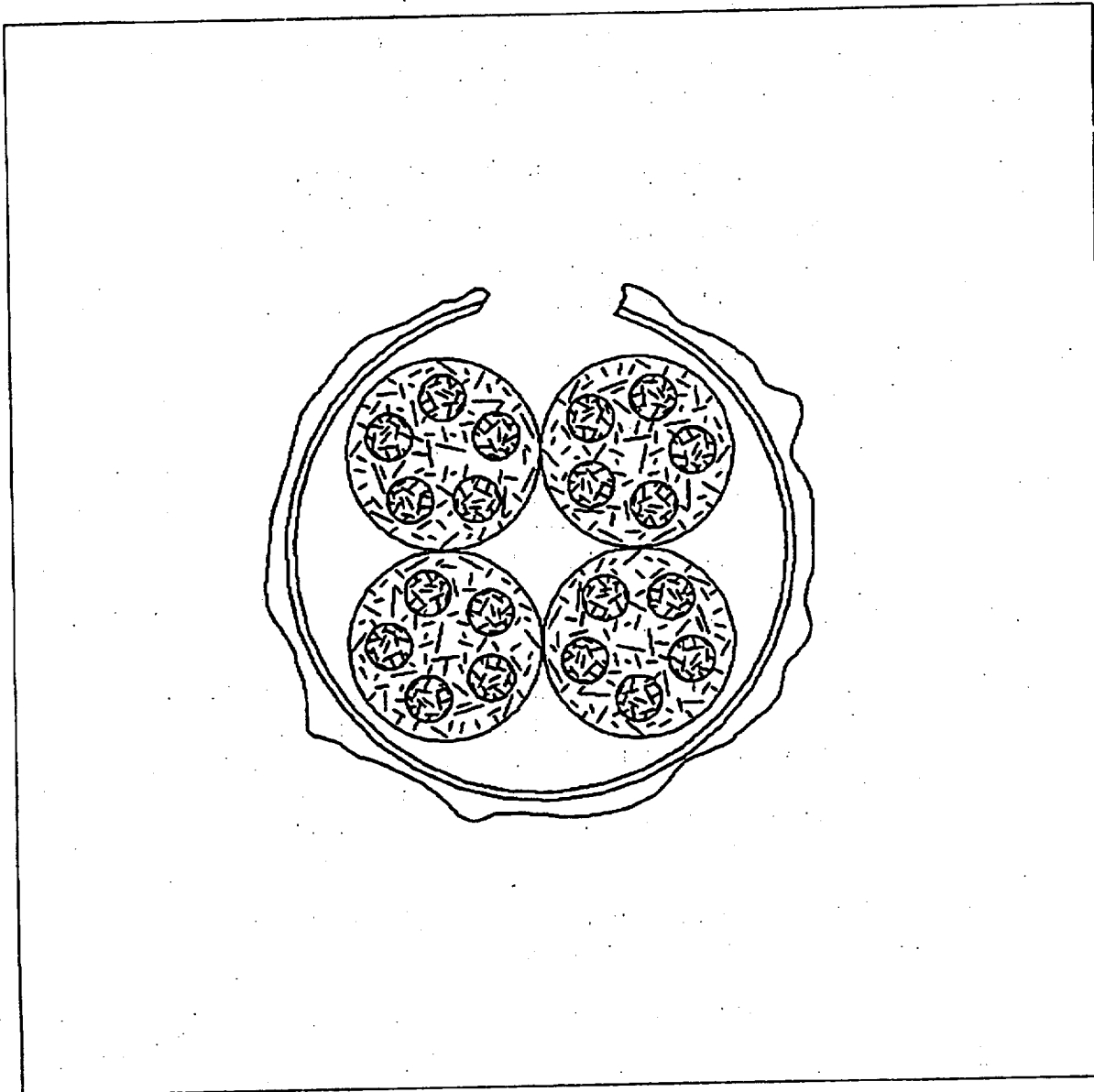


Figure 5.1-1. Degraded Barriers, Degraded Canisters, Glass Fractures

The following explanations will be helpful in understanding the physical processes represented by Figure 5-2:

The three boxes having text starting with, "Dissolution of WF," deal with the method of exchange which transfers oxygen and carbon dioxide from the air to the degrading surface of the WF. These exchange methods are of two types:

- Exchange of oxygen and carbon dioxide from the free surface, which results when the water is standing to some depth in the WP. The free surface (upper) of the water is the only

PREDECISIONAL DOCUMENT

boundary through which oxygen and carbon dioxide can pass, and these gases are transported to the dissolving surface by circulation, which is driven by the buoyant convection of the water heated by the still radioactive WF.

- Exchange of oxygen and carbon dioxide from a film surface, which results when the water is flowing through the WP and reacts with the WF as a thin film. The dissolved gases are transferred from the outer film surface to the WF surface by diffusion. Although the circulation exchange from the free surface is a more efficient process, the diffusion through the film can be very effective because of the short distance involved.

The three boxes having text starting with, "Flush dissolved Gd," deal with the method of removing Gd from the WP. These removal mechanisms are of two types:

- Flow-through flushing in which the removal rate of a species is the product of the flow rate multiplied by the maximum concentration of the species in solution (solubility limit). This mechanism assumes that there is sufficient penetration in the lower portion of the waste package that the water flows through the package. It further assumes that all the water flowing through the WP is sufficiently mixed that it carries the maximum concentration of each species dissolved from the WF.
- Exchange flushing of dissolved material occurs when the lower portion of the package is not penetrated, so that most of the package is filled with water, and a major fraction of the water incident on the WP will flow around the package only picking up dissolved species by physical mixing across the free surface boundary. In this situation the removal rate of all the species is reduced (in comparison with the flow-through flushing) by an exchange factor representing this mixing.

The three scenarios in Figure 5-2 lead to four final configurations, indicated by the four boxes at the bottom. These four configurations are described as follows:

- Fissile material trapped in the altered form with the altered form in its initial geometry; it is expected that this final configuration can be reached only from the breached-top-only scenario because it requires very slow removal rates. This configuration can only arise if the canisters and cans retain their structural integrity, while degrading sufficiently to permit extensive water infiltration.
- Fissile material trapped in the altered form with the altered form slumped to the bottom of the WP in an cylinder segment geometry. It is expected that this configuration can be reached from any scenario, except the bottom breach.
- Fissile material precipitated on a metal surface (WP wall or stainless steel canister fragment) with a very thin slab or disk geometry. It is expected that this configuration can be reached from any scenario, except the bottom breach. There is experimental evidence for more precipitation of analogs of Pu than precipitation of Gd on metal test vessel walls in PCT dissolution tests. Typically, the concentration of Gd in the acidic solution which leaches from the vessel walls will be up to 2 times larger than the concentration in the solution

within the vessel. In contrast, the concentration of an analog of Pu, like cerium, will be 10 times larger in the acidic wall leach than in the solution within the vessel. As discussed in Section 3.1.2, the criticality potential of such selective precipitation is limited by low thickness and potential for re-dissolution.

- **Fissile material trapped in the invert.** A possible mechanism leading to UO_2 precipitation in the invert could be a reduction in the amount of dissolved oxygen, and this less oxidizing environment would cause the U to reduce from the hexavalent to the quadrivalent state, and consequently precipitate. In contrast, the Pu will simply precipitate as soon as it can, so there is more likelihood of precipitation of Pu in the WP before it can reach the invert. Another factor enhancing the rapid precipitation of Pu in the invert is the fact that the colloidal concentration of Pu is likely to be much greater than the Pu which is truly in solution. Pu colloids would likely be filtered out of the water by crushed rock in the invert, or by narrow fractures in the rock below. Yet another possible mechanism for concentration of fissile material in the invert is adsorption onto either zeolites in tuff or degraded concrete or Fe_2O_3 , which could come from the corrosion/oxidation of iron containing metal in the WP barrier or from the corrosion of iron containing WP basked metal.

5.1.1 Breached-Top-Only Scenario, Circulation Flushing Only

Basis

In this scenario only the top of the WP is breached, and the bottom remains unbreached for some long period of time, so that the package remains filled with water (to provide moderation for the criticality) while the WF slowly degrades. Simple flow calculations show that this slow circulation flushing can be supported by infiltration rate between 1 mm/yr and 10 mm/yr. This scenario is possible because of the strong temperature dependence which is expected for the corrosion rate of Alloy 825 or 625 (provided by expert elicitation). The implication of this strong temperature dependence is that there may be some significant probability of penetration of the inner barrier while the WP surface temperature remains above 70°C, but after 10,000 years the WP will have cooled sufficiently that the WP surface temperature will have dropped below 50°C, and the corrosion rate becomes very slow. Calculations with typical parameter values in this model indicate that following initial penetration of the top, penetration of the bottom could take up to 1 million years.

Alteration of WF Process

As long as the WF retains enough decay heat there will be circulation of the water within the WP with cycle times less than a day. Therefore, the dissolving surfaces will be contacted by the water containing sufficient oxygen to maintain the dissolution process (which includes the oxidation of any U decay product of the Pu) of the glass WF. Maintenance of this oxygen in solution may be partly supported by capturing oxygen at the free air-water interface. Oxygen supply (or some other electron acceptor) is important for converting quadrivalent U to hexavalent form, which makes it much more soluble.

Flush/Removal Process

The rate of removal of fissile material and neutron absorbers is primarily determined by the flow rate incident upon the WP, the internal circulation of the water within the WP, the water chemistry (including pH, thermodynamic equilibrium constants, and dissolution rate parameters) which determine the glass alteration rate and solubility of the neutron absorber material, and the exchange of internal and external flows through the holes in the top of the WP.

Final Configuration: Wall Precipitation

Fissile material and the neutron absorbers may be dissolved and re-precipitated on the WP walls as thin mineral deposits. A criticality might occur if much of the fissile material re-precipitates inside the WP while nearly all the neutron absorber remains in solution long enough to be flushed out. Whether such a separation occurs will depend on the basic chemistry and thermodynamic parameters for the fissile and neutron absorbing materials, particularly as expressed in the ratio of solubilities of the neutron absorbers to the solubility of the fissile material. The absolute values of these solubilities are important for determining how much Pu might be left in the WP when the separation occurs. These solubilities are estimated from EQ3/6 calculation results, as described in Section 5.3 and Appendix C. As discussed in Sections 3.1.2, and 5.1, the criticality potential of such selective precipitation is limited by low thickness and potential for re-dissolution.

The quantity of Pu likely to be precipitated may be increased by any pure PuO₂ inclusions in the original WF glass, as is discussed in Section 2.1.2. This configuration is reached by the sequence 1-2-3-4-5-9-12 in Figure 5-1.

Final Configuration: Altered WF in the Initial Geometry

This configuration is expected to have such low probability as to be insignificant. It is discussed briefly here, for the sake of completeness. Furthermore, prior calculations (Reference 2) of k_{eff} have shown this configuration to be the most reactive with respect to criticality, so it may be considered as the worst case.

In this configuration most of the completely altered WF retains its initial geometry. If it is to be critical nearly all the Gd would have to be dissolved and eventually flushed out of the WP; EQ3/6 calculations have indicated that, at pH<4.5 Gd will have significantly higher solubility than U or Pu, but that the solubility is still so low that the Gd cannot be removed from the package in less than 300,000 years.

This configuration is reached by the sequence 1-2-3-4-7-12 in Figure 5-1. If this configuration exists at all, it is expected to be unique to the very low flushing rate of the breached top only scenario.

Final Configuration

Altered WF in Collapsed (Cylinder Segment) Geometry—Fissile material and the neutron absorbers may be dissolved and re-precipitated as part of a pile of altered glass at the bottom of the WP. This configuration is reached by the sequence 1-2-3-4-7-8-12 in Figure 5-1. The collapsed

mass at the bottom of the WP would be expected to have something like an hemicylinder (cylinder segment) shape. The material will be a clay-like mass of silica/silicate and water with some concentration of the fissile and neutron absorber oxides. Because the package is filled with water, the water concentration in the collapsed mass could be as high as 60%, with the remaining 40% being silica and other species (the composition of which will be determined by EQ3/6 calculations).

As a final generalization on the contents of the collapsed altered form, it should be noted that as glass reacts, Pu tends to precipitate as PuO_2 or an hydroxide phase and is retained in the smectite clay phase, likely as colloids, or on metal surfaces. Gd also appears to associate itself with the clay phase. The degree of Pu and Gd segregation outside of the clay phase is unknown.

5.1.2 Breached-Top-and-Side Scenario, Both Flow-Through and Circulation Flushing

Basis

For this scenario the WP will fill only partly, because the water can flow out the holes in the side. Such outflowing holes will establish a water level within the WP, and it is likely that some of the WF canisters will be above and some canisters will be below the water level. Although the holes in the top may be the most likely (because they are the most strongly gravity driven), holes in the side are the next most likely, because the outside will receive most of the film of water from dripping on to the top of the package, while the inside is exposed to a rising and lowering the level of water (resulting from variations in the infiltration rate; e.g., seasonal cycling) trapped inside the package. Intermittent wetting and drying is known to be the most stressing aqueous corrosion condition. Whether the intermittent drying actually occurs will depend on whether the dryout time is long enough and the humidity is low enough to fully dry the temporarily exposed surface.

In this scenario, the exchange between the solution inside the WP and the outside dripping flow will be more rapid than for the breached-top-only scenario, because there is larger surface area for penetration by the fresh infiltrating water. The consequence is that there will be more rapid removal of solubility limited species, as is explained further below.

Alteration of WF

The WFs (canisters) which are below the water level will be altered at a rate similar to that in the breached-top-only scenario. The WFs above the water level are altered by a film of water which is continuously moving and continuously re-supplied with oxygen, so the alteration process may be faster than for the breached-top-only scenario.

Flush/Removal

The WFs which are below the water level in the WP will be flushed by circulation and exchange at a rate similar to that for the breached-top-only scenario. The WFs above the water level will be flushed by a film of water which is continuously moving so the removal process will be much faster than for the breached-top-only scenario. Those WFs above the water level cannot contribute to any criticality so the possibility of criticality in the initial geometry becomes remote. However, the accelerated alteration of the WFs above the water level will increase the probability of achieving one

of the other potentially critical final configurations (altered collapsed, precipitated on wall of metal surface, precipitated/trapped in the invert).

Final Configuration

Altered WF Collapsed Geometry—As with the collapsed geometry configuration discussed in Section 5.1.1, this configuration is reached by the sequence 1-2-3-4-7-8-12 in Figure 5-1. This is the most likely configuration resulting from the general scenario of this section; it is characterized by the glass WFs collapsed, or re-precipitated at the bottom of the WP. Such a configuration would be expected to have an ellipsoidal shape, 20% water (less than the breached-top-only scenario because the package can be only partly filled with water since there are holes in the side of the package), 80% silica/silicate.

Final Configuration

Precipitation of Fissile Material on Metal Surface: (Thin Slab Geometry)—As with the metal surface precipitation geometry configuration discussed in Section 5.1.1, this configuration is reached by the sequence 1-2-3-4-5-9-12 in Figure 5-1. Since the exchange with the outside fluid is much faster than the breached-top-only scenario, it is possible that much of the glass silica can be removed from the WP, leaving a significant amount of U precipitating on the package wall, more in the form of a metal or oxide deposit, rather than embedded in silicates. The likelihood of this alternative is determined by the chemical/thermodynamic parameters which reflect partitioning among degraded/precipitated phases. In addition, as shown above, the pitting corrosion of the WP inner barrier may supply a significant amount of iron, as in the breached-top-only scenario. The resulting geometric configuration could be a thin slab, 50% water.

Final Configuration

Fissile Material Trapped in the Invert: (Near-field External Criticality)—This configuration is reached by both the sequences 1-2-3-4-5-10-14 or 1-2-3-4-5-6-10-14 in Figure 5-1. The external criticality for the breached-top-and-side scenario will be somewhat more likely than for the breached-top-only scenario, since the removal of fissile material is significantly faster. However, the near-field criticality will still be dominated by the breached bottom scenario, and will therefore be described below.

5.1.3 Breached-Top-and-Bottom Scenario, Flushing by Flow-through

Basis

This scenario would have a volumetric flow through the WP at rates up to a maximum of 40 liters per year (corresponding to an infiltration rate=10 mm/yr). This is estimated by multiplying the 0.001 meters per year infiltration rate by the inside cross-section area of the package along the axis, 4 square meters. This volumetric flow could be increased by groundwater focusing due to fractures or other means of permeability enhancement, which could produce up to 4000 liters per year from a focusing factor of 100. No concentration factor is used in this study because a very conservative assumption has already been made with regard to effectiveness of water in removing WF dissolution

PREDECISIONAL DOCUMENT

products: all the water flowing through the WP will contact the dissolving surfaces, or will mix completely with water that has such contact. This assumption is realistic for a WP partly filled with water, but it is very conservative for this much more rapid flushing by flow-through.

Alteration of WF

In this scenario all the WFs are altered by a film of water which is continuously moving and continuously re-supplied with oxygen. In general, this film will move faster and have more dissolved oxygen than either of the other (first two) scenarios. The metal corrosion rate is proportional to the dissolved oxygen concentration over some range of this concentration so this parameter may be important for determining the rate of penetration of the steel canister and can. The glass dissolution rate is relatively independent of oxygen concentration in the solution.

Flush/Removal

The water film is also the primary flushing agent; since it is continuously moving, the removal process will be much faster than for the breached-top-only scenario. This is because the other two scenarios will have most, or much, of the water flowing by the WP without contacting the WFs.

Final Configuration, Altered WF in Collapsed (Ellipsoidal) Geometry

Internal criticality is less likely with a breached top and bottom because any dissolved fissile species would be more likely to be flushed out of the WP. Ordinarily, the absence of a distinct pool of water (such as is contained for the other two scenarios) will preclude the possibility of criticality. However, criticality in this configuration is a possibility if the altered form slumps to the WP bottom as a moist clay. Since the clay can act as a sponge, it may retain a considerable water concentration, even though water continues to flow out of the WP through the holes in the bottom. If this configuration did occur, it would resemble the internal criticality configurations for the previous two degradation scenario alternatives. Because of its expected low probability, this configuration is not reached by any of the scenarios in either Figure 5-1 or Figure 5-2.

Final Configuration, Fissile Trapped in Invert

(External Criticality, Near-Field)—If the breached bottom scenario ends with the fissile material flowing out of the WP in solution, and if the U is re-concentrated by precipitating out of the resulting groundwater stream, a criticality could occur. A precipitation of fissile material could occur in the form of silicates or alkali silicates as the fissile bearing solution flows out of the WP and encounters a less moist environment and leaves an evaporative type deposit. EQ3/6 analysis indicates that the most likely minerals are soddyite or haiweeite. This configuration is reached by either of the sequences 1-2-3-4-5-6-10-14 or 1-2-3-4-5-6-10-14 in Figure 5-1.

If sufficient fissile material and very little neutron absorber were to precipitate in the invert, it would be likely to have a lower water concentration than the internal criticality configurations because of a lack of natural confinement for water, and lack of a clay formation to act as a sponge for water. For this reason this configuration is expected to have a very low probability, and has been assigned a low priority with respect to immediate analysis. It will, however, be evaluated in the near future.

Corrosion of the barrier steel could inhibit criticality in the near-field (invert) because significant amounts of low solubility Fe would precipitate in the same places as would be likely for U precipitation (if any). On the other hand, the presence of iron in solution could increase the precipitation of U, leaving the iron and U separated, which is the opposite of co-precipitation. Still another possibility is that the iron be present as Fe⁺⁺ (possible if the oxygen concentration is very low), which has a strong reducing capability, thereby facilitating the co-precipitation of Pu. EQ3/6 calculations indicate that this will be unlikely.

5.2 PHYSICAL SCENARIOS FOR CERAMIC WASTE FORM DEGRADATION

The data on the performance of ceramic WFs is very limited. A research and development program is currently underway at Lawrence Livermore National Laboratory (LLNL) to develop the physical characteristics and chemical constituents of the ceramic WF to meet the requirements for production, Pu loading, and long-term criticality. However, some information of interest exists in the literature on those ceramics which are candidates for nuclear waste immobilization. This information is summarized below, and serves as the basis of the degradation scenarios developed thus far.

Ceramic materials, especially oxides, are resistant to corrosive attack under a wide range of chemical environments. Pu can be accommodated in zirconolite, pyrochlore, monazite, and zircon. Most of the recent investigations have focused on the Synroc-C family of ceramics, which are a mixture of zirconolite, hollandite, and rutile. Pyrochlore may also be present. Pu releases from zirconolite are about 1×10^{-5} g/m²/day at 70°C to 90°C in deionized water at pH 7. However, zirconolite and other ceramics are susceptible to metamictization as a result of radiation damage. This damage can result in complete amorphization, microcracking, swelling, and decrepitation. The presence of pyrochlore and large grain size appears to enhance this process in Synroc-C. Leach rates can be enhanced by about 10-15 times due only to metamictization with essentially no change in surface area. However, if microcracking, swelling (up to about 6 volume percent) and decrepitation occur, the surface area can be enhanced by 15,000 times the original geometric surface area. These processes can be reduced by reducing the grain size and pyrochlore content. Zircon and monazite are also affected by radiation damage. The dissolution of natural zircon in bicarbonate solution at 87°C increased as a result of alpha damage amorphization by 100 times from 10^{-3} to 10^{-1} weight percent. Natural monazite suffers radiation damage as well, with leach rate increases of up to ten times. However, natural monazite is almost always found in the crystalline state because of its low temperature of recovery from radiation damage.

Metamict radiation damage transformation could occur on the order of a few thousand years following ceramic WF fabrication; this damage is primarily from atoms significantly displaced by recoiling nuclei from the ²³⁹Pu alpha decay to ²³⁵U. It should be noted that a similar radiation damage also occurs in glass, but is less significant in enhancing dissolution rate, because glass does not have a regular crystal structure to begin with, and the interior is already fractured from the initial fabrication process. The likelihood and extent of the metamict transformation from radiation damage in Synroc-C are proportional to the amount of pyrochlore contained in the ceramic and the fraction of the ceramic which contains large grains. The expected refinements in the ceramic technology may reduce the amount of pyrochlore and large grains to the point where the metamict transformation is insignificant.

Synroc-C ceramics dissolution products tend to form a very thin altered layer (much thinner than for glass dissolution). The composition of this thin layer has not been completely characterized with respect to the individual components, and this composition is likely to vary with water chemistry. The layer is probably depleted in CaO, leaving primarily Ti and Zr oxides. The Ti oxide layer is believed to be primarily responsible for the low dissolution rates characteristic of the Synroc-C family of ceramics. Since the ceramic WF dissolution goes through only this thin altered phase, there will be no analog for the two final glass WF configurations which contain primarily glass altered form. Otherwise, the ceramic scenarios resemble those for the glass WFs, except that the dissolution rate is expected to be much smaller, and its dependence on dissolved components (such as silica or H⁺) might be quite different.

The ceramic scenarios are based on the use of Gd as the long-term criticality control material. Recent test data by Jostens, et. al. (Reference 4) suggest that the Gd within the ceramic (Synroc-C) has a combined dissolution rate and/or solubility about one order of magnitude higher than the rest of the ceramic matrix and Pu, so it may be appropriate to use a less soluble material such as Hf as the principal criticality control neutron absorber. However, Hf is much more expensive than Gd, and Gd is a more efficient neutron absorber (particularly at thermal energies) so until more data are available, Gd remains the nominal choice. It is expected, however, that there will be some evaluation of the possibility of utilizing the Hf which is present in natural Zr (approximately 2% to 4.5%), thereby reducing the cost of Zr required for the zirconolite which is the major component of Synroc-C.

As with the glass WF scenarios, the ceramic WF scenarios begin with water incident on the WP followed by breach of the WP barriers and the canister containing the WF to permit the water to attack the ceramic surfaces (beginning at least 5000 years after emplacement). EQ3/6 analysis of the glass WF has indicated that the dissolution of the filler glass surrounding the ceramic cans inside the DHLW type canisters within the WPs will control the pH for the first few thousand years at a value which may be as high as 9 or 10, depending on rates of reaction of filler glass and Cr alloys. Under these conditions, the Pu dissolving from the Synroc-C would remain in solution owing to the formation of carbonate complexes. The solubility of the neutron poison materials under these conditions is likely to be low. However, the amount of Pu in solution is still very low and little Pu would be lost by flushing the system during this period of time.

After the first few thousand years, the DHLW filler glass in the canisters will be converted mostly to clay phases or silicates and the pH will begin to decrease toward neutrality (i.e., the pH would approach that of the original J-13 water as the high pH water is flushed out). The pH may be lowered further to about 4 to 4.5 over many thousands of years by the buildup of oxidation products of Pu, molybdenum (Mo) and niobium (chromic, dichromic, molybdic and niobic acids) from these elements present in the nickel-base inner barrier materials. (If only limited oxidation of these metals to form metal oxides, not acids, occurs, the pH will remain slightly, to moderately, alkaline.) Under the acidic conditions, Pu is not soluble and PuO₂ or other stable precipitates will form. The Gd, Hf, and other rare earth elements (RREs), are also likely to be insoluble under these conditions. In fact, the EQ3/6 analysis of the glass WF has indicated that, although the low pH (below 4.5) may raise the solubility of Gd above that of U or Pu, it is still small enough to assure that enough Gd will remain in the WP to prevent internal criticality for at least 500,000 years.

However, over this period of time, Pu will be converted to U, and U may be soluble under acidic (low pH) conditions as was indicated by the EQ3/6 calculations for glass, and is corroborated by preliminary EQ3/6 calculations for ceramic. Over time, the bulk ceramic material will degrade by a combination of grain boundary dissolution and metamictization as a result of radiation damage. However, due to the low solubility of the ceramic grains, the amount of fissile material in solution will likely be small. Thus the ceramic scenarios which could lead to criticality then have to have nearly complete dissolution of the WF matrix.

Thus, from these studies, two cases for geochemical and criticality analyses of Synroc-C can be deduced. The first considers that the ceramic material is in a metamict state with no increase in surface area. The release rate of Pu can be assumed to increase 10-15 times. The fissile material is assumed to precipitate on the available surfaces as a thin film. It is further assumed that the pH is lowered to less than 5 and remains there so that some fissile and a larger fraction of neutron absorber material are flushed from WP because of the increased solubility of the neutron absorber. The second case is for a complete decrepitation where the release rate is enhanced and the surface area is also enhanced by a factor of 15,000 times. In this latter case, it is assumed that the ceramic rubble will be distributed onto a bed of clays and silicates. The two final configurations are then identified for criticality analysis as follows:

Altered WF in the Initial Geometry—In this configuration most of the completely altered (metamict) WF retains its initial geometry. The release rate of Pu is assumed to be 10-15 times the unaltered rate. The stainless steel container material will corrode at a rate proportional to the dissolved oxygen concentration, driving the pH down. The pH will decrease to less than five over time. The neutron absorber and, at a slower rate, the Pu and U, are slowly removed from the system. The rate of Gd removal is still very low but could cause criticality to occur at very long times.

Altered WF in the Collapsed Geometry—In this configuration most of the completely altered (metamict) WF loses its geometry and collapses as particulate onto a bed of clayey materials and silicates. The exposed surface area is assumed to be enhanced by a factor of 15,000 times. The neutron absorbers (Gd and iron) are assumed to be leached at rates dependent on the pH of the system which is controlled by the infiltration rate and the dissolution rate of the stainless steel container material. Criticality could occur earlier than from the initial geometry since sufficient Gd could have been flushed from the system.

Detailed chemical scenarios for the ceramic WF are described in Section 5.5. These scenarios are similar to those described for the glass WFs. Criticality calculations have been performed for a range of possible conditions for the configurations identified for glass. Hence, only a restricted set of possible scenarios has been run for the ceramic WF. This is given in Section 7.

The EQ3/6 calculations which form the basis of this discussion are summarized in Appendix C, Table C-4.

5.3 CHEMICAL ANALYSIS METHODOLOGY AND GENERAL RESULTS

The preceding two sections (5.1 and 5.2) provide a physical description of the possible degradation scenarios and resulting final configurations. This section describes the methodology for developing

a chemical description, particularly for estimating the amounts of the principal neutronically significant species (U, Pu, and Gd) in the several phases (i.e., liquid, and various solids) of the configurations, as a function of time. The specific estimates for these amounts are given in the configuration descriptions in Sections 6.1 and 6.2, and they serve as inputs to the criticality calculations of Section 7.

The material in this section generally applies to both the glass and ceramic WFs, except as otherwise noted. Chemical analyses specific to the glass and ceramic WFs will be described in Sections 5.4 and 5.5, respectively.

5.3.1 EQ3/6 and Mass Balance Considerations

The geochemical computer codes EQ3NR and EQ6 were used to provide a general overview of the nature of chemical reactions to be expected and of the degradation products likely to result from corrosion of the WFs and containers. EQ6 can be used only to a limited extent in addressing this problem because it lacks a flow through option. Also lacking are thermodynamic data¹ for highly concentrated solutions for some constituents (Pu, U, Gd, Si, Al). These deficiencies placed severe limitations on the extent to which the computations could provide reliable results.

To overcome these limitations the following methodology was adopted: First, EQ3/6 was used to identify the pH and species present when the alkali glass has degraded completely. Second, high concentrations are avoided by assuming adequate flushing. Third, equilibrium calculations with EQ3/6 were used to determine the solubilities of U, Pu, and Gd at specific values of pH during the degradation period of the La-BS glass WF after the removal of the soluble products of the DHLW glass. These results were plotted on graphs that summarize changes in solubility with pH. The graphs also show simple hand-calculated solubility curves applicable to very low concentrations, using the dissolved chemical species indicated by EQ3NR or EQ6 as being important, according to the value of pH. These results are shown in Figure C-1 for Gd, C-2 for Pu, and C-3 for U, which are discussed more fully in Appendix C.

The initial EQ6 runs showed a substantial increase in pH, owing to the dissolution of alkalis from the degradation of DHLW filler glass, accompanied by a correspondingly large increase in concentrations of dissolved constituents. These increases cannot be modeled accurately owing to the lack of an adequate database. The pH was modeled as rising to a maximum of about 10, if CO₂ from the atmosphere had free access to all portions of the WP thereby neutralizing to a large extent the released alkali. The dissolution rate depends strongly on pH. For the EQ6 modeling a rate corresponding to that at pH 10 was used. Together with data on surface area and mass of glass this resulted in an estimate of complete degradation of the glass in about 250 years. The dissolution rate for pH 7 is about one tenth as fast, which gives complete DHLW glass degradation in about 2500 years. In the absence of CO₂ the pH would rise much more, perhaps to 12 or 13. In fact the pH in some glass reaction experiments has risen to a little over 12 (Reference 22). The concentrations of dissolved alkali metal ions, Na and K, would reach a combined total molality of about 4 at the time that all the DHLW had reacted in the absence of dilution by through flowing additional water. The maxima for pH and concentrations of alkalis, borate, and other soluble components of the DHLW

¹ The code could handle the calculations were the data available, specifically Pitzer's parameters.

glass will depend upon the relative corrosion rates of the metals in the containers and the glass WFs, as well as on the infiltration rate of water. As is explained in Section 5.4.1, the corrosion of the metals may produce acid (specifically, chromic acid for $\text{pH} > 7.2$; dichromic for $\text{pH} < 7.2$; and molybdic). This acid would neutralize an equivalent amount of the alkali being released from the DHLW glass. The degradation rates of 304L and Alloy 625 are discussed in Section 4.1. Uncertainty exists as to the long-term degradation rate of both DHLW and La-BS glass WF. For use in the EQ6 modeling a normalized rate, based on the release of boron from a representative glass formulation of 6 g/m^2 in the course of 215 days was taken from Table 1 of Bates (Reference 23) for the degradation rate of the DHLW glass. Alkali is produced by this degradation faster than is acid from the corrosion of the metals. Consequently the pH rises until all the glass has corroded. Thereafter, the pH drops as more acid is added from continuing corrosion of the metals. The greater the degree of fracturing of the DHLW glass, the higher the surface area, the greater the rate of alkali production, and the higher the maximum pH. EQ6 runs used a range of degree of fracturing.

The infiltration rate, or more accurately the rate of flow through the WP, will determine how long the dissolved components of the glass and metals will remain within the (degraded) WP. At a sufficiently high rate of flow the initially high concentrations of Na, K, and borate will be flushed out of the system while the fraction of La-BS glass that has degraded is still very small. Approximate calculations taking into account only the overall dissolution and infiltration rates in conjunction with the composition of the glass indicate that at an infiltration rate of 1 mm/yr . the concentrations of Na and B will decline to values close to those in J-13 water within several hundred years. In that case EQ3/6 can be applied to calculating solubilities at all later times. This can be done because specific pH values can be chosen, rather than times, and the flushing will have reduced the concentrations to the range that can be handled by the available database. Results from these calculations are shown in Tables C-3 and C-4 and Figures C-1 through C-3 in Appendix C. The required mass balances as a function of time were incorporated into the criticality calculations, using solubility as a function of pH. In this way both of the deficiencies noted above can be avoided. Therefore, the calculation of graphs applicable to low concentrations coupled with computations of solubilities in J-13 well water at specific pH values provides suitable data for criticality evaluations.

5.3.2 Thermodynamic Data and Static Mass Balance Relationships for Gd

The solubility of a specific element at a given temperature and pressure is determined by solids which exist in the system and by the components in the solution. For this purpose data were taken from Reference 24 and incorporated into the EQ3/6 database. On this basis the most insoluble Gd solids over the pH range of interest (4 to 10) are GdOHCO_3 , $\text{GdPO}_4 \cdot x\text{H}_2\text{O}$, and $\text{GdF}_3 \cdot 0.5\text{H}_2\text{O}$. Whereas Spahiu and Bruno (Reference 24) do not include data for GdOHCO_3 , they do for NdOHCO_3 . Comparison of data for other compounds and aqueous species of Gd and Nd shows that for analogous substances the thermodynamic data are nearly identical. Consequently, the Nd datum for NdOHCO_3 was used for GdOHCO_3 . The Gd data selected by Spahiu and Bruno (Reference 24) during their literature review and incorporated into the EQ3/6 database are reproduced in Table F-1 in Appendix F. The value of x in $\text{GdPO}_4 \cdot x\text{H}_2\text{O}$ was not specified. However, the X-ray diffraction pattern for the solid actually used to determine the solubility product shows diffraction lines corresponding to rhabdophane, $(\text{Ce}, \text{Y}, \text{La}, \text{Di})\text{PO}_4 \cdot \text{H}_2\text{O}$ (Reference 24, p. 515; the elements enclosed in parentheses, as well as other REEs, substitute freely for each other in the crystal structure; Di is an old symbol for didymium, which was later recognized as being a mixture of neodymium and

PREDECISIONAL DOCUMENT

praseodymium); on this basis x was assigned a value of 1². Throughout the pH range 4 to 10, both the phosphate and the fluoride are less soluble in J-13 water than is the hydroxycarbonate. However, examination of the amounts of phosphate and fluoride available from the WFs and from J-13 water show that there is only enough of these constituents to precipitate a small fraction of the Gd that could be released from La-BS glass. Consequently, the single most important Gd solid is GdOHCO₃.

Experiments show that Gd is insoluble under neutral to alkaline conditions and that under acid conditions it goes into solution (Reference 26). The perspective taken in this report is that over very long time frames equilibrium conditions will be attained. This means that glasses will have been converted to an assemblage of thermodynamically stable solids and that nearly all of the system inventory of chemical components that constitute a significant proportion of the mass, such as Gd, will occur in well characterized solids rather than adsorbed onto other minerals, if these components are still present in the system. To confirm the expectations of the effect of solid solutions (i.e., solids of variable composition as explained above for rhabdophane), ideal solid solution parameters for REE solids were incorporated into the EQ3/6 database. Initial calculations did confirm that the presence of REEs in addition to Gd does indeed decrease the solubility of Gd. However, no data were available to indicate how readily these solid solutions would form, in contrast to separate pure phases for each REE, and a higher solubility of Gd is more conservative (i.e., it would be removed sooner from the vicinity of fissile material). Consequently, solid solutions were not included in the final calculations.

The SKB and EQ3/6 thermodynamic databases contain no data on other potentially insoluble Gd compounds. The only other likely candidates are silicates, inasmuch as the limited data in Reference 27 indicate that REE salts of other anions present in the system, specifically, chromate, dichromate, bromide, chloride, and nitrate are moderately to highly soluble. Because no solubility data for Gd silicates apparently exist, but such compounds are expected to be quite insoluble (Reference 28 and Reference 29), experiments should be conducted to obtain data. If such silicates should prove to be insoluble under acid conditions in the pH range 4 to 7, the Gd would remain with the fissile materials in this pH range as well as at higher pH.

The first step for evaluating the solubility of Gd silicates is a detailed literature search. If this search reveals no data, a simple set of experimental investigations is suggested as the next step. Rare earth silicates have been synthesized at high temperatures and their crystallographic structures determined (Reference 38). Thus, a variety of different Gd silicates could be produced and experiments run to determine solubilities. However, this would not determine whether they would actually form at the low temperatures which would exist in a repository. Multiple approaches may be required because the situation is likely to be complex, reactions may be slow, and perhaps only metastable conditions may be achievable in the short term.

² The actual value of x is of minor importance to the calculations used. No range is given either in Reference 24 nor in the original source paper (Reference 30). The dissolution reaction is, $GdPO_4 \cdot xH_2O = Gd^{3+} + PO_4^{3-} + x H_2O$. The corresponding equilibrium constant is $K = (Gd^{3+})(PO_4^{3-})(H_2O)^x$, where quantities in parentheses refer to thermodynamic concentrations, or activities. In dilute solutions the activity of water is close to one. Thus, except for minor corrections, the last term in the equilibrium constant is essentially one to the power of x (i.e., 1).

PREDECISIONAL DOCUMENT

- A. The first alternative involves the addition of some dilute sodium silicate solution or silica sol to a Gd chloride solution and allowing the solution to age. Perhaps there will be an immediate precipitate, or one may develop on standing. It would not be surprising if a silica gel developed, which might well contain Gd. If so, and with an excess of silica over Gd, this might provide an upper limit on the solubility of a Gd silicate.
- B. The second alternative would be to synthesize some Gd silicate hydrothermally at temperatures up to perhaps 200° C and use this as input to dissolution experiments at lower temperature. Analysis of the high temperature solution, if feasible, would provide an upper solubility limit. Hopefully, this approach would produce a crystalline solid.
- C. A third alternative is to use a Gd-citrate solution, in which the Gd will be complexed by the citrate to prevent it from simply adsorbing onto silica surfaces, together with a silica sol as above. In this way if an association is found between Gd and silica it will be known that a reaction that formed a chemical compound occurred, not just an adsorption phenomenon.

The objective of each of these alternatives is to produce a Gd silicate, then characterize it (e.g., by X-ray diffraction), and finally measure its solubility in such a way that the solubility product can be determined.

It is also recommended that determinations be made for $GdOHCO_3$ in the same way as done for $NdOHCO_3$ (Reference 30). This would remove the reliance on Nd as a surrogate for Gd and reduce the uncertainty of the calculations.

5.3.3 Alkalinity of J-13 Well Water

Harrar, et al. (Reference 31) have provided a summary of analytical data for J-13 well water. The report points out that this water has been analyzed for many years with high consistency in the results. Thus, it seems unlikely that further analyses will differ in any significant respect for the principal constituents, although considerable uncertainty exists in respect to minor and trace ones. In particular, average values for, respectively, pH, alkalinity as bicarbonate, and chloride are 7.41, 128.9 mg/L, and 7.14 mg/L. Analyses of J-13 well water show that most of the measured alkalinity must be due to bicarbonate because the concentrations of other species, such as borate, are inadequate to account for the alkalinity and measurements of evolved CO_2 from the water are more than enough to account for the alkalinity by acid titration. Whereas this average analysis is close to being electrically neutral, thermodynamic (EQ3/6) calculations indicate that it is far from equilibrium with atmospheric CO_2 . Adjustments to the average concentrations of major constituents, e.g., Na^+ and alkalinity, within the range of their standard deviations (S.D.) do permit the identification of compositions consistent with the average measured pH and a partial pressure of CO_2 within the range recommended in Reference 3. For example, EQ3 input of sodium ion (S.D. 2.29 mg/L) as 44.2 mg/L and alkalinity (S.D. 8.6 mg/L) as 133.2 mg/L, leads to pH 7.41 and $\log P_{CO_2} = -2.32$ (4.64E-03 bar). This partial pressure of CO_2 is about 15 times atmospheric and lies only a little outside the logarithmic range of -2.6 to -4.6 used in TSPA-95 (Reference 3). If instead of averaging pH directly, as was done in Harrar, et al. (Reference 31), the corresponding concentrations of hydroxide are averaged (which is appropriate to estimating the pOH of a mixture of waters of differing

composition, aside from taking account of acid-base reactions that would occur upon mixing) and that average converted to pH, the average pH becomes 7.64. An example of adjustments that lead to this pH is sodium ion at 45.8 mg/L and alkalinity of 133.0 mg/L; this yields $\log P_{\text{CO}_2} = -2.54$, about nine times atmospheric and within the range used in TSPA-95 (Reference 3). By comparison, it is interesting to note that measurements by Yang, et al. (Reference 43) of the partial pressure of CO_2 in borehole USW UZ-5 at depths below 100 meters range from 0.08% ($\log P_{\text{CO}_2} = -3.10$) at 153 and 189 m depth to 0.36% ($\log P_{\text{CO}_2} = -2.44$) at 368 m (the deepest reported). All of the EQ3 calculations used to make these adjustments assumed a temperature of 25°C. Adjustments at the actual temperature of J-13 water, 31°C, would differ only slightly.

Because these parameters apply only to the pHs and partial pressures of the CO_2 stated, but for the most part different values of the parameters are of interest, other adjustments were made as needed while preserving the essential chemical characteristics of the water. The nature of these adjustments is made in other sections, as appropriate.

- A. If one specifies the pH and bicarbonate as input to EQ3NR, the code calculates a partial pressure of CO_2 of 4.62E-03 atm., which is about 15 times higher than in air, and, to achieve electrical neutrality between positive and negative ions, a chloride concentration of 11.97mg/L; this alternative will be designated as high alkalinity (HA).
- B. An alternative choice of pH 7.41 and atmospheric CO_2 leads to a bicarbonate concentration of only 8.83 mg/L, but chloride at 76.7 mg/L; this alternative will be designated equilibrium alkalinity (EA). The increase in the chloride content results from the necessity of maintaining electrical neutrality. In this system the chloride undergoes little interaction with other components.
- C. One might also consider specifying the use of H^+ to achieve electrical neutrality, in spite of the probability that slight analytical imbalance in respect to electrical neutrality is likely to give an erroneous answer. Doing so, however, by way of using the analytical bicarbonate and chloride concentrations, yields a calculated pH of 7.938 and a partial pressure of CO_2 of 1.43E-03.

5.3.4 Solubilities of Gd, Pu, and U under Acidic Conditions

As acid concentrations are increased, it is to be expected that the solubility of GdOHCO_3 will increase in accordance with the reaction,



For a chosen fixed partial pressure of CO_2 the logarithm of the dissolved Gd^{+++} can be plotted as a straight line against pH, making use of the equilibrium constant for this reaction, as shown in Figure C-1. (See Appendix C for more detail on the linear equation and how it is derived.) EQ3 calculations for J-13 water composition brought to low pH by addition of dichromic acid, specifically at pHs 5.5, 6, and 6.5, show that indeed Gd^{+++} constitutes most of the dissolved Gd and that the least soluble Gd solids are GdOHCO_3 and $\text{GdPO}_4 \cdot \text{H}_2\text{O}$. A subsequent EQ6 run brought the output from the EQ3 calculation to equilibrium with these solids, as well as with Pu and U solids,

PREDECISIONAL DOCUMENT

PuO₂ and soddyite, respectively. These results are plotted on Figures C-1 through C-3 in Appendix C.

The specific solubility values from the EQ6 runs are given in Tables C-3 and C-4 for the high alkalinity and equilibrium alkalinity assumptions, respectively. The analyses in this study are based on the application of an exponential fit to these Gd solubility data. The relevant points are summarized in Table 5.3.4-1; these values are extracted from the specific cases indicated by * in those tables.

Table 5.3.4-1. Bounding Values of Gd Solubility from EQ6 Runs

Alkalinity assumption	pH=5.5	pH=6.5	log-log slope*
Equilibrium (Table C-3)	44,100 ppm	3 ppm	-4.17
High (Table C-4)	145 ppm	.3 ppm	-2.68

*Slope of the line of log Gd molality as a function of pH, connecting the indicated two points.

The analysis of this section shows that the plot of log Gd molality vs pH should be a straight line for pH below 6.5. This analysis (particularly the chemical balance equation for Gd⁺⁺⁺, above) also gives an idealized value of -3 for this slope. Consistent with these data the following formula will be used for the pH dependence of Gd solubility:

$$\text{max Gd (ppm)} = 3 \times 10^{-3(\text{pH}-6.5)}, \text{ or } 95 \times 10^{-3(\text{pH}-6.0)}$$

This is a mixture of the equilibrium alkalinity assumption with the idealized slope. The equilibrium alkalinity assumption is conservative with respect to the multiplicative factor 3, since this is the larger of the two values in Table 5.3.4-1 at pH 6.5. The exponential factor of 3 is not conservative since it is of lower magnitude than the EA value, and consequently gives a much lower upper limit of Gd solubility (at pH 5.5). It is appropriate, however, because it is more consistent with the measured value of alkalinity as bicarbonate, which is supported by the weight of specific measurements. In the present state of knowledge on the subject, it is not appropriate to rely solely on the measured value because it is at only one pH, and because it is not supported by a generally recognized mechanism for producing the super-saturation in carbon dioxide which appears to occur.

At higher pH the dominant dissolved Gd species changes, first to GdCO³⁺, over the approximate pH range from 7.2 to 7.7, and to Gd(CO₃)₂; for pH higher than 8.5. At pHs intermediate to these ranges the solubility corresponds to the sum of the two most important species. Other species considered are GdOH⁺⁺, Gd(OH)₂⁺, Gd(OH)(aq), and Gd(OH)₄⁻. These reactions and equations for the corresponding lines are given in Appendix C.

Similarly, the plot for Pu and U uses reactions between the appropriate solids and each of the more important dissolved species. These reactions and corresponding equations are also included in Appendix C.

5.3.5 Compositions of Solid Phases Resulting from Degradation of WP Components

The approach used for obtaining a representative composition for the degradation products consisted, first, of taking results from EQ6 runs at the time that the model predicted that all of the DHLW filler glass had reacted, and, second, modifying that composition to a small extent on the basis of static mass balance considerations that would affect this composition under neutral to somewhat acidic conditions. Because of the long time frames, the modeling assumed that the phases formed would be in equilibrium with the solution. Thus, quartz, rather than chalcedony, was assumed. Similarly, clay minerals, rather than a degraded leached glass ("gel"), were assumed. Some solids were, however, suppressed as being unlikely to form at low temperatures, even though the thermodynamics would predict their occurrence; garnet, biotite, and pyroxene, among others, were suppressed. Chalcedony is less thermodynamically stable than quartz, but frequently forms at low temperature. Once formed it persists for geologically long times. The metastable equilibrium between a solution and chalcedony does result in a higher aqueous silica concentration, but both forms of silica are very insoluble. The assumption that quartz forms, which may occur in the time frames involved, means that the lower aqueous silica will result in a higher calculated soddyite solubility, which is more conservative.

By the time the model predicts complete reaction of DHLW filler glass the calculated aqueous concentration has already exceeded the limits ordinarily accepted for use of the type of data presently available. Because of the electrical charges on aqueous ions and various kinds of ionic interactions, such as the formation of complexes and ion pairs, it is necessary to apply corrections to the concentrations of dissolved species in order to utilize thermodynamic data properly. At very low concentrations the relationships are well known and can be calculated with considerable accuracy. As concentrations increase, it is possible to apply approximate additional correction terms, but at very high strengths relations become very complicated. Because some of the data needed for the high concentrations likely to be encountered in the present case are unavailable, some of these additional corrections cannot be applied. Nevertheless, a considerable degree of correction can be, and has been, used in the EQ6 modeling. Appendix D provides a brief discussion of the nature of these corrections and a comparison of the factors calculated by EQ6 using the same correction option utilized during the modeling, with experimentally measured factors (i.e., activity coefficients) at concentrations resembling those expected at this stage of reaction progress. This comparison seems adequate to conclude that, qualitatively, the general character of the reactions has been determined by EQ6. Further rationale for this conclusion appears in Appendices C and E.

The rationale presented in the preceding paragraph does not mean that the calculated aqueous concentrations can be relied upon. However, the solids predicted are in keeping with expectations based on well recognized chemical principles and on static mass balance considerations. Specifically, it is expected that all except traces of the Al, Si, Fe, Mn, Ni, and Zr will be present in the solids. Moreover, under alkaline conditions Ca and Mg should be distributed between clay and carbonate minerals with only small amounts in solution. This also applies to that portion of the alkalis, Na and K, not otherwise associated with borate, carbonate, or bicarbonate. (See Appendix E for a more detailed discussion of mass balance relationships.) Boron should be in solution, or perhaps as a precipitated borate mineral. These chemical expectations are in keeping with the model results.

In other sections of this report the mixture of solid products is referred to as "clay" or as "clayey material" because much of it consists of clay minerals (i.e., nontronite and celadonite) and all of it is expected to be fine grained (i.e., to consist of clay size particles).

The rate of glass degradation is related to the mix of products, as noted above. Some discussion of this topic appears in Appendix C, Section C.2.

5.4 CHEMICAL SCENARIOS FOR GLASS WASTE FORM DEGRADATION

The scenario perspectives shown in Figure 5-3 identify the chemical parameters which determine the possible separations of the fissile material from the neutron absorbers. The alternatives shown in this chart serve as planning guidelines for the EQ3/6 calculations which were performed. These parameters were used in the mass balance equations to determine which species will be removed from the WP as a function of time; they are also used to determine the partitioning among different precipitating species.

5.4.1 Unlimited Access of Air with Alkali Glass Composition

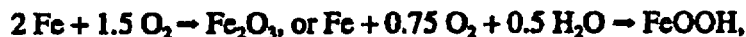
Initially, as noted above, the degradation of DHLW filler glass in the presence of an unlimited supply of air will dominate the chemical evolution. This degradation will result in a substantial increase in pH. This can be viewed simplistically as resulting from the dissolution of a sodium or potassium silicate component of the glass according to:



The silica would precipitate in some insoluble form, such as quartz or chalcedony. However, with unrestricted entry of air into all parts of the WP the hydroxide would be promptly neutralized by atmospheric CO_2 to form bicarbonate ion. This water would still be alkaline, and would attain a high alkalinity (i.e., would require a large amount of acid to bring it to a neutral pH), but the CO_2 would limit the pH to a maximum of about 10.

At the same time atmospheric oxygen would keep oxidation states of U and Pu relatively high. The U should oxidize to the +6 state, if it is not already at that valence in the waste, and remain in that state both in solution and in precipitated solids. The Pu is less readily oxidized and, except in the presence of large concentrations of carbonate and/or bicarbonate, would be mostly in the +5 state in solution, but in the +4 state, as PuO_2 , as a precipitate.

The effect of metal corrosion on pH needs to be taken into account. The net reaction of many metals consists simply of a gain oxygen from the air, e.g.,



with no net effect on H^+ or pH. On the other hand the corrosion of stainless steels and other corrosion resistant metals may entail substantial effect. Specifically, Cr may oxidize to chromate or dichromate, and Mo to molybdate:

PREDECISIONAL DOCUMENT



It is known that conditions as acidic as pH 4 to 5 develop in pits and crevices during corrosion of these metals. It remains unknown, however, whether such reactions will occur on a sufficiently broad scale, or rapidly enough, to lower the pH of an initially strongly alkaline solution to such low pHs. For example, the mineral, eskolaite, Cr_2O_3 , is known to occur "as a major constituent of black pebbles in the bed of the Merume River, Guyana." (Reference 25, p. 197), thus demonstrating that Cr oxide may survive for long times without converting to the higher oxidation state necessary to support acid conditions. This assumption is conservative with respect to criticality (based on the above reasoning that such conditions may arise within the WP) because the result is removal of Gd while leaving fissile material behind.

Experimental measurements of acid production from corrosion of corrosion resistant alloys over long time spans, as might be achieved by suitable accelerated testing, would be very helpful in evaluating the potential for this mechanism to lower pH, and thereby increase Gd solubility. For the potential oxidation of Cr it is recommended that a set of simple tests be conducted. Possibilities for such experiments are:

- A. Agitate finely divided Cr_2O_3 and CrO_2 , in separate experiments, in water or an aqueous solution resembling J-13 well water at about 90°C to enhance the reaction rate, for an extended period of time. Air should be bubbled through the mixture continuously. From time to time samples of the solution should be taken for analysis of dissolved Cr. It is to be hoped that sufficient Cr will enter solution that the oxidation state can be determined, perhaps spectroscopically, inasmuch as the color of Cr^{+++} ion is distinctly different from that of either chromate or dichromate ion.
- B. A similar experiment, but at room temperature, using a rather strong solution of hydrogen peroxide. Bubbling air through the system is probably not desirable, as it may remove oxygen as it breaks down from the peroxide.
- C. Other similar experiments using strong oxidizing agents to enhance reaction rates. Perhaps bubbling ozone through the solution at elevated temperature would produce a measurable reaction.
- D. It seems likely that at sufficiently low pH the oxidation to chromate will proceed. Accordingly, this could be tested, and, if chromate is produced, the rate could be measured as a function of pH with the objective or projecting this to higher pHs of interest for application to production of chromic acid under anticipated repository conditions.

Options to accelerate the reaction (e.g., ultrasound, catalyst, Cl^- in solution) or concentrate the reactant (geometry) may be required to obtain the required data in a reasonable time.

Counter to the potential acid production is the likely continuing influx of J-13 water with its associated alkalinity.

5.4.2 Restricted Access of Air with Alkali Glass Composition

If entry of air into the interior of the WP is severely restricted, the evolution of the system would be entirely different. Scoping calculations with EQ6 indicate that very high pH could be achieved (over 13) and very low oxidation potentials (Eh). These results are in keeping with simple static mass balance considerations. Under such circumstances Gd should be insoluble as $Gd(OH)_3$ and Pu and U as the dioxides. Thus, no nuclear criticality seems possible, inasmuch as all three elements should remain in close proximity to each other.

5.4.3 Unlimited CO_2 and O_2 with No Alkali in the Glass

This case resembles that described in Section 5.4.1, except that the WF glass would have to be the nominal La-borosilicate (not the ATS glass), and the filler would be some non-alkali glass instead of the nominal DHLW filler glass. In this case the early large increase in pH, and consequent accompanying increase in CO_2 absorption from the air to form bicarbonate, would be absent. This would result in a less neutralizing effect for any acid produced by oxidation of Cr and Mo and, therefore, a somewhat lower final pH. Modeling of this scenario, including only La-BS glass and the metals, did not result in early attainment of high concentrations, but did predict acidic pH toward the end of the run. There is a small initial increase in pH, by about 0.01 pH units, owing to the small content of Sr in the glass. Because EQ6 does not implement a flow through option, this case had to be modeled as a closed system. As a consequence, at pHs below about 5.2 the concentrations exceed the limits of reliability as dichromate and molybdate increase in the solution. At this stage of reaction progress the Gd concentration was predicted to have reached over 8000 ppm, but the Pu concentration was only about $2E-05$ ppm and U only about $2E-09$ ppm. In other words all of the Gd released from the waste, except for a very small proportion incorporated into Gd phosphate, would be in solution. In reality the concentrations seem unlikely to get this high for the dichromate and Gd because of the flushing action of infiltrating water. In all other respects the chemistry for this case parallels that described in more detail for unlimited access of CO_2 and O_2 and alkali glass. For this case the use of figures C-1 through C-3 in Appendix C is appropriate since they still represent solubility conditions at low pH with adequate accuracy.

5.4.4 Limited CO_2 and O_2 with No Alkali in the Glass

The results discussed above and straightforward chemical considerations make it clear that under these conditions there will be no large increase in pH as a consequence of dissolution of WFs. Moreover, in this case there will be insufficient O_2 to produce acids from Cr or Mo. Consequently, the pH will never reach strongly acidic conditions. Instead the pH would remain essentially at its initial value with perhaps a small increase in response to the dissolution of Sr from La-BS glass, depletion of dissolved CO_2 and O_2 , etc. The depletion of the initial complement of O_2 will lead to highly reducing conditions and immobilization of both Pu and U as the dioxides. The Gd will remain insoluble in some form, such as $GdOHCO_3$. An EQ6 run for this case produced results in keeping with the expectations. These conditions are not conducive to producing a criticality.

5.4.5 Composition of Solid Degradation Products From Glass

As discussed in Section 5.3.5, EQ6 was used to provide a representative composition for the combined degraded DHLW glass and the Pu immobilization glass. The modeled solid product mixture from EQ6 consists of nontronite, Ca-Mg carbonate, quartz, microcline, celadonite, pyrolusite, nickel silicate, gaylussite (a Na-Ca carbonate), and minor amounts of other compounds, as well as insoluble Gd, Pu, and U phases. These results are consistent with those expected, as described in the preceding paragraph. Ca and Mg are shown to occur mostly in carbonates and celadonite. Na appears in the nontronite, but much remains in solution. K is shown in nontronite, microcline, and solution. Al and Si are constituents of nontronite, celadonite, microcline, and (Si only) quartz. Fe is a major component of the nontronite, and Zr is insoluble as zircon. The modeling for the maximum amount fracturing of the DHLW filler glass, namely, 100 times the surface area, shows a rather large amount of borax, but, if it in fact does form, it is expected to dissolve as more J-13 water infiltrates through the WP. For the expected amount of fracturing, 30 times the surface area, borax does not form, because with the reduced surface area the release rate of sodium and borate into the solution is less, until much more metal has corroded, thereby making the pH substantially lower and changing other aspects of the chemistry. Nevertheless, the minerals formed are nearly the same (similar compositions), although the compositions of the solid solutions differ somewhat. Thus, the principal uncertainty lies in the distribution of the alkalis between solution and solid. Accordingly, the modeled mixture of solids was assumed to be reasonably representative in respect to the elemental content (as distinguished from the mix of minerals), except for the soluble salt, borax. For criticality calculations the boron was conservatively assumed to have been removed. At sufficiently low pH, the alkalis³ and alkaline earths³ in the silicate and carbonate minerals should be leached out, but this modification to the composition was not made. It would have only minor impact on the criticality calculations.

The elemental components of the solids making up the degraded glass clayey material from the EQ3/6 calculation are shown in Table 5.4.5-1.

Table 5.4.5-1. Elemental Components of the Clayey Mass from Degraded Filler Glass and Pu Immobilization Glass

Element	Moles in Solid
H	3.273E+1
C	9.835E-1
O	6.808E+1
Na	3.821E+0
Mg	5.954E-1
Al	1.689E+0
Si	1.378E+1
K	1.249E+0
Ca	2.901E-1

³ The alkali metals include Li, Na, K, Rb, Cs, and Fr. The alkaline earth metals include Be, Mg, Ca, Sr, Ba, and Ra.

PREDECISIONAL DOCUMENT

Table 5.4.5-1. Elemental Components of the Clayey Mass from Degraded Filler Glass and Pu Immobilization Glass (Continued)

Element	Moles In Solid
Mn	5.400E-1
Fe	3.746E+0
Cu	4.218E-2
Zr	7.866E-3
Hf (2 wt% Zr)	8.123E-5
U	1.405E-1
Pu	2.967E-2

5.5 CHEMICAL SCENARIOS FOR CERAMIC WASTE FORM DEGRADATION

Section 5.2 provides a physical description of the general ceramic degradation process. EQ6 calculations indicate that the chemical evolution of a system incorporating a ceramic WF instead of La-BS glass will again be dominated in early time frames by the DHLW filler glass degradation. Thereafter, the pH would decrease in a very similar manner to that for the La-BS glass case, if Cr and Mo oxidize to form acids.

5.5.1 Modeling of Ceramic WF Degradation

Modeling for the ceramic WF used the recommended fracture factor of 30 for DHLW filler glass in all cases. The ceramic was in one instance treated as if it were a homogeneous phase of constant composition, analogous to a glass, and in other cases, one with a fracture factor of 10 and another with 15,000, as a mixture of zirconolite, pyrochlore, Ba-hollandite, and Zr rich rutile. These computer runs all hit the reliability limit as a consequence of the large releases of alkalis and borate from the DHLW glass. Whereas the differences due to the various WFs are small they are sufficient to make noticeable differences in the solubilities at this stage of reaction progress. These differences appear to arise from the slight alkalinity caused by dissolution of La-BS compared to nearly none by ceramic, silica dissolving from the glass, etc. This gives rise to small differences in the carbonate concentration, which, because it is raised to third power in calculating the concentration of U species in this pH range, makes a large difference in the U solubility. For similar reasons GdOHCO₃ appears as one of the insoluble Gd phases for the glass model at this point, but not for the ceramic. However, none of these makes any significant difference to criticality issues because all three elements are still dominantly retained in the initial Pu WF while the pH is high.

PREDECISIONAL DOCUMENT

The only important difference in respect to criticality is the rate of degradation of the WF. This is much smaller than for glass with a fracture factor of 10. Interestingly, the release rate of Pu from the WF, per WP, is still less for the ceramic by a factor of about 40 even for a fracture factor of 15,000.

5.5.2 Composition of Solid Degradation Products From Ceramic

In a somewhat similar manner as was used for the degradation of La-BS glass, a point in reaction progress was chosen at about the stage at which all of the DHLW filler glass had degraded to obtain a representative composition for solid products. In this case a local minimum of pH, 6.36, during the evolution of the fluid composition was chosen, even though the solution concentration was too high to provide reliable results for the composition of the water. The combination of solid products was compatible with expectations for the same reasons as explained previously in Section 5.3.5. The proportions of the minerals and their compositions resemble those for the glass case, although they differ in detail. Although slightly acid, no appreciable amount of alkalis had yet been leached from the clays.

The elemental components of the solids making up the clayey material from the EQ3/6 calculation are shown in Table 5.5.2-1. As noted in Table 5.5.2-1, 2 wt% of the Zr is assumed to be Hf. Most zircon minerals contain 1 to 5% Hf (Reference 27, p. B-19).

Table 5.5.2-1. Elemental Components of the Clayey Mass from Degraded Filler Glass and Pu Immobilization Ceramic

Element	Moles in Solid
H	2.175E+1
C	1.152E-1
O	7.572E+1
Na	1.710E+0
Mg	4.964E-1
Al	1.859E+0
Si	1.210E+1
K	1.088E+0
Ca	4.547E-1
Ti	2.064E+0
Cr	8.051E-1
Mn	6.738E-1
Fe	9.782E+0
Ni	3.703E+0
Zr	3.285E-1
Gd	1.189E-1
Hf (2 wt% Zr)	3.392E-3

PREDECISIONAL DOCUMENT

Table 5.5.2-1. Elemental Components of the Clayey Mass from Degraded Filler Glass and Pu Immobilization Ceramic (Continued)

Element	Moles in Solid
U	1.701E-1
Pu	3.090E-1

5.6 FISSILE MATERIAL TRAPPED IN THE INVERT

²³⁵U and remaining undecayed quantities of ²³⁹Pu are released into solution from the degrading WFs. Most of the fissile material is precipitated immediately after release, but some remains in solution and is flushed from the degraded WP. Eventually the precipitated fissile material will be re-dissolved and flushed from the WP. Although the removal process could take more than one million years, the accumulation of a critical mass by re-concentrating the fissile material in the invert from the solution flowing (or dripping) from the WP is conceptually possible. Thus, the actual possibility of criticalities must be evaluated. Fissile material could be trapped in the invert in several ways: adsorption on or ion exchange into zeolitic materials present in the tuff and the degraded concrete, precipitation due to a reduction in dissolved oxygen, adsorption onto corrosion products of carbon steel, particularly iron oxy-hydroxide, or by take up in microbial species present on these materials.

Tuff contains a variety of zeolites, such as clinoptilolite, with the amount dependent upon its location within the various rock strata. The repository horizon itself contains little zeolitic material. However, large amounts exist between the repository horizon and the water table. These are largely in vitric tuffs in which the glassy phase was converted to the zeolites clinoptilolite, heulandite, and mordenite by hydrothermal reactions. Thus, the potential for adsorption onto tuff in the invert depends on the source of the material. If it comes from the crushed (repository horizon) tuff, it will be low in zeolites, but if it comes from material near the surface, such as the Calico Hills member, it will be high in zeolites. The limited available data on U sorption on zeolitic materials was recently summarized in LANL report (Reference 21). For zeolitic tuffs, sorption coefficients determined in laboratory studies are near zero at pH of 9, but increase as pH decreases to about 6. Experimental in situ work (Reference 41) has shown that the adsorption of U of up to 1 weight percent, from U-bearing groundwater, onto zeolitic material is possible in the range of pH from about 4 to 8.5, based on the heulandite-clinoptilolite group as the active zeolite. In the time frame required to accumulate kilograms of fissile material any ²³⁹Pu adsorbed would likely be decayed to ²³⁵U and ²³⁹Pu is less likely to adsorb to zeolites than ²³⁵U.

An important source of zeolites is the concrete which may degrade to form zeolites directly, along with hydrogarnet, or by its interaction with the glass dissolution products which have been flushed from the WP by the modified J-13 water. One simulation case was run using EQ3/6 with J-13 at pH 12 with gibbsite, diaspore, and many of the calcium silicate hydrates in cement; this computation showed that zeolites may form stably under these conditions. In addition, zeolitic cements can be produced from conventional cement by the addition of alkali and fly ash, a source of alumina and silica. A list of potential calcium-rich zeolitic minerals that could form as a result of these reactions is given in Table 5.6-1. Sodium-rich zeolites are also possible.

PREDECISIONAL DOCUMENT

Another possible mechanism leading to UO_2 precipitation in the invert could be the reduction in the amount of dissolved oxygen. This less oxidizing environment could cause the U to be reduced from the hexavalent to the quadrivalent state, and subsequently precipitate. However, this requires a dramatic decrease in oxygen content. Since it is anticipated that the oxygen content outside of the package will be more rather than less oxidizing due to the additional free surfaces, this will not likely lead to U precipitation. (See Section 3.1.2.) In contrast with U, the Pu in solution will simply precipitate as soon as it can, so there is more likelihood of precipitation of Pu in the WP before it can reach the invert. The colloidal Pu concentration, which is likely to be much greater than the Pu which is truly in solution, would likely be trapped in the clayey phase and not leave the WPs prior to conversion to U. Thus, this mechanism is not expected to lead to the precipitation of fissile material in the invert.

Conflicting data are available in the literature regarding the adsorption of U onto pure iron-containing mineral phases such as goethite (iron oxy-hydroxide) and hematite (iron oxide) (Reference 21). One set of data indicates that the corrosion products readily adsorb U while the other does not. Thus, the corrosion products, which will fall onto and become part of the invert, could potentially adsorb U present in the effluent water from the WPs. However, the presence of iron will reduce the potential for a criticality. In addition, microbial action can lead to the formation of complexes that can adsorb radionuclides. Adsorption has been demonstrated for heavy metals, but little work has been conducted with radionuclides. Further work is needed in order to include these mechanisms in the criticality calculations. Thus, it is currently assumed that the adsorption onto zeolites, formed from concrete degradation or reaction, is the most likely mechanism for the presence of fissile material in the invert.

Table 5.6-1 Representative List of Calcium-Rich Zeolites Which Could Result from Concrete Degradation

Zeolite Name	Zeolite Formula
Epistilbite	$CaAl_2Si_4O_{16} \cdot 5(H_2O)$
Chabazite	$CaAl_2Si_4O_{16} \cdot 5(H_2O)$
Dachardite	$(Ca, Na_2, K_2)_7Al_{10}Si_{20}O_{80} \cdot 25(H_2O)$
Gismondine	$CaAl_2Si_2O_8 \cdot 4(H_2O)$
Heulandite*	$(Na, Ca)_{2-3}Al_3(Al, Si)_2Si_{13}O_{38} \cdot 12(H_2O)$
Laumontite	$CaAl_2Si_4O_{12} \cdot 4(H_2O)$
Clinoptilofite*	$(Na, K, Ca)_{2-3}Al_3(Al, Si)_2Si_{13}O_{38} \cdot 12(H_2O)$
Cowlesite	$CaAl_2Si_2O_{10} \cdot 5-6(H_2O)$
Garronite	$Na_2Ca_2Al_{12}Si_{20}O_{64} \cdot 27(H_2O)$
Levyne	$(CaNa_2K_2)_7Al_8Si_{12}O_{38} \cdot 18(H_2O)$
Mordenite	$(Ca, Na_2, K_2)Al_2Si_{10}O_{34} \cdot 7(H_2O)$
Scolecite	$CaAl_2Si_3O_{16} \cdot 3(H_2O)$
Stellerite	$CaAl_2Si_7O_{18} \cdot 7(H_2O)$
Stilbite	$NaCa_2Al_3Si_{13}O_{38} \cdot 14(H_2O)$

PREDECISIONAL DOCUMENT

Table 5.6-1 Representative List of Calcium-Rich Zeolites Which Could Result from Concrete Degradation
(Continued)

Svetozarite	$(Ca, K, Na)_2Al_2Si_{12}O_{28} \cdot 6(H_2O)$
Thomsonite	$NaCa_2Al_3Si_4O_{28} \cdot 6(H_2O)$
Wairakite	$CaAl_2Si_4O_{12} \cdot 2(H_2O)$
Yugawaralite	$CaAl_2Si_6O_{18} \cdot 4(H_2O)$

* Same formula, but slightly different structures, and usually different ratios among Na, K, Ca.

6. REPRESENTATIVE WASTE FORM DEGRADATION CONFIGURATIONS

The final configurations described in this section are representative of the range of potential criticalities which can occur. Section 6.1 discusses the degraded configurations to be further evaluated for the glass WF, and Section 6.2 provides the same discussion for the ceramic WF.

6.1 TYPICAL CONFIGURATIONS FROM GLASS WASTE FORM DEGRADATION

The WF degradation scenarios discussed in Section 5.1 identified two classes of configurations of the degraded glass WF which must be evaluated for criticality. These configurations are:

- The degraded WF slumped into a mass of clayey material forming a hemicylinder at the bottom of the WP (internal criticality)
- The accumulation of fissile material in the invert (external, near-field criticality).

Section 6.1.1 and 6.1.2 will provide further detail on the typical variations of above two classes of configurations. These configurations are modeled and analyzed using MCNP4A as discussed in Section 7. Section 6.1.3 will provide details of scenarios which do not lead to credible critical configurations.

The scenarios leading to these configurations are discussed in Section 5.4 and the input data applied to the scenarios is provided in Section 4.

6.1.1 Altered WF Slumped to Bottom of WP

As discussed in Section 5.1, degradation of both the DHLW glass and the Pu immobilization glass WF by water, occurs in two general stages: formation of a "gel-like" alteration layer at the degrading glass surface, followed by reprecipitation of clays and minerals both near the initial alteration point and elsewhere within the package. The majority of the DHLW glass would be expected to have degraded prior to the degradation of the Pu glass because it is exposed first and has a degradation rate that is potentially an order of magnitude higher (Section 4.1) than that of the Pu glass.

During the period that the WF is degrading, insoluble fissile isotopes will precipitate into the clayey material. If the Gd is also insoluble, it will precipitate into the clayey material together with the fissile isotopes and prevent criticality. However, during the period of stainless steel corrosion, the pH may be lowered sufficiently that Gd is relatively soluble as shown in Sections 5.3 and 5.4. Under these conditions the Gd will not accumulate in the clayey material. For this reason, the clayey material is considered the most likely location for a criticality within the waste package. The criticality calculations are based on a uniform distribution of neutronically significant species (U, Pu, Gd) within the clay, according to amounts determined as a function of time from the mass balance calculations described in Section 3.2.1. Figure 6.1.1-1 shows the physical geometry used for the criticality calculations, which encompasses a range of concentrations of the neutronically significant species, as described in Section 7.1. Figure 6.1.1-1 does not show any undegraded WF as a distinct entity; the alternatives for the location of this material are described in subsections 6.1.1.1 and 6.1.1.2.

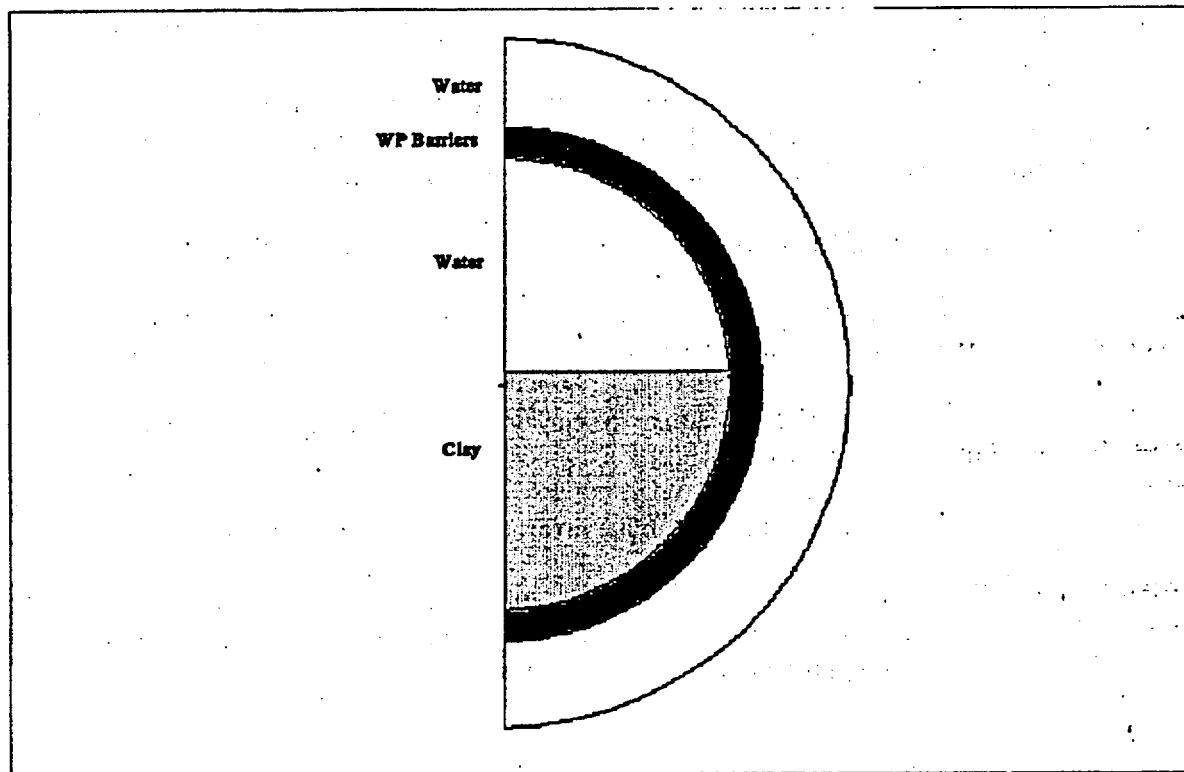


Figure 6.1.1-1. WP Model for Homogenized Clayey Material Slumped to Bottom

A representative composition of the elements in the clayey solids is determined by the mineral species remaining at the end of typical EQ3/6 runs modeling the chemical reaction over time of the glass with water and the other components in the WP (particularly the steel of the canisters and cans). These runs are described in Section 5.4. This clayey composition is assumed to be representative of the range which could occur under credible degradation scenarios. The elemental components of the solids making up the clay are shown in Table 5.4.5-1. Typically, a clay would have a density of approximately 2.3 g/cm^3 (Reference 25) and this value is assumed appropriate for the degraded glass clayey material.

Although the DHLW glass contains a significant amount of depleted U, it degrades much faster than the Pu glass and an indeterminate fraction is transported outside the WP before significant amounts of U are released from the Pu glass. EQ3/6 cannot differentiate between isotopes or original sources for elements and, therefore, cannot distinguish the fraction of U that is ^{235}U or ^{238}U . For this reason, the depleted U is not included in the clayey composition.

The height of the cylinder segment of homogenized clayey material will depend on the amount of clay remaining and the amount of water trapped in the clay. Because material has been transported into and out of the WP, the actual volume of clay remaining is unknown. For this evaluation, it was assumed that the volume of the clay is equivalent to that displaced by the original four glass pour

canisters within the WP. Clays contain water in two forms: a fixed amount of hydrogen (bound as H_2O or OH) and a variable amount of free water. The bound H for the degraded glass clayey material has the same atom density as H in 33.7 volume percent free water and is already represented in Table 5.4.5-1. The volume fraction of free water in the clayey material is dependent on many conditions and, therefore, is variable.

Several less likely variations of the final configuration are also considered. These are concentration of all Pu, U, and Gd in the top of the clay; concentration of all Pu, U, and Gd in the bottom of the clay; and concentration of all Pu, U, and Gd at one end of the WP. The first variation could conceivably occur if a large amount of the DHLW glass were to degrade and slump to, or precipitate at, the bottom of the WP before the structure of the pour canisters have collapsed. When collapse of the pour canisters does occur, this will leave the Pu glass canisters and any non-slumped DHLW glass clay, on top of the clayey material. This would result in a final configuration with an upper layer of Pu/U/Gd bearing clay and a bottom layer of clay containing little or no Pu/U/Gd. Figure 6.1.1-2 shows the stratified clay layers for these configurations. The latter two cases appear less likely as they would require a mechanism for physically shifting the degrading Pu glass canisters to one end of the package after the DHLW glass clay has slumped, or cause them to settle to the bottom of a high water fraction DHLW glass clay. Tilting of the package due to a support failure could cause the cans to shift to one end of the package, but the clay would also be shifted. Settling of the Pu glass canisters to the bottom of the clay could result while they are still relatively intact in high water fraction clay, or as a result of shaking during a seismic event. However, this would make it difficult to remove the Gd as it would be trapped under a protective layer of non-Pu/U/Gd clayey material. Stratification of the heavier clayey components from the lighter ones once complete alteration of both glasses has occurred is not supported by natural analogs. A scenario involving flushing of a large fraction of the clay components by flowing water, leaving a reduced volume of clayey material with concentrated Pu/U/Gd would result in a similar configuration. A flushed clay scenario is unlikely since the bulk of the clayey materials is relatively unreactive. The geometries for concentration of Pu/U/Gd in a bottom layer of the clay are identical to those shown in Figure 6.1.1-2, except that the concentration occurs in the bottom layer. Figure 6.1.1-3 shows the geometry modeled with all of the Pu/U/Gd clayey material in one half of the package.

6.1.1.1 Undissolved WF separated from the clayey material

It is most conservative to assume that the undissolved WF remains outside the clayey material. [Note that the term "undissolved" is used rather than "undegraded" to reflect the fact that the WF can degrade to the extent of fragmenting while still retaining its initial chemical composition so that the Gd is not separated from the fissile isotopes.] Detailed modeling of the physical degradation process is beyond the scope of this study, so this conservative assumption is taken as the nominal case and serves as the basis for most of the calculations in Section 7.

6.1.1.2 Undissolved WF distributed uniformly within the clayey material

It is likely that much of the WF will fragment before it dissolves. Under such circumstances a significant fraction of the fragments could be distributed in the clayey material where they would ultimately dissolve at a later time. The extreme manifestation of this process is to have all the undissolved WF fragments uniformly distributed throughout the clayey mass. In this case, the clay

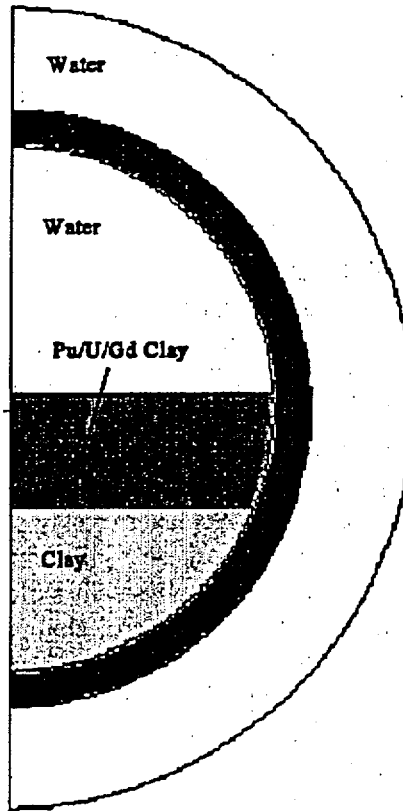


Figure 6.1.1-2. WP Model for Concentration of all Pu/U/Gd in Top Layer of Clay

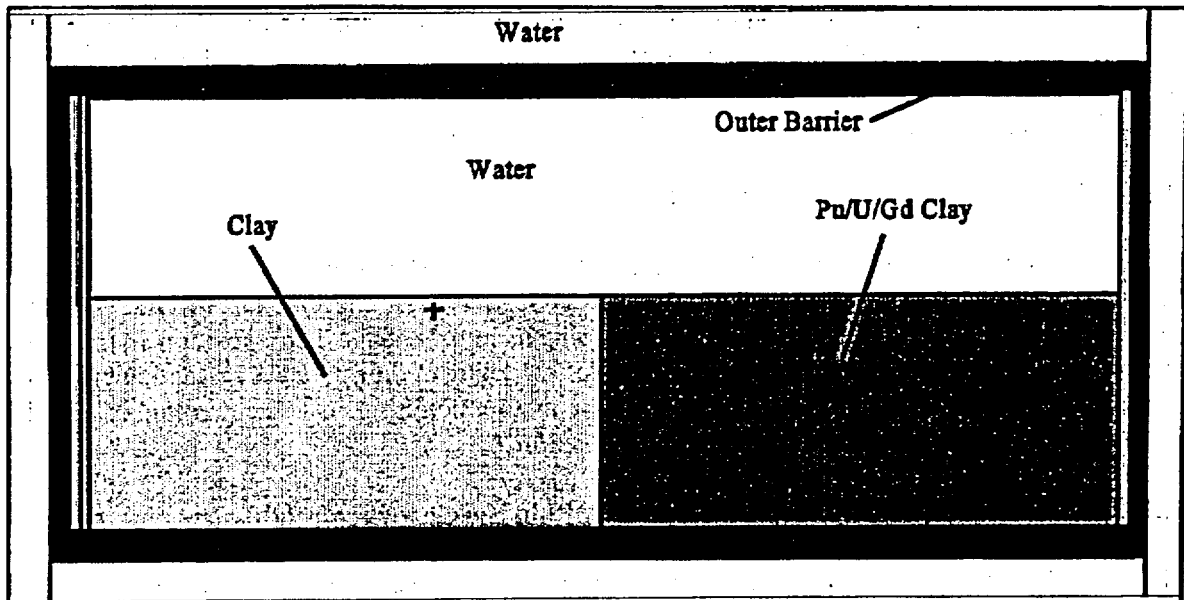


Figure 6.1.1-3. WP Model for Concentration of Pu/U/Gd on One End of WP

mass depicted in Figure 6.1.1-1 would contain the chemical components of all the undissolved WF in addition to the clay elements and the neutronically significant species (U, Pu, and Gd) precipitated after being released from the already dissolved WF. The amount of undissolved WF components and neutronically significant species in the clay will, obviously, vary during the time when the WF is dissolving. This variation is determined from the mass balance equations given in Section 3.2.1.

6.1.2 Invert Accumulation

Fissile and neutron absorber material which has been flushed out of the degraded WP must pass through the invert material. As discussed in Section 5.6, the invert material will likely be a mixture of tuff and degraded concrete, as well as degradation products of the WP, particularly the carbon steel outer container. Fissile material could be trapped in the invert in several ways: adsorption on zeolitic materials present in the tuff and the degraded concrete, precipitation due to a change in dissolved oxygen, adsorption onto corrosion products of carbon steel (particularly iron oxy-hydroxide), or by take up in microbial species present on these materials. The U could then concentrate in this mixture at some level depending on the amount that could potentially be adsorbed on these materials.

The analysis in Section 5.6 indicated that the most likely mechanism for fissile material accumulation in the invert will be from adsorption and ion exchange with calcium-rich zeolites like those listed in Table 5.6-1. A representative configuration which could result involves concrete degradation to a representative calcium-rich zeolite, chabazite $\text{CaAl}_2\text{Si}_4\text{O}_{12}\cdot 6(\text{H}_2\text{O})$, and its base aggregate. The aggregate is assumed to be crushed, welded tuff (no zeolite) from the repository with a porosity of 0.139 (Reference 39 p.7-11, Reference 40, p. 16). Chabazite, $\text{CaAl}_2\text{Si}_4\text{O}_{12}\cdot 6(\text{H}_2\text{O})$, is a representative calcium-rich zeolite with a high hydrate content which could form from the reaction of the glass reaction products present in effluent water and the degraded concrete as discussed in Section 5.6. Chabazite will be assumed to represent the mix of zeolites which might be present in the invert. The chabazite (or similar zeolite) could adsorb up to 1 weight percent U based on the results from laboratory experiments (Reference 41). The invert has a cylinder segment geometry similar to the clayey material configuration inside the WP, and the accumulation of ^{235}U would likely conform to roughly this geometry.

Other mechanisms such as the adsorption onto existing zeolitic material in the tuff invert and the precipitation of U as a result of reduction in dissolved oxygen were not considered likely or have lower accumulation concentrations. The adsorption onto steel corrosion products and the interactions with microbes may be possible, but it will be necessary to obtain data and/or models for these processes before these mechanisms can be evaluated.

6.1.3 Other Configurations

Two other configurations discussed in Section 5.1 will not be further considered as part of this analysis: fissile precipitation on container walls, and degraded forms in configurations similar to the initial configuration. The latter is considered similar to the initial WF configuration previously evaluated in Reference 2 and need not be further evaluated as a degraded WF from a criticality standpoint. As discussed previously in Section 3.1.2, the criticality potential of the former

configuration is limited by the low thickness of the precipitate (high leakage geometries) and the potential for re-dissolution. Thus it will not be further considered.

6.2 TYPICAL CONFIGURATIONS FROM CERAMIC WASTE FORM DEGRADATION

The configurations that could lead to a potential criticality for the ceramic WFs include the slumped to bottom case, for internal criticality, and invert accumulation for external criticality. Other configurations are possible, but these are unlikely to lead to significant potential for criticality.

6.2.1 Slumped to Bottom

If the altered WF disintegrates completely as a result of metamictization, the resulting mass will slump (collapse) to the bottom of the WP onto any remaining clayey material and silicates. This material could present a criticality concern if the Gd is removed as a result of the decrease in pH of the system.

The model for the homogenized clayey material that could slump to the bottom was shown in Figure 6.1.1.-1. The configuration for the ceramic is assumed to be that described for the Pu glass and the generation scenario is also assumed to be the same. The majority of the DHLW glass would be expected to have degraded prior to the degradation of the ceramic material due to the fact that it is exposed first and has a degradation rate significantly higher than that of the Pu ceramic material. The DHLW glass will have degraded into clayey material and other minerals which have slumped to the bottom of the package, along with any remaining pieces of the DHLW glass canisters and the degraded ceramic canisters and WFs. It has been assumed that the ceramic material at this point in time will have undergone considerable metamictization and disintegrated into small particles which are dispersed into the clayey material. Both the bulk, early in time, and the particulate ceramic material, later in time, will be slowly dissolving. The Pu, U and Gd released into solution will either precipitate as other mineral phases or remain in solution, depending on the system pH and chemistry. These mineral phases will precipitate back onto the particles or onto the clayey material. The composition of the clayey material was defined in Section 5.5.2 and listed in Table 5.5.2-1. The clayey material has density of 3.0 g/cm^3 which is calculated as the mass ratio of the elemental components from Table 5.5.2-1 to those in Table 5.4.5-1 times the density used for the degraded glass clayey material (2.3 g/cm^3). The geometry of the dispersion of the ceramic WF into the clayey material would be similar to that shown in Figure 6.1.1.-1.

Several less likely variations of the final configuration were discussed in Section 6.1.1. These variations were not analyzed for the ceramic case since the volume of the clayey materials will be lower and the amount of contained water will be considerably less than that for glass, reducing the effect on k_{eff} of these variations.

6.2.2 Invert Accumulation

The accumulation of fissile material outside the WP is essentially independent of the original WF, with only the time range of the accumulation being affected. Therefore, the discussion in Section 6.1.2 is equally applicable to the degraded ceramic WF.

6.2.3 Other Configurations

Other configurations for internal criticalities which are possible include precipitation on the walls, and slow dissolution of the ceramic in a degraded but initial shape. The amount of material that could precipitate and collect on the walls has been calculated to be very small and would not result in a critical state. Slow dissolution of an altered WF which retains its shape, even though its has transformed to a metamict state, would result in both the fissile and neutron absorber materials being slowly flushed from the system. Thus, this configuration does not present a criticality concern.

PREDECISIONAL DOCUMENT

INTENTIONALLY LEFT BLANK

7. CRITICALITY CALCULATIONS (k_{eff})

The criticality potential of Pu immobilized in glass and ceramic for intact configurations has been previously analyzed (Reference 2). It was shown that as long as the neutron absorbing species (Gd) remains with the fissile species (U, Pu), a criticality is not possible (even with the presence of an optimum amount of water to serve as moderator). Some simple generic configurations resulting from the degradation of the glass and ceramic WFs were also analyzed. Criticality of these degraded WFs was shown to require both significant separation of the absorber material from fissile material and significant intermixing with moderator material (water).

This study has extended the initial analyses to evaluate the variety of configurations represented by the material compositions and geometries identified in Sections 4 and 6. The criticality potential of a variety of compositions (of the principal neutronically significant species) in degraded configurations within a WP was evaluated by calculating the effective multiplication factor, k_{eff} , using the Monte-Carlo neutron transport code, MCNP4A. The criticality potential of accumulations of ^{235}U transported outside the WP into the invert was also evaluated. A multi-variate regression fit was then made to the data for configurations inside the WP to predict k_{eff} as a function of Pu, U, and Gd mass. The regression equations are programmed into the mass balance program (described in Section 3.2.1 and listed in Appendix B) and are used to determine when sufficient fissile material has been separated from the Gd, or intact WF for k_{eff} thresholds to have been reached.

This general methodology is described further in Sections 7.1 and 7.2. A summary of the coupled mass balance/criticality results is given in Section 7.3. Section 7.4 gives comparisons of four Pu canisters per WP versus one Pu canister per WP and can-in-can glass versus can-in-can ceramic.

7.1 BASIC CALCULATIONS WITH MCNP

The calculations described in this section are performed to indicate the minimum amount of Gd required to keep the k_{eff} below thresholds of 0.98 and 0.93 for combinations of different ^{239}Pu and ^{235}U masses covering the credible range from the degraded WFs inside the WP. In addition, calculations to determine the minimum mass of ^{235}U which must be accumulated in the invert to exceed these same thresholds are performed.

7.1.1 Clayey Configuration from Degradation of DHLW Glass and Pu Immobilization Glass

Based on the scenario and configuration analyses described in Sections 5.1 and 6.1, the primary criticality analysis is focused on a clayey material containing the fissile species dissolved from the glass and (possibly) some of the Gd dissolved from the glass in a cylinder segment (hemicylinder) geometry. The cylinder segment represents an accumulation of material in the WP shell and is similar to a hemicylinder but is more than 50% of the WP volume. Figure 6.1.1-1 shows a typical cross-sectional view of the model configuration. The inner dimensions of a degraded WP are approximated in the model inner radius of the shell as 78.25 cm and the inner length as 304 cm.

PREDECISIONAL DOCUMENT

A representative composition of the elements in the clayey solids is determined by the mineral species remaining at the end of typical EQ3/6 runs modeling the chemical reaction over time of the glass with water and the other components in the WP (particularly the steel of the canisters and cans). These runs are described in Section 5.3.5. This clayey composition is assumed to be representative of the range which could occur under credible degradation scenarios as discussed in Section 6.1.1. The elemental components of the solids making up the clay are shown in Table 5.4.5-1 and the minerals/compounds composing the solids are discussed in Section 5.4.5.

DHLW glass contains a significant amount of depleted U. However, DHLW glass degrades much faster than the Pu glass so a significant fraction may be transported outside the WP during a period of alkalinity before significant amounts of U are released from the Pu glass. EQ3/6 cannot differentiate between isotopes or original sources for elements. For this reason, no depleted U is included in the base calculations. However, there is an estimate of the sensitivity of k_{eff} to include various amounts of ^{238}U in the clayey mixture as discussed in Section 7.5.4.

Clays contain water in two forms: a fixed amount of hydrogen (bound as $\cdot\text{H}_2\text{O}$ or OH) and a variable amount of free water. The bound H for the degraded glass clayey material has the same atom density as H in 33.7 volume percent free water. The volume fraction of free water in the clayey material is unknown and is varied to find the highest k_{eff} value for Gd, U, and Pu mass combinations. The H in water or in the clayey compounds moderates (slows down) the neutrons from fission so that they can more effectively be absorbed to cause fissions. As the neutrons are moderated, they can also be more effectively absorbed by materials that don't fission. An optimum amount of H can be found which maximizes the ratio of fissions to absorptions (optimum moderation).

A number of ^{239}Pu and ^{235}U mass combinations covering the credible range from the degraded WFs inside the WP were identified based on preliminary mass balance calculations. The free water fraction and the Gd mass for these ^{239}Pu and ^{235}U combinations were varied to find the maximum amount of Gd required to meet the k_{eff} threshold values of 0.93 and 0.98. For all of the ^{239}Pu and ^{235}U mass combinations the highest required mass of Gd was found at zero water fraction (no free water but including all the H in bound water). Furthermore, it was found that, generally, the ^{239}Pu was worth significantly more in k_{eff} than the equivalent mass of ^{235}U because of the ^{239}Pu resonance neutron absorption (with subsequent fission) centered at approximately 0.25 eV. This resonance becomes very important in the presence of Gd because the high thermal absorption of Gd leads to a skewed neutron energy distribution with a reduced neutron flux in the thermal region and relatively high flux in the higher energy regions which expose the neutrons to the ^{239}Pu resonance. In the absence of Gd, the ^{239}Pu is still worth more (in terms of k_{eff}) than ^{235}U , but the difference in worth is not nearly so significant.

To establish the methodology for identifying accumulations of material where criticality could occur (screening configurations), calculations were performed for various amounts of Gd to provide cases with k_{eff} values ranging from 0.9 to 1.0 for given combinations of ^{235}U and ^{239}Pu . Details of these cases are shown in Appendix G and a discussion of criticality (k_{eff}) thresholds is given in Section 3.1.4.

The discussion of clay composition used for input to the MCNP calculations can be summarized as follows:

- A. The static (time independent) components of the clay are those given in Table 5.4.5-1; except for U and Pu, these components reflect contributions from both the filler glass and the WF glass, as filtered through EQ3/6, which reflects their individual solubilities.
- B. The concentrations of U and Pu are determined as a function of time from the dynamic mass balance equations, reflecting only the fractions of those elements that have been released by WF dissolution up to the time of calculation. These mass balance equations utilize solubilities determined by analyses using EQ3/6 and the appropriate thermodynamic equilibrium coefficients. The concentration of Gd is varied to provide a distribution of resulting k_{eff} values.
- C. The specific set of U, Pu, and Gd concentrations actually used in MCNP calculations are taken to be representative of the range of values determined by the mass balance equations for times up to 100,000 years.
- D. This nominal case is equivalent to assuming, with respect to U, Pu, and Gd, that the undissolved WF is outside the clay. This is the configuration described in Section 6.1.1.1.

The nominal configuration described in the previous paragraph is the extreme conservative case, in which none of the Gd remaining in the undissolved WF is available for criticality control. The opposite extreme is for all the undissolved WF to be uniformly distributed throughout the clay, so that the remaining undissolved Gd can have the maximum criticality control effect. Since this configuration represents the extreme of non-conservatism with respect to the parameter of Gd concentration in the potentially critical mass (the clay), it has not been used as the nominal configuration. Criticality calculations have, however, been made for this configuration, and it was found that the general conclusions of the study were not affected. Although the criticality potential was reduced by comparison with the nominal configuration, it still remains significant. The comparison of results for these two opposite configurations is given in section 7.3.3

7.1.2 Clayey Configuration from Degradation of DHLW Glass and Pu Immobilization Ceramic

Because the major component of both a waste glass and waste ceramic is the DHLW filler glass, the examination of the degradation process into a clayey configuration will be similar for the two WFs, and this discussion will be similar to that in Section 7.1.1.

A representative composition of the clayey solids for the degraded DHLW glass/ceramic is taken from an EQ3/6 run modeling the chemical reaction over time of the DHLW glass and Pu immobilization ceramic with water and the other components in the WP. As with the glass WF, this clayey composition is assumed to be representative of the range which could occur under credible degradation scenarios as discussed in Section 6.2.1. This clayey composition would also represent chunks of partly degraded ceramic in a glass clay. The elemental components of the solids making

up the clayey material are shown in Table 5.5.2-1. As noted in Table 5.5.2-1; 2 wt% of the Zr is assumed to be Hf. The effect of varying the wt% of Hf is discussed in Section 7.5.5.

It should be noted that, with both the glass and ceramic WFs, most of the clayey material comes from the filler glass which is essentially the same for both cases. There are however differences in clayey composition due to the quite different chemical compositions of the WFs and the much longer time to degradation for the ceramic WF. The most important of these differences neutronically is the much higher Hf (a major neutron absorber) concentration due to the greater zirconium concentration in the ceramic WF. These different WFs also result in somewhat different mineral inventories for the clayey mass as output by the EQ3/6 runs. Of these ancillary differences, the one of greatest importance is the lower water of hydration in the clayey mass from the ceramic WF: equivalent of 20.7 volume percent water as contrasted with 33% for glass. This difference in water of hydration is manifested by the lower H amount in Table 5.5.2-1 as compared with Table 5.4.5-1.

A number of ^{239}Pu and ^{235}U mass combinations were run for the glass WF. For combinations of ^{239}Pu and ^{235}U requiring more than about 2.5 kg Gd to fall below a k_{eff} of 0.98, the highest value of k_{eff} was found at zero water fraction (no free water but including bound H). For combination of ^{239}Pu and ^{235}U requiring less than about 2.5 kg Gd, the highest value of k_{eff} was found at 0.10 or greater water fraction. Because of the approximately 0.25 eV resonance in the ^{239}Pu fission cross-section, the ^{239}Pu was worth significantly more than the equivalent mass of ^{235}U in the presence of Gd. In the absence of Gd, the ^{239}Pu is still worth more than ^{235}U , but the difference in worth is not nearly so significant. Note that the degraded ceramic waste clayey composition contains only about two-thirds of the H as the degraded glass waste clayey composition. The lower water fraction, coupled with the Hf from the ceramic (with lower required mass of Gd), cause the peaking at a higher free-water fraction than the corresponding degraded glass cases.

Just as for the glass WF, calculations were performed for various amounts of Gd to provide cases with k_{eff} values ranging from 0.9 to 1.0 for given combinations of ^{235}U and ^{239}Pu . Details of these cases are shown in Appendix G.

This discussion of clay composition can be summarized in the same manner as was done for the glass WF in the last two paragraphs of Section 7.1.1, except that the WF is now ceramic, and the static compositions are found in Table 5.5.2-1, which, unlike Table 5.4.5-1, also contains a typical value for Gd.

7.1.3 Accumulations of ^{235}U Outside the WP In or On the Invert

Scenarios for accumulating fissile material outside the WP in or on the invert are discussed in Section 5.6. The accumulation of fissile material outside the WP is essentially independent of the original WF, with only the time range of the accumulation being affected. No credible mechanism for precipitating U compounds out of solution was identified in the geochemical analysis discussed in Section 6.1.3 and 6.2.3. Adsorption by zeolites in the tuff or ferrous oxides is possible but is limited to relatively low concentrations. In the time frame required to accumulate kilograms of fissile material any ^{239}Pu adsorbed would likely be decayed to ^{235}U . Therefore, this analysis focuses on accumulations of ^{235}U alone. Since the fractions of absorbers transported from the WP is uncertain and variable with conditions (pH), no credit for absorbers or other material from the WP

is taken in this analysis. The results in this section are equally applicable for either the glass or ceramic Pu immobilization WFs.

As discussed in Section 6.1.2, the concrete has been assumed to degrade to a representative calcium-rich zeolite, chabazite $\text{CaAl}_2\text{Si}_4\text{O}_{12}\cdot 6\text{H}_2\text{O}$, and its base aggregate as discussed in Section 6.1.2. The aggregate is assumed to be crushed, welded tuff from the repository with a porosity of 0.139 (0.10 volume fraction filled with water). The chabazite is assumed to adsorb approximately 1 weight percent U based on the results from laboratory experiments (Reference 41). In the model the invert depth is 0.75 m and the drift is 5.5 m which is consistent with current scoping designs. Calculations were performed for a cylinder segment geometry similar to the clayey configuration in the WP. The length of the accumulation was varied as well as the hydrogen content (100%, 90%, and 80%) to find optimum moderation. The chabazite has the highest water fraction of a group of calcium-rich zeolites and the 0.10 volume fraction filling by water of the aggregate porosity is high, therefore justifying the investigation of the effect of reduction in hydrogen content to cover other compositions. The lengths run are 150 cm, 300 cm, and infinity. The 150 cm length and 300 cm length correspond to roughly 25 kg and 50 kg of ^{235}U , respectively. The results of the calculations are shown in Table 7.1.3-1. Note that none of the cases exceed the 0.98 criticality threshold. The 90% of base hydrogen loading cases are closest to optimum moderation (k_{eff} peak) and do exceed a 0.93 criticality threshold for about 204 cm or 34 kg (interpolating) of ^{235}U .

Table 7.1.3-1 Accumulations of 1 wt% ^{235}U in Chabazite (40%) and Aggregate (60%) from Degraded Concrete in a 75 cm Deep Cylinder Segment

Hydrogen Fraction In Chabazite/Aggregate	150 cm / 25 kg ^{235}U	300 cm / 50 kg ^{235}U	- length
100% H	0.9178 ± .0020	0.9459 ± .0018	0.9544 ± .0019
90% H	0.9201 ± .0023	0.9469 ± .0043	0.9616 ± .0023
80% H	.	.	0.9589 ± .0026

7.2 MULTI-VARIATE REGRESSIONS FOR DEGRADED GLASS AND CERAMIC WASTE FORMS

Using the results of the MCNP4A runs discussed in Sections 7.1.1 and 7.1.2, multi-variate regressions were developed for both the degraded glass and ceramic WFs. This will allow k_{eff} to be computed as a function of the mass (in kg) of Pu, U, and Gd in the hemicylinder of clayey material. For each WF, multiple regressions were required to generate a good fit to the wide range of Pu, U and Gd contents. These regressions are only applicable for predicting Pu/U/Gd combinations which yield k_{eff} values from 0.9 to 1.0, as the majority of the MCNP4A data (given in Attachment G) was within this range. In most cases, a linear regression in the form of

$$k_{\text{eff}} = c_1 + c_2 \text{Pu} + c_3 \text{U} + c_4 \text{Gd} \quad (1)$$

PREDECISIONAL DOCUMENT

was sufficient to provide a good fit to the MCNP4A data. For larger amounts of Pu and U in the clayey material, the amounts of Gd required to produce k_{eff} values in the above range became non-linear, and the following equation provided a better fit than Equation 1:

$$k_{eff} = c_1 + c_2 Pu + c_3 U + c_4 \ln(Gd) \quad (2)$$

For each WF, Table 7.2-1 provides the constants for Equations 1 or 2 (as applicable), their ranges of applicability, and the R^2 value indicating the goodness-of-fit.

Table 7.2-1. Coefficients for Glass and Ceramic WF Regressions

Waste Form	Eq.	Applicable Range	c_1	c_2	c_3	c_4	R^2
Glass	1	Gd = 0 kg	0.53431	0.01514	0.00819	0	0.991
Glass	1	0kg < Gd ≤ 1kg	0.72902	0.00803	0.00397	-0.26981	0.953
Glass	1	1kg < Gd < 4kg	0.72582	0.00532	0.00233	-0.09609	0.945
Glass	2	Gd ≥ 4 kg	0.82278	0.00342	0.00148	-0.17762	0.984
Ceramic	1	Gd ≤ 0.2 kg	0.44828	0.01012	0.00483	-0.36997	0.978
Ceramic	1	0.2 kg < Gd ≤ 1 kg	0.62518	0.00658	0.00301	-0.17972	0.981
Ceramic	1	1 kg < Gd ≤ 2.5 kg	0.67725	0.00478	0.00205	-0.08524	0.978
Ceramic	2	Gd > 2.5 kg	0.75870	0.00298	0.00135	-0.11954	0.981

All of the above regressions were performed in Microsoft Excel version 5.0 spreadsheets, the results from which are provided in Appendix G. Since the percentage of water in the clayey material was not to be considered in the mass-balance the above regressions utilized the water fractions which yielded the peak k_{eff} values for conservatism. As discussed in Sections 7.1.1 and 7.1.2, this peak was at the zero water fraction for most cases, with the exception being Gd ≤ 2.5 kg in the ceramic cases, for which a water fraction of 0.1, or greater, yielded the highest k_{eff} values.

7.3 COUPLED MASS BALANCE/CRITICALITY EVALUATIONS AND RESULTS

The mass balance equations of Section 3.2.1 were used to compute the amounts of Pu, U, and Gd in the clayey precipitate as a function of time, using the three programs listed in Appendix B. These programs incorporate the formula for Gd solubility from 5.3.4, and the regression for k_{eff} as a function of Pu, U, and Gd concentration for both glass and ceramic WFs, as developed in Section 7.2. The first two of the programs in Appendix B reflect the two modes of analysis:

- Screening for the values of Pu, U, and Gd concentration in the clayey material at which a criticality first occurs (pugdcr.c)
- Listing the time history of k_{eff} (pugdkeff.c).

The initial WF dissolution rate is reduced with time so that it is proportional to the remaining WF surface area, which is assumed to be proportional to the 2/3 power of the remaining WF mass. The third program (critload.c) is used to search for the limiting values of dissolution rate multiplied by fracture factor, referred to as the dissolution product factor (DPF), particularly as a function of Pu loading, as described in Section 7.4.1.

The oxidized Cr, which is responsible for the acidification of the solution in the WP, is assumed to come from corrosion of the stainless steel only (canister and WF containing cans). Since the stainless steel is mostly in sheet form, the surface area, and consequently the dissolution rate, is constant until most of the steel has degraded, so in this approximation the dissolution rate has been left constant. The basic input parameters for these analyses are in the ranges listed in Table 7.3-1.

Table 7.3-1. Summary of Input Parameters for Criticality Evaluations

Parameter	High value	Low value
pH ⁽¹⁾	7.5	5.5
Gd solubility (ppm) ⁽²⁾	3000	0.02
Pu solubility (ppm) ⁽²⁾	6x10 ⁻³	1
U solubility (ppm) ⁽²⁾	20	1
Glass WF DPF (g/m ² /day) ⁽⁴⁾	20x10 ⁻³	.5x10 ⁻³
Ceramic WF DPF (g/m ² /day) ⁽⁴⁾	20x10 ⁻³	.5x10 ⁻³
Stainless Steel corrosion rate (µm/1000yr) ⁽⁵⁾	0.15	0.05
Infiltration rate (mm/yr) ⁽⁶⁾	10	0.1

- ⁽¹⁾ This limited range is appropriate after the dissolution of most of the filler glass, when the released alkali ions have been removed by from the WP by flushing.
- ⁽²⁾ The high value of Gd solubility is determined by the formula in Section 5.3.4; the low value is taken from the pH=7.5 value in Table C-4. Note that the high value of Gd solubility corresponds to the low value of pH, and vice-versa.
- ⁽³⁾ These ranges fall within the larger range of possibilities given in Table 4.2-1.
- ⁽⁴⁾ These are typical of the mid-range of the products of the dissolution rate values in Table 4.1-1 with the fracture factor values in Table 4.1-2. It should be noted that the same range has been used for both the ceramic and glass WFs. This represents an assumption of an unlikely high degree of metamictization made for purposes of comparability only.
- ⁽⁵⁾ This range is consistent with the values given in Table 4.1-3.
- ⁽⁶⁾ This range is the same as given in Table 4.3-1.

The primary scenario for reaching a critical configuration in these evaluations is the removal of Gd from the WP by flushing as quickly as it is released from the degrading WF, as long as the pH is low which means that the Gd solubility is high. A variation on this scenario is the accumulation of Gd precipitate while the Gd release rate from the WF is faster than the Gd removal rate. The criticality is then delayed until the Gd release rate is slowed sufficiently that the removal rate can catch up and reduce the Gd in the precipitate to the point where there is sufficient fissile material for criticality.

The programs listed in Appendix B begin the corrosion of stainless steel immediately after the breach of the WP barriers, which is taken to be 3500 years, as discussed in Section 3.1.1. These programs begin the buildup of fissile material in the clayey precipitate 2500 years later, which is the additional time for most of the filler glass to degrade (at a fracture factor of 30 and a DHLW glass dissolution rate of 10^{-3} g/m²/day) and the alkali components to be flushed from the WP, so that the corroding stainless steel can reduce the pH to the point where the Gd solubility is so large, that almost all of the Gd can be flushed from the WP as fast as it is released from the WF. In this total 6000 years, 22% of the ²³⁹Pu will have decayed into ²³⁵U, so the programs begin the buildup with this ratio. It should be noted that this time to start of buildup is shorter than the 8000 year estimate given in Section 7.3.1 in connection with Figure 7.3.1-4. The shorter estimate given here means that less ²³⁹Pu will have decayed to ²³⁵U which is conservative, since the ²³⁹Pu is more reactive with respect to criticality than the ²³⁵U as is shown by the actual k_{eff} calculations summarized in Appendix G.

In the time between the breach of the WP and the onset of acid conditions following degradation of the filler glass, some of the WF could also be degraded and release some fissile material. If the pH is high enough (above 9) to make the U and Pu very soluble, a significant fraction of the amounts released from the WF could be removed from the WP during this short time. Since it is not certain that the alkali from the dissolving filler glass will drive the pH sufficiently high, particularly with the presence of the acidifying chromate from the corroding stainless steel, it has been assumed that all of the U and Pu released from the WF will be retained in the clayey precipitate. It is further assumed that any Gd released during this interim time will be re-dissolved and removed from the WP when the filler glass has fully degraded and the solution becomes acidic from the corroding stainless steel. The algorithms used do account for the loss of Cr which is released during this time, thereby reducing the period when the package solution can be acidic, which, in turn, reduces the potential for criticality.

The stainless steel containing Cr is used for both the canisters and the WF cans. The WF cans, being only 3/8 as thick as the canisters, will corrode completely long before the canisters, so they will not affect the duration of acid conditions. The corroding WF cans will increase the steady state Cr in solution, but only by their fraction of the canister mass, 25%. Furthermore, this increased Cr in solution will only last as long as the cans are corroding. Therefore, in keeping with the approximations used in this study, the Cr in the WF cans has been omitted.

7.3.1 Glass WF Results

The nominal criticality behavior for the WPs with degraded Pu glass WFs is summarized by Figures 7.3.1-1 through 7.3.1-7. These are explained by the following paragraphs.

Figure 7.3.1-1 gives k_{eff} as a function of time after the start of WF dissolution, for the nominal stainless steel corrosion rate of 0.1 μ m/yr, and for a family of values of the DPF (WF dissolution rate in g/m²/day multiplied by the fracture factor). All times in this study are measured from the start of WF dissolution, approximately 5,000 years (Section 3.1.1). The values chosen for the DPF are typical of the mid-range given in Table 4.3-2. For these typical values, the analysis results in sufficient chromate in solution to lower the pH to between 5 and 6 so that the Gd goes into solution as quickly as it is released by the WF dissolution, and is flushed from the WP so that it cannot collect in the precipitate (clayey material). As the fissile material is released from the WF and accumulates

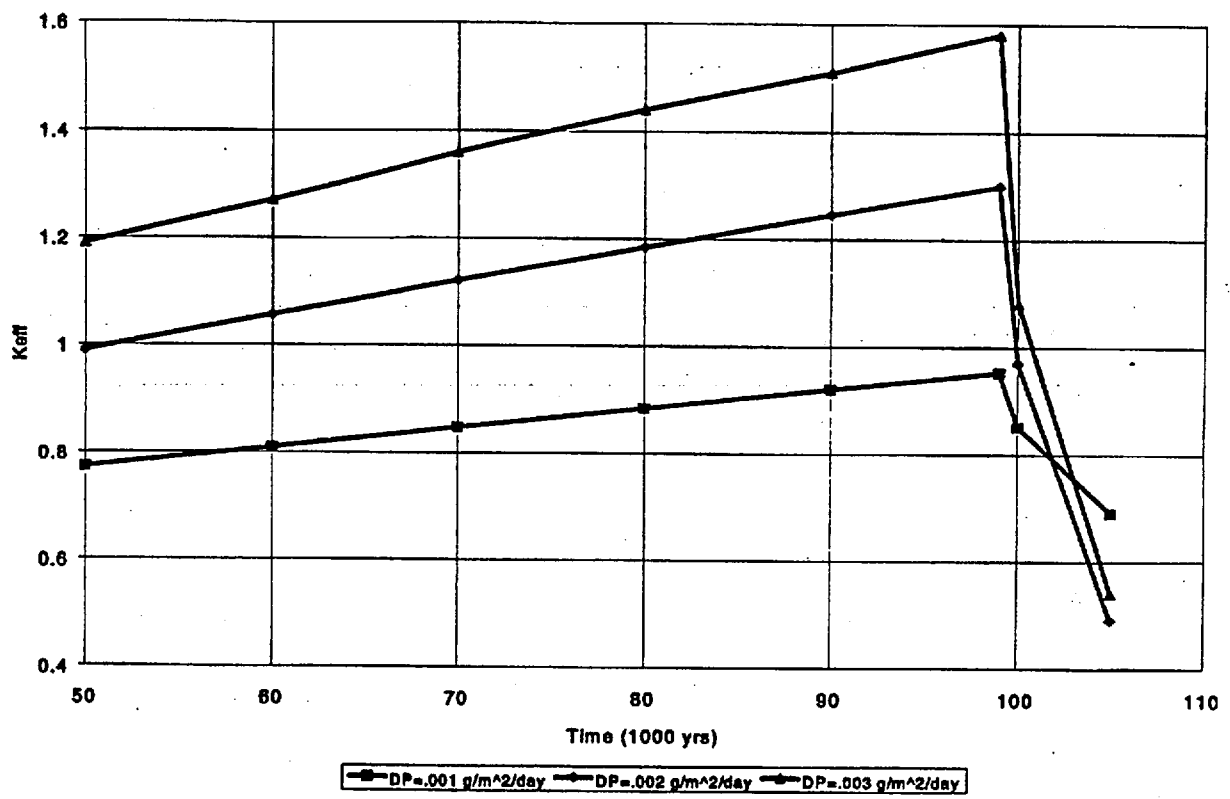


Figure 7.3.1-1. K_{eff} vs Time Glass Waste Form, Infiltration Rate = 1 mm/yr, Stainless Steel Corrosion Rate = 0.1 $\mu\text{m/yr}$

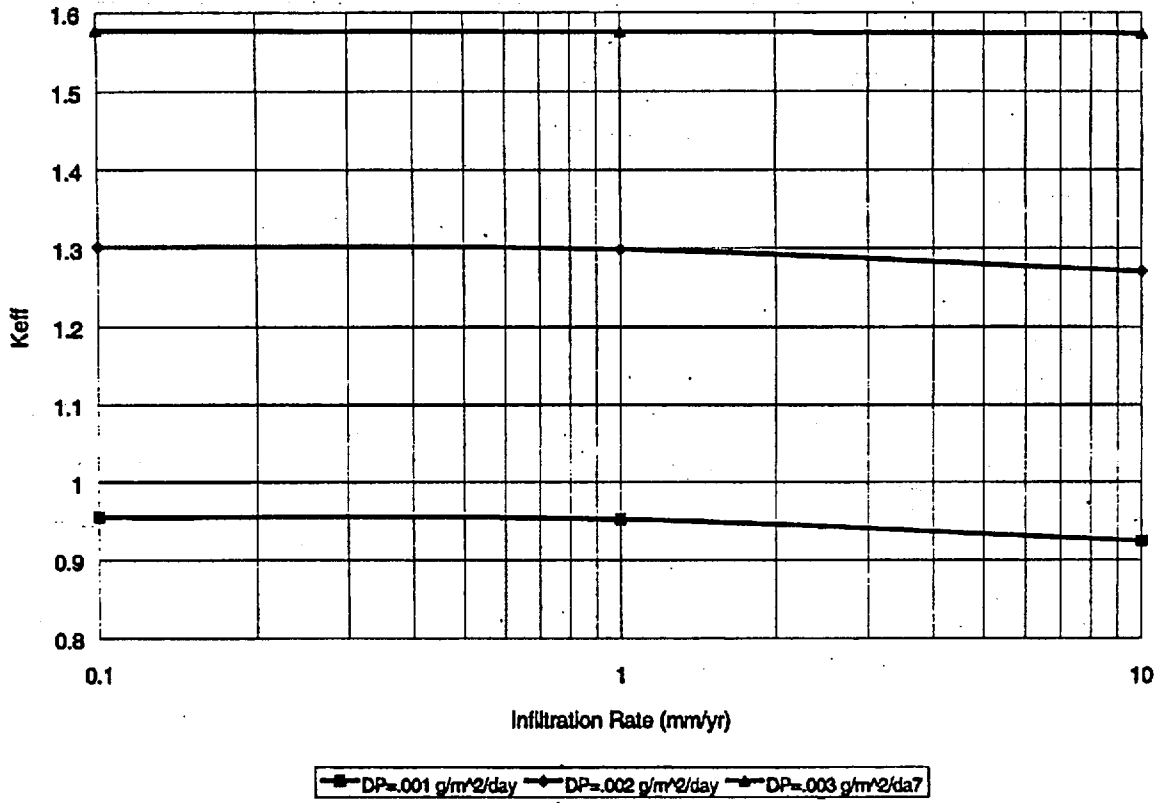


Figure 7.3.1-2. Peak k_{eff} vs Infiltration Rate, DPF Family, Glass WF Stainless Steel Corrosion Rate = 0.1 $\mu\text{m/yr}$

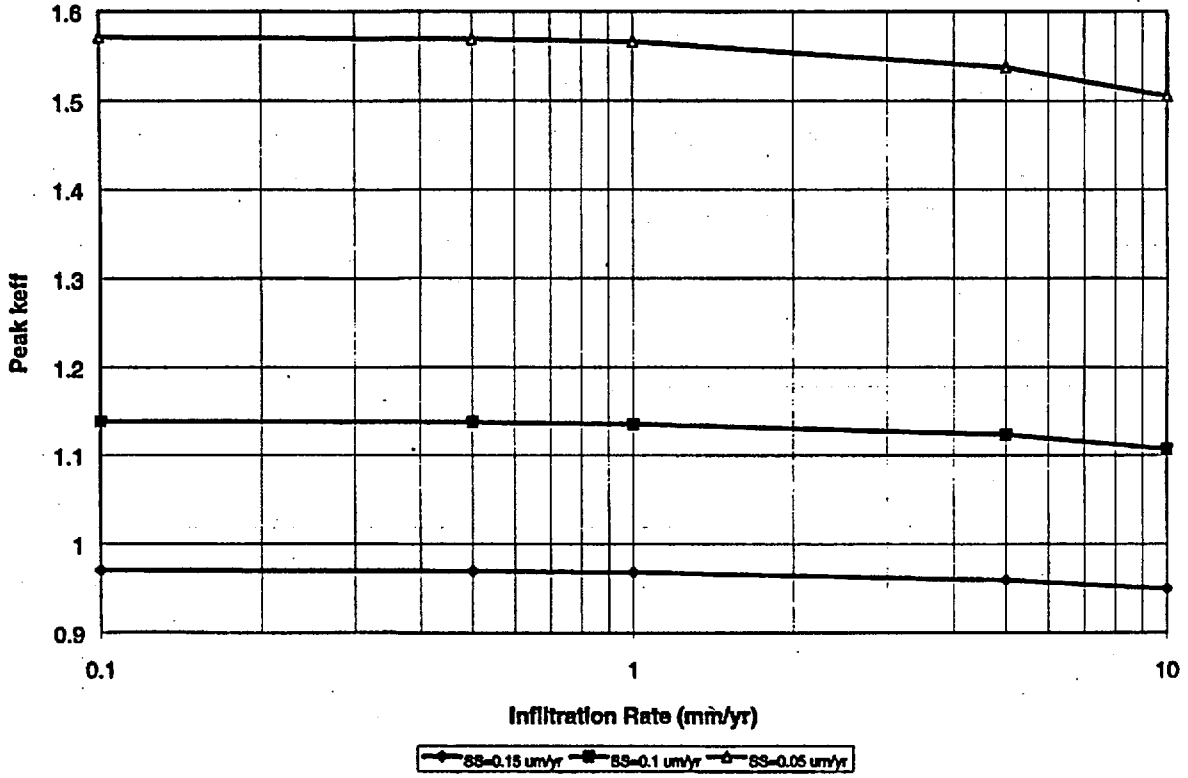


Figure 7.3.1-3. Glass WF: Peak k_{eff} as a Function of Infiltration Rate for Typical Values of Stainless Steel Corrosion Rate at DPF = $1.5E-3$ ($\text{g/m}^2/\text{day}$)

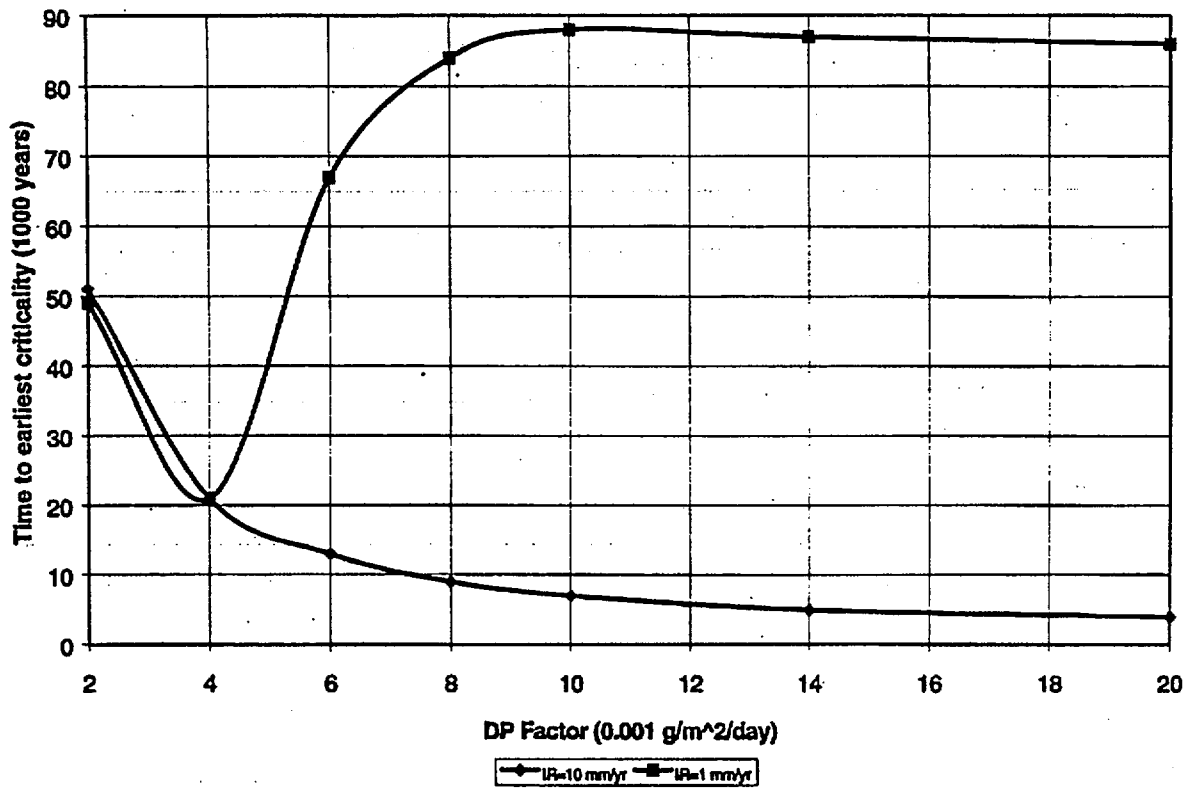


Figure 7.3.1-4. Glass WF: Years (1000) to Earliest Criticality, Stainless Steel Corrosion Rate = 0.1 $\mu\text{m}/\text{yr}$, pH = 5.5

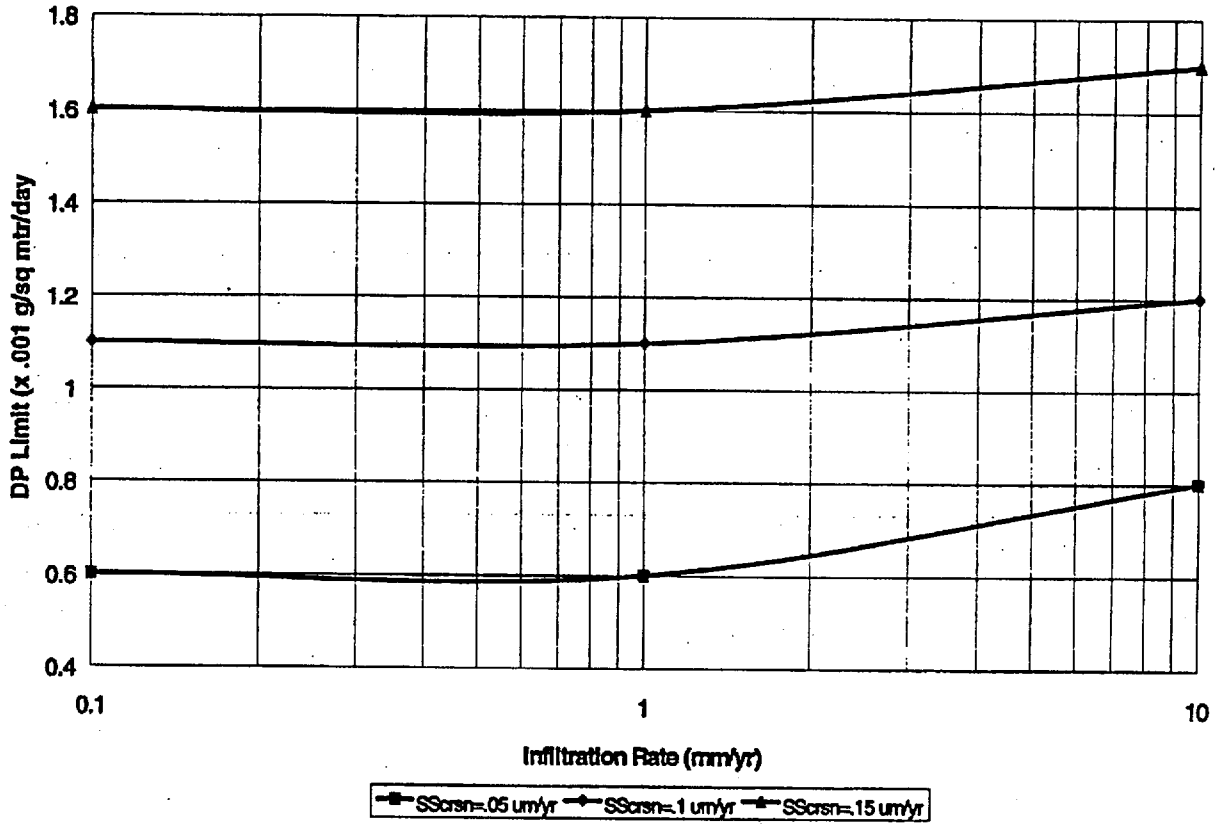


Figure 7.3.1-5. DPF Limit for $k_{eff} = 0.98$, Glass WF

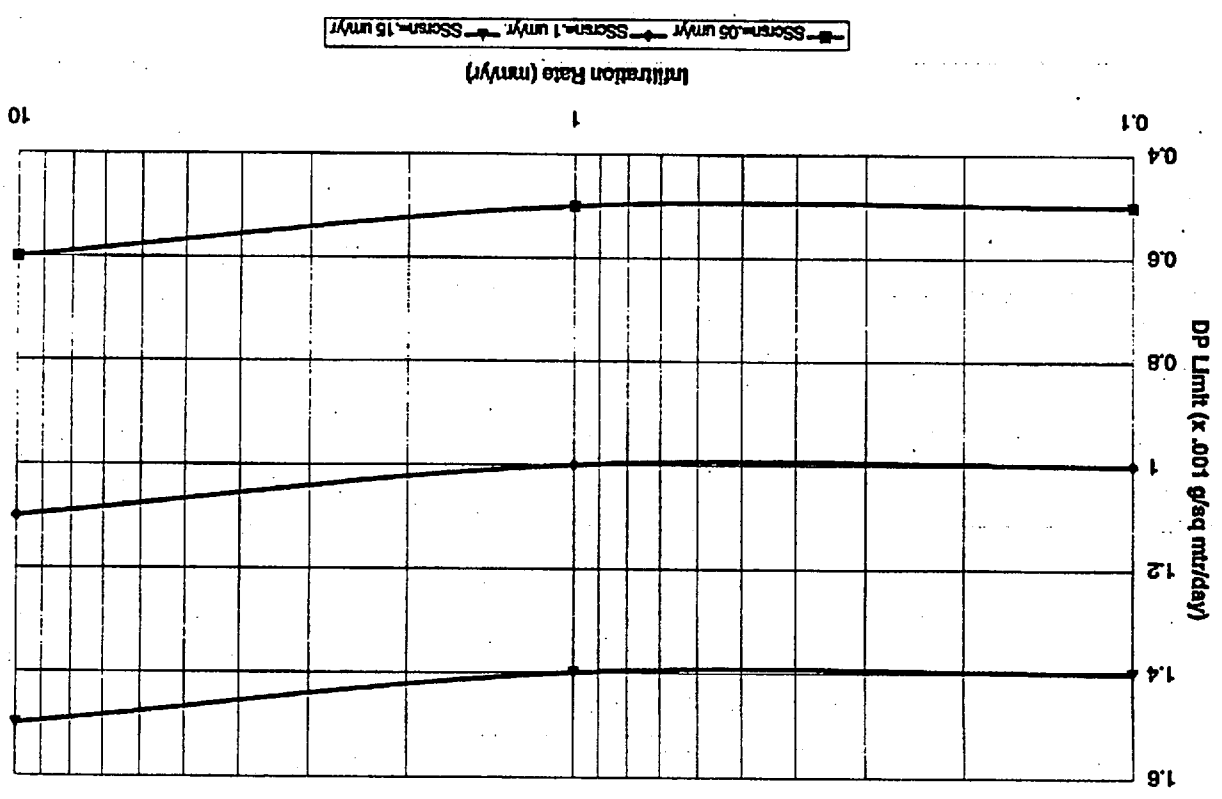


Figure 7.3.1-6. DPF Limit, $K_d = 0.83$, Glass WF

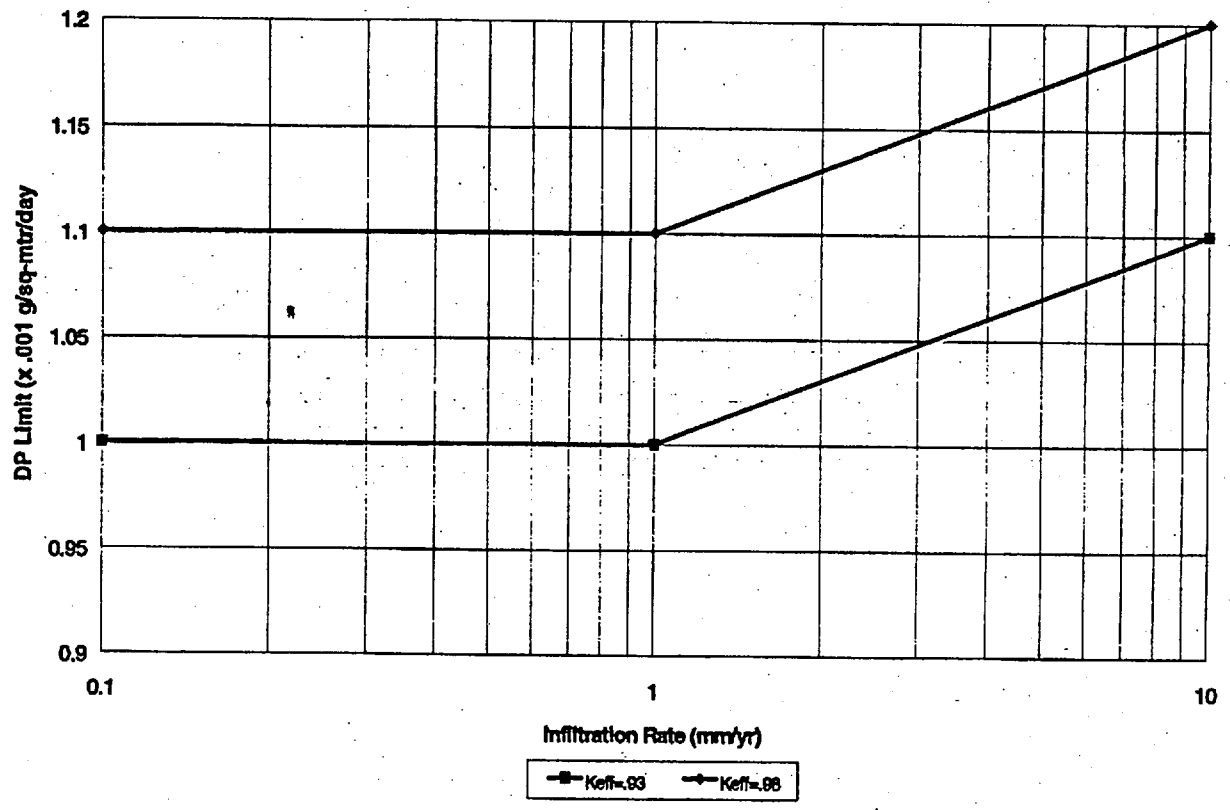


Figure 7.3.1-7. DPF Limit, $k_{eff} = 0.96$ and 0.93 , Glass WF Stainless Steel Corrosion Rate = 0.10

with time in the clayey material, k_{crit} shows a steady increase. Under the assumed dissolution rate for the stainless steel, all of the steel has degraded by approximately 99,000 years, after which the chromate in solution declines as it is flushed from the WP so that the pH rises and Gd precipitates with the result that k_{crit} drops to an insignificant value within the next 2000 years. Comparison of the curves for the three values of DPF shows a strong dependence on this parameter. This is because the model determines the peak k_{crit} by the amount of fissile material which is released from the WF to precipitate in the clayey mass while the pH is low (before all the stainless steel has corroded). The higher the DPF, the more fissile mass can accumulate before Gd starts precipitating to lower the k_{crit} . It should be noted that the values of k_{crit} greater than 1.0 and lower than .9 are for comparison purposes only; their absolute values are not meaningful, since the regression is only tested for the limited range 0.9 to 1.0.

Figure 7.3.1-2 gives the peak k_{crit} over time as a function of the infiltration rate for a family of WF DPFs. In general, increasing the infiltration rate from 0.1 to 10 mm/yr results in higher amounts of U being removed from the package, thus reducing the concentration of U in the clayey material and lowering k_{crit} . Increasing the infiltration rate from 0.1 to 10 mm/yr will also reduce the chromate concentration in solution, thereby increasing the pH, which in turn lowers the Gd solubility so that some can precipitate into the clayey material and lower k_{crit} . Decreasing the infiltration rate from 0.1 mm/yr to 0.05 mm/yr has little effect on k_{crit} because the Gd solubility is so high that the Gd can be removed from the WP much faster than it is released from the WF dissolution. The Gd solubility is presumed to saturate at some point; if it occurs at 15,000 ppm, then an infiltration rate below 0.05 mm/yr will be too slow to remove the Gd as fast as it is released from the WF (for the range of DPF indicated in this Figure 7.3.1-2) so some Gd will precipitate in the clayey material and the package cannot become critical.

Figure 7.3.1-3 gives peak k_{crit} over time as a function of infiltration rate for a family of stainless steel corrosion rates (0.05 to 0.15 $\mu\text{m}/\text{yr}$). The k_{crit} generally increases as the corrosion rate decreases, because the length of time with low pH is increased allowing for higher buildup of fissile material in the clayey precipitate. (Although the concentration of chromate, and hence the Gd solubility, decreases with decreasing stainless steel corrosion rate, the Gd solubility still remains high enough for the prompt removal of any Gd released by WF degradation.) Further reduction of the corrosion rate will further increase the fissile buildup period. This fissile buildup trend is reversed when the corrosion rate falls below 2×10^{-5} $\mu\text{m}/\text{yr}$ because the resulting chromate concentration is too low to maintain a sufficiently low pH to sustain the necessary Gd solubility against the alkalinity of the incoming water. The behavior with infiltration rate is similar to that shown in Figure 7.3.1-2. The only exception to these two observations is for the highest infiltration rate with the lowest corrosion rate. In this case the Gd solubility is so low that the Gd cannot be removed as fast as it is released. The overall degradation rate of the WFs is a function of dissolution rate (function of chemistry), fracture factor, and flow rate. The dissolution rate multiplied by the WF fracture factor is defined as the DPF.

Figure 7.3.1-4 gives the earliest possible time to criticality as a function of WF DPF for infiltration rates of 10.0 and 1.0 mm/yr. To illustrate the effect of precipitation and re-dissolution of Gd, the minimum value of pH possible has been raised from 5.5 (the value used in most of the other cases of this study) to 5.8, which has the effect of lowering the maximum Gd solubility from 3000 ppm to 378 ppm. For this artificial limitation of solubility, there is no criticality for infiltration rate equal

to 0.1 mm/yr because the Gd removal rate never catches up with the Gd release rate from the degrading WF.

The results in Figure 7.3.1-4 generally show the earliest possible time decreasing with increasing DPF because the increasing rate of buildup of fissile material in the clayey mass means that a critical mass will be reached sooner, except for the DPF's above 4 for the 1.0 mm/year infiltration rate cases. In this situation the Gd is released from the WF at a faster rate than it can be removed (even with the enhanced Gd solubility). In this somewhat anomalous situation the higher DPF means that more Gd will precipitate before the removal rate can catch up with the release rate and begin to remove some of the previously precipitated Gd. This larger mass of Gd precipitate will require a longer time to re-dissolve and remove with the result that the higher DPF will be associated with a longer time to earliest possible criticality. There are no points for DPF below 4×10^{-3} , because this value is only slightly above the DPF limit of between 2 and 3×10^{-3} (as is seen in Figure 7.3.1-5). It should be noted that infiltration rate of 0.1 mm/yr does not give any criticality over the parameter range of interest.

It should be noted that the times to earliest criticality in Figure 7.3.1-4 are measured from the time at which all of the filler glass is degraded (when there is no longer a large supply of alkali to prevent the low pH which can be produced by the chromate resulting from the stainless steel corrosion). This time is expected to be no less than approximately 8000 years (3,500 years for the penetration of the WP barriers plus 1100 years for penetration of the canister, as explained in Section 3.1.1, followed by 3,000 years for the complete dissolution of the filler glass). This means that the total time to earliest criticality in Figure 7.3.1-4 is actually 12,000 years (4,000 indicated in the figure for a DPF of $0.020 \text{ g/m}^2/\text{day}$ plus the 8,000 to start). Furthermore, the figure shows that the earliest total time to criticality, except for the range of DPF's from 0.003 to $0.006 \text{ g/m}^2/\text{day}$, will be greater than 40,000 years, as long as the infiltration rate is not much more than 1 mm/yr. It should be noted that this approximately 8000 year starting point for measuring time to criticality is somewhat longer than the 6000 year estimate in Section 7.3, to be more realistic.

Figures 7.3.1-5, 7.3.1-6, and 7.3.1-7 show the sensitivity of DPF limit to the change in regulatory definitions of criticality. Figures 7.3.1-5 and 7.3.1-6 give the DPF limit for criticality, where criticality is defined as k_{cr} above 0.98 and 0.93, respectively. The rationale for each of these alternatives is given in Section 3.1.4. If the DPF of the WF is above the indicated limit, the criticality is considered to be possible. Naturally, the DPF limits for $k_{cr}=0.93$ (Figure 7.3.1-6) are lower than the corresponding limits for $k_{cr}=0.98$ (Figure 7.3.1-5). Both figures show little change of this DPF limit with infiltration rate; this is because the question of whether criticality can occur is answered primarily by whether the period of low pH (corroding stainless steel) lasts long enough for a critical mass of fissile material to accumulate in the clayey mass. Figure 7.3.1-7 gives a direct comparison between the effects of the 0.98 and 0.93 thresholds, which is to increase the DPF limit by approximately 10%.

7.3.2 Ceramic WF Results

The nominal criticality behavior for the WPs with degraded Pu ceramic WFs is summarized by Figures 7.3.2-1 through 7.3.2-7. These results are generally similar to the corresponding figures for

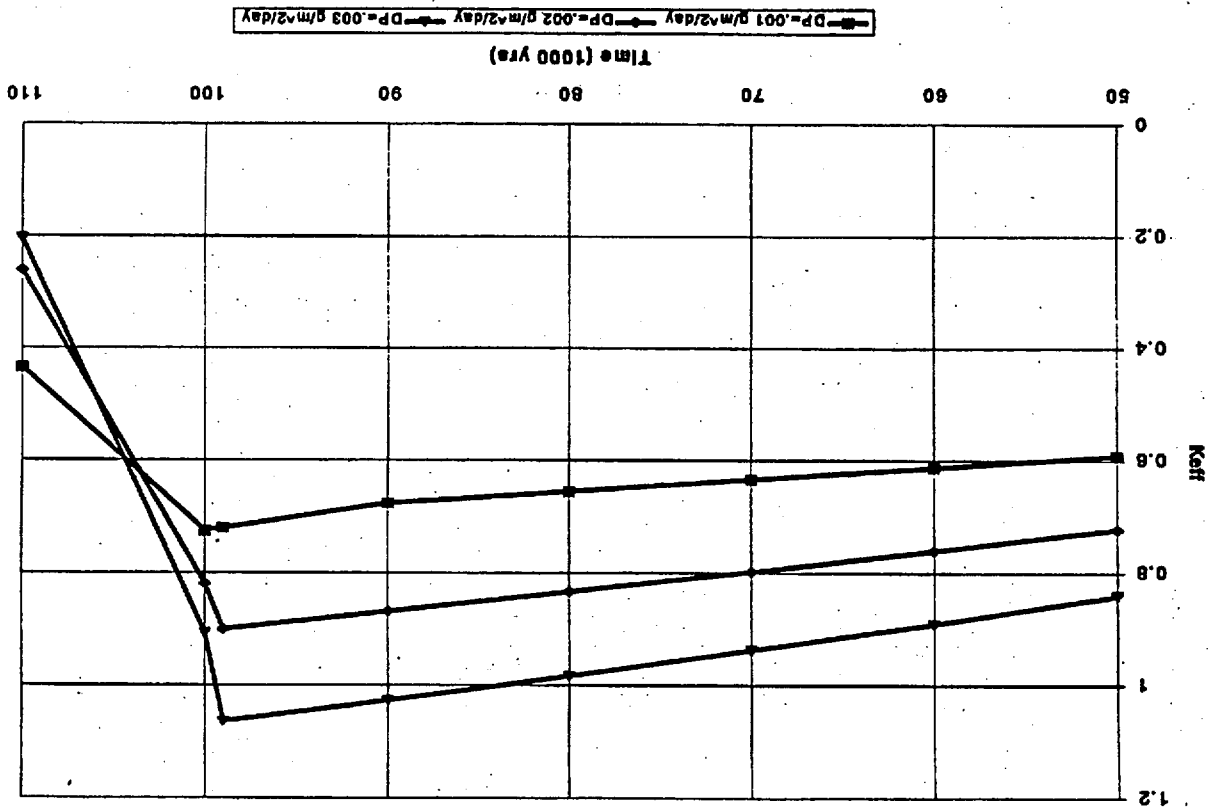


Figure 7.3.2-1. K_{eff} Time, Ceramic WF Infiltration Rate = 1 mm/yr, Stainless Steel Corrosion Rate = 0.1 μm/yr

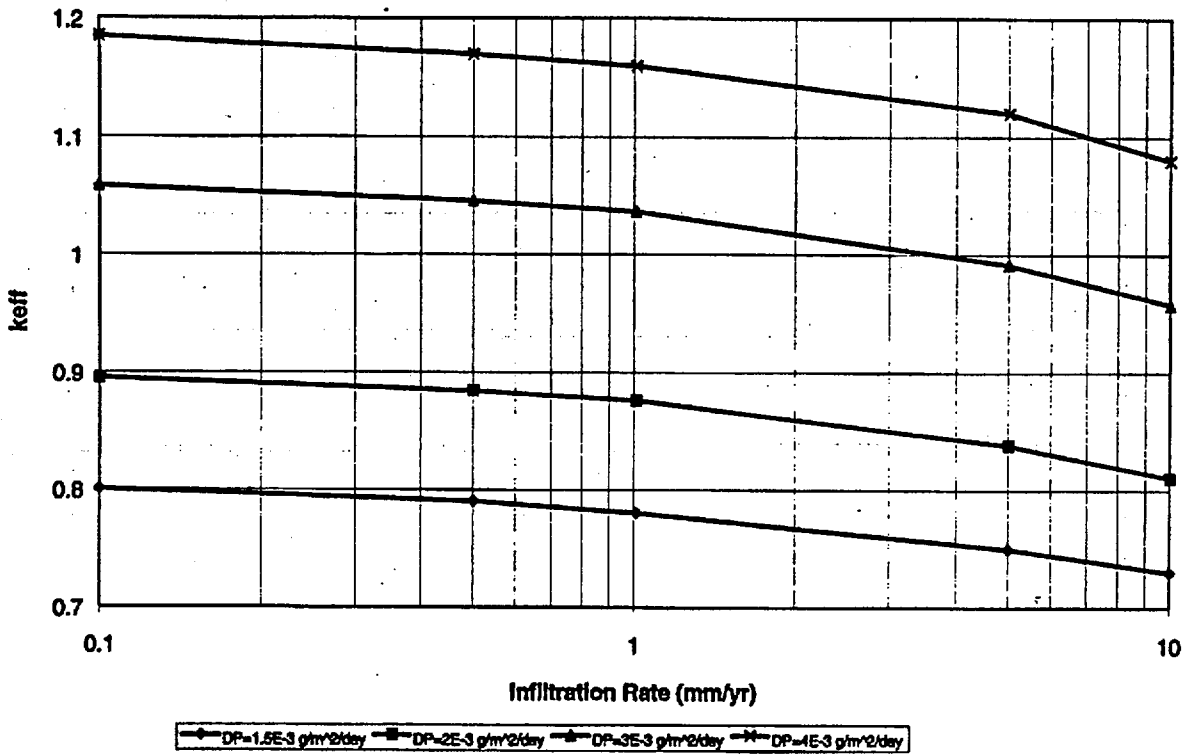


Figure 7.3.2-2. Ceramic WF: k_{eff} as a Function of Infiltration Rate for Typical Values of WF Dissolution Rate x Factor (Dissolution Product)

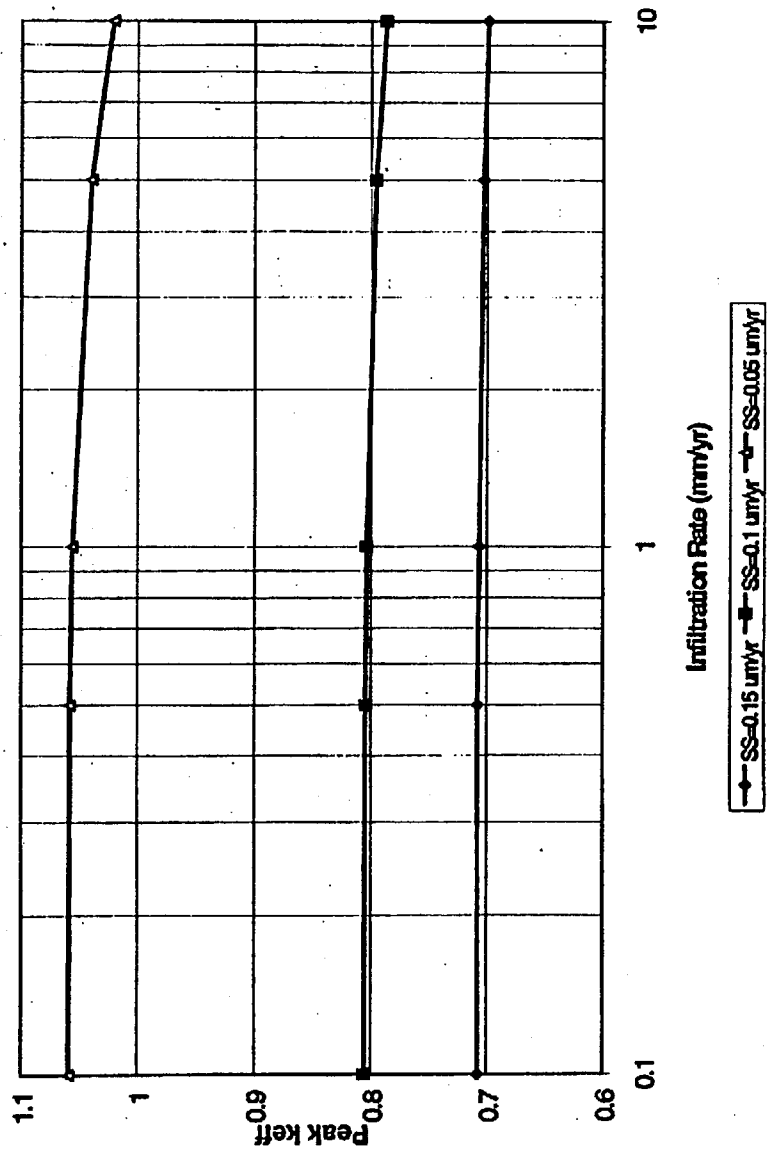


Figure 7.3.2-3. Ceramic WF: Peak k_{eff} as a Function of Infiltration Rate for Typical Values of Stainless Steel Corrosion Rate at DPF = $1.5E-3$ (g/m²/day)

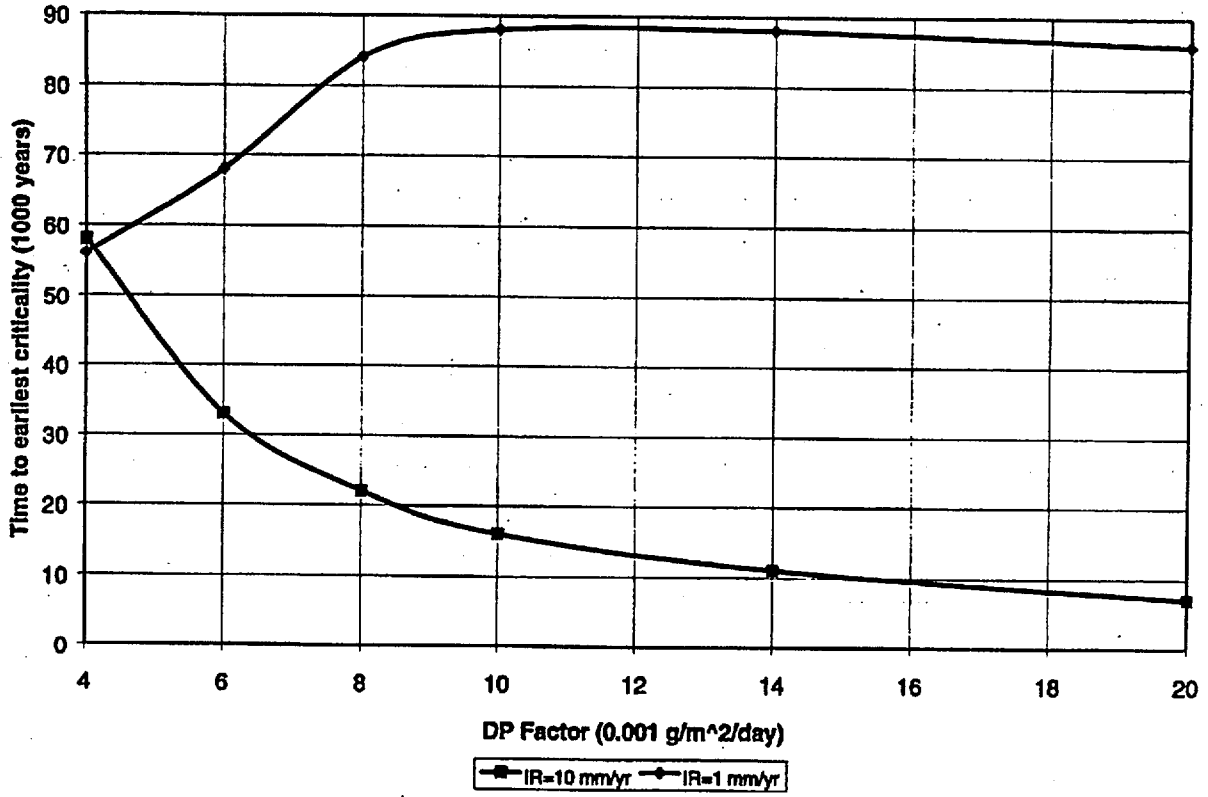


Figure 7.3.2-4. Ceramic WF: Years (1000) to Earliest Criticality for Stainless Steel Corrosion Rate = 0.1 μ m/yr

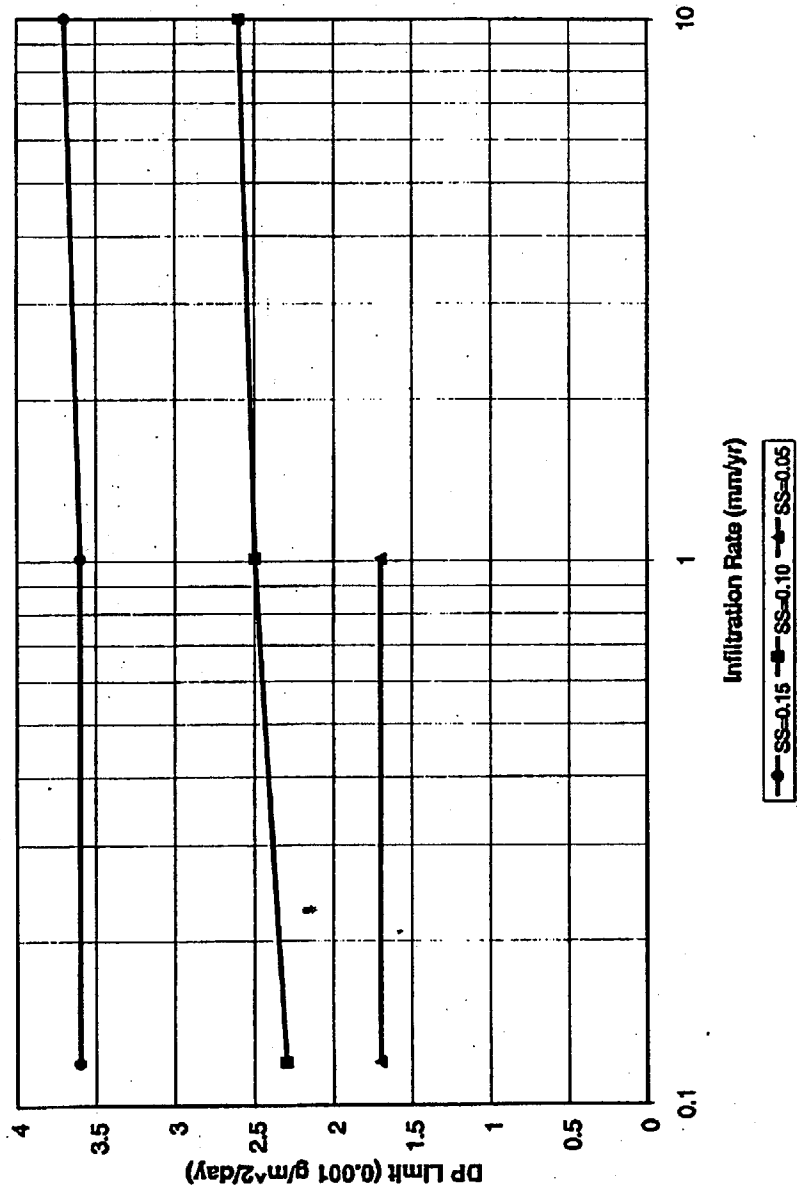


Figure 7.3.2-6. Ceramic WF: DPF Limits for $K_{sp} = 0.88$

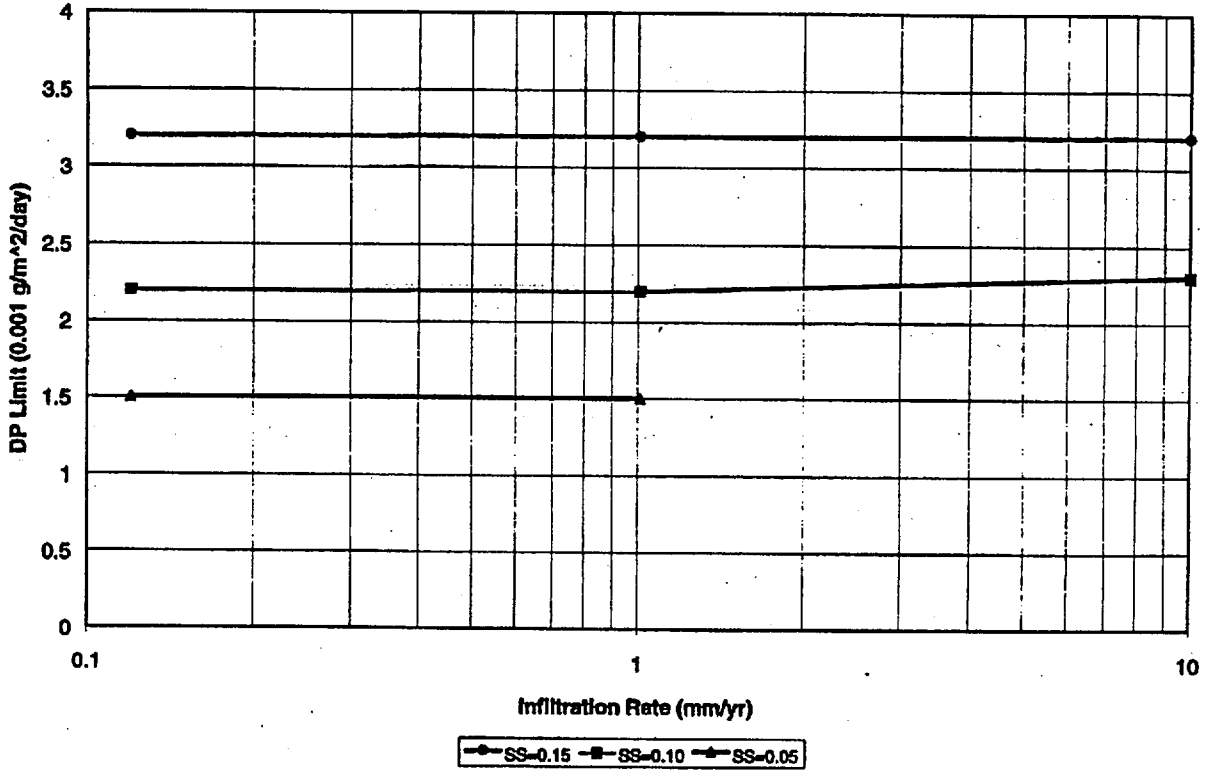


Figure 7.3.2-6. Ceramic WF: Dissolution Product Limit for $k_{cr} = 0.98$

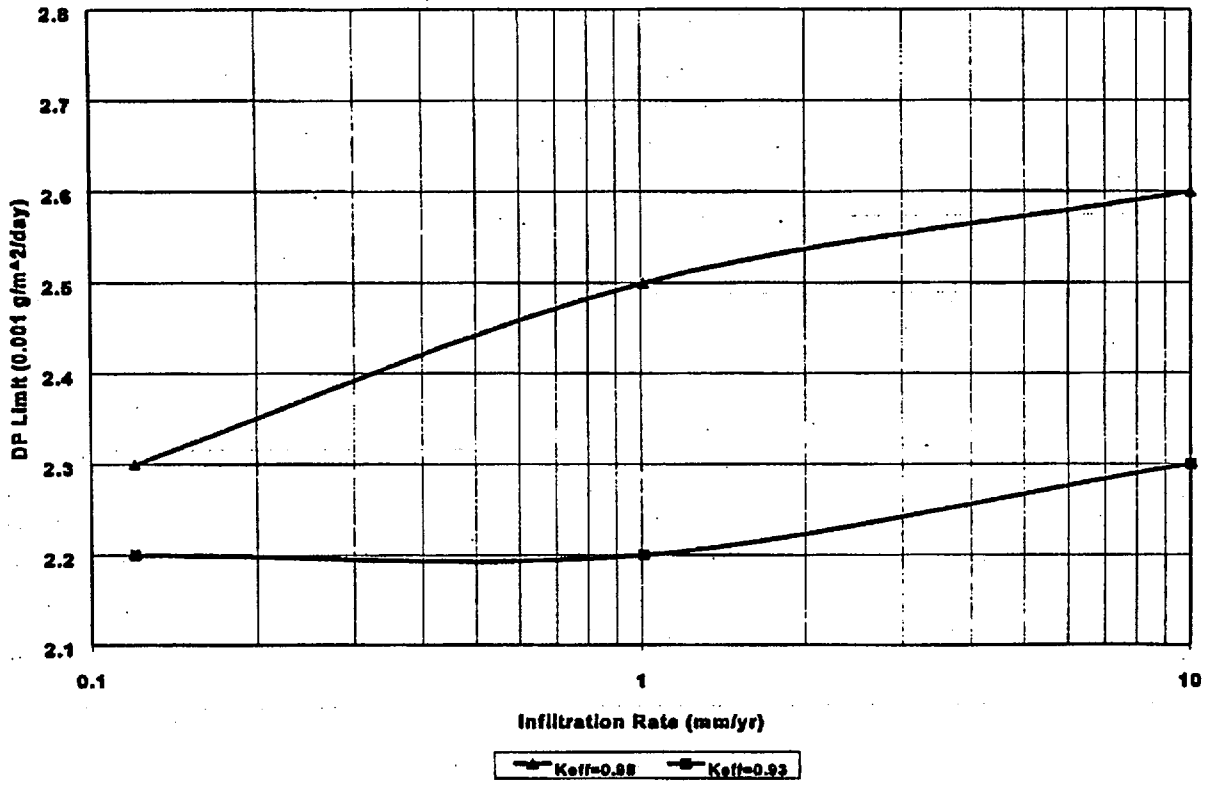


Figure 7.3.2-7. DPF Limit, $k_{eff} = 0.98$ and 0.93 , Ceramic WF, Stainless Steel Corrosion Rate = $0.1 \mu\text{m/yr}$

the glass WF, except that the ceramic cases show lower k_{eff} and higher WF DPF limits than for the glass WFs. More specific discussion is given in the following paragraphs.

In Figure 7.3.2-1 the drop off beyond the peak at 99,000 years looks more gradual for the corresponding glass case, Figure 7.3.1-1. However, that is primarily an artifact of the larger range of k_{eff} in the glass case.

Figure 7.3.2-4 shows generally longer times to earliest criticality than the corresponding glass values (Figure 7.3.1-4). The exception is for the anomalous situation in which the earliest criticality occurs after most of the initially precipitated Gd has been re-dissolved and removed. For these cases the earliest times for glass and ceramic are approximately the same, for the same values of DPF and infiltration rate. This is because the earliest criticality occurs while there is still more than one kilogram of Gd remaining in the precipitate (for both glass and ceramic WFs), and this much Gd overwhelms the effect of the small amount of Hf which distinguishes the ceramic from the glass. It should also be noted that glass case extends down to a DPF equal to 0.002 while the ceramic case only extends down to 0.004. This is consistent with the ceramic DPF limit being more than twice that of the glass, as is shown in Figure 7.4.3-1.

7.3.3 Undissolved WF distributed in clay

The alternative configuration with the undissolved WF fragmented and distributed uniformly in the clay has been analyzed to yield results similar to those given in the previous sections (7.3.1 and 7.3.2). Since this alternative configuration is understood to be non-conservative, the results will not be presented in detail; only the general behavior will be described, and the principal differences between the nominal and alternative configurations will be presented in tabular form.

For the alternative configuration there can be no criticality until most of the WF has dissolved to release the Gd, which can then be removed from the clay (which, in the present approximation, is equivalent to removing the Gd from the waste package, which will occur if the pH remains low enough to keep the Gd soluble). Even with major Gd removal from the waste package, there will still be enough Gd in the clay that, generally, criticality cannot occur unless at least 90% of the original fissile inventory remains in the clay. This requirement (for criticality), that the fissile isotopes remain within the waste package until most of the WF has dissolved, is not a significant constraint, since the U and Pu will be quite insoluble except at high pH, which can only occur during, approximately, the first 10,000 years. This time period corresponds to the time period of filler glass dissolution (during which there is major release of alkali ions, and/or the time period of degradation of any concrete liner of the emplacement drift).

The major difference in the criticality behavior between the nominal and the alternate configurations is in the DPF threshold (limit), as can be seen from the comparison in Table 7.3.3-1. As shown in the comparison provided in Table 7.3.3-1, the alternative configuration (WF fragments in the clay) requires much higher DPF than does the nominal configuration (WF outside the clay); in other words, this case has a much higher DPF threshold (at least 0.0082 g/m²/day). For the WF in clay there is little difference between glass and ceramic WFs, because there is always a significant amount of Gd in the clay when criticality occurs, so the small amount of Hf naturally present in the ceramic is of little benefit.

PREDECISIONAL DOCUMENT

Table 7.3.3-1. Comparison of DPF thresholds (SS crsn rate = 0.10 $\mu\text{m}/\text{yr}$, Infiltration rate = 1 mm/yr), for indicated Pu loading, in units of 0.001 $\text{g}/\text{m}^2/\text{day}$

Pu loading	WF outside clay	WF fragments in clay
Glass WF, full Pu	1.1	8.3
Ceramic WF, full Pu	2.5	8.5
Glass WF, 0.55 Pu	2.3	8.7
Ceramic WF, 0.55 Pu	7.5	9.8

Table 7.3.3-1 shows, for the alternative configuration (WF fragments in the clay), only a small increase in DPF threshold with decrease in Pu loading (to 0.55 of the nominal 205 kg/waste package). This is because the stainless steel lifetime (which is assumed to be the time period during which Gd has a high solubility so that significant quantities of it can be removed from the waste package) is approximately 100,000 years for the nominal corrosion rate of 0.1 $\mu\text{m}/\text{yr}$. Increasing the WF dissolution rate (as reflected in the DPF) so that the WF lifetime is significantly less than the stainless steel corrosion lifetime does not significantly increase the potential for criticality. If the stainless steel corrosion rate were higher than 0.1 $\mu\text{m}/\text{yr}$, the threshold DPF for alternative configuration (WF in clay) would be correspondingly higher than the values shown in Table 7.3.3-1.

The lowest threshold DPF (0.0082 $\text{g}/\text{m}^2/\text{day}$) for the alternative configuration corresponds to a WF dissolution in approximately 110,000 years. This is consistent with the times to earliest possible criticality occurrence shown in Table 7.3.3-2, for a slightly higher DPF.

Table 7.3.3-2. Time to earliest criticality (x1000 yrs*) At DPF=10 (x0.001 $\text{g}/\text{m}^2/\text{day}$)

Infiltration rate	WF outside clay	WF fragments in clay
Glass WF 1 mm/yr	88	79
Ceramic WF 1 mm/yr	88	83
Glass WF 10 mm/yr	7	80
Ceramic WF 10 mm/yr	16	84

* Measured from start of WF dissolution, approximately 5000 yrs.

The DPF used in Table 7.3.3-2 corresponds to a WF dissolution time of approximately 90,000 years. As would be expected, the alternative configuration (WF fragments in the clay) cases all correspond to nearly complete dissolution of the WF. In contrast, the nominal configuration cases (WF outside the clay) for 10 mm/yr infiltration rate have much lower earliest possible criticality, corresponding to the possibility of criticality with only small amounts of fissile species, because there is absolutely no Gd present. In contrast, the nominal cases with the infiltration rate only 1 mm/yr show an earliest time to criticality of 88,000 years. With this slower infiltration rate, the Gd cannot be removed from the waste package as fast as it is released from the WF. Consequently, it is available for criticality control. With this slow infiltration rate, there can be no criticality until the release rate drops

sufficiently (because of the smaller remaining WF surface area) to permit the Gd removal process to catch up.

7.4 WASTE FORM DESIGN CONSIDERATIONS

7.4.1 Pu Loading Alternatives

The Pu loading per WP can be reduced by reducing the wt% of Pu in the WF (below the nominal design of 10%) and/or reducing the number of Pu waste containing canisters per WP. With respect to criticality, the effect of both these strategies is the same, as long as they have the same amount of Pu per WP.

Figure 7.4.1-1 shows reduction of Pu loading increases the DPF limit, thereby increasing the likelihood that the actual DPF will be under the limit, and criticality will be avoided. For a reduction of Pu to 50% of the nominal design value (5% of the WF instead of 10%, or 2 WF canisters per package instead of 4) the increase in DPF limit is approximately linearly proportional to decrease in Pu. For a reduction to 30% of the nominal design, the increase in DPF limit is more than linearly proportional. This case has such a strong effect because criticality can only occur if enough fissile has been released from the WF while the stainless steel is still corroding, and this very low Pu loading brings the system close to the balance between the two. This contrast becomes even stronger for the high infiltration rate (10 mm/yr) because it takes much less flushing action to keep up with the smaller release rate of Gd.

It should be noted that the curves in Figure 7.4.1-1 end for fraction loadings below 0.3. For the scenarios considered in this study, criticality will not be possible below these loadings, so these lowest fraction loadings could be considered as threshold Pu loadings. Consistent with explanation of increase in DPF limit with increase in infiltration rate given in the previous paragraph, these threshold loadings are seen to increase with increasing infiltration rate (noting that the threshold loading for infiltration rates of 0.1 mm/yr and 1.0 mm/yr are close to resolve at this approximation).

Figure 7.4.1-2 shows the analogous results for the ceramic WF. The low end of the range of loading factors presented in this figure corresponds to the threshold below which criticality will not be possible for the ceramic WF. (The small increase with infiltration rate is not resolved at the precision of this study.)

7.4.2 Gd:Pu Ratio Alternatives

The effectiveness of Gd in limiting the possibility of criticality is generally expected to be proportional to the amount of Gd incorporated into the WF. However, for the low pH scenarios which constitute the majority of the ones evaluated in this study, the critical configurations are mostly Pu and U in the clayey precipitate which contains virtually no Gd (it having been flushed away because of its high solubility under acidic conditions, as is explained in Section 5.3). Under these conditions, reducing the Gd in the original WF has little effect, as long as it does not fall below a few percent of the Pu, on a mole basis.

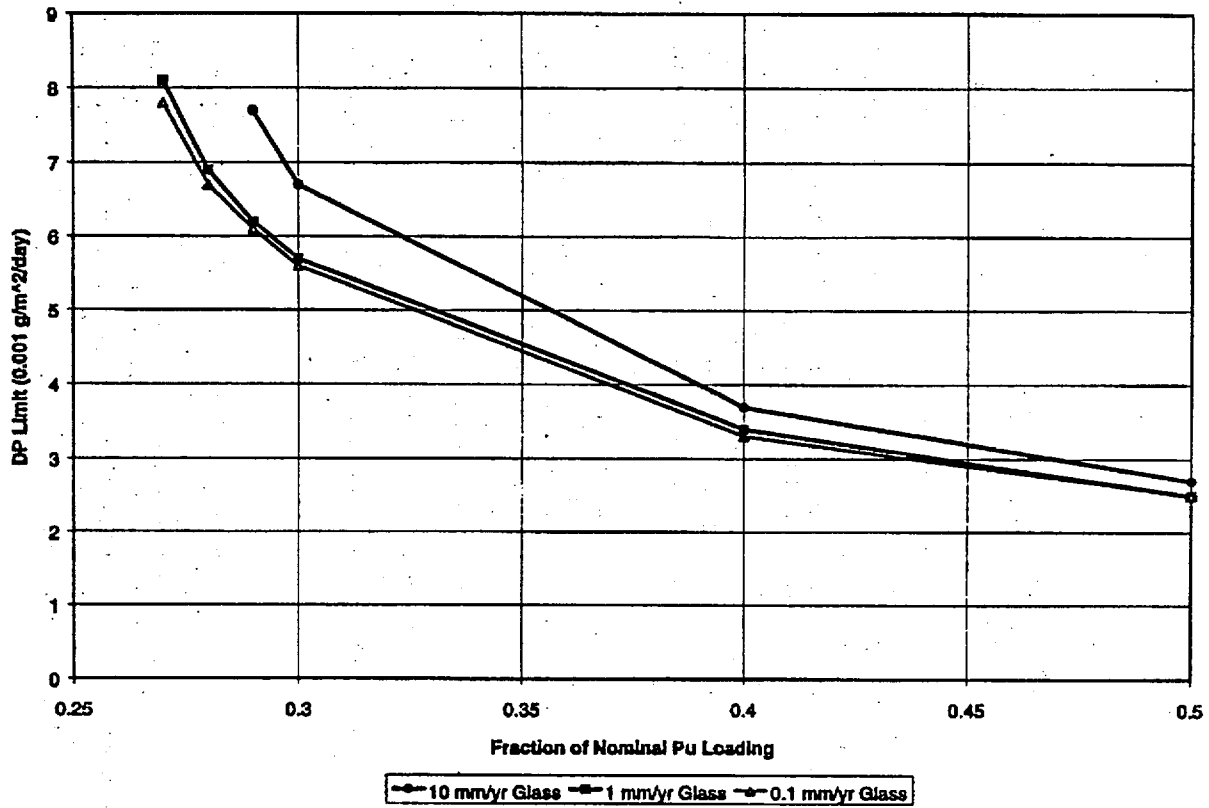


Figure 7.4.1-1. Glass WF: DPF Limit as a Function of Pu Loading Fraction for Stainless Steel Corrosion Rate = 0.1 $\mu\text{m}/\text{yr}$

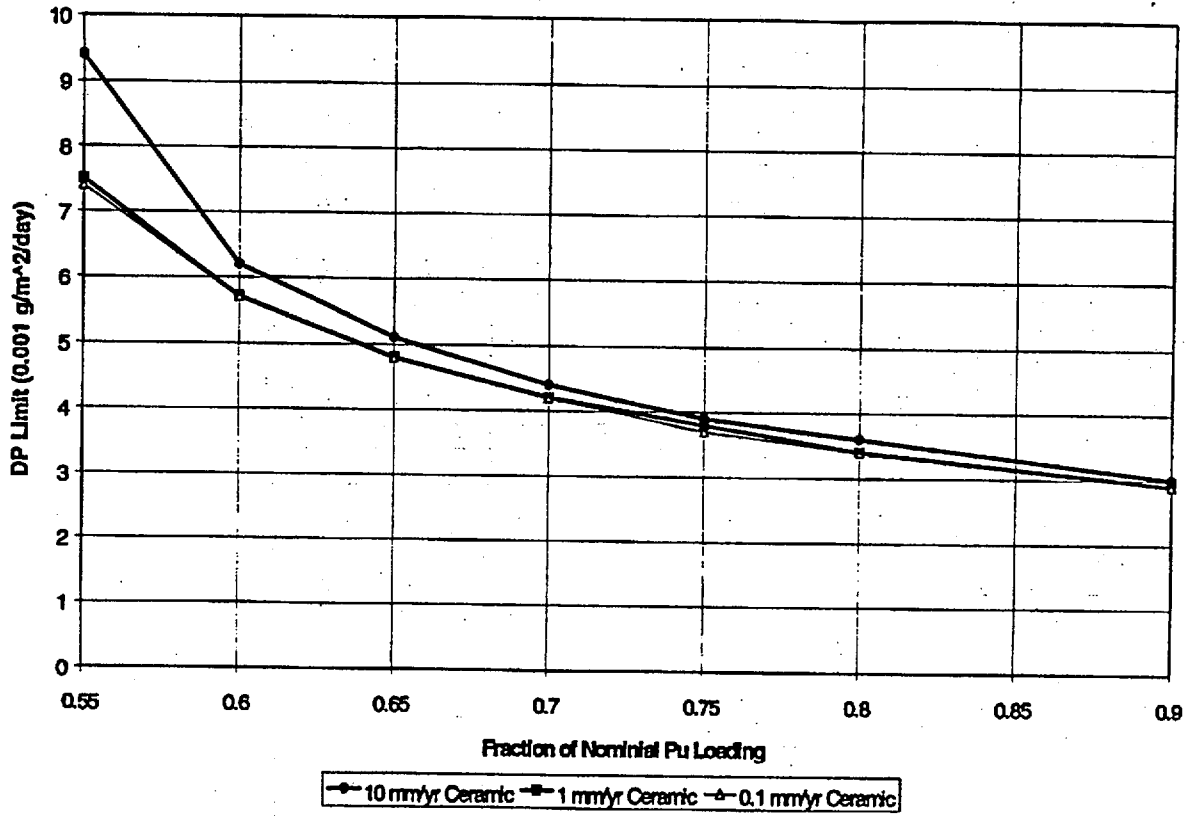


Figure 7.4.1-2. Ceramic WF: DPF Limit as a Function of Pu Loading Fraction, for Stainless Steel Corrosion Rate = 0.1 μ m/yr

The Gd:Pu ratio can have some effect, however, on the earliest time to criticality for those scenarios in which the initial rate of Gd removal is not fast enough to remove all the Gd as it is released from the degrading WF. In such cases, the Gd precipitates, but is re-dissolved if the stainless steel lasts longer than the glass. The earliest time to criticality will be proportional to the amount of Gd released from the WF. This effect is illustrated in Figure 7.4.2-1, which shows the earliest possible time to criticality for Gd:Pu mole ratios 1:2 and 2:1, as well as the nominal design of 1:1. As would be expected, increasing the amount of Gd in the waste-form is seen to increase the time to earliest possible criticality. As long as all the Gd is flushed as fast as it is released from the WF, the exact release rate (as manifested in the DPF) will not make much difference; this is the case for the nominal WF design and for the half strength Gd loading. For the double Gd loading, the release rate of Gd will overwhelm the flushing capability (for this particular set of conditions: Infiltration rate = 0.3 mm/yr and stainless steel corrosion rate = 0.1 $\mu\text{m}/\text{yr}$), so the greater the DPF, the more Gd will be released and the time to re-dissolve before criticality can occur.

7.4.3 Glass vs Ceramic

Figures 7.4.3-1 and 7.4.3-2 compare glass and ceramic DPF limits as a function of stainless steel corrosion rate and infiltration rate, respectively. They show that the DPF limit for ceramic is more than twice that for glass, and that both are relatively insensitive to infiltration rate. The higher DPF limit for ceramic is a benefit of the Hf naturally present in the ceramic zirconolite.

7.5 ADDITIONAL RELEVANT RESULTS

7.5.1 Effects of Non-Homogeneous Fissile Distribution

The probable configuration of the degraded glass clayey material is relatively homogeneous as investigated in Section 7.1.1; while there may be localized heterogeneities, overall the clayey material can best be represented as a homogeneous mixture. Even though the DHLW glass potentially degrades orders of magnitude faster than the Pu immobilization glass, the Pu immobilization glass will likely be distributed within the DHLW clay as it degrades. MCNP4A runs were performed for three variations on the base geometry for the degraded glass WF (zero volume % additional water) to investigate heterogeneous effects on k_{eff} by concentrating the Pu/U/Gd into a smaller volume and including the bulk of the clayey material in a separate volume. As discussed in Section 6.1.1, these variations are concentration of all Pu, U, and Gd in the bottom of the clay; concentration of all Pu, U, and Gd in the top of the clay; and concentration of all Pu, U, and Gd at one end of the WP. Table 7.5.1-1 provides the k_{eff} results for the concentration of various amounts of Pu, U and Gd in various volumes of clay at the bottom of the WP, as well as the k_{eff} results for corresponding uniformly distributed cases.

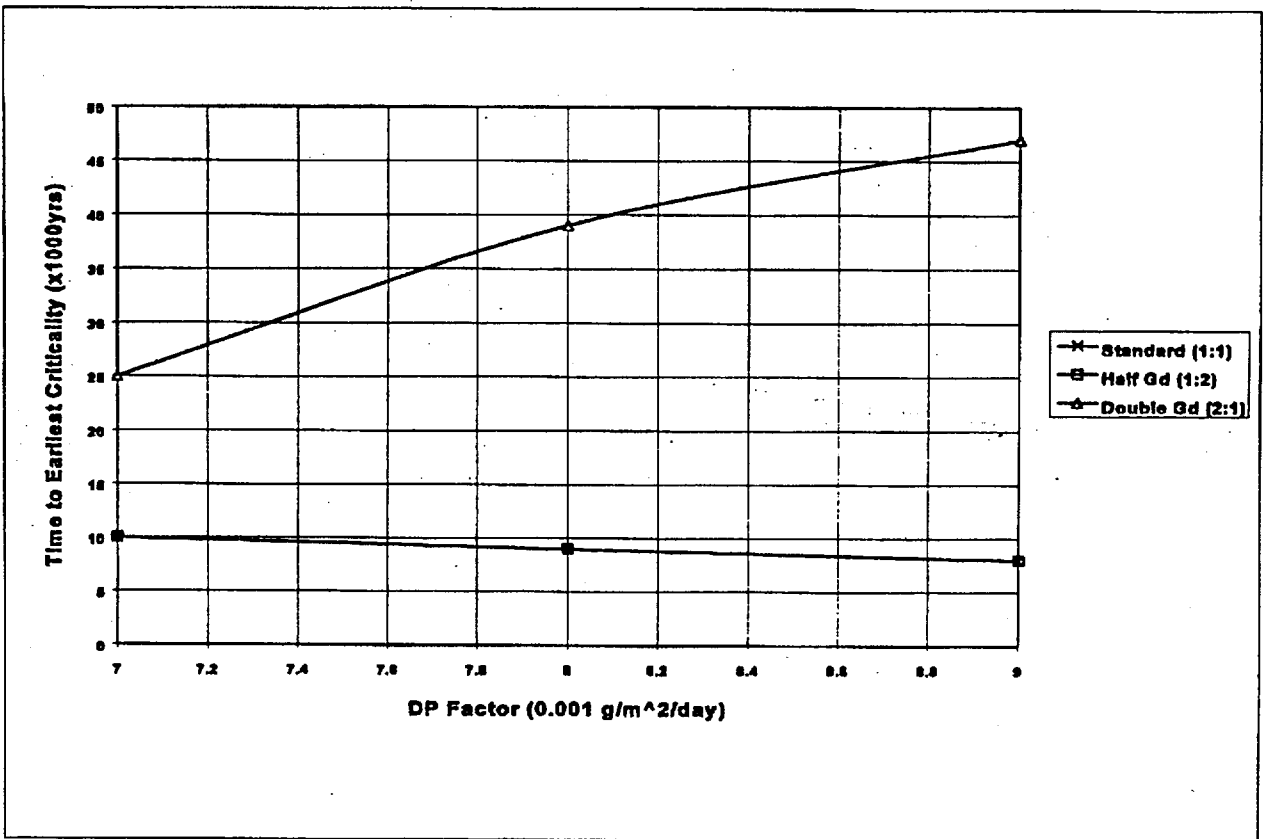


Figure 7.4.2-1. Reverse Behavior of Time to Earliest Criticality as a Function of DPF for a Family of Gd:Pu Mole Ratios
(Infiltration Rate = 0.3 mm/yr, Stainless Steel Corrosion Rate = 0.1 μ m/yr)

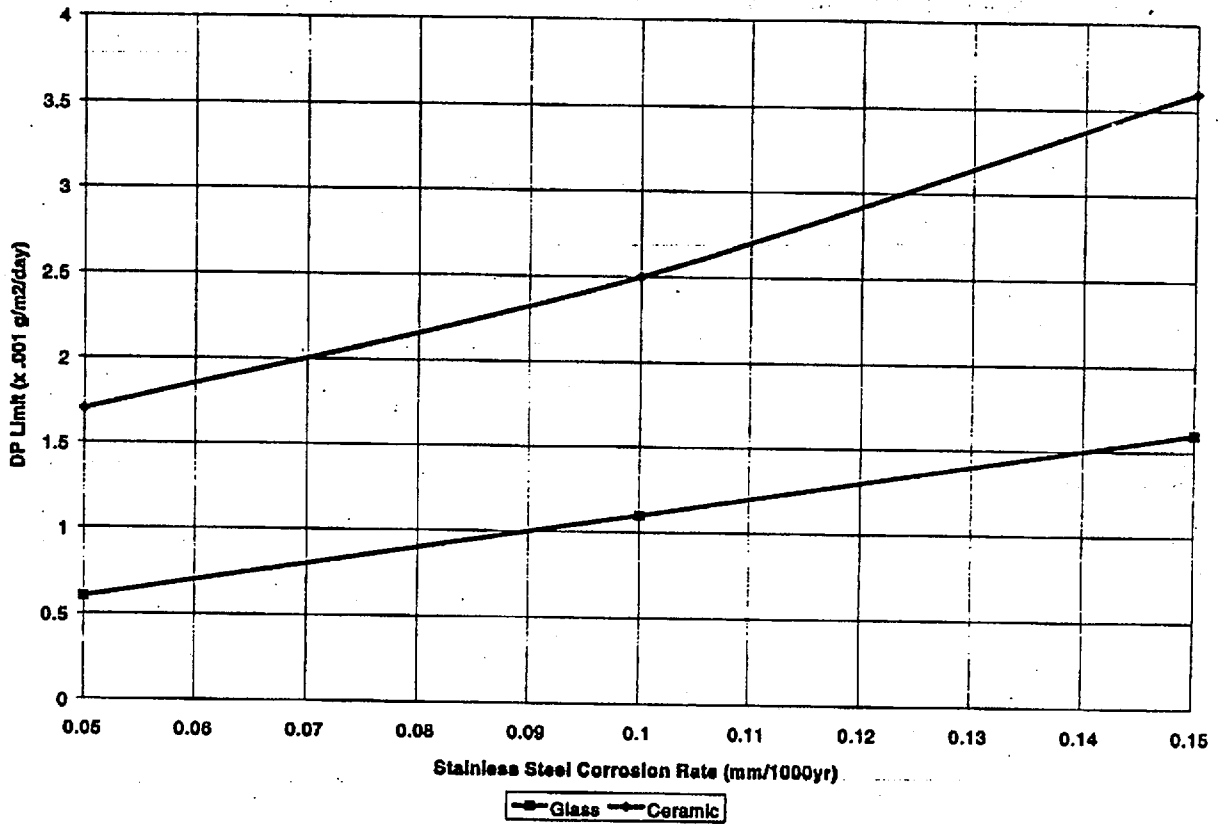


Figure 7.4.3-1. DP Limit, Glass and Ceramic Compared ($k_w = 0.98$) for Infiltration Rate = 1 mm/yr

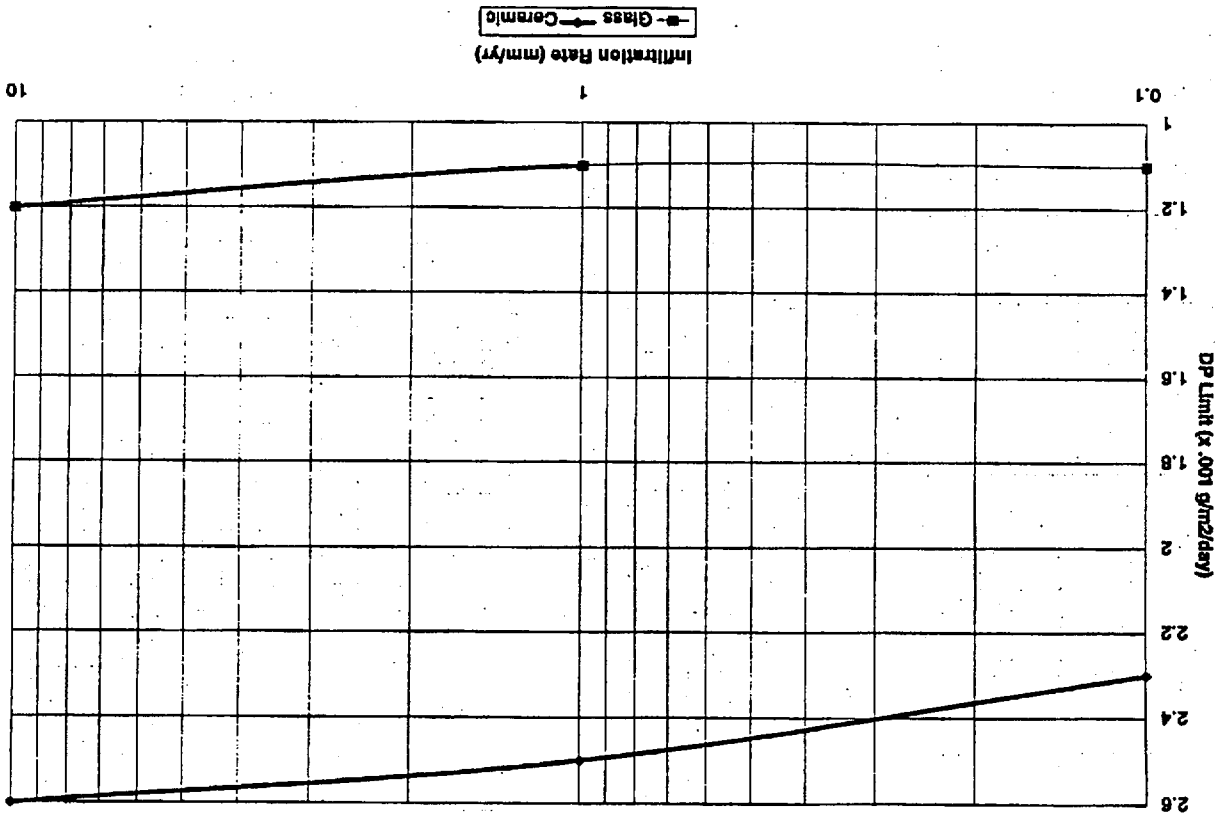


Figure 7.4.3-2. DPF Limit vs Infiltration Rate, Glass and Ceramic Compared ($k_{sp} = 0.98$) for Stainless Steel Corrosion Rate = 0.1 μ m/yr

PREDECISIONAL DOCUMENT

Table 7.5.1-1. Effect on k_{eff} of Pu/U/Gd Concentration in Bottom of Clay

Kg Pu	Kg U	Kg Gd	Uniformly Distributed	Pu/U/Gd in bottom 75% of clay	Pu/U/Gd in bottom 50% of clay	Pu/U/Gd in bottom 25% of clay
40	150	3.5	0.9548 ± 0.0053	1.0044 ± 0.0039	1.0375 ± 0.0054	1.0529 ± 0.0047
40	50	2.25	-	-	0.9022 ± 0.00244	-
40	50	2.5	-	-	0.8807 ± 0.0031	-
40	50	1.25	0.9344 ± 0.0041	0.9774 ± 0.0042	1.0132 ± 0.0050	1.0008 ± 0.0060
25	25	0.75	-	-	0.8824 ± 0.0044	-
25	25	0.25	0.9602 ± 0.0047	1.0194 ± 0.0040	1.0651 ± 0.0044	1.0521 ± 0.0052
10	65	0.875	-	-	0.8838 ± 0.0081	-
10	65	0.5	0.9194 ± 0.0041	0.9645 ± 0.0044	1.0032 ± 0.0049	0.9947 ± 0.0049

Table 7.5.1-2 provides similar information for a single amount of Pu, U and Gd, concentrated to various degrees at the top of the clay hemicylinder. In this variation, extreme concentrations of Pu/U/Gd in the top of the clay approach a higher leakage slab geometry and significantly reduce k_{eff} over that of the uniformly distributed base case. Figure 7.5.1-1 below summarizes the overall effect of uniform and non-uniform (top and bottom) Pu/U/Gd distributions on k_{eff} for the 25 kg Pu, 25 kg U, and 0.25 kg Gd cases.

Table 7.5.1-2. Effect on k_{eff} of Pu/U/Gd Concentration in Top of Clay

Pu	U	Gd	Uniformly Distributed	Pu/U/Gd in top 75% of clay	Pu/U/Gd in top 50% of clay	Pu/U/Gd in top 25% of clay
25	25	.25	0.9602 ± .0047	0.99384 ± 0.0049	0.9883 ± 0.0062	0.8608 ± 0.0052

In the final variation, various amounts of Pu, U, and Gd were concentrated at one end of the clay hemicylinder. Table 7.5.1-3 provides the results of this variation.

Table 7.5.1-3. Effect on k_{eff} of Concentrating Pu/U/Gd on One End of WP

Pu	U	Gd	Uniformly Distributed	Pu/U/Gd all in right half of clay
40	150	3.5	0.9548 ± .0053	1.1187 ± 0.0052
40	50	2.25	-	0.9670 ± 0.0038
40	50	2.5	-	0.9485 ± 0.0057
40	50	1.25	0.9344 ± .0041	1.0872 ± 0.0050
25	25	0.75	-	0.9475 ± 0.0043
25	25	0.25	0.9602 ± .0047	1.1511 ± 0.0049
10	65	0.875	-	0.9581 ± 0.0050
10	65	0.5	0.9194 ± .0041	1.0798 ± 0.0064

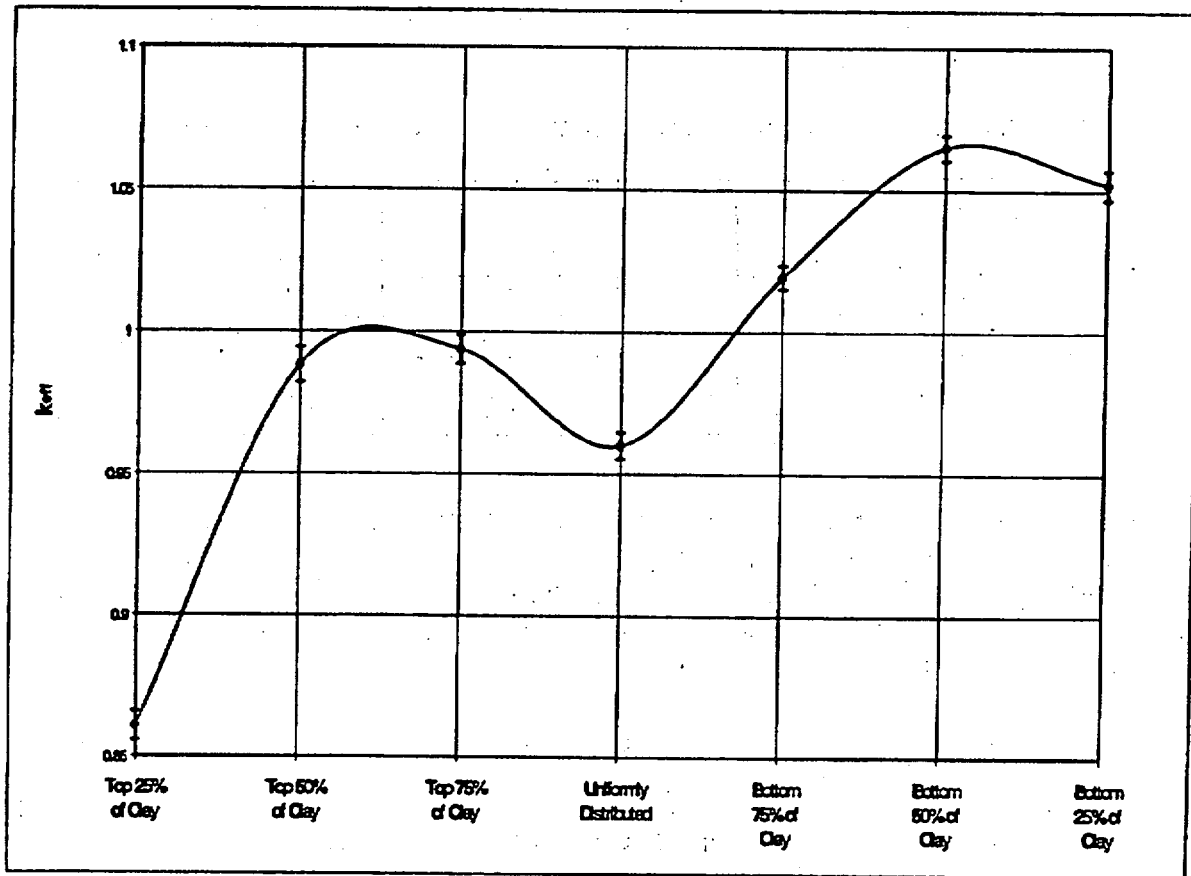


Figure 7.5.1-1. Effects on k_{eff} of Pu/U/Gd Distribution Within the Clay for the 25kg/25kg/0.25kg Case

These cases indicate that the value of k_{eff} can increase when the Pu/U/Gd are concentrated, and the maximum increase generally occurs when concentration occurs in approximately 50% of the total clayey material volume. The most significant increase occurs in the accumulation in one end cases, but these are the least probable. The most likely mechanism for achieving this configuration is flushing of a large fraction of the clay components which are more soluble than the U and Pu by flowing water, leaving a reduced volume of clayey material with more concentrated Pu and U. This concentration scenario could result in up to a 4.5% increase in k_{eff} over the results presented in Section 7.1.1. However, this scenario is unlikely since the bulk of the clayey materials are no more soluble than the Pu and U in the neutral pH region.

The results of the cases described in this section also indicate that the density of U, Pu, and Gd in the clayey material has a more significant affect on k_{eff} than geometry or volume except in extreme variations. Four additional cases as listed in Table 7.5.1-4 were run to demonstrate the relatively small affect of cutting the volume of the clayey accumulation in half (half the mass of all the clayey

PREDECISIONAL DOCUMENT

material components including U, Gd, and Pu). The model for these cases is the nominal cylinder segment within the waste package with half the length as that used in the nominal cases. For the cases listed in Table 7.5.1-4, k_{eff} is reduced only from 1.5% to 2.0% as compared to the full volume/length cases.

Table 7.5.1-4. Effect on k_{eff} of Half Volume on One End of WP (Same Concentration)

Pu (kg)	U (kg)	Gd (kg)	Full Volume	Half Volume Right Half of Clay (Same Concentration)
21	14	0.	0.9643 ± 0.0028	0.9482 ± 0.0048
25	25	0.25	0.9602 ± 0.0047	0.9424 ± 0.0055
50	75	2.0	0.9728 ± 0.0049	0.9548 ± 0.0049
140	30	8.0	0.9742 ± 0.0048	0.9594 ± 0.0041

In summary, it can be concluded that although a graded distribution of fissile material within the clayey precipitate can lead to an increased k_{eff} with respect to a uniform distribution, most such graded distributions are relatively unlikely to occur. It can also be concluded that the composition of the clayey material in terms of mass/volume of the principal neutronically significant species has the primary affect on k_{eff} .

7.5.2 Evaluation of Sm as Replacement Option for Gd

As discussed in Section 2.1.2, Sm has been suggested as an alternative for Gd. Four near-critical glass cases were run to compare the worth of Sm with that for Gd. The case descriptions and results for both Gd and Sm are listed in Table 7.5.2-1. In addition, four corresponding cases with neither Gd or Sm were run. The Sm is shown to be only a fraction of the worth of Gd. Several additional cases were run to determine the approximate mass of Sm required to replace the Gd (equivalent k_{eff}). A comparison of values in Table 7.5.2-1 indicates that ratios from 2 up to 4 to 1 of Sm to Gd is required in these degraded configurations.

Table 7.5.2-1. Comparison of Gd and Sm in Degraded DHLW Glass/Pu Immobilization Glass

Case Description	Gd	Mole Equivalent Sm	Approximate Sm Mass Required (kg)	No Absorber
25 kg ²³⁹ Pu, 25 kg ²³⁵ U, 0.25 kg Gd	0.9602 ± .0047	1.0811 ± .0044	1.0	1.1008 ± .0045
10 kg ²³⁹ Pu, 65 kg ²³⁵ U, 0.375 kg Gd	0.9734 ± .0043	1.0945 ± .0052	1.3	1.1610 ± .0042
50 kg ²³⁹ Pu, 75 kg ²³⁵ U, 2 kg Gd	0.9728 ± .0049	1.1868 ± .0058	5.0	1.3954 ± .0048
140 kg ²³⁹ Pu, 30 kg ²³⁵ U, 8 kg Gd	0.9742 ± .0048	1.1340 ± .0052	16.0	1.4950 ± .0047

7.5.3 Investigation of Dryout in the Degraded Glass Clayey Configuration

Because the degraded glass configuration discussed in Section 7.1.1 showed a decrease in k_{eff} as the free water fraction was increased from zero, 3 cases were run to determine whether k_{eff} might increase significantly if the clay were to dry out (losing some water of hydration) after starting at a near critical configuration (i.e., find optimum moderation by H). Four combinations of Pu/U/Gd are used with Gd masses ranging between 0. and 10. Kg. The first step of the dryout process is modeled by the removal of the water reflector above the clayey configuration; the second step is reduction of the bound H to 80 % of its initial value; the third step is reduction of H to 50% of its initial value; the final step is reduction of H to 25% of its initial value. The results for these cases are shown in Table 7.5.3-1. The point of optimum moderation and degree of peaking (or whether or not it occurs at all) is a primarily a function of Gd (Pu) mass. As discussed in Section 7.1.1, the mass of Gd required to meet k_{eff} thresholds is primarily a function of Pu mass. As the mass of Gd increases, the water fraction at which peaking occurs and the degree of peaking increases. Note that the maximum increase, which occurs at 50% the initial value of H, is about 5% in k_{eff} , indicating that the potential increase in k_{eff} following dryout could affect the Gd mass required to meet criticality thresholds for the base calculations. The peak at 50% of the initial value of H for the 2 kg and 10kg of Gd cases coincides with the optimum ratio of H and Pu/U/Gd presented in Section 7.5.1 for concentration effects.

Table 7.5.3-1. Investigation of Dryout of Degraded Glass Configuration

Case Description	Base	No Reflector	80% H	50% H	25% H
21 kg ²³⁹ Pu / 14 kg ²³⁵ U / 0.0 kg Gd	0.9643 ± 0.0028	0.9609 ± .0028	0.9667 ± .0037	0.9399 ± .0045	0.8466 ± .0052
25 kg ²³⁹ Pu / 25 kg ²³⁵ U / 0.25 kg Gd	0.9602 ± .0047	-	0.9571 ± .0053	0.9320 ± .0044	0.8842 ± .0058
50 kg ²³⁹ Pu / 75 kg ²³⁵ U / 2.0 kg Gd	0.9728 ± .0049	0.9721 ± .0046	0.9756 ± .0048	0.9824 ± .0048	0.9447 ± .0076
140 kg ²³⁹ Pu / 60 kg ²³⁵ U / 10.0 kg Gd	0.9738 ± .0030	0.9677 ± .0042	0.9926 ± .0047	1.0193 ± .0050	0.9941 ± .0068

7.5.4 Effects of ²³⁸U in Degraded Glass Clayey Composition

As discussed in Section 7.1.1, the amount of ²³⁸U in the clayey composition is unknown and was, therefore, not included in the base cases. Approximately 2 weight percent of the DHLW glass is depleted U, initially providing over 100 kg of ²³⁸U in a WP containing 4 pour canisters. Three different Pu/U/Gd mass combinations were run with 25, 50, and 100 kg of ²³⁸U included in the clayey composition. The results are shown in Table 7.5.4-1. Note that 100 kg of ²³⁸U reduces k_{eff} by about 2.6% to 3.4% (increasing worth with decreasing Pu).

PREDECISIONAL DOCUMENT

Table 7.5.4-1. Comparison of ^{235}U in Degraded DHLW Glass/Pu Immobilization Glass

Pu/U/Gd Masses (kg)	0 kg ^{235}U	25 kg ^{235}U	50 kg ^{235}U	100 kg ^{235}U
40/50/1	0.9795 ± .0049	0.9768 ± .0052	0.9618 ± .0031	0.9535 ± .0055
21/14/0	0.9843 ± .0028	0.9835 ± .0040	0.9487 ± .0039	0.9387 ± .0045
10/65/0.375	0.9734 ± .0043	0.9587 ± .0043	0.9537 ± .0037	0.9395 ± .0044

The neglect of the effect of ^{235}U in the nominal analyses of this study is conservative. It may also be realistic, since the high pH initial phase of filler glass degradation will likely result in the removal of the ^{235}U present in the initial filler glass. This analysis is also an indication of the potential criticality control benefits of adding depleted U to the waste package. However, the greatest benefit from such a policy would be for external criticality.

7.5.5 Variation of Hf Content in the Degraded Ceramic WF

The zirconium (Zr) in the original ceramic was assumed to be composed of 2 wt% Hf as described in Section 7.1.2. Zr ores can typically contain up to 5 wt% Hf (Reference 27). Several additional cases were run to investigate the effect of varying the wt% of Hf in Zr from the original 2 wt%. The results for these cases are shown in Table 7.5.5-1. These results indicate that high wt% of Hf in Zr are required, but even low wt% of Hf does have a beneficial effect which will reduce the criticality potential of marginal cases. In fact, the lower mass requirements for Gd in order to meet k_{eff} thresholds of ceramic vs glass shown by the comparison in Section 7.4.2 is due to the Hf which is incorporated into the natural Zr. The difference of Hf in each of the respective clayey materials can be seen by comparing the Hf concentration between Table 5.4.5-1 and Table 5.5.2-1.

Table 7.5.5-1. Variation of Hf Wt% in Zr for the Degraded Ceramic WF

Pu/U/Gd Masses (kg)	0 wt% Hf	2 wt% Hf	4 wt% Hf	20 wt% Hf*	100 wt% Hf*
25/90/0.5	0.9841 ± .0038	0.9724 ± .0037	0.9612 ± .0040	-	-
10/130/0.5	0.9978 ± .0044	0.9915 ± .0042	0.9827 ± .0054	-	-
50/10/0	1.0080 ± .0035	0.9925 ± .0039	0.9862 ± .0044	0.9161 ± .0038	0.7164 ± .0039
50/75/1.2	-	0.9761 ± .0041	-	0.9088 ± .0047	-

* These concentrations far beyond the typical naturally occurring fraction in Zr (2 to 4 wt%).

An additional set of cases were run to determine the wt% of Hf required to replace 0.5 kg of Gd and are shown in Table 7.5.5-2. Based on the assumed clayey material compositions and volumes, there are approximately 1.7 kg of Hf in the waste package at 2 wt% Hf in Zr. Based on the cases run, approximately 33 wt% of the Zr would be required to be Hf to equal the effect on k_{eff} of 0.5 kg of Gd. This translates to approximately 28.05 kg Hf to equal 0.5 kg of Gd or a factor of 56 to 1. Considering that there are about 135 kg of Gd in the 4-pack waste package (about 34 kg in single

PREDECISIONAL DOCUMENT

canister) in its intact form and that essentially no Hf is lost during the degradation process, replacement of Gd by Hf could be a feasible option.

Table 7.5.5-2. Calculations to Determine Equivalent Hf Wt% in Zr to Replace 0.5 kg Gd for the Degraded Ceramic WF

	25 kg ²³⁹ Pu / 90 kg ²³⁵ U/ 0. kg Gd	10 kg ²³⁹ Pu / 130 kg ²³⁵ U/ 0. kg Gd
4 wt% Hf	1.0806 ± .0035	1.1010 ± .0044
10 wt% Hf	1.0558 ± .0052	1.0718 ± .0062
20 wt% Hf	1.0110 ± .0042	1.0361 ± .0056
30 wt% Hf	0.9814 ± .0043	1.0041 ± .0038
35 wt% Hf	0.9559 ± .0046	0.9815 ± .0048
40 wt% Hf	0.9462 ± .0041	0.9644 ± .0040
45 wt% Hf	-	0.9520 ± .0046

PREDECISIONAL DOCUMENT

INTENTIONALLY LEFT BLANK

8. MAJOR FINDINGS AND RECOMMENDATIONS

8.1 DESIGN IMPLICATIONS

Analysis of a representative set of potentially critical configurations leads to the following findings which directly impact WF design:

- A critical parameter for determining criticality risk is the DPF that is defined as the product of the intrinsic material dissolution rate per unit surface area, multiplied by the ratio of total WF surface area (outer surface area plus the generally much larger internal surface area exposed by fracturing) to outer WF surface area (or inner surface area of the WF can). Threshold (limiting) DPF values have been determined for the nominal WFs for both glass and ceramic, using the principal degradation modes considered in this study. Any WF that has an actual DPF less than its corresponding threshold DPF cannot go critical.
- The DPF threshold for the nominal ceramic WF is approximately twice the value for the nominal glass WF (for the nominal environmental conditions and dissolution rates). This is primarily due to the Hf present in the ceramic, which serves as a backup neutron absorber under those conditions in which the primary absorber, Gd, becomes soluble and is removed from the WP. The Hf is present in the ceramic because it occurs naturally in small amounts in the same ore as the zirconium, which is a principal component of the ceramic. If a comparable concentration of Hf is incorporated in the glass form, the DPF threshold of the glass WF would be comparable to that of the ceramic WF.
- The results of this study could not distinguish between the long term performance of the ceramic and the glass WFs, because of a lack of definitive data on the following:
 - Long-term dissolution rates of the WFs (per unit surface area)
 - Effective surface area (enhanced by internal fracturing)
 - The degree to which Hf can be incorporated into the glass WF matrix without limiting the Pu carrying capability to less than the target 10%.
- For the WFs and degradation modes considered here, it is possible to preclude the possibility of criticality by reducing the Pu loading from the nominal 205 kg per WP. For the ceramic WF this loading should be reduced to 100 kg, and for the glass WF the value should be 50 kg. This factor of 2 difference arises because of the presence of Hf in the ceramic form as discussed above. As with the DPF threshold, this difference can be negated by adding Hf to the glass WF. The required reduction in Pu loading can be achieved either by using a co-disposal concept (mixing DHLW canisters with Pu canisters in a WP), or by reducing the concentration of Pu in the WF.
- The potential for criticality may be reduced by adding depleted uranium as WP filler between the pour canisters. The addition of 200 kg depleted U will, typically, lower the k_{eff} of a nearly critical configuration by 0.05). If the depleted U is encapsulated in a matrix chemically similar to that used for the Pu WF (either glass or ceramic), it will tend to be

mobilized at the same rate as the U in the WF. Once mobilized, the depleted U will transport with the chemically identified fissile ^{235}U which is the decay product of the ^{239}Pu , thereby significantly reducing the potential for external criticality (which will be evaluated in a future report).

8.2 CONDITIONS THAT CAN LEAD TO CRITICALITY

The type and quantity of neutron absorber included in the proposed immobilized Pu WFs are sufficient to prevent criticality in intact configurations, even if the WP is filled with water (highest possible concentration of moderator). For criticality to occur in, or near, a WP of immobilized Pu WF, most of the neutron absorber has to be separated from the fissile material. The following conditions could arise from the interaction of the WP materials and the environment, which could result in sufficient separation of fissile material and neutron absorber.

- A low pH (less than 6.0) may permit the principal added neutron absorber, Gd, to have at least 1000 times the solubility of U or Pu. Under certain (possible) flow conditions, this difference in solubility could result in so much of the Gd being removed from the WP, that there is the potential for a criticality event.
- The corrosion of the WP stainless steel (specifically the stainless steel of the pour canister) may result in the oxidation of Cr or Mo to a high enough valence state that the water becomes acidic. The resulting pH of the water in the WP depends on the rate at which the acid that is produced is flushed from the system; for the current range of estimated infiltration rate from the environment into the drift (1 to 10 mm/yr), and standing water contained in 10% of the WP volume, the pH could be lowered to a value of 5. Elimination of most of the stainless steel components of the WP would obviously limit the potential for acidification.
- If the above conditions hold during the time period of principal WF degradation, the relatively insoluble fissile material being released from the degrading WF may precipitate in a clay mass which could contain sufficient water to moderate a criticality.
- If all of the above conditions hold, the earliest time of criticality occurrence is typically 100,000 years; under certain "worst case" conditions, the earliest time to criticality could be as low as 12,000 years.

8.3 CONDITIONS THAT CAN PRECLUDE THE PROCESSES WHICH CAN LEAD TO CRITICALITY

The following conditions will tend to prevent the occurrence of the conditions that can lead to criticality (listed above):

- The acidity produced by the corroding stainless steel may be neutralized by the alkalinity of the incoming water (which may be maintained at a high pH by remnants of the concrete drift liner).

PREDECISIONAL DOCUMENT

- Certain elements present in the WP may form precipitates of Gd that have not yet been identified in the chemical literature. Such precipitates could limit the solubility of Gd, even at low pH.
- Even if there are conditions that lead to high Gd solubility, there may be sufficient penetration of the package bottom that the fissile material does not precipitate in a compact cylinder sector at the bottom of the WP.

8.4 SENSITIVITY CONSIDERATIONS

- The occurrence of criticality is relatively independent of the infiltration rate, except at rates above 20 mm/yr (four times the present estimated value), which tend to shift the pH toward neutrality, thereby limiting the potential for Gd removal and resulting criticality.
- For a given amount of fissile material and neutron absorber collected in the clayey material at the bottom of the WP, an inhomogeneous distribution of fissile material may result in a k_{eff} significantly larger than the homogeneous distribution. For example, if a cylinder sector of homogeneous distribution has a $k_{\text{eff}}=0.96$, a concentration of the fissile material and neutron absorber in the upper half would give a $k_{\text{eff}}=0.99$ and concentration in the lower half would give $k_{\text{eff}}=1.07$. These represent the optimum inhomogeneity with respect to criticality enhancing horizontal stratification; further concentration to the upper and lower 25% results in $k_{\text{eff}}=0.86$ and 1.05, respectively. Major horizontal stratification is relatively unlikely, but there are a few physical mechanisms that could produce such distributions. These possible variations do not affect the basic results of this study, but they do indicate that there could be worse cases.

8.5 RECOMMENDATIONS

The analyses of this study revealed information gaps, particularly in the application of physical and chemical models. The following items summarize these issues and the data collections/investigations which will remedy these deficiencies. These recommendations are grouped together logically rather than by priority.

- Conduct simple experiments to quantitatively evaluate Cr and Mo oxidation states resulting from the oxidation of corrosion resistant alloys. These should start with a solution of fine particulates of Cr_2O_3 and CrO_2 , and use one, or more, oxidation rate acceleration techniques. The experiments should also be done at neutral pH to quantify the acidification initiation process, and at low pH to determine whether the acidification process is sustained.
- Conduct a thorough literature search for Gd solubility information, particularly to determine the thermodynamic properties of any Gd silicates. These data need to be obtained for the pH range of interest.

PREDECISIONAL DOCUMENT

- Conduct a simple set of experimental investigations to fill in data gaps determined by the literature search. The objective of each of these experiments should be to produce a Gd silicate, then characterize it (e.g., by X-ray diffraction), and finally measure its solubility in such a way that the solubility product can be determined. The following are some specific alternatives:
 - Addition of dilute sodium silicate solution or silica sol to a Gd chloride solution and allowing the solution to age.
 - Synthesis of Gd silicate hydrothermally at temperatures up to 200°C and utilization of this Gd silicate as input to dissolution experiments at lower temperature. Analysis of the high temperature solution, if feasible, would provide an upper solubility limit. Hopefully, this approach would produce a crystalline solid.
 - Examine the evolution of a Gd-citrate solution, in which the Gd will be complexed by the citrate to prevent it from simply adsorbing onto silica surfaces, together with a silica sol as above. In this way if an association is found between Gd and silica it will be known that a reaction that formed a chemical compound occurred, not just an adsorption phenomenon.
- Develop an upgraded version of EQ3/6, and/or AREST, with a practical method of accounting for dilution of confined solutions by incoming water (flow-through), and with an improved thermodynamic database, reflecting recently gathered data such as the above two items.
- To more reliably validate findings from the thermodynamic models (e.g., EQ3/6) dissolution tests need to be developed that simulate long-term leaching behavior in an environment that provides unlimited air to the system (more accurately reflecting the actual environment expected).
- Update analyses based on data expected from ongoing dissolution studies for the following:
 - Stainless steel corrosion rates
 - La-BS glass
 - Ceramic (including appropriate degrees of metamictization).

Feed results of this analysis to the formulation teams to ensure a product specification that meets repository disposal criteria (k_{eff} below threshold values for credible configurations).

- Conduct risk-based analysis, using on the most current performance data, to show consequences of those scenarios that exhibit the potential for a criticality event.
- Evaluate the effect of incorporating large amounts of depleted U in the WF or WP.

PREDECISIONAL DOCUMENT

9. REFERENCES

1. *Total System Performance Assessment of a Geologic Repository Containing a Plutonium Waste Form Rev 00*, CRWMS (Civilian Radioactive Waste Management System) M&O (Management and Operating Contractor), August 15, 1996.
2. *Report on Evaluation of Plutonium Waste forms for Repository Disposal, Rev 01*, DI: A00000000-01717-5705-00009 REV 01, CRWMS M&O, March 29, 1996.
3. *Total System Performance Assessment - 1995: An Evaluation of the Potential Yucca Mountain Repository*, DI: B00000000-01717-2200-000136 REV 01, CRWMS M&O.
4. Jostons, A., Ridal, A., Mercer, D.J., Vance, E. R. 1995. *Experience Gained with the Synroc Demonstration Plant at ANSTO and its Relevance to Plutonium Immobilization*, Australian Nuclear Science and Technology Organization.
5. *Second Waste Package Probabilistic Criticality Analysis: Generation and Evaluation of Internal Criticality Configurations*, DI#:BBA0000000-01717-2200-00005, REV 00) CRWMS M&O, March 27, 1996
6. *Characteristics Data Base (CDB_H)*. A00000000-02268-1200-20005, Vol 1, REV 01, CRWMS M&O.
7. Benson, L. V., and McKinley, P. W., 1985, *Chemical Composition of Ground Water in the Yucca Mountain Area, Nevada, 1971-84*, USGS Open File Report, USGS-OFR-85-484.
8. Ogard, A. E., and Kerrisk, J. F. 1984, *Groundwater Chemistry Along Flow Paths Between a Proposed Repository site and the Accessible Environment*. LA-10188-MS. Los Alamos, New Mexico: Los Alamos National Laboratory.
9. Wilder, D. G. 1993. *Preliminary Near-Field Environment Report Volume II: Scientific Overview of Near-Field Environment and Phenomena*. UCRL-LR-107476 Vol 2. Livermore, California: Lawrence Livermore National Laboratory (LLNL).
10. Shaw, H., personal communication attached to Interoffice Correspondence LV.WP.PG.11/96-263. Subject: *Waste form parameters for Pu immobilized in glass*. From P. Gottlieb to File, 11/13/96.
11. Van Konynenburg, R.A., personal communication attached to Interoffice Correspondence LV.WP.PG.11/96-264. Subject: *Waste form parameters for Pu immobilized in ceramic*. From P. Gottlieb to File, 11/13/96.
12. McCoy, J. K. 1996. *Nominal compositions for materials*, CRWMS M&O IOC# LV.WP.JKM.09/96-223, September 17, 1996.

PREDECISIONAL DOCUMENT

13. Bates, J. K.; Ellison, A. J. G.; Emery, J. W.; Hoh, J. C. 1996. *Glass as a Waste Form for the Immobilization of Plutonium*, Mat. Res. Soc. Symp. Proc. 412, 57-64.
14. Plodinec, M. J. 1995. *Scenarios for the Evaluation of the Criticality Potential of High Actinide Glasses*, WSRC-RP-95-1016 Rev 0, Westinghouse Savannah River Corporation.
15. *Environmental Effects on Corrosion in the Tuff Repository*, U.S. Nuclear Regulatory Commission, NUREG/CR-5435, February, 1990.
16. *Progress Report on the Results of Testing Advanced Conceptual Design Metal Barrier Materials Under Relevant Environmental Conditions For A Tuff Repository*, UCID-21044. Livermore, California: Lawrence Livermore National Laboratory. December 1987.
17. *Pitting, Galvanic, and Long-term Corrosion Studies on candidate Container Alloys for the Tuff Repository*, U.S. Nuclear Regulatory Commission, NUREG/CR-5709, January 1992.
18. *Immersion Studies on Candidate Container Alloys for the Tuff Repository*, U.S. Nuclear Regulatory Commission, NUREG/CR-5598, May 1991.
19. *Inconel Alloy 625*, 5th Edition, Inco Alloys International, Publication T-42, 1985.
20. *Survey of Degradation Modes of Candidate Materials for High-Level Radioactive-Waste Disposal Containers, Volume 2 - Oxidation and Corrosion*, UCID-21362. Livermore, California: Lawrence Livermore National Laboratory, August 1992.
21. Triay, I. R.; Meijer, A.; Conca, J. L.; Kung, K. S.; Rundenberg, R. S.; Strietelmeier, E. S. 1996. *Summary and Synthesis Report on Radionuclide Retardation for the Yucca Mountain Site Characterization Project*. Milestone Report 3784, Los Alamos, New Mexico: Los Alamos National Laboratory.
22. Ebert, W. L. 1995. *The Effects of the Glass Surface Area/Solution Volume Ratio on Glass Corrosion: A Critical Review*. Argonne National Laboratory Report, ANL-94/34, 289pp.
23. Bates, J.; Strachan, D.; Ellison, A.; Buck, E.; Bibler, N.; McGrail, B. P.; Bourcier, W.; Grambow, B.; Sylvester, K.; Wenzel, K.; and Simonsen, S. 1995. *Glass Corrosion and Irradiation Damage Performance*, Plutonium Stabilization & Immobilization Workshop, Washington, D.C., December 11-14.
24. Spahiu, K., and Bruno, J. 1995. *A selected thermodynamic database for REE to be used in HLNW performance assessment exercises*, SKB Technical Report 95-35, Swedish Nuclear Fuel and Waste Management Co., Stockholm, 80pp, January.
25. Roberts, W. L.; Rapp, G. R., Jr.; and Weber, J. 1974. *Encyclopedia of Minerals*. van Nostrand, New York, 693 pp.

PREDECISIONAL DOCUMENT

26. Bourcier, B, personal communication to P. L. Cloke attached to Interoffice Correspondence LV.WP.PG.11/96-265. Subject: *Rare Earth Elements*. From P. Gottlieb to File, 11/13/96.
27. Weast, R. C., ed., *CRC Handbook of Chemistry and Physics*. 61st edition, CRC Press, Inc., Boca Raton, Florida. pp B-73-B166 (1980).
28. McGrail, P, personal communication to P. L. Cloke attached to Interoffice Correspondence LV.WP.PG.11/96-266. Subject: *Rare Earth Precipitates*. From P. Gottlieb to File, 11/13/96.
29. Choppin, G. R., personal communication to P. L. Cloke attached to Interoffice Correspondence LV.WP.GP.11/96-267. Subject: *Silica Experiments*. From P. Gottlieb to File, 11/13/96.
30. Jonasson, R. G.; Bancroft, G. M.; and Nesbitt, H. W. 1985. *Solubilities of some hydrous REE phosphates with implications for diagenesis and sea water concentrations*, *Geochim. Cosmochim. Acta*, Volume 49, number 10, pp 2133-2140, October.
31. Harrar, J. E.; Carley, J. F.; Isherwood, W. F.; and Raber, E. 1990. *Report of the Committee to Review the Use of J-13 Well Water in Nevada Nuclear Waste Storage Investigations*, UCID-21867, Livermore, California: Lawrence Livermore National Laboratory.
32. Bourcier, W. L. 1994. *Critical Review of Glass Performance Modeling*, ANL-94/17, Argonne National Laboratory (ANL), 63pp.
33. Bourcier, W. L., *Waste Glass Corrosion Modeling: Comparison with Experimental Results*, *Mat. Res. Soc. Symp., Proceedings*, Vol. 333, pp. 69-82., 1994.
34. Bourcier, W. L.; Carroll, S. A.; and Phillips, B. L. 1994. *Constraints on the Affinity Term for Modeling Long-Term Glass Dissolution Rates*, *Mat. Res. Soc. Symp., Proceedings*, Vol. 333, pp. 507-512.
35. Ebert, W. L., personal communication to P. L. Cloke attached to Interoffice Correspondence LV.WP.PG.11/96-268. Subject: *European Waste Disposal Efforts*. From P. Gottlieb to File, 11/13/96.
36. Bourcier, W. L.; Weed, H. C.; Nguyen, S. N.; Nielsen, J. K.; Morgan, L.; Newton, L.; and Knauss, K. G. 1992. *Solution Compositional Effects on the Dissolution Kinetics of Borosilicate Glass*, *Proceedings, Seventh International Symposium on Water-Rock Interactions*, pp. 81-84.
37. Latimer, W. M. 1952. *The Oxidation States of the Elements and Their Potentials in Aqueous Solutions*. 2nd ed., Prentice-Hall, Inc., New York, Appendix II.
38. Felsche, J. 1973. "The Crystal Chemistry of the Rare-Earth Silicates," Dunitz, J. D., (ed.), *Structure and Bonding*, Volume 13, Springer-Verlag, New York, pp. 100-197.

PREDECISIONAL DOCUMENT

39. Wilson, M. L.; Gauthier, J. H.; Barnard, R. W.; Barr, G. E.; Dockery, H. A.; Dunn, E.; Eaton, R. R.; Guerin, D. C.; Lu, N.; Martinez, M. J.; Nilson, R.; Rautman, C. A.; Robey, T. H.; Ross, B.; Ryder, E. E.; Schenker, A. R.; Shannon, S. A.; Skinner, L. H.; Helsey, W. G.; Gansemer, J. D.; Lewis, L. C.; Lamont, A. D.; Triay, I. R.; Meijer, A.; Morris, D. E. 1994. *Total-System Performance Assessment for Yucca Mountain - SNL Second Iteration (TSPA-1993)*. Volume 1, SAND93-2675, pp. 7-11. Sandia, New Mexico: Sandia National Laboratories.
40. Broxton, D. E.; Warren, R. G.; Hagar, R. C.; Luedemann, G. 1986. *Chemistry of Diagenetically Altered Tuffs at a Potential Nuclear Waste Repository, Yucca Mountain, Nye County, Nevada*. LA-10802-MS, pp. 16, 52. Livermore, California: Lawrence Livermore National Laboratory.
41. Katayama, N.; Kubo, K.; Hirono, S. 1974. "Genesis of Uranium Deposits of the Tono Mine, Japan," in *Formation of Uranium Ore Deposits*, IAEA-SM-183/19, International Atomic Energy Agency, pp. 437-452.
42. Briggs, J. Blair, ed., Updated November 4, 1996. *International Handbook of Evaluated Criticality Safety Benchmark Experiments*, NEA/NSC/DOC(95)03/I, Nuclear Energy Agency, Organization for Economic Co-operation and Development, MIX-COMP-THERM-001, MIX-SOL-THERM-001, MIX-SOL-THERM-002, MIX-SOL-THERM-004, PU-SOL-THERM-001 through -007, PU-SOL-THERM-009, PU-SOL-THERM-010, PU-SOL-THERM-11, PU-SOL-THERM-013, HEU-MET-THERM-003, HEU-MET-THERM-006, HEU-COMP-THERM-004, HEU-SOL-THERM-001 through -003, HEU-SOL-THERM-007 through -009, HEU-SOL-THERM-013 through -016, HEU-SOL-THERM-021.
43. Yang, I. C.; Rattray, G. W.; and Yu, P. 1996. *Interpretations of Chemical and Isotopic Data from Boreholes in the Unsaturated-Zone at Yucca Mountain, Nevada*, Water-Resources Investigations Report WRIR 96-4058, U.S. Geological Survey.

PREDECISIONAL DOCUMENT

APPENDIX A
MATERIAL PROPERTIES AND REPOSITORY ENVIRONMENT PARAMETERS

PREDECISIONAL DOCUMENT

Intentionally Left Blank

PREDECISIONAL DOCUMENT

TABLES

	Page
A-1 La-BS Glass Waste Form Composition	A-1
A-2 Projected Composition of Savannah River Site DHLW Filler Glass	A-2
A-3 Waste Package Metal Composition	A-3
A-4 Thermal History	A-3
A-5 Composition of Water Incident on the Waste Package	A-5

PREDECISIONAL DOCUMENT

INTENTIONALLY LEFT BLANK

APPENDIX A

MATERIAL PROPERTIES AND REPOSITORY ENVIRONMENT PARAMETERS

This appendix provides parameters of the waste form and the repository environment; these parameters are used as input for the detailed process codes such as EQ3/6.

Waste Form Composition

The La-BS glass composition listed in Table A-1 has been provided by informal memo (Reference 10). The fourth significant figure is for reference only, since the calculations in this study are only considered to three significant figure resolution, and since the final composition is still subject to some change.

Table A-1. La-BS Glass Waste Form Composition

Component	Wt%
SiO ₂	25.8
B ₂ O ₃	10.4
Al ₂ O ₃	19.04
ZrO ₂	1.15
La ₂ O ₃	11.01
Nd ₂ O ₃	11.37
SrO	2.22
PuO ₂	11.39*
Gd ₂ O ₃	7.61**

* Equivalent to 10 Wt% Pu

** Equivalent to 6.6% Wt% Gd, which is a 1:1 mole ratio to Pu.

It should be noted that this glass composition has been optimized to eliminate the need for lead (Pb), because of the current restriction against acceptance of materials regulated as hazardous under the Resource Conservation and Recovery Act for disposal in the first repository.

Filler Glass Composition

The DHLW filler glass has not been finally specified; however, the blend composition given in Reference 6, Table 3.3.8, should be close to the final composition. This is repeated in Table A-2.

PREDECISIONAL DOCUMENT

Table A-2. Projected Composition of Savannah River Site DHLW Filter Glass

Component	wt%
Al ₂ O ₃	3.98
B ₂ O ₃	10.28
BaSO ₄	0.14
Ca ₃ (PO ₄) ₂	0.07
CaO	0.85
CaSO ₄	0.08
Cr ₂ O ₃	0.12
Cs ₂ O	0.08
CuO	0.19
Fe ₂ O ₃	7.04
FeO	3.12
K ₂ O	3.58
Li ₂ O	3.16
MgO	1.36
MnO	2.00
Na ₂ O	11.00
Na ₂ SO ₄	0.36
NaCl	0.19
NaF	0.07
NiO	0.93
PbS	0.07
SiO ₂	45.57
ThO ₂	0.21
TiO ₂	0.99
U ₃ O ₈	2.20
Zeolite	1.87
ZnO	0.08
Others	0.58

PREDECISIONAL DOCUMENT

Waste Package Metal Composition

The compositions of the metals expected to be used for the WP barriers and the canisters and WF cans are given in the Table A-3. These values are from standard metals handbooks; the specific chain of authority for each is given in Reference 12.

Table A-3. Waste Package Metal Composition

Steel Type/Use	Nominal Composition, % by Mass						
	Si	Cr	Mn	Fe	Ni	Nb	Mo
A516/outer barrier	0.275		1.03	98.7			
625/inner barrier		21.5			65.9	3.65	9
304L/canister, cans		19		71	10		

Thermal History

Figure 4.2-8 in Reference 3 provides thermal history at the WP top surface up to 10,000 years. This can be idealized and extrapolated to 100,000 years as shown in Table A-4.

Table A-4. Thermal History

Time (yrs)	Temperature (°C)
5000	66.0
6000	59.5
7000	55.5
8000	53.0
9000	51.0
10000	50.0
15000	45.1
20000	40.6
30000	34.3
40000	31.4
50000	29.7
60000	28.6
80000	27.3
100000	26.5

PREDECISIONAL DOCUMENT

For initial calculations, these values are used without any spatial temperature change into the invert material. If the temperature variation into the invert is needed, or more detail is needed in the thermal profile, thermohydrologic modeling calculations should be done to address the specific scenarios.

Water Compositions

The two water compositions to use as a starting point for calculations are the J-13 water composition (using J-13 average given below) and the 10xJ-13 composition also given in Table A-5. The oxidation state of the system should be taken as oxidizing using the dissolved O₂ values analyzed and reported in Table A-5. It should be noted that because the calcium, bicarbonate, and pH are linked through the equilibria with calcite and CO₂ gas, the carbonate content of the concentrated case should be calculated assuming equilibrium with calcite. The starting CO₂ gas concentration should be taken as about 1200 ppm in the gas phase. Computational assumptions regarding the accessibility of the gas phase to the aqueous phase will affect the equilibrium fluid composition evolution and therefore both closed system and "atmospheric" buffered system behavior should be investigated. In addition, because the ambient fluids are supersaturated with aqueous silica with respect to quartz saturation, the concentrated case should use equilibrium with quartz at the starting temperature to set the initial aqueous silica concentration.

Liquid Flux Scenarios

- No flux (diffusion only)
- Low flux: 0.1 mm/yr
- Medium flux: 1.0 mm/yr (base case)
- High flux: 10 mm/yr

It is suggested in TSPA-95 (Reference 3) that the liquid flux might cycle through these scenarios with an approximately 100,000 year period based on the larger period of the Milankovitch glacial cycle.

Transport processes investigated should cover a range of Peclet numbers from very low (diffusion dominated) to very high (advection dominated).

Table A-5. Composition of Water Incident on the Waste Package

Water Scenario	Na ⁺ mg/l	K ⁺ mg/l	Ca ²⁺ mg/l	Mg ²⁺ mg/l	NO ₃ ⁻ mg/l	HCO ₃ ⁻ mg/l	Cl ⁻ mg/l	F ⁻ mg/l	SO ₄ ²⁻ mg/l	SiO ₂ mg/l	pH	O ₂ mg/l
J-13A ⁱ	42	5.0	12	2.1	NA	124	7.1	2.4	17	57	7.2	5.7
J-13B ⁱⁱ	45	5.3	11.5	1.76	10.1	NA	6.4	2.1	18.1	64.3	6.9	5.7
J-13avg ⁱⁱⁱ	45.8	5.04	13.0	2.01	8.78	128.9	7.14	2.18	18.4	61.1	7.41	NR
Evaporated ^{iv}	460	50	106	13.1	87.5	29.7	764	6.0	184	6.1	7.90	8.4

- i. J-13A analysis from Reference 7. Note that Li⁺ and Sr²⁺, which were measured at microg/l concentrations, have been left out of this report. NA stands for "not analyzed".
- ii. J-13B analysis from Reference 8. Note that Li, Fe, and Mn, which were measured at microg/l concentrations, have been left out of this report. NA stands for "not analyzed".
- iii. J-13avg is set of values given in Table 3-2 of Reference 9. NR stands for "not reported".
- iv. The values in this line were generated by an EQ6 simulation of an evaporation of approximately 90 percent of the water. These values were used to generate the results reported in Table C-3 in Appendix C.

PREDECISIONAL DOCUMENT

INTENTIONALLY LEFT BLANK

PREDECISIONAL DOCUMENT

**APPENDIX B
PROGRAM TO TRACK WASTE PACKAGE DEGRADATION PARAMETERS**

A00000000-01717-5705-00014 REV 01

PREDECISIONAL DOCUMENT

February 1997

PREDECISIONAL DOCUMENT

Intentionally Left Blank

PREDECISIONAL DOCUMENT

APPENDIX B
PROGRAM TO TRACK WASTE PACKAGE DEGRADATION PARAMETERS

```
/* pugdcr.c Computes remaining Pu, Gd, U considering both waste form (WF) dissolution and subsequent removal of these species from the waste package by flow through, and by, the waste package. The basic timestep is 1000 years. To identify the time at which criticality might occur, the program compares remaining U, Pu and Gd against the regression of minimum Gd mass required to avoid criticality for the collapsed WF configuration. This minimum Gd has been determined by a regression using over 100 points of keff as a function of Gd, U, and Pu. To get the best linear fit, the results were grouped into three ranges of Gd concentration: below 1 kg, between 1 kg and 4 kg, and above 4 kg. The resulting piecewise linear function is used for screening purposes only; any potentially critical configuration is subject to an MCNP calculation with the indicated masses of Pu, U, and Gd to verify criticality.
```

The bookkeeping of the Pu, U, and Gd considers that as these components are released from the WF, they immediately go into solution to the extent of their solubility with the remainder assumed to precipitate into some insoluble form. The insoluble forms are collectively referred to as clay. The components of the clay are incremented as these components are dissolved from the WF, except for the amounts which go into solution and are flushed out. The amount of a species removed from the waste package is simply computed as the product of the volumetric flow-through or exchange flushing of the waste package, multiplied by the maximum concentration of the species (solubility). At the present time exchange flushing is simply represented by a lower volumetric rate. The program may be updated to incorporate a specific exchange factor multiplying the basic infiltration rate. This exchange factor would be one for flow-through, and something between .1 and .001 for exchange flushing. However, this feature is not implemented in the present version.

This version also considers the amount of Cr in steel and in solution, so that the latter can determine pH, which, in turn determines the solubility of Gd (and possible later application to U and Pu solubility, if we want detailed consideration of the high pH time phase). For large ratio of flushing to steel dissolution rate, almost all the released Cr will be flushed out at each time step, so the difference equation for incrementing the dissolved Cr (cro) becomes unstable. For this reason the Cr in solution is approximated by the steady state value: release rate from steel divided by flushing rate. To assure that this steady state can be reached, there is a startup of steel dissolution, with timestep reduced to 10 years to assure stability, preceding the startup of waste form dissolution. The startup of steel dissolution will always precede the startup of wasteform dissolution because the canister and cans must be penetrated before the dissolution of the wasteform can begin. If some of the wasteform were released before the pH dropped to the region relevant here (less than 7) there would be a question of whether the Gd were only temporarily sequestered in $GdOHCO_3$ which would dissolve upon lowering of the pH (to 6 or lower), or whether, instead, it was trapped in a highly inert clay.

This version can be adapted to evaluate the reduction of the Pu loading or of the number of waste form canisters per package. To reduce the Pu loading of each waste form canister, change the three statements marked *RdcPct*. To reduce the number of waste form canisters per package, change the three statements marked *RdcCnstrs*. It should be noted that these two strategies give identical results for the same fractional reduction from full 10 percent loading of the 4 waste form canister package.

The effect of varying Gd:Pu mole ratio can be modeled by simply changing the amount of Gd, specified by the statement marked *RdcGd*. It should be noted that such a change has little effect, except for the cases in which Gd is released at such a high rate, and faces a relatively low solubility, so that it precipitates for some time before most of it can go back into solution and be flushed from the package. */

```
#include <stdio.h>
#include <stdlib.h>
```

PREDECISIONAL DOCUMENT

```

#include <math.h>
#include <string.h>
#define PI 3.14159

void main()
(int i,j,k,yr,outflag,
  maxyrs=300, //Maximum time in 1000 yrs
  printyr=10, //Interval for printout in 1000 yrs
  critical=0, //Indicator of whether criticality has occurred on this case
  printcase; //For printing first criticality year
float x,puclay,pugls,uclay,ugls, gdclay, gdgl, fclay, lam,maxgd0,fracfac,
  fgls,fl,ftotal,gdtotal,pudecayg,pudecays,glstrate,glstrateg,fracarea,
  sltnratet,tgls,totalwf,dpuclay,duclay,dgdclay,crs,cro,rc,ph,crom,
  r0, //Stainless steel corrosion rate in microns/yr.
  tswf=6.0, //Start of waste form dissolution (1000 yr)
  tss=3.5, //Start of stainless steel corrosion (1000 yr)
  crs0=400, //Initial Cr in 4 canisters (neglecting Cr in cans)

  puhalf=24.1/.693, //Half-life of Pu in 1000 yrs
  pu00=205, //Initial Pu in 4 canister waste package *RdcPct*, *RdcCnstrs*
  pu0=pu00*exp(-tswf/puhalf), //Pu at start of waste form dissolution
  u0=pu00*(1-exp(-tswf/puhalf)), //U at start of waste form dissolution
  gd0=134, //Initial Gd at mole per mole ratio with Pu *RdcPct*,*RdcGd,*RdcCnstrs*
  pkgarea=4.8, //Horizontal cross sectional area inside waste pkg
  pkgvoid= 3.5, //Void volume inside waste package
  keff=.98, //Threshold for criticality screening
  hco3=0, //Bicarbonate in incoming J13 water, not used now
  minph=5.8,
  totalwf0=10*pu00; //Assume Pu is 10% of waste form *RdcPct*
float dslnrate, inflrate, maxpu, maxgd, maxu;
char dummy[80],outs[10],glasscase;
FILE *fin, *fout,*ferr;
fin=fopen("pugdcr.in","r");
fout=fopen("pugdcr.out","w");
ferr=fopen("junk.out","w");
fgets(dummy,79,fin); //Read through glass vs ceramic heading
fgets(dummy,79,fin); //Read for glasscase
glasscase=tolower(dummy[0]);
if(glasscase=='y') fprintf(fout,"Glass\n\n");
else if(glasscase=='n') fprintf(fout,"Ceramic\n\n");
else
  {printf("Incorrect wasteform\n");
  exit(0);}
fgets(dummy,79,fin); //Read through column headings on input file
while(fscanf(fin,"%f %f %f %f %f %f %f %f", //Input parameters for this case
  &maxpu,&maxgd0,&maxu,&dslnrate,&inflrate,&minph,&fracfac,&r0)!=EOF)
  {printf(fout,"maxPu=%6.2f maxU=%8.2f maxGd=%5.2f minpH=%5.2f\n",
  frac fac=%5.2f\n",maxpu,maxu,maxgd0,minph,fracfac);
  cro=1e-10; //Initialize Cr corresponding to pH=12
  crs=crs0;
  outflag=0; //flag for non-acidic condition
  fracarea=fracfac*15.5, //waste form srfc area per waste pkg
  lam=inflrate; //lmm/yr gives a 1000 yr turnover
  pugls=pu0; //Initialize Pu amount in WF
  gdgl=gd0; //Initialize Gd amount in WF
  ugls=u0; //Initialize U amount in WF
  puclay=0; //Initialize Pu amount removed from WF and still in pkg
  uclay=0; //Initialize U amount in solution (still in pkg)

```

PREDECISIONAL DOCUMENT

```

gdclay=0; //Initialize Gd amount removed from WF and still in pkg
critical=0; //Initialize criticality indicator
printcase=0; //Initialize
fgls=pugls+ugls; //Initialize fissile in WF
fclay=0; //Initialize fissile in solution
totalwf=totalwf0; //Initialize waste form mass
ftotal=fgls+fclay; //Initialize total fissile
gdtotal=gdgls+gdclay; //Initialize total Gd
yr=0; //Initialize time after start of waste form dissolution
glstrate=dslntrate*fracarea* //Dissolution rate times initial surface area
        .001* //Convert gm to kg
        365*1000; //Convert days to 1000 years
//glstrate/=4; //For reducing the number of canisters/pkg *RdcCnstrs*
sltnrate=inflrate*pkgarea* //Volumetric flow incident on package
        .001* //Convert mm/yr to meters/yr
        .001* //Prepare to multiply by concentration in ppm (gm=>kg)
        1000; //Convert yrs to 1000 yrs
tgls=3*totalwf0/glstrate; //Pu WF lifetime, assuming 10%Pu
fprintf(fout, "WF Dslnn rt=%f Stl dslnn rt=%5.3f Infl rt=%f WF life=%f\n",
        dslntrate, r0, inflrate, tgls);
r0*=39.9; //kg/1000yr: cm2*(g/cc)*.1(mm/cm)*(4canisters)*Crfrac/1000
for(i=0; i<(tswf-tss)*100; i++) //10 yr timestep to start ss corrosion
    (if(crs>0) rc=r0/100;
    else rc=0;
    crs-=rc;
    if(crs<0) crs=0;
    cro+=rc-lam*cro/100;
    if(cro<=0) cro=0;
fprintf(ferr, "%d %f %f\n", i, crs, cro);
fprintf(ferr, "\n\n");
x=(cro/52.01/pkgvoid)-hco3;
if(x>0) ph= -log10(x); //1 mole H per mole Cr (dichromate);
//1/52.01 moles Cr/gm Cr; divide by vol to reduce cro from mass to
//concentration; neutralize with bicarbonate not used now
else outflag=1;
fprintf(fout, "Cr in steel=%f Cr in sltn=%f pH=%f\n", crs, cro, ph);
fprintf(fout, "%8s%8s%8s%8s%8s%8s%8s\n",
        "Time", "Pu WF", "U WF", "Gd WF",
        "Pu Clay", "U Clay", "Gd Clay", "Crmate");
while((yr<maxyrs)&&(outflag==0)&&(ftotal>30))
    (maxgd=maxgd0*pow(10, -3*(ph-6.0));
    if(crs>0)
        (rc=r0;
        crs-=rc;
        cro=rc/lam;) //Calculate from steady state to avoid instability
    else cro=1e-10;
    if(crs<0) crs=0;
    x=(cro/52.01/pkgvoid)-hco3;
    if(x>0) ph= -log10(x); //Same as above
    else break;
    if(ph<minph) ph=minph;
    if(ph>9) ph=9;
    pudecayg=(pugls>0?pugls/puhalf:pugls); //WF Pu->U this 1000 yrs
    if((yr<tgls)&&(totalwf>0)) //Compute total WF dissolution for this step
        glstrate=glstrate*pow(1-(yr+.5)/tgls, 2); //Adjust for reduced surface area
    else if ((yr>=tgls)&&(totalwf>0)) glstrate= totalwf;
    else glstrate=0;
    pudecays=(puclay>0?puclay/puhalf:0); //solution Pu->U this 1000 yrs

```

```

duclay = g1rate*ug1s*(totalwt>0?1/totalwt:0)
//Increment clay U from Wfssltcn
-(uclay>sltnrate*maxu?sltnrate*maxu: //Push only maxu
(uclay>0?uclay:0)); //No decrement if none left
//
if(duclay<0) duclay=0;
uclay+duclay+pudcay; //Increment solution U for solution Pu>U
if(uclay<0) uclay=0;
if(totalwt>0)
ug1s+pudcayg-g1rate*ug1s/totalwt; //Decrement U in Wf
duclay=g1rate*ug1s*(totalwt>0?1/totalwt:0)
//Increment clay Pu from Wf dsltn
-(uclay>sltnrate*maxpu?sltnrate*maxpu: //Push only maxpu
(uclay>0?uclay:0)); //No decrement if none left
//
if(dpuclay<0) dpuclay=0;
puc1ay+dpuclay-pudcay; //decrement solution Pu from solution Pu>U
if((pug1s>0) && (totalwt>0))
pug1s-pudcayg+g1rate*pug1s/totalwt; //Decrement Pu in Wf
else pug1s=0;
dgdc1ay=g1rate*gd1s*(totalwt>0?1/totalwt:0)
//Increment clay Gd from Wf dsltn
-s1tnrate*maxgd; //Push only maxgd
if(dgdclay<0) dgdc1ay=0; //Prevents re-dissolution of Gd from clay
gdclay+dgdc1ay;
if(gdclay<0) gdclay=0; //Substitute test if gd can be re-dissolved from clay
gd1s-g1rate*gd1s*(totalwt>0?1/totalwt:0); //Decrement Gd in Wf
totalwt-g1rate; //Decrement Wf for dissolution this step
if (totalwt<0) totalwt=0;
fc1ay=uclay+puc1ay; //Update f1s1e in clay
fg1s=ug1s+pug1s; //Update f1s1e in Wf
total=fg1s+fc1ay; //Update total f1s1e
gdtotal=gd1s+gdclay; //Update total Gd
yr+1;
//Increment time (by 1000 yrs)
stcpy(outs, ' ');
if(g1sclass== 'n')
if(gdclay>2.5)
if(log(gdclay)<(.7587-ketf+.00298*puc1ay+.00135*uc1ay)/.11954)
stcpy(outs, 'Clay10');
if(critical=0)
if(critical=1)
printcase=1;)))
else if (gdclay>1)
if(gdclay<(.67725-ketf+.00478*puc1ay+.00205*uc1ay)/.08524)
stcpy(outs, 'Clay1');
if(critical=0)
if(critical=1)
printcase=1;)))
else if (gdclay>.2)
if(gdclay<(.62516-ketf+.006578*puc1ay+.003005*uc1ay)/.17972)
stcpy(outs, 'Clay.2');
if(critical=0)
if(critical=1)
printcase=1;)))
else if (gdclay<(.448283597-ketf+.010123*puc1ay+.004829*uc1ay)/.36997)
stcpy(outs, 'Clay.0');
if(critical=0)
if(critical=1)
printcase=1;)))

```


PREDECISIONAL DOCUMENT

```

/* pugdkeff.c Version to simply calculate keff using the appropriate regression.

The remainder of this intro is the same as the previous program, pugdcr.c

#include <stdio.h>
#include <stdlib.h>
#include <math.h>
#include <string.h>
#define PI 3.14159

void main()
(int i,j,k,yr,outflag,firsttime,adjustcr,yr0,yrmax,
 maxyrs=300, //Maximum time in 1000 yrs
 printyr=10, //Interval for printout in 1000 yrs
 critical=0, //Indicator of whether criticality has occurred on this case
 printcase; //For printing first criticality year
float x,puclay,pugls,uclay,ugls, gdclay, gdgls,fclay,lam,maxgd0,fracfac,
 fgl,fl,ftotal,gdtotal,pudecayg,pudecays,glstrate,glstrateg,fracarea,
 sltnratet,tgls,totalwf,dpuclay,duclay,dgdclay,crs,cro,rc,ph,crom,keffmax,
 r0, //Stainless steel corrosion rate in microns/yr read from input
 kold=0, //initialization to determine peak
 tswf=6.0, //Start of waste form dissolution (1000 yr)
 tss=3.5, //Start of stainless steel corrosion (1000 yr)
 crs0=400, //Initial Cr in 4 canisters only
 cnl=100, //SS Cr below which degradation rate shrinks with area
 puhalf=24.1/.693, //reciprocal of Pu decay rate per 1000 yrs
 pu00=205, //Initial Pu in 4 canister waste package
 pu0=pu00*exp(-tswf/puhalf), //Pu at start of waste form dissolution
 u0=pu0*(1-exp(-tswf/puhalf)), //U at start of waste form dissolution
 gd0=134, //Initial Gd at mole per mole ratio with Pu
 pkgarea=4.8, //Horizontal cross sectional area inside waste pkg
 pkgvoid= 3.5, //Void volume inside waste package
 keff=.98, //Threshold for criticality screening
 hco3=0, //Alkalinity as bicarbonate, not used now
 minph=6.0, //pH floor to limit Gd solubility; overridden by input
 totalwf0=10*pu00; //Assume Pu is 10% of waste form

float dslntrate, inflrate, maxpu, maxgd, maxu;
char dummy[80],outs[10],glasscase;
FILE *fin, *fout,*ferr;
fin=fopen("pugdkeff.in","r");
fout=fopen("pugdkeff.out","w");
ferr=fopen("junk.out","w");
fgets(dummy,79,fin); //Read through glass vs ceramic heading
fgets(dummy,79,fin); //Read for glasscase
glasscase=tolower(dummy[0]);
if(glasscase=='y') fprintf(fout,"Glass\n\n");
else if(glasscase=='n') fprintf(fout,"Ceramic\n\n");
else
{printf("Incorrect wasteform\n");
 exit(0);}
fgets(dummy,79,fin); //Read through column headings on input file
while(fscanf(fin,"%f %f %f %f %f %f %f %f", //Input parameters for this case
 &maxpu,&maxgd0,&maxu,&dslntrate,&inflrate,&minph,&fracfac,&r0)!=EOF)
{fprintf(fout,"maxPu=%6.2f maxU=%6.2f maxGd=%6.2f minpH=%5.2f\
Frac fac=%5.1f\n",maxpu,maxu,maxgd0,minph,fracfac);
 cro=1e-10; //Initialize Cr corresponding to pH=12
 crs=crs0;
 kold=0;

```

PREDECISIONAL DOCUMENT

```

keffmax=0;
firsttime=1; //to determine peak keff
adjustcr=0; //flag for adjusting for shrinking SS area
outflag=0; //flag for non-acidic condition
fracarea=fracfac*15.5, //waste form srfc area per waste pkg
lam=inflrate*pkgarea/pkgvoid; //For calculating Cr removal and conc
pugls=pu0; //Initialize Pu amount in glass
gdgls=gd0; //Initialize Gd amount in glass
ugls=u0; //Initialize U amount in glass
puclay=0; //Initialize Pu amount removed from glass and still in pkg
uclay=0; //Initialize U amount in solution (still in pkg)
gdclay=0; //Initialize Gd amount removed from WF and still in pkg
critical=0; //Initialize criticality indicator
printcase=0; //Initialize
strcpy(outs, " ");
fgls=pugls+ugls; //Initialize fissile in glass
fclay=0; //Initialize fissile in solution
totalwf=totalwf0; //Initialize waste form mass
ftotal=fgls+fclay; //Initialize total fissile
gdtotal=gdgls+gdclay; //Initialize total Gd
yr=0; //Initialize time after start of waste form dissolution
glrateg=dslntrate*fracarea* //Dissolution rate times initial surface area
.001* //Convert gm to kg
365*1000; //Convert days to 1000 years
sltnratet=inflrate*pkgarea* //Volumetric flow incident on package
.001* //Convert cm/yr to meters/yr
.001* //Prepare to multiply by concentration in ppm (gm=>kg)
1000; //Convert yrs to 1000 yrs
tgls=3*totalwf0/glrateg; //WF lifetime
fprintf(fout, "WF Dssltnn rt=%f Stl dssltn rt=%5.3f Infl rt=%6.2f WFlife=%f\n",
dslntrate, r0, inflrate, tgls);
r0*=39.9; //kg/1000yr: cm2*(steel g/cc)*.1(mm/cm)*(4canisters)*Crfrac/1000
for(i=0; i<(tswf-tss)*100; i++) //10 yr timestep to start ss corrosion
(if(crs>0) rc=r0/100; //Assume no ph dependence for ss crsrn rte
else rc=0;
crs=-rc;
if(crs<0) crs=0;
cro+=rc-lam*cro/100;
if(cro<=0) cro=0;
fprintf(ferr, "%d %f %f\n", i, crs, cro);)
fprintf(ferr, "\n\n");
x=(cro/52.01/pkgvoid)-hco3;
if(x>0) ph= -log10(x); //1 mole H per mole Cr;
//1/52.01 moles Cr/gm Cr; divide by vol to reduce cro from mass to
//concentration; neutralize with bicarbonate
else ph=7.4;
fprintf(fout, "Cr in steel=%f Cr in sltn=%f pH=%f\n", crs, cro, ph);
fprintf(fout, "%8s%8s%8s%8s%8s%8s%8s%8s\n",
"Time", "Pu WF", "U WF", "Gd WF",
"Pu Clay", "U Clay", "Gd Clay", "Crmate", "Keff");
while((yr<maxyrs)&&(outflag==0)&&(ftotal>30))
(maxgd=maxgd0*pow(10, -3*(ph-6.0)));
if(crs>0)
(if(crs>cn1) rc=r0;
else if(adjustcr==0)
(adjustcr=1;
yr0=yr;))
if(adjustcr==1)

```

PREDECISIONAL DOCUMENT

```

(x=(yr-yr0+.5)*r0/cnl;
if (x<1) rc=r0*pow(1-x,2); //adjust for shrinking SS area
else rc=0;)
if(rc>0) crs=-rc;
else crs=0;
cro=rc/lam;}
else cro=1e-10;
if(crs<0) crs=0;
x=(cro/52.01/pkgvoid)-hco3;
if(x>0) ph=-log10(x); //Same as above
else ph=7.4;
if(ph<minph) ph=minph;
if(ph>9) ph=9;
pudecayg=(pugls>0?pugls/puhalf:pugls); //glass Pu=>U this 1000 yrs
if((yr<tgls)&&(totalwf>0)) //Compute total glass dissolution for this step
glstrate=glstrateg*pow(1-(yr+.5)/tgls,2); //Adjust for reduced surface area
else if ((yr>=tgls)&&(totalwf>0)) glstrate= totalwf;
else glstrate=0;
pudecays=(puclay>0?puclay/puhalf:0); //solution Pu=>U this 1000 yrs
duclay= glstrate*ugls*(totalwf>0?1/totalwf:0)
//Increment clay U from glassdssltn
-(uclay>sltnratet*maxu?sltnratet*maxu: //Flush only maxu
(uclay>0?uclay:0)); //No decrement if none left
// if(duclay<0) duclay=0; //to prevent re-dissolution from clay
uclay+=duclay+pudecays; //Increment solution U for solution Pu=>U
if(uclay<0)uclay=0;
if(totalwf>0):
ugls+=pudecayg-glstrate*ugls/totalwf; //Decrement U in glass
dpuclay=glstrate*pugls*(totalwf>0?1/totalwf:0)
//increment clay Pu from glass dsltn
-(puclay>sltnratet*maxpu?sltnratet*maxpu: //Flush only maxpu
(puclay>0?puclay:0)); //No decrement if none left
// if(dpuclay<0) dpuclay=0;
puclay+=dpuclay-pudecays; //decrement solution Pu from solution Pu=>U
if(puclay<0)puclay=0;
if((pugls>0)&&(totalwf>0))
pugls-=pudecayg+glstrate*pugls/totalwf; //Decrement Pu in glass
else pugls=0;
dgdclay=glstrate*gdgls*(totalwf>0?1/totalwf:0)
//Increment clay Gd from glass dssltn.
-sltnratet*maxgd; //Flush only maxgd
// if(dgdclay<0) dgdclay=0; //Prevents re-dissolution of Gd from clay
gdclay+=dgdclay;
if(gdclay<0) gdclay=0; //Substitute test if gd can be re-dissolved from clay
gdgls=-glstrate*gdgls*(totalwf>0?1/totalwf:0); //Decrement Gd in glass
totalwf=-glstrate; //Decrement glass for dissolution this step
if (totalwf<0) totalwf=0;
fclay=uclay+puclay; //Update fissile in clay
fgls=ugls+pugls; //Update fissile in glass
ftotal=fgls+fclay; //Update total fissile
gdtotal=gdgls+gdclay; //Update total Gd
yr+=1; //Increment time (by 1000 yrs)
if(glasscase=='n')
(if(gdclay>2.5) //for ceramic
keff=.7587+.00298*puclay+.00135*uclay-.11954*log(gdclay);
else if (gdclay>1)
keff=.67725+.00478*puclay+.00205*uclay-.08524*gdclay;
else if (gdclay>.2)

```


PREDECISIONAL DOCUMENT

```
/* critload.c This is a version of pugdcr.c which searches for the
limiting fracture factor, above which a criticality can occur for a series of Pu
loading cases.
```

```
The remainder of this intro is the same as the previous program, pugdcr.c
```

```
#include <stdio.h>
#include <stdlib.h>
#include <math.h>
#include <string.h>
#define PI 3.14159
```

```
void main()
```

```
{int i,j,k,yr,outflag,endload,enddp,
    maxyrs=300, //Maximum time in 1000 yrs
    printyr=10, //Interval for printout in 1000 yrs
    critical=0, //Indicator of whether criticality has occurred on this case
    printcase; //For printing first criticality year
float x,puclay,pugls,uclay,ugls, gdclay, gdgls,fclay,lam,fracfac,
    fgl,fl,ftotal,gdtotal,pudecayg,pudecays,glrate,glrateg,fracarea,
    sltnratet,tgls,totalwf,dpuclay,duclay,dgdclay,crs,cro,rc,ph,crom,
    ffstep,ffstart,loadfac,puglslast,uglslast,puclaylast,uclaylast,
    gdglslast,gdclaylast,crolast,totalwfmax,totalwflast,fclaylast,
    r0, //Stainless steel corrosion rate in microns/yr
    tswf=6.0, //Start of waste form dissolution (1000 yr)
    tss=3.5, //Start of stainless steel corrosion (1000 yr)
    crs0=400, //Initial Cr in 4 canisters (neglecting Cr in cans)

    puhalf=24.1/.693, //Reciprocal of Pu-239 decay rate
    pu00=205, //Initial Pu in 4 canister waste package
    pu0=pu00*exp(-tswf/puhalf), //Pu at start of waste form dissolution
    u0=pu00*(1-exp(-tswf/puhalf)), //U at start of waste form dissolution
    gd0=134, //Initial Gd at mole per mole ratio with Pu
    pkgarea=4.8, //Horizontal cross sectional area inside waste pkg
    pkgvoid= 3.5, //Void volume inside waste package
    keff=.98, //Threshold for criticality screening
    hco3=0, //Bicarbonate in incoming J13 water, not used now
    minph=5.8, //Overridden by input
    maxpu=6.1e-3, //Pu solubility limit
    maxu=1.0, //U solubility limit
    maxgd0=95.0, //Multiplying factor for pH dependent Gd solubility limit
    totalwf0=10*pu00; //Assume Pu is 10% of waste form

float dslntrate, inflrate, maxgd;
char dummy[80],outs[10],glasscase;
FILE *fin, *fout,*ferr;
fin=fopen("critload.in","r");
fout=fopen("critload.out","w");
ferr=fopen("junk.out","w");
fgets(dummy,79,fin); //Read through glass vs ceramic heading
fgets(dummy,79,fin); //Read for glasscase
glasscase=tolower(dummy[0]);
if(glasscase=='y') fprintf(fout,"Glass\n\n");
else if(glasscase=='n') fprintf(fout,"Ceramic\n\n");
else
    (printf("Incorrect wasteform\n");
    exit(0));
fgets(dummy,79,fin); //Read through column headings on input file
while(fscanf(fin,"%f %f %f %f %f %f %f %f", //Input parameters for this case
```

PREDECISIONAL DOCUMENT

```

&keff,&loadfac,&ffstart,&ffstep,&dslntrate,&infrate,&minph,&r0)!=EOF)
(fprintf(fout,"Keff=%5.3f FFstart=%5.3f FFstep=%5.3f Loadfac = %5.3f\
minpH=%5.2f\n",keff,ffstart,ffstep,loadfac,minph);
endload=0;
fracfac=ffstart;
while((fracfac<20)&&(endload==0)) //fracfac incremented each iteration
(cro=1e-10; //Initialize Cr corresponding to pH=12
crs=crs0;
outflag=0; //flag for non-acidic condition
fracarea=fracfac*15.5, //waste form srfc area per waste pkg
lam=infrate*pkgarea/pkgvoid; //Turnover rate for cr stdy state and removal
pugls=pu0*loadfac; //Initialize Pu amount in WF & adjust for Pu loading
gdgls=gd0*loadfac; //Initialize Gd amount in WF & adjust for Pu loading
ugls=u0*loadfac; //Initialize U amount in WF & adjust for Pu loading
puclay=0; //Initialize Pu amount removed from WF and still in pkg
uclay=0; //Initialize U amount in solution (still in pkg)
gdclay=0; //Initialize Gd amount removed from WF and still in pkg
critical=0; //Initialize criticality indicator
printcase=0; //Initialize
fgls=pugls+ugls; //Initialize fissile in WF
fclay=0; //Initialize fissile in solution
totalwf=totalwf0; //Initialize waste form mass
ftotal=fgls+fclay; //Initialize total fissile
gdtotal=gdgls+gdclay; //Initialize total Gd
yr=0; //Initialize time after start of waste form dissolution
glstrateg=dslntrate*fracarea* //Dissolution rate times initial surface area
.001* //Convert gm to kg
365*1000; //Convert days to 1000 years
sltnratet=infrate*pkgarea* //Volumetric flow incident on package
.001* //Convert mm/yr to meters/yr
.001* //Prepare to multiply by concentration in ppm (gm=>kg)
1000; //Convert yrs to 1000 yrs
tgls=3*totalwf0/glstrateg; //Pu WF lifetime, assuming 10%Pu
fprintf(fout,"WF Dslntrn rt=%f Stl dslntrn rt=%5.3f Infl rt=%f WF life=%f\n",
dslntrate,r0,infrate,tgls);
for(i=0;i<(tswf-tss)*100;i++) //10 yr timestep to start ss corrosion
(if(crs>0) rc=r0*39.9/100; //kg/1000yr:
cm2*(g/cc)*.1(mm/cm)*(4canisters)*Crfrac/1000
else rc=0;
crs-=rc;
if(crs<0)crs=0;
cro+=rc-lam*cro/100;
if(cro<=0) cro=0;)
x=(cro/52.01/pkgvoid)-hco3;
if(x>0) ph=-log10(x); //1 mole H per mole Cr (dichromate);
//1/52.01 moles Cr/gm Cr; divide by vol to reduce cro from mass to
//concentration; neutralize with bicarbonate not used now
else outflag=1;
fprintf(fout,"Cr in steel=%f Cr in sltn=%f pH=%f\n",crs,cro,ph);
fclaylast=0;
while((yr<maxyrs)&&(outflag==0))
(maxgd=maxgd0*pow(10,-3*(ph-6.0));
if(crs>0)
(rc=r0*39.9; //kg/1000yr: cm2*(g/cc)*.1(mm/cm)*(4canisters)*Crfrac/1000
crs-=rc;
cro=rc/lam;) //Calculate from steady state to avoid instability
else cro=1e-10;
if(crs<0)crs=0;

```

PREDECISIONAL DOCUMENT

```

x=(cro/52.01/pkgvoid)-hco3;
if(x>0) ph= -log10(x); //Same as above
else break;
if(ph<minph) ph=minph;
if(ph>7) outflag=1;//All Cr is used up so no chance for criticality
pudecayg=(pugls>0?pugls/puhalf:pugls);//WF Pu=>U this 1000 yrs
if((yr<tgl)&&(totalwf>0))//Compute total WF dissolution for this step
  glsrate=glsrate*pow(1-(yr+.5)/tgl,2);//Adjust for reduced surface area
else if ((yr>=tgl)&&(totalwf>0)) glsrate= totalwf;
else glsrate=0;
pudecays=(puclay>0?puclay/puhalf:0);//solution Pu=>U this 1000 yrs
duclay= glsrate*ugls*(totalwf>0?1/totalwf:0)
//Increment clay U from WFDsilt
-(uclay>sltndratet*maxu?sltndratet*maxu: //Flush only maxu
(uclay>0?uclay:0)); //No decrement if none left
// if(duclay<0) duclay=0;
uclay+=duclay+pudecays; //Increment solution U for solution Pu=>U
if(uclay<0)uclay=0;
if(totalwf>0)
  ugls+=pudecayg-glsrate*ugls/totalwf; //Decrement U in WF
dpuclay=glsrate*pugls*(totalwf>0?1/totalwf:0)
//increment clay Pu from WF dsilt
-(puclay>sltndratet*maxpu?sltndratet*maxpu: //Flush only maxpu
(puclay>0?puclay:0)); //No decrement if none left
// if(dpuclay<0) dpuclay=0;
puclay+=dpuclay-pudecays; //decrement solution Pu from solution Pu=>U
if(puclay<0)puclay=0;
if((pugls>0)&&(totalwf>0))
  pugls-=pudecayg-glsrate*pugls/totalwf; //Decrement Pu in WF
else pugls=0;
dgdclay=glsrate*gdgls*(totalwf>0?1/totalwf:0)
//Increment clay Gd from WF dsilt
-sltndratet*maxgd; //Flush only maxgd
// if(dgdclay<0) dgdclay=0; //Prevents re-dissolution of Gd from clay
gdclay+=dgdclay;
if(gdclay<0) gdclay=0; //Substitute test if gd can be re-dissolved from clay
gdgls-=glsrate*gdgls*(totalwf>0?1/totalwf:0); //Decrement Gd in WF
totalwf-=glsrate; //Decrement WF for dissolution this step
if (totalwf<0) totalwf=0;
fclay=uclay+puclay; //Update fissile in clay
fgls=ugls+pugls; //Update fissile in WF
ftotal=fgls+fclay; //Update total fissile
if(fclay<fclaylast+.001) //No fissile left
  (endload=1;
  fprintf(fout,"Fissile used up Pu=%6.1f U=%6.1f\n",puclay,uclay);
  outflag=1;
else fclaylast=fclay;
gdtotal=gdgls+gdclay; //Update total Gd
yr+=1; //Increment time (by 1000 yrs)
strcpy(outs," ");
if(glasscase=='n') //Criticality for clay
  (if(gdclay>2.5)
  (if(log(gdclay)<(.7587-keff+.00298*puclay+.00135*uclay)/.11954)
  (strcpy(outs,"Clay10");
  if(critical==0)
  (critical=1;
  printcase=1;)))
  else if (gdclay>1)

```


PREDECISIONAL DOCUMENT

```
    crolast=cro;)  
    strcpy(outs, " ");  
    printcase=0;] //end of timestep loop  
    if(critical==0)  
        fprintf(fout, 'No criticality Loadfac=%5.3f FF=%5.1f Time=%d\n\n',  
            loadfac, fracfac, yr);  
    else endload=1; //We've found the lowest DP for this load factor  
    fracfac+=ffstep; //Increment fracfac for next iteration of this loop  
    if(endload==0) fprintf(fout, 'No criticality Loadfac=%5.3f\n\n', loadfac);))
```

PREDECISIONAL DOCUMENT

**APPENDIX C
SUMMARY OF RESULTS OF EQ3/6 CALCULATIONS**

A00000000-01717-5705-00014 REV 01

PREDECISIONAL DOCUMENT

February 1997

PREDECISIONAL DOCUMENT

Intentionally Left Blank

CONTENTS

	Page
C.1 CHEMISTRY AND ANALYSIS	C-1
C.2 DATA AND RELATIONSHIPS USED FOR COMPUTING SOLUBILITIES OF GADOLINIUM, PLUTONIUM, AND URANIUM AS A FUNCTION OF pH	C-9
C.3 GLASS DEGRADATION RATES	C-13

FIGURES

C-1 Plot of idealized concentration of dissolved Gd species in equilibrium with GdOHCO ₃ (solid), corresponding total idealized Gd solubility, and EQ6 calculations of solubility. Heavy dashed line is for normal atmospheric partial pressure of CO ₂ , and heavy solid line is for CO ₂ partial pressure of 1.43x10 ⁻³ atm. Symbols at the ends of straight lines are provided only to enable the reader to identify lines for each aqueous species by use of the legend. They are not model results.	C-6
C-2 Plot of idealized concentration of dissolved Pu species in equilibrium with PuO ₂ (solid), corresponding total idealized Pu solubility, and EQ6 calculations of solubility. Heavy solid line is for normal atmospheric partial pressure of CO ₂ , and heavy dashed line is for CO ₂ partial pressure of 1.43x10 ⁻³ atm. Symbols at the ends of straight lines are provided only to enable the reader to identify lines for each aqueous species by use of the legend. They are not model results.	C-7
C-3 Plot of idealized concentration of dissolved U species in equilibrium with soddyite (except for pH>9, when the solid is haiweeite), corresponding total idealized U solubility, and EQ6 calculations of solubility. Heavy solid line is for normal atmospheric partial pressure of CO ₂ , and heavy dashed line is for CO ₂ partial pressure of 1.43x10 ⁻³ atm. Symbols at the ends of straight lines are provided only to enable the reader to identify lines for each aqueous species by use of the legend. They are not model results.	C-8

TABLES

C-1 Modeling Results, Element Specific, Glass Waste with Average J-13 Well Water	C-2
C-2 Modeling Results, Element Specific, Ceramic Waste with Average J-13 Well Water ..	C-4
C-3 Solubility data for Gd, Pu, and U in J-13 water at various pHs. Data at log fCO ₂ = -3.5000	C-5
C-4 Solubility data for Gd, Pu, and U in J-13 water at various pHs. Data at log fCO ₂ = -2.3357	C-5

PREDECISIONAL DOCUMENT

INTENTIONALLY LEFT BLANK

APPENDIX C SUMMARY OF RESULTS OF EQ3/6 CALCULATIONS

C.1 CHEMISTRY AND ANALYSIS

Tables in this appendix provide a summary of results from numerous calculations that are most relevant to nuclear criticality issues. The calculations were done with the EQ3/6 package of computer codes, which simulate reaction progress toward a final equilibrium state. The tables include only a small fraction of the results from individual runs. The output also reports the concentrations of all other aqueous species and the names and amounts of numerous solid phases predicted to form during the course of reaction.

Various assumptions had to be made to conduct these simulations. In view of the long time frame it was assumed in most computer runs that the eventual result would be the true equilibrium assemblage, not some metastable condition, as might persist even at the end of laboratory experiments lasting several years. Thus, quartz and PuO_2 , not chalcedony and $\text{Pu}(\text{OH})_4$, respectively, were assumed to be the stable phases. Another assumption was that once the metal barriers, i.e., the carbon steel corrosion allowance, the Alloy 625 corrosion resistant barrier, and the 304L stainless steel containers for the glasses were breached at 5000 years there would be sufficient internal convection to keep the J-13 well water circulating among the Alloy 625 internal surface, all of the exposed 304L, and the fractured DHLW and La-BS glasses. This was modeled as a closed system in view of the lack of a flow-through/flushing option within EQ6.

Because of the lack of Pitzer's coefficients for activity coefficients for many of the constituents, it was not possible to use a closed system to model the final stages of reaction progress. The leaching of the DHLW glass has the potential to produce extremely high ionic strengths, well beyond the capability of the activity coefficient option that had to be used. Similarly, the assumption of approach to equilibrium results in a prediction of oxidation of the Cr in the metals to chromates; this, too, would increase the ionic strength dramatically and simultaneously produce acid conditions perhaps to a pH as low as 4. In view of these limitations only the initial stages of closed system reaction progress, up to the point where the results may still be qualitatively correct, are reported in this appendix. Closed system run results are included in Tables C-1 and C-2.

To obtain useful chemical data for the later stages of reaction progress recognition was taken of the likelihood that the high concentrations of initial reaction products would be flushed from the system by continuing influx of J-13 well water. Similarly, much of any acid produced would be flushed out. This allowed computation of solubilities of suitable solid phases, specifically, GdOHCO_3 , PuO_2 , soddyite, and haiweeite, in J-13 well water at specific values of pH. The composition of the water did, of course, have to be changed somewhat to correspond to the modified pHs, as explained in section C-2. The results of these calculations are reported in Tables C-3 and C-4 and are plotted in Figures C-1, C-2, and C-3. Table C-3 provides the results for normal atmospheric pressure of CO_2 , and Table C-4 for a higher partial pressure computed from the measured pH and alkalinity of J-13 well water.

Table C-1. Modeling Results, Element Specific, Glass Waste with Average J-13 Well Water

Run #	Time or zd	Log Total Aqueous Molalities/ppm				Pu, U, and Gd Solids		Description	Comment
		Gd	Pu	U	Name	Log Mol/gt			
J13avwp50 pH = 8.83	58 y	-0.03/ 1.36E+01	-4.72/ 4.31	-1.47/ 7.55E+03	GdOHCO ₃ ⁺ PuO ₂ Rhabdophane	-2.10/1.24 -2.18/1.84 -3.87/0.02	LaBS glass, DHLW glass, 304L, & Alloy 625 reaction with J-13 water. SKB thermodynamic data added to data base. Glass fracture factor (FF) = 100. Cr allowed to oxidize fully to chromate.	Limit of accurate calculations with available data, i.e., about ionic strength 1 as here.	
J13avwp50c pH = 8.79	7.8 y	-7.13/ 0.012	-10.76/ 0.42E-05	-4.12/ 18.2	GdOHCO ₃ PuO ₂ Sodylyte Rhabdophane	-4.21 -4.23 -3.21 -4.12	LaBS glass (FF=6), DHLW glass (FF=30), 304L, & Alloy 625 reaction with J-13 water. SKB thermodynamic data added to data base. Cr allowed to oxidize fully to chromate.	Maximum pH. Note that slower rate of DHLW reaction compared to that of Cr alloys keeps this maximum lower.	
J13avwp50c pH=8.15	101 y	-7.32/ 7.0E-03	-11.89/ 4.71E-07	-5.09/ 1.82	GdOHCO ₃ PuO ₂ Sodylyte Rhabdophane	-3.09/-0.13 -3.13/0.18 -2.10/1.89 -4.28/0.01	Continuation	Ionic strength = 0.78, i.e. approximate limit of accurate calculations.	
J13avwp50c pH = 7.14	816 y	-5.37/ 5.27E-01	-12.28/ 1.03E-07	-7.44/ 6.83E-03	GdOHCO ₃ PuO ₂ Sodylyte Rhabdophane LaF ₃ -ss	-2.30/0.78 -2.35/1.08 -1.44/8.67 -3.70/0.03 -4.98/-0.01	Continuation	Approximate limit of applicability of results; ionic strength = 4.2	
J13avwp54 pH = 5.18	436 y	-1.21/ 8.23E+0 3 ¹	-10.12/ 1.57E-05	Not included in waste form for this run	PuO ₂ Rhabdophane	-1.22/14.4 -7.12/<0.01	LaBS glass, 304L, & Alloy 625. SKB thermodynamic data added to data base. FF = 100. Limited O ₂ & CO ₂	Ionic strength 2.3 - somewhat beyond range of accurate calculations	
J13avwp54 pH = 4.95	672 y	-0.91/ 1.48E+0 4 ¹	-9.92/ 2.19E-05	Not included	PuO ₂ Rhabdophane	-0.82/28.9 -7.22/9.45	Continuation	Ionic strength 4.7 - applicability limit.	

Table C-1. Modeling Results, Element Specific, Glass Waste with Average J-13 Well Water (Continued)

Run #	Time or z†	Log Total Aqueous Moles/liter/ppm			Pu, U, and Gd Solids		Description	Comment
		Gd	Pu	U	Name	Log Mol/gf		
113avwp56b pH = 10.06	58 y	-5.80/ 2.30E-01	-3.77/ 38.61	-1.47/ 7.52E+03	Gd(OH)CO ₃ PuO ₂ Rhabdophane	-4.51/0.05 -3.69/0.05 -3.42/0.06	LABS glass, DHLW glass, 304L & Alloy 625 reaction with J-13 water. SKB thermodynamic data added to data base. FF= 100. Cr not allowed to oxidize to chromate.	No solid U species. Ionic strength = 1.24. - limit for accuracy. Note High U solubility
113avwp56b pH = 10.15	104 y	-6.70/ 2.75E-01	-3.12/ 1.61E+02	-1.18/ 1.34E+04	Na4UO ₆ (CO ₃) ₂ Gd(OH)CO ₃ Rhabdophane	-3.27/0.13 -4.24/0.01 -2.48/0.11	Continuation	No solid Pu species N.B. Solubility of Pu and U are High
113avwp56b pH = 10.28	643 y	-5.56/ 3.41E-01	-2.24/ 1.10E+03	-2.20/ 1.17E+03	Na4UO ₆ (CO ₃) ₂ Gd(OH)CO ₃ Rhabdophane	-0.67/32.0 -2.37/0.67 -2.10/0.06	Continuation	No solid Pu species. GdPO4·H2O = -3.34
113avwp56b pH = 9.69	30,342 y	-6.28/ 7.63E-02	-5.31/ 1.07	-0.69/ 2.51E+04	PuO ₂ Na4UO ₆ (CO ₃) ₂ Gd(OH)CO ₃ Rhabdophane	-0.73/44.43 -1.02/22.53 -0.67/34.0 -3.34/0.07	Continuation	33.94 moles of solvent water, out of initial 55.51, still present. This means 15.3 g of U in solution vs. 22.5 in solid. Ionic strength never got outside range that could be handled approximately.
113avwp58 pH = 9.83	58 y	-6.04/ 1.34E-01	-4.73/ 4.25	-1.47/ 7.55E+03	Gd(OH)CO ₃ PuO ₂ Rhabdophane	-2.10/1.24 -2.16/1.64	Like run 113avwp50, but formation of quartz, tridymite, and coesite suppressed.	Ionic strength 1.2, - limit for accuracy. No U solid
113avwp58 pH = 10.06	234 y	-5.79/ 2.06E-01	-2.79/ 3.13E+02	-2.35/ 8.32E+02	Gd(OH)CO ₃ Na4UO ₆ (CO ₃) ₂ PuO ₂ Rhabdophane	-1.49/5.20 -0.88/31.0 -1.58/8.58 -3.49/0.05	Continuation	N.B. High solubilities of Pu and U Ionic strength 4.0, - applicability limit.

† High values of dissolved Gd, but within limits for which calculations give acceptable results.

‡ Values are log gram-atoms of metal (or cation) and grams of metal, not the entire weight of the solid.

‡ Equilibrium constant taken to be equal to that for Nd(OH)CO₃.

Table C-2. Modeling Results, Element Specific, Ceramic Waste with Average J-13 Well Water

Run #	Time or z†	Log Total Aqueous Molalities/ppm				Pu, U, and Gd Solids		Description	Comment
		Gd	Pu	U	Name	Log Mol/g†			
J13avcer1 pH = 8.82	28 y	-8.30/ 7.79E-05	-9.84/ 3.43E-05	-3.18/ 1.54E+02	PuO ₂ Soddyite Rhabdophane	-5.48/-0.01 -2.69/0.49 -3.88/-0.01	Ceramic waste, modeled as a homogeneous special reactant (FF = 10), DHLW glass (FF = 30), 304L, and Alloy 625 reaction with J-13 water. SKB data base. Cr allowed to oxidize fully. Mid-range of reaction rate (1.0E-5.6 g/m ² /day)		
J13avcer1 pH = 7.44	542 y	-8.32/ 5.79E-04	-12.4/ 7.48E-08	-8.30/ 7.57E-02	PuO ₂ Soddyite Rhabdophane	-4.19/0.02 -1.35/10.6 -4.64/-0.01	Continuation	Ionic strength 4.75, - applicability limit.	
J13avcer2 pH = 8.80	29 y	-9.27/ 8.29E-05	-9.89/ 3.07E-02	-3.22/ 1.38E+02	PuO ₂ Soddyite Rhabdophane	-5.24/-0.01 -2.69/0.49 -3.88/-0.01	Ceramic waste modeled as consisting of separate phases of zirconolite, pyrochlore, Zr-containing rutile, and Be-hollandite. Used dissolution rate of 1.0E-5.5 g/m ² /day for zirconolite and pyrochlore, 10 times faster for Be-hollandite, and 1/2 the rate for rutile. FF = 10 for all phases, and 30 for DHLW. Reaction also with 304L, Alloy 625, and J-13 water.	Course of reaction essentially the same as for glass, except for smaller amounts of other components of the glass, such as B) being added to the solution.	
J13avcer2 pH = 7.08	715 y	-8.24/ 8.98E-04	-12.25/ 1.05E-07	-7.51/ 8.66E-03	PuO ₂ Soddyite Rhabdophane	-3.81/0.03 -1.40/0.48 -4.49/0.01	Continuation	Ionic strength 4.78, - applicability limit.	

† Values are log gram-atoms of metal (or cation) and grams of metal, not the entire weight of the solid.

Table C-3. Solubility data for Gd, Pu, and U in J-13 water at various pHs[†]. Data at log fCO₂ = -3.5000[‡]

pH	Gd, ppm	Gd, m	Gd, log m	Pu, ppm	Pu, m	Pu, log m	U, ppm	U, m	U, log m
5.5	44134*	0.3236098	-0.489978	6.15E-06	2.907E-11	-10.53651	0.00471	2.282E-06	-7.641733
6	67.2	0.0004275	-3.369025	1.48E-06	6.085E-12	-11.21715	0.00231	8.718E-09	-8.012441
6.4938	3.06*	1.962E-05	-4.707278	4.77E-07	1.956E-12	-11.70867	0.002	6.471E-09	-8.072047
7.01	0.122	7.76E-07	-8.110183	1.56E-07	6.411E-13	-12.19307	0.00193	8.011E-09	-8.096327
7.5187	0.0138	6.779E-08	-7.056548	6.78E-08	2.78E-13	-12.55559	0.00218	9.141E-09	-8.039024
8.01	0.00506	3.218E-08	-7.492453	5.34E-08	2.191E-13	-12.65938	0.00478	2.009E-08	-7.896988
8.9689	0.0151	6.961E-08	-7.157334	2.22E-08	9.114E-12	-11.04031	2.56	1.077E-05	-4.967857
8.8131	0.129	8.199E-07	-6.036278	12	5.532E-05	-4.257154	41300	0.1951271	-0.709682

Table Notes:

- * These values were used to establish the pH dependence of Gd solubility over the range of primary interest.
- ‡ Assumes flushing of dissolved waste products
- † Solids are: GdOHCO₃; PuO₂; Soddyite at pH < 8.01, Halwoelite at pH = 8.97, Na₂UO₇(CO₃)₂ at pH 8.81

Table C-4. Solubility data for Gd, Pu, and U in J-13 water at various pHs[†]. Data at log fCO₂ = -2.3357[‡]

pH	Gd, ppm	Gd, m	Gd, log m	Pu, ppm	Pu, m	Pu, log m	U, ppm	U, m	U, log m
5.5	144.9*	0.0009222	-3.035162	5.19E-06	2.127E-11	-10.67214	0.00457	1.921E-06	-7.716391
6.6998	6.31	4.018E-05	-4.396228	1.71E-06	7.021E-12	-11.15358	0.00323	1.362E-06	-7.865868
6.4963	0.32*	2.034E-06	-5.691663	6.23E-07	2.555E-12	-11.59262	0.00299	1.254E-06	-7.901587
7.0018	0.0431	2.739E-07	-6.562331	3.14E-07	1.287E-12	-11.89053	0.00701	2.946E-06	-7.530812
7.5018	0.0183	1.161E-07	-6.935148	2.77E-07	1.135E-12	-11.94518	0.0615	2.582E-07	-6.567871
7.9775	0.0259	1.646E-07	-6.783651	0.0000014	5.731E-12	-11.24175	2.38	9.912E-06	-5.003859
9	0.269	1.726E-06	-5.763062	0.148	6.134E-07	-6.212225			

Table Notes:

- * These values were used to establish the pH dependence of Gd solubility over the range of primary interest.
- ‡ Assumes flushing of dissolved waste products
- † Solids are: GdOHCO₃; PuO₂; Soddyite at pH < 7.98. Did not achieve saturation in U at pH 9.

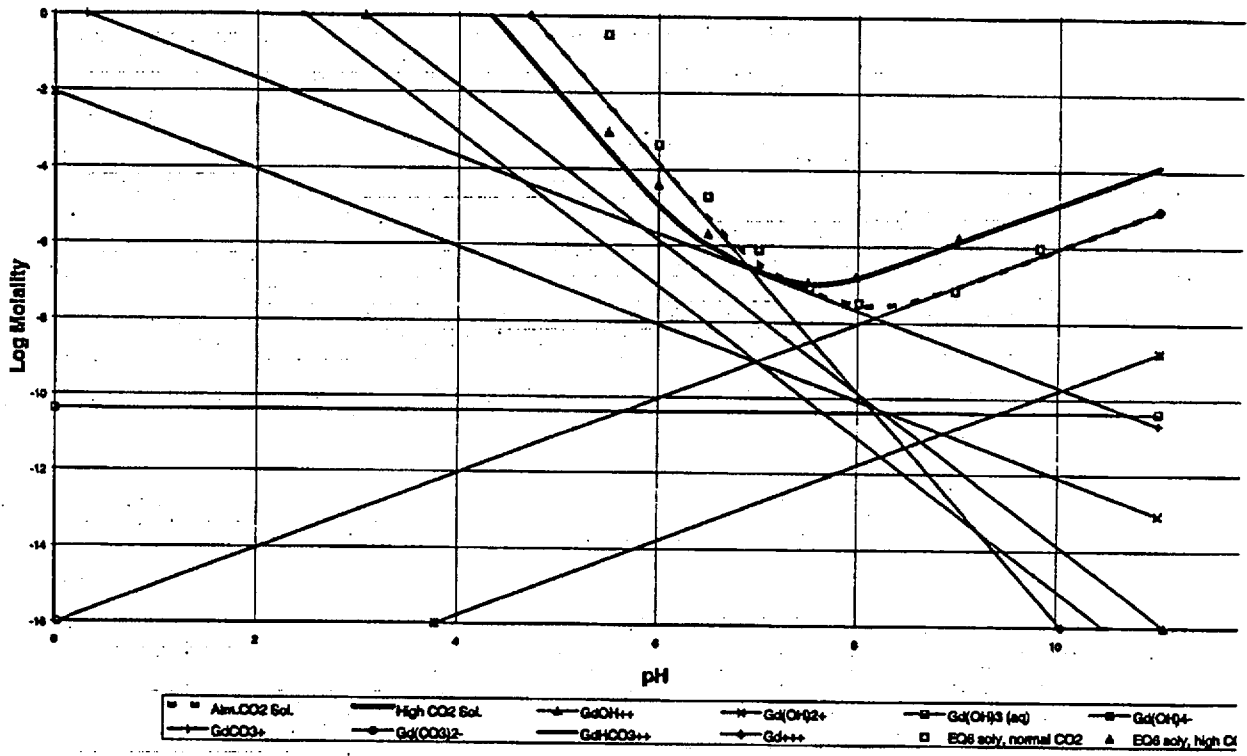


Figure C-1. Plot of idealized concentration of dissolved Gd species in equilibrium with GdOHCO₃ (solid), corresponding total idealized Gd solubility, and EQ6 calculations of solubility. Heavy dashed line is for normal atmospheric partial pressure of CO₂, and heavy solid line is for CO₂ partial pressure of 1.43x10⁻³ atm. Symbols at the ends of straight lines are provided only to enable the reader to identify lines for each aqueous species by use of the legend. They are not model results.

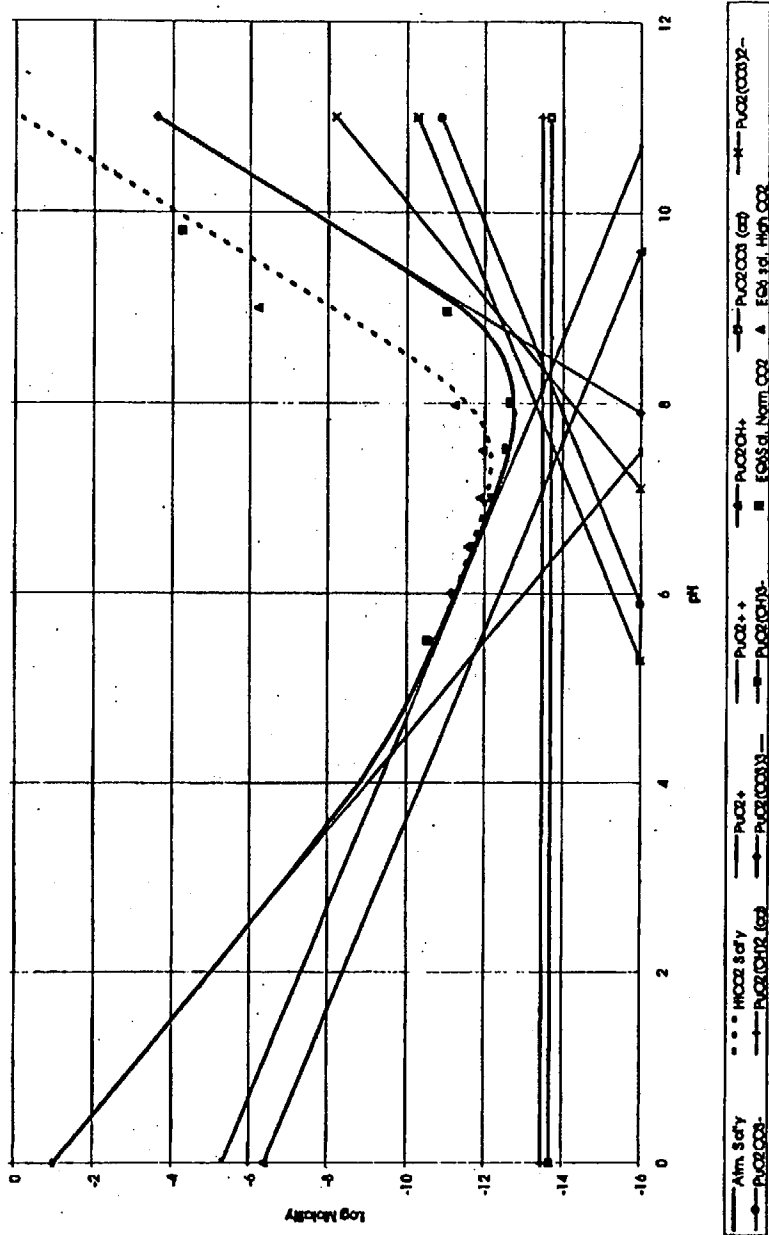


Figure C-2. Plot of idealized concentration of dissolved Pu species in equilibrium with PuO₂ (solid), corresponding total idealized Pu solubility, and EQ6 calculations of solubility. Heavy solid line is for normal atmospheric partial pressure of CO₂, and heavy dashed line is for CO₂ partial pressure of 1.43x10⁻⁵ atm. Symbols at the ends of straight lines are provided only to enable the reader to identify lines for each aqueous species by use of the legend. They are not model results.

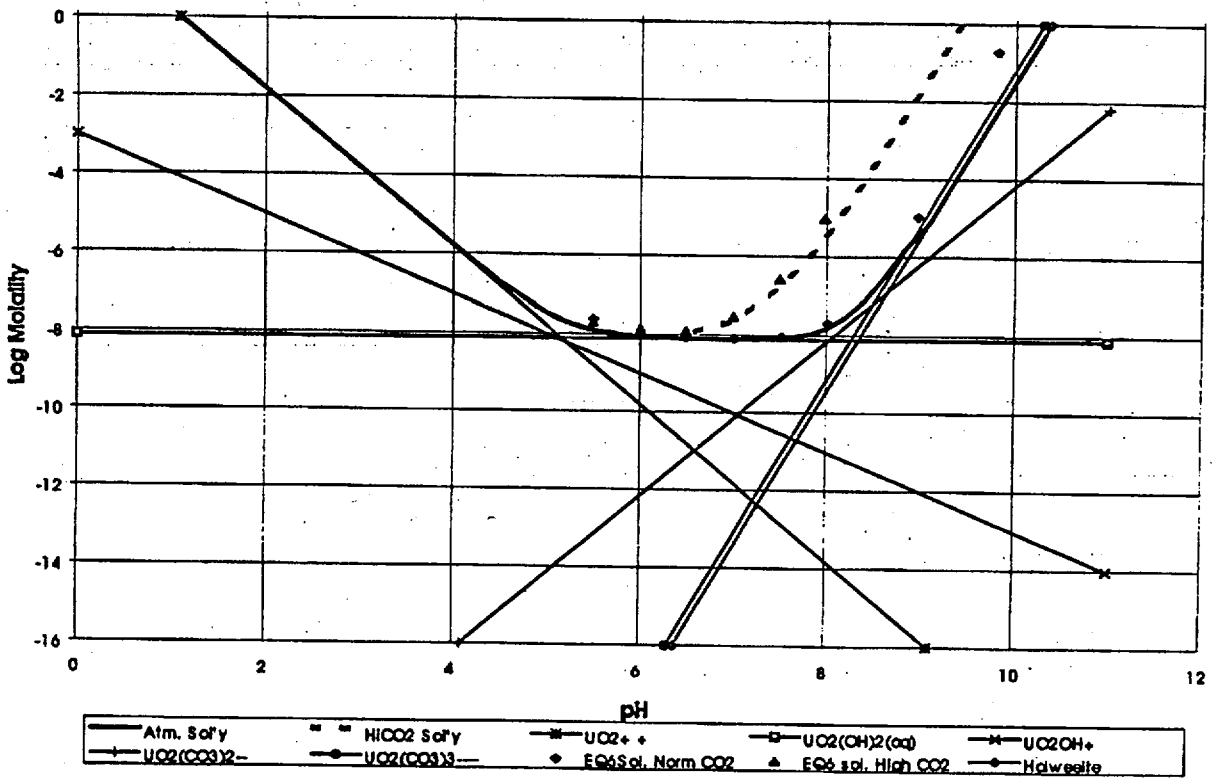


Figure C-3. Plot of idealized concentration of dissolved U species in equilibrium with soddyite (except for pH>9, when the solid is haiweelite), corresponding total idealized U solubility, and EQ6 calculations of solubility. Heavy solid line is for normal atmospheric partial pressure of CO₂, and heavy dashed line is for CO₂ partial pressure of 1.43x10⁻⁸ atm. Symbols at the ends of straight lines are provided only to enable the reader to identify lines for each aqueous species by use of the legend. They are not model results.

C.2 DATA AND RELATIONSHIPS USED FOR COMPUTING SOLUBILITIES OF GADOLINIUM, PLUTONIUM, AND URANIUM AS A FUNCTION OF pH

This section includes relationships used to compute, on a simplified basis, the solubilities of Gd, Pu, and U as a function of pH. The first steps in this process are to ascertain, first, what solids that contain the element of interest are present, and, second, what dissolved species that contain that element have the highest concentrations. This was accomplished by using the base composition of J-13 well water, but changing the pH to obtain relationships at several values of pH from the EQ3/6 codes. This necessitated increasing the concentrations of other ions in order to achieve electrical balance, or neutrality, at pH values other than that measured in J-13 well water itself. For lower pHs it was assumed that dichromate ion was appropriate, and at higher pH, sodium ion. In all cases it was assumed that the solutions were saturated in CO₂, either at the normal atmospheric value at sea level, or at the pressure corresponding to the measured values of pH and alkalinity, ascribed entirely to bicarbonate, in J-13 well water. The latter value is 4.62E-03 atm.

The solubility of a given element equals the sum of the concentrations of all of the dissolved species. Thus, the concentration of each species must be known. They have been determined approximately in the simplified approach used here by utilizing the data shown in Table F-1 in Appendix F together with other data supplied with the codes EQ3NR and EQ6. In the simple approach all activity coefficients have been assumed to be equal to unity, i.e., an ionic strength of zero has been assumed. This way of proceeding provides an overview of the nature of the relationship between solubility and pH, but will not yield accurate values. In most instances the calculated solubilities will be lower than actual ones because activity coefficients will normally be less than one. (See Appendix D for a more complete explanation of the relevant equations.)

The EQ3 calculations at low pH show that most of the dissolved Gd will exist as Gd⁺⁺⁺ ion and that the solid controlling the solubility is GdOHCO₃. (Gadolinium phosphate is actually less soluble, but the concentration of phosphate in J-13 well water is inadequate to precipitate more than a small part of the gadolinium being released from the waste form.) In view of the facts that data were not available for GdOHCO₃ and that data for Nd compounds are nearly identical to those for Gd, NdOHCO₃ was used as a proxy for GdOHCO₃. See section 5.3.2 for further discussion of thermodynamic data. The data in the EQ3/6 data base have been made consistent with the "basis" species selected for use with that code, e.g., H⁺ and H₂O, rather than OH⁻, and HCO₃⁻; rather than CO₃²⁻.

For low pH the reaction that incorporates the considerations noted above is



PREDECISIONAL DOCUMENT

The equilibrium constant for this reaction can be derived from the following reactions and equilibrium constants:

Number	Reaction	Log K
1	$GdOHCO_3 + 2 H^+ = Gd^{+++} + HCO_3^- + H_2O$	2.8404
2	$CO_2(g) + H_2O = HCO_3^- + H^+$	-7.8136
3	$HCO_3^- = H^+ + CO_3^{--}$	-10.3288
4	$OH^- + H^+ = H_2O$	13.9951

The values for the logarithms for the equilibrium constants, Log K, were taken from the EQ3/6 data base version data0.b19.skb. In principle the constant for reaction 1 derives from the value reported in Table F-1 in Appendix F for $NdOHCO_3$ + reaction 4 - reaction 3. The reader can readily confirm that this combination of reactions, substituting $GdOHCO_3$ for $NdOHCO_3$, does result in reaction 1. To combine equilibrium constants in correspondence to combining reactions, one must multiply by constants for reactions that are added and divide by constants for reactions that are subtracted. In this way species that are eliminated by the addition or subtraction are similarly eliminated from the product/quotient of the constants. Alternatively the logarithms of the constants may be added and subtracted. Thus, as the reader can easily confirm, the log K for reaction 1 is log K for $NdOHCO_3$ from Table F-1 plus log K for reaction 4 (taken as 14.00) minus log K for reaction 3 (taken as -10.34). This actually yields 2.8239 for log K for reaction 1. Evidently, perhaps for internal consistency with the data reported by Reference 20, slightly different values were used when the REE data were incorporated into the EQ3/6 data base for reactions 3 and 4, e.g. -10.34 and 14.00, respectively. The equilibrium constant for reaction 3, for example, is

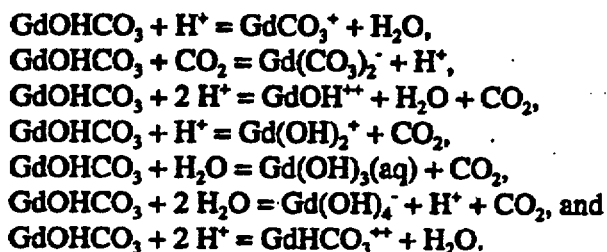
$$K = (H^+)(CO_3^{--})/(HCO_3^-) = 10^{-10.3288} = 4.69 \text{ E-11,}$$

where parentheses indicate activities, or, in this approximation, concentrations. The relationship between activities and concentrations is explained more fully in Appendix D, together with some examples of activity coefficients.

These same principles are applied in deriving the constant for reaction A from reactions 1 and 2, namely subtracting reaction 2 from reaction 1. This yields log K for reaction A as 10.6540 which is equivalent to $K = 4.508E+10 = (Gd^{+++})(CO_2)/(H^+)^3$. The concentration of carbon dioxide, (CO_2) , is taken equal to its partial pressure. The logarithm of this equation is $\log K = \log (Gd^{+++}) + \log P_{CO_2} - 3 \log (H^+)$. $\log (H^+) = -pH$, so this becomes $\log K = \log (Gd^{+++}) + \log P_{CO_2} + 3 pH$. On substituting actual values, specifically, $\log K = 10.6540$ and $\log P_{CO_2} = -3.5$ (atmospheric P_{CO_2} at sea level), and rearranging this becomes $\log (Gd^{+++}) = 14.154 - 3 pH$; for the case of enhanced CO_2 ; i.e., a partial pressure of $4.62E-03$ atm., the equation is $\log (Gd^{+++}) = 12.9897 - 3 pH$. The equation for atmospheric P_{CO_2} is plotted in Figure C-1.

PREDECISIONAL DOCUMENT

Other reactions in Table F-1 were combined in a similar fashion to derive equations for the equilibrium between GdOHCO_3 and GdCO_3^+ , $\text{Gd}(\text{CO}_3)_2^-$, GdHCO_3^{++} , GdOH^{++} , $\text{Gd}(\text{OH})_2^+$, $\text{Gd}(\text{OH})_3(\text{aq})$, and $\text{Gd}(\text{OH})_4^-$. These are:



Corresponding lines are plotted in Figure C-1. The equations for these lines for normal atmospheric pressure of CO_2 are, respectively,

$$\begin{aligned} \text{Log}(\text{GdCO}_3^+) &= 0.3098 - \text{pH}, \\ \text{Log}(\text{Gd}(\text{CO}_3)_2^-) &= -16.0344 + \text{pH}, \\ \text{Log}(\text{GdOH}^{++}) &= 6.1442 - 2 \text{pH}, \\ \text{Log}(\text{Gd}(\text{OH})_2^+) &= -2.0656 - \text{pH}, \\ \text{Log}(\text{Gd}(\text{OH})_3(\text{aq})) &= -13.8754, \\ \text{Log}(\text{Gd}(\text{OH})_4^-) &= -19.7852 + \text{pH}, \text{ and} \\ \text{Log}(\text{GdHCO}_3^{++}) &= -0.3098 - \text{pH}. \end{aligned}$$

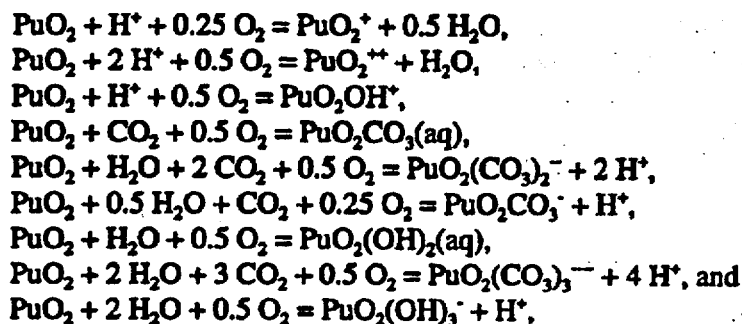
The heavy dashed line in this figure shows the sum of the concentrations for all of these species for atmospheric partial pressure of CO_2 , and the solid heavy line shows the same sum for a partial pressure of $4.62\text{E}-03$ atm.

Exactly parallel steps were taken for Pu and U, and the results plotted in Figures C-2 and C-3 respectively. For these elements the number of solution species included in the EQ3/6 data base is much greater. Only the most important (i.e., highest concentrations for the conditions under investigation) aqueous species were selected on the basis of EQ3NR computer runs. Specifically, these were PuO_2^+ , PuO_2^{++} , PuO_2OH^+ , $\text{PuO}_2\text{CO}_3(\text{aq})$, $\text{PuO}_2(\text{CO}_3)_2^-$, PuO_2CO_3 , $\text{PuO}_2(\text{OH})(\text{aq})$, $\text{PuO}_2(\text{CO}_3)_3^-$, and $\text{PuO}_2(\text{OH})_3^-$ for Pu, and UO_2^{++} , $\text{UO}_2(\text{OH})_2(\text{aq})$, UO_2OH^+ , $\text{UO}_2(\text{CO}_3)_2^-$, and $\text{UO}_2(\text{CO}_3)_3^-$ for U. The least soluble solid for Pu is PuO_2 over the entire pH range shown. The situation for U is more complicated than for the other elements because at pHs above about 8.2 the least soluble solid is no longer soddyite, as it is for lower pH, but in the vicinity of pH 8 to 9, haiweeite, and near 10, $\text{Na}_4\text{UO}_2(\text{CO}_3)_3$. For haiweeite, it was assumed in the simple approach that the concentration of Ca in solution was limited by equilibrium with calcite. When calcite is absent, as would be the case at low pH owing to the dissolution of calcite, this relationship could not be used, but the EQ3/6 calculations likewise show that haiweeite is more soluble than soddyite. In the plots the solubility line for normal atmospheric CO_2 coincides with the solubility of haiweeite at pH above about 8.5. Because the concentration of Na could not be estimated simply, and because approximate calculations show that the solubility of $\text{Na}_4\text{UO}_2(\text{CO}_3)_3$ and haiweeite are very similar at the highest pHs shown, no attempt was made to plot a line for this sodium uranyl carbonate. At the higher partial pressure of CO_2 haiweeite becomes more soluble than soddyite, owing to the greater dependence on the carbonate content in the presence of calcite. The plots are terminated at

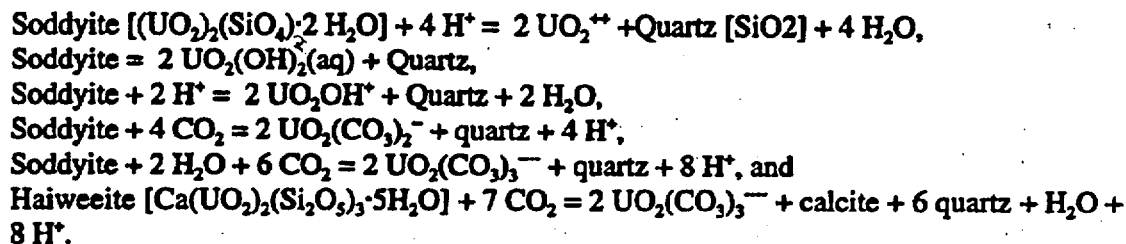
PREDECISIONAL DOCUMENT

pH 11 because conditions more alkaline than pH 10 to 11 cannot be attained in equilibrium with atmospheric CO₂.

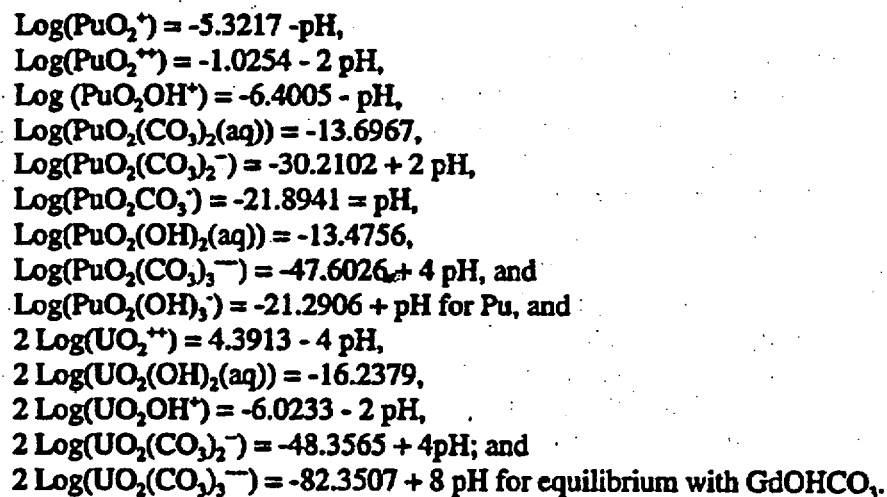
Reactions for Pu and U are as follows:



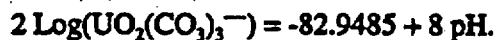
for which the oxygen partial pressure is fixed at atmospheric, and



The corresponding equations for the lines are:



The line for haiweeite in equilibrium with calcite and the tricarbonat complex is



The often discussed strong increase in solubility for U (and Pu) with increasing pH is clearly shown in these figures.

The results of EQ6 solubility calculations are also plotted on these figures. As expected they are higher than the ideal conditions shown by the lines, as a consequence of the non-zero ionic strength. This deviation becomes greater the further from neutral are the solutions, because, under those conditions, the ionic strength is necessarily greater than in J-13 well water near neutral. Nevertheless, the agreement between the solubilities calculated by EQ6, taking ionic strength and all other components of the well water into account, and the ideal plots, is generally very good. For criticality calculations the actual EQ6 results were used and interpolated using the slope of the simple theoretical lines. The results of the EQ6 calculations are included in Tables C-3 and C-4.

C.3 GLASS DEGRADATION RATES

The degradation rate of alkali glass in time frames of decades to centuries remains uncertain. Nevertheless, after a few thousand years it is assumed in this report that it is completely degraded. The dissolution rate depends strongly on pH. For the EQ6 modeling a rate corresponding to that at pH 10 was used. Together with data on surface area and mass of glass this resulted in an estimate of complete degradation of the glass in about 250 years. The dissolution rate for pH 7 is about one tenth as fast, which gives complete DHLW glass degradation in about 2500 years. LLNL (References 32, 33, and 34) have performed modeling of experimental results using EQ6. These models make use of an approximation to thermodynamic properties of the "gel", or leached glass observed during the experiments and incorporates this approximation into a relatively simple kinetic rate relationship (transition state theory, but with the use of only a few parameters). The net result is that the rate of reaction of the glass, as incorporated into the model, increases linearly with pH and declines exponentially as concentration of silica dissolved in the water increases. The rate of linear increase of the rate with pH and the exponential factor for silica dependence were derived from fitting model results to experimental data. At later stages of reaction progress the model incorporates a decrease in this silica concentration as a consequence of the precipitation of clays and removal of silica from the solution. This leads to an increase in the glass degradation rate. Taking this concept further, to the stage in which the sodium ion concentration has become large, it seems possible that build-up of alkalis will similarly decrease the rate of glass reaction. This could result in sufficient slowing of reaction that all the borate remains in solution and gets flushed out as more water infiltrates into the waste package. Similarly, the sodium and potassium not incorporated into other solids, such as clays, would be largely flushed out, leaving only enough to maintain equilibrium with these solids. Indeed, this seems more probable than the reaction proceeding to the stage of borax precipitation. However, because there is no experimental evidence for such an effect, it cannot be relied upon for the present analyses.

Reference 22 summarizes several experiments on the effects of species other than silica and hydrogen ion on glass corrosion. Specifically, the reports state that Ca and Mg have no perceptible effect at low concentrations, but that at pH > 6 (for the CGS glass on which the tests were performed) the dissolution rate is reduced by added silica, and that for pH < 6 added Al reduces the rate. High concentrations of Mg investigated by Barkatt, et al. and cited by Reference 22, however, did produce "severe quenching". No data were reported on the potential effects of high concentration of Na. No references on the effect of Na were found during the preparation of this

PREDECISIONAL DOCUMENT

report. The German nuclear waste program has to some degree investigated the effects of brines on the dissolution of nuclear waste glasses. Argonne National Laboratory (Reference 35) was not aware of whether these investigations examined quenching effects of high concentrations of these elements on the corrosion rates. Knowledge of what effect, if any, high sodium concentrations have on the degradation rate would improve our understanding of reactions within the waste package and have implications as to the nature of reactions between the effluent from the package on the invert. Accordingly, it is recommended that 1) the existing literature be examined carefully, and 2) if these investigations do not provide adequate answers, flow through tests like those conducted by LLNL (Reference 36) be conducted for Na and borate as they were for Ca and Mg, but at high concentrations. Such experiments would reduce the uncertainty in how long the DHLW waste will endure and would likewise reduce the uncertainty in modeling the interactions between water containing dissolved fissile material and/or Gd with tuff in the invert or below the drift and with other materials emplaced in the drift.

PREDECISIONAL DOCUMENT

**APPENDIX D
ACTIVITY COEFFICIENTS**

**A000000000-01717-5705-00014 REV 01
PREDECISIONAL DOCUMENT**

February 1997

PREDECISIONAL DOCUMENT

...
...
...
...
...
...
...

Intentionally Left Blank

APPENDIX D ACTIVITY COEFFICIENTS

As noted in section 5.3.5, corrections to analytical, or stoichiometric, concentrations are required to use thermodynamic data properly. These corrections, known as activity coefficients, arise because of the electrical charges on aqueous ions and various kinds of ionic interactions, such as the formation of complexes and ion pairs.

For this purpose the so-called "B-dot" equation was used in the EQ3/6 calculations. In addition to the corrections applied at much lower concentrations this equation takes account of the formation of complexes or ion pairs, and uses a measure of the concentration, the ionic strength, accordingly. Ionic strength is 1/2 the sum of the concentrations of individual ions, expressed in molality, times the square of their corresponding charges. It would be preferable to use the Pitzer equations, for which data are incomplete. The Pitzer approach proceeds very differently, in general taking into account only very stable complexes, such as sulfate and carbonate ions. It considers neither ion pairs nor their effect on ionic strength; rather it uses a set of fitting parameters to model the interactions. The derivation of these parameters requires specific measurements in solutions resembling those being modeled.

Activity coefficients have been evaluated experimentally, e.g., by measuring vapor pressures and utilizing appropriate related thermodynamic relationships. This permits determining the activity of a dissolved salt as a whole, but not activity coefficients of individual ions. Thus, comparisons between measured and calculated values must be based on actual solutions in which positive and negative ions are electrically balanced, not on single ions.

Consider the dissociation reaction, $X_{\nu+}Y_{\nu-} = \nu_+X^{z+} + \nu_-Y^{z-}$. (Clearly, $|\nu_+z| = |\nu_-z|$.) Let a represent the activity of the salt, a_+ the activity of the positive ion, and a_- that of the negative ion. Then the activity of the salt is defined as $a = a_+^{\nu_+} a_-^{\nu_-}$, and the mean ionic activity is defined as $a_{\pm} = a^{1/\nu}$ where $\nu = \nu_+ + \nu_-$. Similarly, the mean ionic molality is defined as $m_{\pm} = m(\nu_+^{\nu_+} \nu_-^{\nu_-})^{1/\nu}$. The activity coefficient, $\gamma_{\pm} = a_{\pm} / m_{\pm} = (\gamma_+^{\nu_+} \gamma_-^{\nu_-})^{1/\nu}$. Another important concept is that of ionic strength, because at low concentrations the logarithm of the activity coefficient varies linearly with the square root of ionic strength. Ionic strength = 0.5 times the sum of the concentration of an ion times the square of its charge. Thus, using the example above for a concentration, m , for $X_{\nu+}Y_{\nu-}$, the ionic strength would be $0.5[\nu_+m(z^+)^2 + \nu_-m(z^-)^2]$. EQ3/6 makes use of the term, "true ionic strength," which refers to ionic strength computed on the basis of species actually present, taking into account complexes and ion pairs. Similarly, "True" means the ionic activity coefficient is computed from the mean ionic activity divided by the mean ionic concentration of free, or uncomplexed, ions. Stoichiometric ionic strength is calculated as if everything in solution, except very stable complexes like carbonate and sulfate, is completely dissociated. The activities must be the same no matter how they are computed. The distinction between the stoichiometric and "true" quantities depends upon whether only the concentrations of uncomplexed ions are considered in calculating the molalities or whether the total amount in solution is used.

Table D-1 shows a comparison between measured activity coefficients and those calculated by EQ3/6. The greatest deviations are for the nitrates, up to about 50%. The others lie below about 20%. Thus, for qualitative purposes the errors should give answers within about an order of

PREDECISIONAL DOCUMENT

magnitude of the correct result. To be sure, when these errors are combined into equilibrium constants the errors for individual ions may add, but in some cases a deviation in the same direction may occur in both the numerator and the denominator, thereby to some degree canceling the error. For example, if the correct values were 0.4 and 0.5, but both deviated by 10% positively from those numbers, the ratio would be the same; i.e. $0.4/0.5 = 0.44/0.55$. It is concluded that the EQ3/6 results up to an ionic strength of about 4 can be used qualitatively to indicate the general nature of the reactions that would actually occur.

Table D-1. Comparison Table for Activity Coefficients - EQ3/6 Calculations Compared with Measured Data

Salt	Ionic Strength		Gamma \pm , EQ3/6		Gamma \pm , (Reference 37)
	Stoichiometric	"True"	Stolch ¹	"True"	Stoichiometric
NaCl	1.0	0.940	0.597	0.635	0.68
NaCl	2.0	1.788	0.568	0.634	0.67
NaCl	3.0	2.541	0.552	0.652	0.71
NaCl	4.0	3.213	0.543	0.678	0.78
LaCl ₃	1.2	1.028	0.308	0.360	0.28
LaCl ₃	3.0	2.236	0.258	0.349	0.27
LaCl ₃	6.0	3.758	0.220	0.370	0.38
KCl	1.0	0.988	0.601	0.608	0.608
KCl	2.0	1.958	0.589	0.602	0.578
KCl	3.0	2.898	0.600	0.622	0.571
KCl	4.0	3.803	0.621	0.653	0.579
MnSO ₄	0.8	0.359	0.111	0.248	0.17
MnSO ₄	2.0	0.764	0.074	0.194	0.11
MnSO ₄	4.0	1.298	0.055	0.169	0.073
Al(NO ₃) ₃	1.2	0.384	0.035	0.414	0.18
Al(NO ₃) ₃	3.0	1.574	0.207	0.349	0.14
Al(NO ₃) ₃	6.0	4.232	0.292	0.379	0.19
Ca(NO ₃) ₂	0.8	0.481	0.382	0.478	0.42
Ca(NO ₃) ₂	1.5	0.681	0.302	0.434	0.38
Ca(NO ₃) ₂	3.0	1.854	0.254	0.422	0.35
Ca(NO ₃) ₂	6.0	3.180	0.218	0.437	0.35
MgSO ₄	0.8	0.307	0.109	0.284	0.13
MgSO ₄	2.0	0.628	0.073	0.232	0.088
MgSO ₄	4.0	1.040	0.054	0.208	0.064
Na ₂ SO ₄	0.8	0.480	0.355	0.445	0.36
Na ₂ SO ₄	1.5	1.078	0.280	0.394	0.27
Na ₂ SO ₄	3.0	1.931	0.238	0.377	0.20

¹ Computed as stoichiometric ionic strength, i.e., the mean ionic activity/stoichiometric concentration (molality of the dissolved salt).

PREDECISIONAL DOCUMENT

**APPENDIX E
JUSTIFICATION OF STATIC MASS BALANCE METHODOLOGY**

A00000000-01717-5705-00014 REV 01

PREDECISIONAL DOCUMENT

February 1997

PREDECISIONAL DOCUMENT

Intentionally Left Blank

PREDECISIONAL DOCUMENT

CONTENTS

	Page
E.1 STATIC MASS BALANCE ESTIMATIONS	E-1
E.2 DETAILED CONSIDERATIONS	E-1
E.2.1 DHLW Glass	E-1
E.2.2 La-BS Glass	E-5

PREDECISIONAL DOCUMENT

INTENTIONALLY LEFT BLANK

A000000000-01717-5705-00014 REV 01
E-ii
PREDECISIONAL DOCUMENT

February 1997

APPENDIX E JUSTIFICATION OF STATIC MASS BALANCE METHODOLOGY

E.1 STATIC MASS BALANCE ESTIMATIONS

The basic need is to estimate where Gd, Pu and U reside as a function of time. Calculations at both high and low ionic strength (I) indicate that under oxidizing conditions over the pH range likely to develop both Pu and U remain essentially insoluble, or, if soluble, little has been released from the waste form up to those times. Therefore, the emphasis is on Gd. Gd appears to be highly insoluble in the system and conditions of interest, except at low pH. Thus, estimates are needed as to when Gd begins to dissolve and when it is all in solution. These times depend on other components of the waste that affect the pH, i.e., most constituents of the waste package.

The pH is an intensive variable, or a potential (specifically the negative decadic logarithm of the chemical potential of hydrogen ion). What is really needed, however, is knowledge of how much acid may be generated first to neutralize the solution and second to dissolve Gd; i.e., the corresponding extensive variable.

The complexities of comparing the pH are compounded by lack of adequate thermodynamic and physicochemical data at the high concentrations expected. Notably lacking are parameters needed to calculate chemical potentials at high concentrations, the Pitzer parameters. Such data are unlikely to be available any time soon.

On the other hand, static¹ mass balance relationships with the limited thermodynamic data for Gd, mineralogical (crystallochemical) relations, rates of waste degradation, chemical compositions of waste package, and water flux components, do permit semi-quantitative determinations of the amounts of acid and the aqueous concentration of Gd as a function of time. Whereas accurate quantitative data are desirable, the semi-quantitative results suffice for making conservative choices.

E.2 DETAILED CONSIDERATIONS

E.2.1 DHLW Glass

This appendix focuses on the effects of reactions with the DHLW glass. Reactions with the metals has been covered adequately in section 5.4.1.

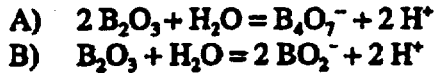
Components of DHLW Glass—The most important of these, because they have the highest concentrations are SiO_2 , B_2O_3 , Al_2O_3 , Na_2O , and K_2O . Of lesser importance are BaO , Fe oxide, CaO , Cl, etc.

¹ "Static mass balance" refers to the distribution of elemental masses in the phases present at a fixed point in time. Dynamic mass balance refers to rates of transfer of mass from one phase to another as well as transfers into or out of the system.

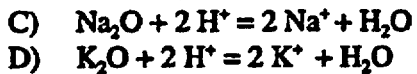
PREDECISIONAL DOCUMENT

The SiO_2 upon being released from the glass will largely precipitate as silica (quartz, chalcedony or some other form of SiO_2) and as a component of silicates (clay, feldspar, etc.). The net effect on acid content is small and is for the present purposes neglected.

B_2O_3 presents more of a problem. Looked upon in a simplified, or stepwise, fashion it will enter solution to form some variety of borate ion, e.g., according to reactions like:



Coupled with this one must consider the behavior of the alkalis, Na and K. The simple steps here are:



This is equivalent to the ion exchange process which occurs in the early stage of glass dissolution leading to a pH of ~ 10 .

Notable in this respect is that the dissolution of the alkalis has exactly the opposite effect on acid content as does boron. Moreover, the alkali content exceeds the equivalent amount of boron in the waste. Thus a portion of the alkalis may be considered as neutralizing the effect of dissolution of B_2O_3 . In this connection the relationship,



becomes relevant. Reaction E results from combining reactions A and B so as to eliminate B_2O_3 . The net result in acid production in going from B_2O_3 to B_4O_7^- is the same regardless of whether it is considered as happening directly or stepwise.

What does this mean for determining the amount of Gd in solution? To answer this some indication of where B resides at various times is required. Initially reaction with J-13 water increases the pH as a consequence of reactions C and D predominating over A and/or B. Calculations with EQ6 indicate that much of the boron should precipitate as borax, $\text{Na}_2\text{B}_4\text{O}_7 \cdot 10\text{H}_2\text{O}$. This would involve the reaction,



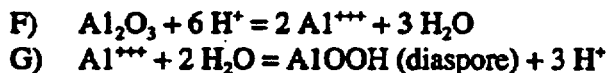
which has no direct effect on the amount of acid. Thus, it is irrelevant to the acid/base inventory as to whether borax precipitates or not. Nevertheless, how much gets flushed from the system by through flowing water does matter, as noted below.

If the borate exists in solution as B_4O_7^- , rather than as BO_2^- , less acid will be required later to convert the borate to boric acid (dissolved or precipitated) as would in effect be necessary for the solution to become significantly acid. The conservative assumption is that the B exists as B_4O_7^- , either dissolved or solid, as this would mean that Gd would start dissolving sooner. Therefore, for the

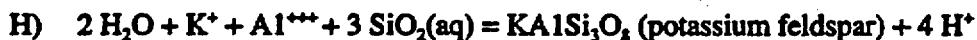
PREDECISIONAL DOCUMENT

purpose at hand, it is assumed that the $B_4O_7^-$ arising from reaction A is compensated by an equivalent amount of alkali coming from reactions C and D. The remainder of the alkali in solution will be assumed to correspond to dissolved carbonate and anions produced by metal corrosion. This logic means that the $GdOHCO_3$ would start to dissolve when the carbonate and bicarbonate are neutralized, but before any borate remaining in the solution starts to be neutralized. Another implication of this logic is that the pH when the bicarbonate is neutralized is 7, because acid dissociation constants are being ignored; this is a necessary consequence of the inability to calculate the relevant relationships at high concentrations.

The situation for Al is once again rather simple. All except trace amounts of Al released from the glass will precipitate as some insoluble compound. Specific reactions include:



The acid consumption in reaction F is exactly compensated by acid production in reaction G



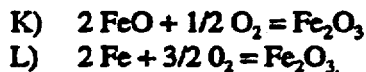
Acid production from reaction H compensates for acid in reactions D and F. The EQ3/6 data base uses the formula $Na_{1/3}Fe_2Al_{1/3}Si_{11/3}O_{10}(OH)_2$ for Na-nontronite, and a corresponding one for K-nontronite. The iron is ferric. The precipitation reaction may be written as:



Thus, reaction I compensates for the appropriate portions of reactions C, F, and J:



The net result is that Al will not have a perceptible impact on the acid/base inventory. It should be noted that the oxidation state of Fe in the glass, or in metals, is irrelevant to this inventory in the presence of atmospheric O_2 , coupled with common observation that Fe in aerated waters soon oxidizes to the ferric state:



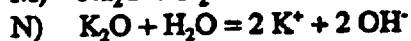
To a large extent the behavior of the alkalis has already been discussed. The remaining point relates to reactions H, I, and others of a similar nature in which Na and K become incorporated into silicates. In all of these cases the amount of alkali incorporated corresponds to an equivalent amount of Al that substitutes for Si in tetrahedrally coordinated crystallographic sites.

The unique chemistry of the waste package permits utilization of these relations to determine approximately the inventory of the alkalis in the silicates, which in this case are expected to consist mostly of clay minerals. The ability to do this rests on the basis that neither the waste package nor J-13 water contains much Ca or Mg. Thus, as a first approximation the content of these elements in clay may be ignored. Otherwise the Al that provides for their charge balance in tetrahedral sites

in silicates would need to be taken into account. In addition, the Al must reside predominantly in the tetrahedral sites. Because of the high iron content of the waste package and the high oxidation state, this appears to be the case. Ferric iron can be expected to occupy the octahedral sites in smectite clay, of which nontronite represents the ferric iron end members. (Data in the EQ3/6 data base represent other end members having no iron and having the octahedral sites and part of the tetrahedral sites occupied by Al, beidellite, or the octahedral sites 5/6 occupied by Al and 1/6 by Mg and all tetrahedral sites by Si, montmorillonite). To the extent that these or similar components of smectite develop, the approximation made here will be less accurate. EQ6 modeling indicates that at the times of interest the Na and K end-members predominate.

The net result of the considerations above is that this inventory of alkalis is assumed to be equivalent to that of Al. The latter is derived from the alteration rate of the glass multiplied by the mole fraction of Al in the glass and the time.

Reactions C and D can be viewed instead of consuming H^+ as producing OH^- :



(These could be derived from C and D by adding twice the water dissociation reaction, $H_2O = H^+ + OH^-$)

In the presence of atmospheric CO_2 , or some other moderate partial pressure of CO_2 in a repository, the hydroxide would react to bicarbonates:



The bicarbonate would in turn hydrolyze partially thereby increasing the pH to a maximum in the range of 9 to 11, depending upon specific circumstances.



The extent of this hydrolysis cannot be determined by the simple mass balance considerations identified here. Such a calculation requires the use of equilibrium constants and, in the present instance in which high concentrations prevail, the missing parameters. (Actually, Pitzer data for the major dissolved components do exist, but the analyses required also must take account of the alkalis precipitated, Al and Si, as is apparent above, and Pitzer data evidently are not available for Al and Si. Thus, calculations that omit Al and Si would be of limited value.)

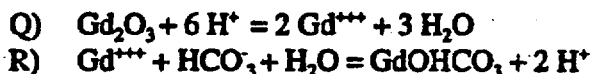
This inability to determine the proportion of HCO_3^- and CO_3^{2-} leads to another uncertainty in ascertaining the amount of acid required to lower the pH to where Gd becomes soluble. The conservative approach is to assume the presence of HCO_3^- only, complexed with Na^+ , etc., or not, inasmuch as this would require less acid. In other words the extra hydroxide produced by reaction P is ignored. Because the second dissociation constant of carbonic acid is about $5.0E-11$, but the pH on the basis of EQ6 calculations is not expected to be significantly higher than 10 (e.g., an activity of hydrogen ion of $1.0E-10$), only about 1/3 of the HCO_3^- will hydrolyze. Half of this will still be

PREDECISIONAL DOCUMENT

accounted for by ignoring the hydrolysis. Thus, the acid demand will be high, according to this approximation, by about 1/6, and by less for lower pHs.

E.2.2 La-BS Glass

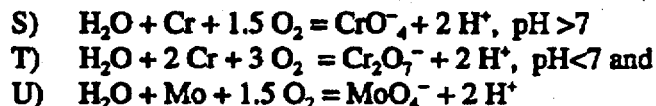
Considerations here parallel those for DHLW glass. The only significant difference arises for the Rare Earth Elements (REEs).



Considerations of the known or estimated thermodynamics of Gd, for both solids and solution, indicate the Gd will be in one or another solid mostly GdOHCO₃, except at pH < 7.² See Figure C-1 in Appendix C. Thus about 2/3 of the acid consumption, or alternatively hydroxide production, will be immediately compensated by hydroxycarbonate precipitation of REEs. The remainder will be taken into account. Pu and daughter ²³⁵U are expected to form insoluble compounds with no net acid inventory effects. The same is expected for Zr and Sr.

Metals

As noted previously in section 5.4.1, the reactions



express the generation of acid from the corrosion of the metals.

Calculations

The relations noted above permit an approximate calculation of the chemistry at specified times during the period of high concentrations without reliance on computations that lie outside the capabilities of existing data bases. The specifications of the dimensions of the various components of a glass waste package, together with the composition of the DHLW glass permit the calculation of the number of moles of glass per kg of J-13 water as about 83.51 moles. (In EQ6 quantities must be normalized to 1 kg of water, and the composition of special reactants, such as glass, to the mass which contains gram-atoms of individual elements that total to one, i.e., to one "mole." These normalizations result in there being approximately 83.51 moles of glass per kg of water. The dissolution rate uses a high rate of degradation of the glass, appropriate to pH 10, and a high degree of fracturing of the glass, about 100 times the surface area. Other data were used for other scenarios in this report.) The dissolution rate, converted to moles, is about 0.3334 moles per year. This means that the DHLW glass will be completely reacted in about 250 years. At that time the total input of

² By happenstance the pH at which the GdOHCO₃ starts becoming much more soluble approximately corresponds to neutral. This means that the rapid dissolution of the GdOHCO₃ begins at about the same time as excess base is neutralized. It wouldn't matter much, however, if the pH were a unit higher or lower inasmuch as this would represent only 10⁻⁴m of excess acid or base.

PREDECISIONAL DOCUMENT

Na and K to the water will be 83.51 moles of glass times the sum of the mole fractions of Na and K in the glass, $9.317E-02$, to yield a total amount of alkali released of 7.781 moles per kg of water. The Al in the clay at this time will be approximately the mole fraction of Al in the DHLW glass times 83.51 moles, or 1.371 moles. In this calculation the contribution of Al from the La-BS glass is neglected because little will have been released. The sodium coupled to borate will be 1/2 the release of boron from the DHLW, or 2.605 moles. The chromate produced up to this time will come primarily from the 304L stainless steel and alloy 625. The release rate from 304L is about $8.537E-03$ moles/yr, with a Cr mole fraction of 0.2 and from alloy 625 about $2.114E-03$ moles/yr with mole fractions of Cr of 0.2538 and for Mo of 0.0576. In 250 years this amounts to $0.427 + 0.134 = 0.561$ moles of Cr and 0.030 moles of Mo. The equivalents of acid from this metal corrosion would then be twice those amounts or $2(0.561 + 0.030) = 1.182$. This leaves unneutralized alkali equal to the amount released, 7.781, minus that in clays, 1.371, minus that coupled to borate, 2.605, minus that already neutralized by acid production, 1.182, to give 2.623 moles of Na and K that are not in some way compensated by acidic components. This is approximately equivalent to the amount of bicarbonate to be neutralized by further acid production from the metal corrosion. The acid production rate, from the data shown above, is 1.182 equivalents divided by 250 years, or $4.728E-03$ equivalents/year. At this rate the alkali would require about 555 years to become neutralized. Thus the total time from the beginning of the degradation of the waste until the water reached approximate neutrality would be about 800 years. This in effect assumes that the borate and accompanying Na and K have been flushed out of the system. On the other hand for a closed system the borate should be retained. The time to neutralize the borate and the carbonate would be about $(7.781 - 1.371 - 1.182)/4.72E-03$, or 1107 years. The total time from breach of the waste package would then be about 1360 years.

The results of an EQ6 computer calculation using the same rates for the closed system indicated that the $GdOHCO_3$ would begin to dissolve rapidly at about 1700 years. In other words this calculation, based in large part on the principles elaborated upon in earlier sections of this appendix, as well as on rates of reaction of components of the waste package, resulted in a similar time estimate for neutralization of the alkali. This suggests that the same approach, which totally avoids any reliance on equilibrium calculations at high concentrations, can provide approximate chemical relationships during the period of high pH and alkali metal ion content. Some aspects of this approach, e.g., the composition of clay minerals, the precipitation or lack thereof of borax, and the point at which $GdOHCO_3$ begins to dissolve relative to conversion of borate to boric acid, seem amenable to experimental verification.

PREDECISIONAL DOCUMENT

**APPENDIX F
GADOLINIUM THERMODYNAMIC DATA**

A0000000-01717-5705-00014 REV 01

PREDECISIONAL DOCUMENT

February 1997

PREDECISIONAL DOCUMENT

Intentionally Left Blank

A00000000-01717-5705-00014 REV 01
PREDECISIONAL DOCUMENT

February 1997

PREDECISIONAL DOCUMENT

APPENDIX F
GADOLINIUM THERMODYNAMIC DATA

Table F-1. Gadolinium and Neodymium Thermodynamic Data

Reaction	Log K*
$GdOH^{2+} \rightleftharpoons Gd^{3+} + OH^{-}$	-6.0
$Gd(OH)_2^{+} \rightleftharpoons Gd^{3+} + 2OH^{-}$	-11.8
$Gd(OH)_3(aq) \rightleftharpoons Gd^{3+} + 3OH^{-}$	-17.5
$Gd(OH)_4^{-} \rightleftharpoons Gd^{3+} + 4OH^{-}$	-22.1
$GdCO_3^{+} \rightleftharpoons Gd^{3+} + CO_3^{2-}$	-7.8
$Gd(CO_3)_2^{-} \rightleftharpoons Gd^{3+} + 2CO_3^{2-}$	-13.1
$GdHCO_3^{2+} \rightleftharpoons Gd^{3+} + HCO_3^{-}$	-2.1
$GdH_2PO_4^{2+} \rightleftharpoons Gd^{3+} + H_2PO_4^{-}$	-2.4
$GdHPO_4^{+} \rightleftharpoons Gd^{3+} + HPO_4^{2-}$	-5.7
$Gd(HPO_4)_2^{-} \rightleftharpoons Gd^{3+} + 2HPO_4^{2-}$	-9.6
$GdPO_4(aq) \rightleftharpoons Gd^{3+} + PO_4^{3-}$	-12.2
$Gd(PO_4)_2^{3-} \rightleftharpoons Gd^{3+} + 2PO_4^{3-}$	-20.7
$GdSO_4^{+} \rightleftharpoons Gd^{3+} + SO_4^{2-}$	-3.4
$Gd(SO_4)_2^{-} \rightleftharpoons Gd^{3+} + 2SO_4^{2-}$	-5.1
$GdF^{2+} \rightleftharpoons Gd^{3+} + F^{-}$	-4.1
$GdF_2^{+} \rightleftharpoons Gd^{3+} + 2F^{-}$	-7.2
$GdCl^{2+} \rightleftharpoons Gd^{3+} + Cl^{-}$	-0.3
$GdNO_3^{+} \rightleftharpoons Gd^{3+} + NO_3^{-}$	-0.8
$Gd(s) + 3H^{+} + 0.75 O_2(g) \rightleftharpoons Gd^{3+} + 1.5H_2O$	178.6
$Gd(OH)_3(am) \rightleftharpoons Gd^{3+} + 3OH^{-}$	-24.0
$Gd(OH)_3(s) \rightleftharpoons Gd^{3+} + 3OH^{-}$	-26.4
$Gd_2O_3(c, monocl.) + 6H^{+} \rightleftharpoons 2Gd^{3+} + 3H_2O$	53.8
$Gd(OH)CO_3(s) \rightleftharpoons Gd^{3+} + OH^{-} + CO_3^{2-}$	-
$Gd_2(CO_3)_3(s) \rightleftharpoons 2Gd^{3+} + 3 CO_3^{2-}$	-34.7
$GdPO_4 \cdot x H_2O(s) \rightleftharpoons Gd^{3+} + PO_4^{3-} + x H_2O$	-24.3
$GdF_3 \cdot 0.5H_2O(s) \rightleftharpoons Gd^{3+} + 3F^{-} + 0.5 H_2O$	-16.9
$Nd(OH)CO_3(s) \rightleftharpoons Nd^{3+} + OH^{-} + CO_3^{2-}$	-21.5

*Selected by Reference 20 and incorporated into the EQ3/6 data base.

PREDECISIONAL DOCUMENT

INTENTIONALLY LEFT BLANK

PREDECISIONAL DOCUMENT

**APPENDIX G
CRITICALITY DATA POINTS**

PREDECISIONAL DOCUMENT

Intentionally Left Blank

PREDECISIONAL DOCUMENT

TABLES

	Page
G-1	MCNP4A k_{eff} Results for Glass Waste Form Cases G-1
G-2	MCNP4A k_{eff} Results for Ceramic Waste Form Cases G-8
G-3	Accumulations of 1 wt% ^{235}U in Chabazite (40%) and Aggregate (60%) from Degraded Concrete in a 75 cm Deep Cylinder Segment G-16
G-4	Effect on k_{eff} of Pu/U/Gd Concentration in Bottom of Clay G-16
G-5	Effect on k_{eff} of Pu/U/Gd Concentration in Top of Clay G-16
G-6	Effect on k_{eff} of Concentrating Pu/U/Gd on One End of WP G-17
G-7	Effect on k_{eff} of Half Volume on One End of WP (Same Concentration) G-17
G-8	Comparison of Gd and Sm in Degraded DHLW Glass/Pu Immobilization Glass .. G-18
G-9	Investigation of Dryout of Degraded Glass Configuration G-18
G-10	Comparison of ^{238}U in Degraded DHLW Glass/Pu Immobilization Glass G-19
G-11	Variation of Hf Wt% in Zr for the Degraded Ceramic Waste Form G-19
G-12	Calculations to Determine Equivalent Hf Wt% in Zr to Replace 0.5 kg Gd for the Degraded Ceramic Waste Form G-19

PREDECISIONAL DOCUMENT

INTENTIONALLY LEFT BLANK

APPENDIX G CRITICALITY DATA POINTS

Tables G-1 and G-2 contain the results of the MCNP4A criticality calculations, in the form of $k_{eff} \pm$ two times the standard deviation (approximate 95% confidence interval), for the clayey material formed from the degraded glass and ceramic waste forms, respectively. Following each table are the output produced by the Excel V.5 regression function. Shading in Tables G.1 and G.2 indicates the points used for the regressions (typically the peak k_{eff} value for a range of water fractions in the clay), and each regression output indicates the range for which it applies. The MCNP4A input file name for each case is given in parentheses below the k_{eff} data point. Tables G-3 through G-10 provide the results of other MCNP4A cases used in Section 7 with the input file name indicated below each data point. Regressions were not developed for these variations.

Table G-1. MCNP4A k_{eff} Results for Glass Waste Form Cases

^{235}Pu (kg)	^{235}U (kg)	Gd (kg)	0 Volume % Water	10 Volume % Water
0	53.09	0	0.9691 \pm 0.0039 (cd0z0)	0.9530 \pm 0.0036 (cd1z0)
0.5	50	0	0.9499 \pm 0.0040 (ca0a0)	0.9357 \pm 0.0028 (ca1a0)
3.96	41.3	0	0.9315 \pm 0.0039 (cd0y0)	0.9133 \pm 0.0037 (cd1y0)
3.96	53.09	0	1.0308 \pm 0.0043 (cd0q0)	-
5	41	0	0.9467 \pm 0.0046 (ca0b0)	0.9280 \pm 0.0033 (ca1b0)
5.18	50.57	0	1.0214 \pm 0.0044 (cd0r0)	-
10	35	0	0.9710 \pm 0.0036 (cd0e0)	-
10	65	0.25	1.0183 \pm 0.0044 (cd0p3)	-
10	65	0.375	0.9734 \pm 0.0043 (cd0p4)	-
10	65	0.5	0.9184 \pm 0.0041 (cd0p5)	-
10	100	0.75	1.0030 \pm 0.0055 (cd0p8)	-
10	100	1	0.9340 \pm 0.0038 (cd0c1)	-
10	130	1.25	0.9840 \pm 0.0043 (cd0b13)	-
10	130	1.5	0.9393 \pm 0.0045 (cd0b15)	-
10	165	1.75	1.0017 \pm 0.0037 (cd0a18)	-
10	165	2	0.9608 \pm 0.0044 (cd0a2)	-

PREDECISIONAL DOCUMENT

Table G-1. MCNP4A k_{eff} Results for Glass Waste Form Cases (Continued)

^{239}Pu (kg)	^{235}U (kg)	Gd (kg)	0 Volume % Water	10 Volume % Water
10	165	2.25	0.9409 ± 0.0050 (c0IA23)	-
15	25	0	0.9689 ± 0.0031 (ca10I0)	-
18.1	21.8	0	0.9622 ± 0.0046 (cc10x0)	0.9415 ± 0.0034 (cc11x0)
17.26	24.04	0	0.9927 ± 0.0040 (cc10s0)	-
18.83	21.78	0	1.0000 ± 0.0047 (ca10c0)	-
18.9	15.8	0	0.9495 ± 0.0038 (cc10v0)	0.9353 ± 0.0034 (cc11v0)
18.9	21.8	0	0.9994 ± 0.0044 (cc10w0)	0.9800 ± 0.0030 (cc11w0)
20.97	17.24	0	0.9928 ± 0.0051 (ca10c0)	-
21	12	0	0.9501 ± 0.0035 (ca10k0)	-
21	14	0	0.9843 ± 0.0028 (ca10j0)	-
21	17.2	0	0.9983 ± 0.0030 (cc10u0)	0.9782 ± 0.0037 (cc11u0)
22.35	14.47	0	0.9841 ± 0.0035 (cc10i0)	-
23.47	8.21	0	0.9541 ± 0.0037 (ca10f0)	-
23.5	9	0	0.9618 ± 0.0039 (ca10h0)	-
23.93	9.87	0	0.9777 ± 0.0037 (ca10g0)	-
24	9	0	0.9689 ± 0.0035 (ca10i0)	-
25	5	0	0.9513 ± 0.0038 (c0kF0)	-
25	25	0	1.1006 ± 0.0045 (c0kE0)	-
25	25	0.25	0.9602 ± 0.0047 (c0kEp3)	-
25	60	0.5	1.0343 ± 0.0044 (c0kDp5)	-
25	60	0.75	0.9597 ± 0.0047 (c0kDp8)	-
25	80	1	0.9058 ± 0.0039 (c0kD1)	-
25	90	1	1.0128 ± 0.0039 (c0kC1)	-
25	90	1.25	0.9620 ± 0.0033 (c0kC13)	-

PREDECISIONAL DOCUMENT

Table G-1. MCNPAA k_{eff} Results for Glass Waste Form Cases (Continued)

^{239}Pu (kg)	^{235}U (kg)	Gd (kg)	0 Volume % Water	10 Volume % Water
25	90	1.5	0.8185 ± 0.0053 (c0kC15)	-
25	90	2	0.8554 ± 0.0033 (c0kC2)	-
25	125	1.5	1.0213 ± 0.0041 (c0kB15)	-
25	125	1.75	0.9872 ± 0.0038 (c0kB18)	-
25	125	2	0.8530 ± 0.0051 (c0kB2)	-
25	125	2.5	0.8989 ± 0.0032 (c0kB25)	-
25	160	2	1.0377 ± 0.0052 (c0kA2)	-
25	160	2.5	0.9784 ± 0.0043 (c0kA25)	-
25	160	3	0.8434 ± 0.0043 (c0kA3)	-
25	160	3.5	0.8033 ± 0.0032 (c0kA35)	-
27.65	11.58	0	1.0461 ± 0.0039 (c0l0e0)	-
40	15	0.5	0.9684 ± 0.0041 (c0jEp5)	-
40	50	1	0.9795 ± 0.0049 (c0jD1)	-
40	50	1.25	0.9344 ± 0.0041 (c0jD13)	-
40	85	1.5	1.0026 ± 0.0043 (c0jC15)	-
40	85	1.75	0.9678 ± 0.0043 (c0jC18)	-
40	85	2	0.9307 ± 0.0046 (c0jC2)	-
40	120	2	1.0262 ± 0.0055 (c0jB2)	-
40	120	2.5	0.9716 ± 0.0058 (c0jB25)	-
40	120	3	0.9319 ± 0.0042 (c0jB3)	-
40	150	3	0.8938 ± 0.0041 (c0jA3)	-
40	150	3.5	0.9548 ± 0.0053 (c0jA35)	-
40	150	4	0.9295 ± 0.0044 (c0jA4)	-
50	10	0.7	0.9759 ± 0.0041 (c0id.7)	0.8595 ± 0.0038 (c1id.7)

PREDECISIONAL DOCUMENT

Table G-1. MCNP4A k_{eff} Results for Glass Waste Form Cases (Continued)

^{239}Pu (kg)	^{235}U (kg)	Gd (kg)	0 Volume % Water	10 Volume % Water
50	10	1	0.9065 ± 0.0049 (c10d1)	-
50	30	1	0.9851 ± 0.0046 (c10e1)	0.9683 ± 0.0038 (c11e1)
50	30	1.2	0.9464 ± 0.0040 (c10g12)	-
50	30	1.5	0.9036 ± 0.0045 (c10i15)	-
50	75	1.5	1.0413 ± 0.0046 (c10b15)	-
50	75	2	0.9728 ± 0.0049 (c10b2)	0.9427 ± 0.0049 (c11b2)
50	75	2.5	0.9221 ± 0.0048 (c10b25)	-
50	75	3	0.8818 ± 0.0039 (c10b3)	-
50	110	2.5	1.0025 ± 0.0039 (c1y0f25)	-
50	110	3	0.9827 ± 0.0042 (c1y0f3)	0.9345 ± 0.0048 (c1y1f3)
50	110	3.5	0.9240 ± 0.0044 (c1y0f35)	-
50	110	4	0.8983 ± 0.0038 (c1y0f4)	-
50	140	3	1.0197 ± 0.0047 (c10a3)	-
50	140	3.5	0.9844 ± 0.0048 (c10a35)	0.9551 ± 0.0047 (c11a35)
50	140	4	0.9538 ± 0.0035 (c10a4)	-
50	140	4.5	0.9307 ± 0.0041 (c10a45)	-
50	140	5	0.9067 ± 0.0051 (c10a5)	-
85	20	2	1.0228 ± 0.0045 (c10hd2)	-
85	20	2.5	0.9751 ± 0.0045 (c10hd25)	0.9478 ± 0.0048 (c11hd25)
85	20	3.5	0.9072 ± 0.0057 (c10hd35)	-
85	50	3	1.0003 ± 0.0049 (c10hc3)	-
85	50	3.5	0.9669 ± 0.0045 (c10hc35)	0.9338 ± 0.0039 (c11hc35)
85	50	4	0.9374 ± 0.0054 (c10hc4)	-
85	50	4.5	0.9207 ± 0.0042 (c10hc45)	-

PREDECISIONAL DOCUMENT

Table G-1. MCNP4A k_{eff} Results for Glass Waste Form Cases (Continued)

^{239}Pu (kg)	^{235}U (kg)	Gd (kg)	0 Volume % Water	10 Volume % Water
85	80	4	0.8892 ± 0.0039 (c10hb4)	-
85	80	5	0.9465 ± 0.0042 (c10hb5)	0.9048 ± 0.0034 (c11hb5)
85	80	6	0.9139 ± 0.0037 (c10hb6)	-
85	80	7	0.8827 ± 0.0034 (c10hb7)	-
85	110	5	0.8974 ± 0.0037 (c10ha5)	-
85	110	6	0.9576 ± 0.0049 (c10ha6)	0.9185 ± 0.0039 (c11ha6)
85	110	7	0.9302 ± 0.0047 (c10ha7)	-
85	110	8	0.9110 ± 0.0049 (c10ha8)	-
140	30	6	1.0261 ± 0.0042 (c10gb6)	-
140	30	8	0.9742 ± 0.0048 (c10gb8)	0.9298 ± 0.0039 (c11gb8)
140	30	10	0.9361 ± 0.0044 (c10gb10)	-
140	30	12	0.9088 ± 0.0041 (c10gb12)	-
140	60	8	1.0132 ± 0.0047 (c10ga8)	-
140	60	10	0.9738 ± 0.0030 (c10ga10)	0.9230 ± 0.0051 (c11ga10)
140	60	13	0.9293 ± 0.0045 (c10ga13)	-
140	60	16	0.8967 ± 0.0040 (c10ga16)	-

PREDECISIONAL DOCUMENT

Multi-variate Fit for Data in Table G-1

Gd = 0
S U M M A R Y
O U T P U T

<i>Regression Statistics</i>	
Multiple R	0.996015434
R Square	0.992046745
Adjusted R Square	0.991289292
Standard Error	0.002692529
Observations	24

ANOVA

	<i>df</i>	<i>SS</i>	<i>MS</i>	<i>F</i>	<i>Significance F</i>
Regression	2	0.018990096	0.009495048	1309.714101	9.03071E-23
Residual	21	0.000152244	7.24971E-06		
Total	23	0.01914234			

	<i>Coefficients</i>	<i>Standard Error</i>	<i>t Stat</i>	<i>P-value</i>	<i>Lower 95%</i>	<i>Upper 95%</i>
Intercept	0.534305374	0.008671112	61.61901216	3.24263E-25	0.516272806	0.552337942
X Variable 1	0.015139723	0.00029707	50.96353843	1.70368E-23	0.014521933	0.015757514
X Variable 2	0.008186415	0.000161328	50.74381442	1.86419E-23	0.007850914	0.008521916

0kg < Gd =< 1 kg
S U M M A R Y
O U T P U T

<i>Regression Statistics</i>	
Multiple R	0.98173069
R Square	0.96379514
Adjusted R Square	0.95293369
Standard Error	0.00891743
Observations	14

ANOVA

	<i>df</i>	<i>SS</i>	<i>MS</i>	<i>F</i>	<i>Significance F</i>
Regression	3	0.021169	0.007056	88.73534	1.65834E-07
Residual	10	0.000795	7.95E-05		
Total	13	0.021964			

	<i>Coefficients</i>	<i>Standard Error</i>	<i>t Stat</i>	<i>P-value</i>	<i>Lower 95%</i>	<i>Upper 95%</i>
Intercept	0.72901967	0.018931	38.50903	3.33E-12	0.686838459	0.771200872
X Variable 1	0.00802842	0.000545	14.74322	4.13E-08	0.006815088	0.009241755
X Variable 2	0.00396649	0.000256	15.50521	2.54E-08	0.003396494	0.004536484
X Variable 3	-0.26981017	0.017231	-15.6588	2.31E-08	-0.308202375	-0.231417958

PREDECISIONAL DOCUMENT

Multi-variate Fit for Data in Table G-1 (Continued)

1kg < Gd < 4kg

SUMMARY OUTPUT

<i>Regression Statistics</i>	
Multiple R	0.97444126
R Square	0.94953577
Adjusted R Square	0.94544408
Standard Error	0.01026583
Observations	41

ANOVA

	<i>df</i>	<i>SS</i>	<i>MS</i>	<i>F</i>	<i>Significance F</i>
Regression	3	0.07337	0.024457	232.0642	4.88914E-24
Residual	37	0.003899	0.000105		
Total	40	0.077269			

	<i>Coefficients</i>	<i>Standard Error</i>	<i>t Stat</i>	<i>P-value</i>	<i>Lower 95%</i>	<i>Upper 95%</i>
Intercept	0.7256189	0.011405	63.62472	2.1E-39	0.702510868	0.748726932
X Variable 1	0.00532057	0.00021	25.39324	5.19E-25	0.004896028	0.005745111
X Variable 2	0.00233011	9.19E-05	25.35103	5.5E-25	0.002143876	0.002516346
X Variable 3	-0.09609022	0.003957	-24.281	2.48E-24	-0.104108703	-0.088071735

Gd ≥ 4kg

SUMMARY OUTPUT

<i>Regression Statistics</i>	
Multiple R	0.993123
R Square	0.986294
Adjusted R Square	0.98413
Standard Error	0.004847
Observations	23

ANOVA

	<i>df</i>	<i>SS</i>	<i>MS</i>	<i>F</i>	<i>Significance F</i>
Regression	3	0.032123	0.010708	455.7565592	7.17427E-18
Residual	19	0.000446	2.35E-05		
Total	22	0.032569			

	<i>Coefficients</i>	<i>Standard Error</i>	<i>t Stat</i>	<i>P-value</i>	<i>Lower 95%</i>	<i>Upper 95%</i>
Intercept	0.822783	0.009632	85.42133	4.95487E-26	0.802622863	0.842943124
X Variable 1	0.003415	1E-04	34.16284	1.59967E-18	0.00320616	0.003624657
X Variable 2	0.001461	6.33E-05	23.06844	2.3432E-15	0.001328599	0.001593747
X Variable 3	-0.17762	0.005139	-34.5599	1.28861E-18	-0.18837243	-0.16685882

PREDECISIONAL DOCUMENT

Table G-2. MCNP4A k_{eff} Results for Ceramic Waste Form Cases

Pu (kg)	U (kg)	Gd (kg)	0 Volume % Water	10 Volume % Water	20 Volume % Water	30 Volume % Water
0.16	110.8	0	-	0.9843 ±0.0040 (s1pg3)	-	-
0.33	110.1	0	-	0.9873 ±0.0045 (s1pg4)	-	-
0.49	117	0	-	1.0150 ±0.0042 (s1pg7)	-	-
7.99	101	0	-	1.0144 ±0.0039 (s1pg8)	-	-
10	35	0	-	0.8978 ±0.0024 (s1IE0)	-	-
10	65	0	0.8473 ±0.0049 (s0ID0)	0.8817 ±0.0040 (s1ID0)	-	-
10	100	0	0.9848 ±0.0040 (s0IC0)	1.0242 ±0.0038 (s1IC0)	1.0450 ±0.0035 (s2IC0)	1.0392 ±0.0038 (s3IC0)
10	100	0.2	0.9394 ±0.0037 (s0ICp2)	0.9847 ±0.0040 (s1ICp2)	0.9788 ±0.0038 (s2ICp2)	-
10	100	0.3	0.9101 ±0.0043 (s0ICp3)	0.9352 ±0.0045 (s1ICp3)	0.9482 ±0.0043 (s2ICp3)	0.9469 ±0.0038 (s3ICp3)
10	100	0.5	0.8728 ±0.0049 (s0ICp5)	0.8972 ±0.0039 (s1ICp5)	0.8988 ±0.0041 (s2ICp5)	-
10	130	0.3	0.9977 ±0.0044 (s0IBp3)	1.0359 ±0.0041 (s1IBp3)	1.0480 ±0.0040 (s2IBp3)	1.05030 ±0.0038 (s3IBp3)
10	130	0.5	0.9810 ±0.0039 (s0IBp5)	0.9915 ±0.0042 (s1IBp5)	1.0018 ±0.0037 (s2IBp5)	-
10	130	0.8	0.9141 ±0.0048 (s0IBp8)	0.9360 ±0.0045 (s1IBp8)	0.9382 ±0.0037 (s2IBp8)	-
10	130	1	-	0.9050 ±0.0048 (s1IB1)	-	-
10	165	0.5	1.0331 ±0.0052 (s0IAp5)	-	-	-
10	165	0.8	1.0000 ±0.0041 (s0IAp8)	-	-	-
10	165	1	0.9783 ±0.0037 (s0IA1)	0.9988 ±0.0057 (s1IA1)	1.0024 ±0.0038 (s2IA1)	0.9922 ±0.0045 (s3IA1)
10	165	1.4	0.9270 ±0.0051 (s0IA14)	0.9484 ±0.0035 (s1IA14)	0.9378 ±0.0039 (s2IA14)	-
10	165	1.8	0.8975 ±0.0039 (s0IA18)	0.8960 ±0.0045 (s1IA18)	-	-
11.57	87.8	0	-	0.9964 ±0.0049 (s1pg6)	-	-
12.82	91.94	0	-	1.0133 ±0.0038 (s1pg2)	-	-
16.22	83.18	0	-	1.0163 ±0.0050 (s1pg1)	-	-
17.27	75.7	0	-	0.9984 ±0.0043 (s1pg5)	-	-

PREDECISIONAL DOCUMENT

Table G-2. MCNP4A k_{eff} Results for Ceramic Waste Form Cases (Continued)

Pu (kg)	U (kg)	Gd (kg)	0 Volume % Water	10 Volume % Water	20 Volume % Water	30 Volume % Water
25	5	0	0.6940 ±0.0036 (s0kF0)	0.8997 ±0.0028 (s1kF0)	-	-
25	25	0	0.8139 ±0.0033 (s0kE0)	0.8332 ±0.0023 (s1kE0)	-	-
25	60	0	0.9593 ±0.0042 (s0kD0)	0.9891 ±0.0044 (s1kD0)	1.0062 ±0.0037 (s2kD0)	0.99620 ±0.0041 (s3kD0)
25	60	0.2	0.9107 ±0.0040 (s0kDp2)	0.9352 ±0.0035 (s1kDp2)	0.9426 ±0.0041 (s2kDp2)	-
25	60	0.3	-	0.9181 ±0.0042 (s1kDp3)	0.9166 ±0.0026 (s2kDp3)	0.9056 ±0.0035 (s3kDp3)
25	90	0.2	1.0001 ±0.0047 (s0kCp2)	1.0359 ±0.0044 (s1kCp2)	1.0481 ±0.0044 (s2kCp2)	-
25	90	0.3	0.9826 ±0.0044 (s0kCp3)	1.0142 ±0.0044 (s1kCp3)	1.0242 ±0.0037 (s2kCp3)	1.0203 ±0.0027 (s3kCp3)
25	90	0.5	0.8451 ±0.0042 (s0kCp5)	0.8724 ±0.0037 (s1kCp5)	0.9759 ±0.0032 (s2kCp5)	-
25	90	0.8	0.9012 ±0.0039 (s0kCp8)	0.9188 ±0.0032 (s1kCp8)	0.9182 ±0.0047 (s2kCp8)	-
25	90	1	-	0.8784 ±0.0041 (s1kC1)	0.8823 ±0.0042 (s2kC1)	-
25	125	0.5	1.0295 ±0.0048 (s0kBp5)	-	-	-
25	125	0.8	0.9848 ±0.0041 (s0kBp8)	-	-	-
25	125	1	0.9664 ±0.0039 (s0kB1)	0.9789 ±0.0040 (s1kB1)	0.9877 ±0.0054 (s2kB1)	0.9762 ±0.0041 (s3kB1)
25	125	1.4	0.8240 ±0.0050 (s0kB14)	0.9323 ±0.0033 (s1kB14)	0.9242 ±0.0039 (s2kB14)	-
25	125	1.8	0.8881 ±0.0042 (s0kB18)	0.8938 ±0.0044 (s1kB18)	-	-
25	160	1.4	0.9924 ±0.0038 (s0kA14)	-	-	-
25	160	1.8	0.9848 ±0.0040 (s0kA18)	0.9898 ±0.0041 (s1kA18)	0.9586 ±0.0032 (s2kA18)	-
25	160	2	0.9270 ±0.0048 (s0kA2)	0.9592 ±0.0038 (s1kA2)	-	-
25	160	2.3	-	0.9281 ±0.0040 (s1kA23)	-	-
40	15	0	0.9100 ±0.0045 (s0jE0)	0.9355 ±0.0031 (sy1jE0)	0.9266 ±0.0032 (sy2jE0)	-
40	15	0.1	-	0.9071 ±0.0041 (sy1jE.1)	-	-
40	50	0	1.0212 ±0.0048 (s0jD0)	-	-	-
40	50	0.2	0.9824 ±0.0039 (s0jDp2)	1.0139 ±0.0046 (sy1jd.2)	-	-

PREDECISIONAL DOCUMENT

Table G-2. MCNP4A k_{eff} Results for Ceramic Waste Form Cases (Continued)

Pu (kg)	U (kg)	Gd (kg)	0 Volume % Water	10 Volume % Water	20 Volume % Water	30 Volume % Water
40	50	0.3	0.9832 ±0.0039 (s0 Dp3)	0.9885 ±0.0039 (sy1 d.3)	0.9833 ±0.0043 (sy2 d.3)	-
40	50	0.5	0.9303 ±0.0035 (s0 Dp5)	0.9500 ±0.0044 (sy1 d.5)	-	-
40	50	0.8	-	0.9012 ±0.0042 (sy1 d.8)	-	-
40	85	0.5	1.0082 ±0.0047 (s0 Cp5)	-	-	-
40	85	0.8	0.9753 ±0.0041 (s0 Cp8)	0.9951 ±0.0040 (sy1 c.8)	-	-
40	85	1	0.9548 ±0.0046 (s0 C1)	0.9870 ±0.0055 (sy1 c1)	0.9559 ±0.0039 (sy2 c1)	-
40	85	1.2	-	0.9421 ±0.0035 (sy1 c12)	-	-
40	85	1.4	0.9154 ±0.0033 (s0 C14)	-	-	-
40	85	1.5	-	0.9152 ±0.0042 (sy1 c15)	-	-
40	85	1.8	0.8826 ±0.0038 (s0 C18)	-	-	-
40	120	1.4	0.9855 ±0.0049 (s0 B14)	-	-	-
40	120	1.5	-	0.9940 ±0.0039 (sy1 b15)	-	-
40	120	1.8	0.8599 ±0.0038 (s0 B18)	0.9852 ±0.0041 (sy1 b18)	-	-
40	120	2	0.8427 ±0.0045 (s0 B2)	0.9442 ±0.0035 (sy1 b2)	0.9192 ±0.0045 (sy2 b2)	-
40	120	2.5	-	0.9085 ±0.0043 (sy1 b25)	-	-
40	120	3	0.8947 ±0.0033 (s0 B3)	0.8809 ±0.0038 (sy1 b3)	-	-
40	150	1.8	1.0127 ±0.0048 (s0 A18)	-	-	-
40	150	2	0.9988 ±0.0021 (s0 A2)	1.0102 ±0.0045 (sy1 a2)	-	-
40	150	2.5	0.9680 ±0.0040 (s0 A25)	0.9668 ±0.0032 (sy1 a25)	0.9368 ±0.0042 (sy2 a25)	-
40	150	3	-	0.9408 ±0.0035 (sy1 a3)	-	-
40	150	3.5	0.9248 ±0.0045 (s0 A35)	0.9099 ±0.0040 (sy1 a35)	-	-
50	10	0	0.9849 ±0.0048 (sy0 e0)	0.9925 ±0.0039 (sy1 e0)	0.9830 ±0.0050 (sy2 e0)	-
50	10	0.1	-	0.9621 ±0.0040 (sy1 e.1)	-	-

PREDECISIONAL DOCUMENT

Table G-2. MCNP4A k_{eff} Results for Ceramic Waste Form Cases (Continued)

Pu (kg)	U (kg)	Gd (kg)	0 Volume % Water	10 Volume % Water	20 Volume % Water	30 Volume % Water
50	10	0.2	-	0.9440 ±0.0035 (sy1le.2)	-	-
50	10	0.3	-	0.9173 ±0.0040 (sy1le.3)	-	-
50	10	0.5	-	0.8821 ±0.0025 (sy1le.5)	-	-
50	30	0.2	-	1.0113 ±0.0050 (sy1ld.2)	-	-
50	30	0.3	0.9645 ±0.0035 (sy0ld.3)	0.8943 ±0.0050 (sy1ld.3)	0.9877 ±0.0035 (sy2ld.3)	-
50	30	0.5	-	0.8530 ±0.0039 (sy1ld.5)	-	-
50	30	0.8	-	0.8032 ±0.0042 (sy1ld.8)	-	-
50	30	1	-	0.8767 ±0.0035 (sy1ld1)	-	-
50	75	1	-	0.9978 ±0.0061 (sy1lc1)	-	-
50	75	1.2	0.9598 ±0.0043 (sy0lc12)	0.9761 ±0.0041 (sy1lc12)	0.9574 ±0.0038 (sy2lc12)	-
50	75	1.5	-	0.9440 ±0.0049 (sy1lc15)	-	-
50	75	2	-	0.9013 ±0.0042 (sy1lc2)	-	-
50	110	1.5	-	1.0184 ±0.0046 (sy1lb15)	-	-
50	110	2	0.9648 ±0.0036 (sy0lb2)	0.9695 ±0.0048 (sy1lb2)	0.9454 ±0.0036 (sy2lb2)	-
50	110	2.5	-	0.9346 ±0.0034 (sy1lb25)	-	-
50	110	3	-	0.9054 ±0.0049 (sy1lb3)	-	-
50	140	2	1.0153 ±0.0042 (sy0la2)	1.0277 ±0.0044 (sy1la2)	-	-
50	140	2.5	0.9873 ±0.0040 (sy0la25)	0.9891 ±0.0042 (sy1la25)	0.9630 ±0.0048 (sy2la25)	-
50	140	3	0.9659 ±0.0041 (sy0la3)	0.9608 ±0.0046 (sy1la3)	-	-
50	140	3.5	0.9459 ±0.0045 (sy0la35)	0.9334 ±0.0045 (sy1la35)	-	-
50	140	4	0.9238 ±0.0047 (sy0la4)	0.9158 ±0.0037 (sy1la4)	-	-
85	20	1	1.0121 ±0.0050 (sy0hd1)	-	-	-
85	20	1.5	0.9751 ±0.0044 (sy0hd15)	0.9915 ±0.0042 (sy1hd15)	0.9626 ±0.0040 (sy2hd15)	-

Table G-2. MCNPA K^m Results for Ceramic Waste Form Cases (Continued)

Pu (kg)	U (kg)	Gd (kg)	0 Volume % Water	10 Volume % Water	20 Volume % Water	30 Volume % Water
85	20	2	0.9440 ± 0.0039 (sy0hd2)	0.9483 ± 0.0037 (sy1hd2)	-	-
85	20	2.5	-	0.9154 ± 0.0040 (sy1hd2s)	-	-
85	20	3	0.8882 ± 0.0040 (sy0hd3)	0.8872 ± 0.0032 (sy1hd3)	-	-
85	50	2	0.9909 ± 0.0039 (sy0hc2)	1.0059 ± 0.0030 (sy1hc2)	-	-
85	50	2.5	0.9718 ± 0.0042 (sy0hc2s)	0.9754 ± 0.0041 (sy1hc2s)	0.9410 ± 0.0044 (sy2hc2s)	-
85	50	3	0.9510 ± 0.0043 (sy0hc3)	0.9457 ± 0.0044 (sy1hc3)	-	-
85	50	3.5	0.9333 ± 0.0037 (sy0hc3s)	0.9225 ± 0.0037 (sy1hc3s)	-	-
85	50	4	0.9142 ± 0.0031 (sy0hc4)	0.8987 ± 0.0043 (sy1hc4)	-	-
85	80	3	0.8981 ± 0.0062 (sy0hb3)	-	-	-
85	80	4	0.8805 ± 0.0049 (sy0hb4)	0.9517 ± 0.0052 (sy1hb4)	-	-
85	80	5	0.8318 ± 0.0055 (sy0hb5)	-	-	-
85	80	6	0.8050 ± 0.0037 (sy0hb6)	-	-	-
85	110	4	1.0016 ± 0.0058 (sy0hb4)	-	-	-
85	110	5	0.8723 ± 0.0043 (sy0hb5)	0.9825 ± 0.0041 (sy1hb5)	-	-
85	110	6	0.8505 ± 0.0042 (sy0hb6)	-	-	-
85	110	7	0.8371 ± 0.0038 (sy0hb7)	-	-	-
85	110	8	0.8208 ± 0.0042 (sy0hb8)	-	-	-
140	30	6	0.8850 ± 0.0048 (sy0gb6)	-	-	-
140	30	8	0.8705 ± 0.0058 (sy0gb8)	0.9545 ± 0.0047 (sy1gb8)	-	-
140	30	10	0.8428 ± 0.0055 (sy0gb10)	-	-	-
140	30	13	0.9118 ± 0.0045 (sy0gb13)	-	-	-
140	30	16	0.8813 ± 0.0048 (sy0gb16)	-	-	-
140	60	8	1.0005 ± 0.0055 (sy0gb8)	-	-	-

PREDECISIONAL DOCUMENT

Table G-2. MCNP4A k_{eff} Results for Ceramic Waste Form Cases (Continued)

Pu (kg)	U (kg)	Gd (kg)	0 Volume % Water	10 Volume % Water	20 Volume % Water	30 Volume % Water
140	60	10	0.8764 ± 0.0050 (sy0ga10)	-	-	-
140	60	13	0.9410 ± 0.0048 (sy0ga13)	0.9247 ± 0.0047 (sy1ga13)	-	-
140	60	16	0.9189 ± 0.0046 (sy0ga16)	-	-	-
140	60	20	0.8958 ± 0.0046 (sy0ga20)	-	-	-

PREDECISIONAL DOCUMENT

Multi-variate Fit for Data in Table G-2

Gd ≤ 0.2 kg 10 vol% water

**S U M M A R Y
O U T P U T**

<i>Regression Statistics</i>	
Multiple R	0.989728786
R Square	0.97956307
Adjusted R Square	0.97649753
Standard Error	0.01414546
Observations	24

ANOVA

	<i>df</i>	<i>SS</i>	<i>MS</i>	<i>F</i>	<i>Significance F</i>
Regression	3	0.191814248	0.063938083	319.5401841	4.6591E-17
Residual	20	0.004001881	0.000200094		
Total	23	0.195816129			

	<i>Coefficients</i>	<i>Standard Error</i>	<i>t Stat</i>	<i>P-value</i>	<i>Lower 95%</i>	<i>Upper 95%</i>
Intercept	0.448283597	0.017456824	25.6795616	8.72327E-17	0.411869317	0.484697878
X Variable 1	0.010123316	0.000411235	24.61685163	1.98167E-16	0.009265494	0.010981137
X Variable 2	0.004829273	0.000159848	30.21161614	3.65561E-18	0.004495836	0.00516271
X Variable 3	-0.369966327	0.043758439	-8.454742251	4.91028E-08	-0.46124479	-0.278687864

1kg ≥ Gd > 0.2 kg 10 vol% water

**S U M M A R Y
O U T P U T**

<i>Regression Statistics</i>	
Multiple R	0.99178904
R Square	0.9836455
Adjusted R Square	0.981309142
Standard Error	0.006428997
Observations	25

ANOVA

	<i>df</i>	<i>SS</i>	<i>MS</i>	<i>F</i>	<i>Significance F</i>
Regression	3	0.052204394	0.017401465	421.0167438	6.57672E-19
Residual	21	0.000867972	4.1332E-05		
Total	24	0.053072366			

	<i>Coefficients</i>	<i>Standard Error</i>	<i>t Stat</i>	<i>P-value</i>	<i>Lower 95%</i>	<i>Upper 95%</i>
Intercept	0.625156627	0.011353715	55.06185881	3.39616E-24	0.601545281	0.648767973
X Variable 1	0.006578083	0.000221579	29.68731585	1.23668E-18	0.006117285	0.007038882
X Variable 2	0.003004992	8.81515E-05	34.08895629	7.17718E-20	0.002821671	0.003188313
X Variable 3	-0.179719764	0.006187864	-29.04391106	1.93886E-18	-0.192588133	-0.166851394

PREDECISIONAL DOCUMENT

Multi-variate Fit for Data in Table G-2 (Continued)

2.5 kg ≥ Gd > 1 kg 10 vol% water

SUMMARY OUTPUT

<i>Regression Statistics</i>	
Multiple R	0.990167266
R Square	0.980431214
Adjusted R Square	0.977878763
Standard Error	0.00549085
Observations	27

ANOVA

	<i>df</i>	<i>SS</i>	<i>MS</i>	<i>F</i>	<i>Significance F</i>
Regression	3	0.034742436	0.011580812	384.1137208	8.82283E-20
Residual	23	0.000693437	3.01494E-05		
Total	26	0.035435873			

	<i>Coefficients</i>	<i>Standard Error</i>	<i>t Stat</i>	<i>P-value</i>	<i>Lower 95%</i>	<i>Upper 95%</i>
Intercept	0.677252597	0.010017981	67.60370212	5.79212E-28	0.656528853	0.697976341
X Variable 1	0.004775255	0.000140711	33.93653106	3.7676E-21	0.004484172	0.005066338
X Variable 2	0.002054091	6.45478E-05	31.82279974	1.60533E-20	0.001920564	0.002187618
X Variable 3	-0.085239645	0.003605516	-23.64145799	1.22562E-17	-0.092698212	-0.077781078

20 kg ≥ Gd > 2.5 kg 0% water

SUMMARY OUTPUT

<i>Regression Statistics</i>	
Multiple R	0.982507166
R Square	0.965320331
Adjusted R Square	0.960985373
Standard Error	0.006620516
Observations	28

ANOVA

	<i>df</i>	<i>SS</i>	<i>MS</i>	<i>F</i>	<i>Significance F</i>
Regression	3	0.029281375	0.009760458	222.6827108	1.19974E-17
Residual	24	0.00105195	4.38312E-05		
Total	27	0.030333325			

	<i>Coefficients</i>	<i>Standard Error</i>	<i>t Stat</i>	<i>P-value</i>	<i>Lower 95%</i>	<i>Upper 95%</i>
Intercept	0.758701628	0.01039263	73.00381514	1.06424E-29	0.737252298	0.780150957
X Variable 1	0.002976227	0.000118259	25.16698109	9.1943E-19	0.002732152	0.003220302
X Variable 2	0.001352482	6.56335E-05	20.60657155	9.08191E-17	0.001217021	0.001487943
X Variable 3	-0.119536382	0.004856555	-24.61340884	1.53825E-18	-0.129559817	-0.109512946

PREDECISIONAL DOCUMENT

Table G-3. Accumulations of 1 wt% ²³⁸U in Chabazite (40%) and Aggregate (60%) from Degraded Concrete in a 75 cm Deep Cylinder Segment

Hydrogen Fraction in Chabazite/Aggregate	Segment Length		
	150 cm / 25 kg ²³⁸ U	300 cm / 50 kg ²³⁸ U	= Length
100% H	0.9178 ± .0020 (insegd)	0.9459 ± .0018 (insegg)	0.9544 ± .0019 (infsegd)
90% H	0.9201 ± .0023 (insegf)	0.9469 ± .0024 (insege)	0.9816 ± .0023 (infsege)
80% H	-	-	0.9589 ± .0026 (infsegf)

Table G-4. Effect on k_{av} of Pu/U/Gd Concentration in Bottom of Clay

Pu (kg)	U (kg)	Gd (kg)	Uniformly Distributed	Pu/U/Gd in Bottom 75% of Clay	Pu/U/Gd in Bottom 50% of Clay	Pu/U/Gd in Bottom 25% of Clay
40	150	3.5	0.9548 ± 0.0053 (c0jA35)	1.0044 ± 0.0039 (a0jA5)	1.0375 ± 0.0054 (b0jA7)	1.0529 ± 0.0047 (d0jA14)
40	50	2.25	-	-	0.9022 ± 0.0044 (b0jB45)	-
40	50	2.5	-	-	0.8807 ± 0.0031 (b0jB5)	-
40	50	1.25	0.9344 ± 0.0041 (c0jD13)	0.9774 ± 0.0042 (a0jD17)	1.0132 ± 0.0050 (b0jD25)	1.0006 ± 0.0060 (d0jD17)
25	25	0.75	-	-	0.8824 ± 0.0044 (b0kE15)	-
25	25	0.25	0.9602 ± 0.0047 (c0kEp3)	1.0194 ± 0.0040 (a0kEp3)	1.0651 ± 0.0044 (b0kEp5)	1.0521 ± 0.0052 (d0kE1)
10	65	0.87 5	-	-	0.8838 ± 0.0081 (b0lD18)	-
10	65	0.5	0.9194 ± 0.0041 (c0lDp5)	0.9845 ± 0.0044 (a0lDp7)	1.0032 ± 0.0049 (b0lD1)	0.9947 ± 0.0049 (d0lD2)

Table G-5. Effect on k_{av} of Pu/U/Gd Concentration in Top of Clay

Pu (kg)	U (kg)	Gd (kg)	Uniformly Distributed	Pu/U/Gd in Top 75% of Clay	Pu/U/Gd in Top 50% of Clay	Pu/U/Gd in Top 25% of Clay
25	25	.25	0.9602 ± 0.0047 (c0kEp3)	0.9938 ± 0.0049 (e0kEp3)	0.9883 ± 0.0082 (f0kEp5)	0.8608 ± 0.0052 (g0kE1)

PREDECISIONAL DOCUMENT

Table G-6. Effect on k_{eff} of Concentrating Pu/U/Gd on One End of WP

Pu (kg)	U (kg)	Gd (kg)	Uniformly Distributed	Pu/U/Gd All in Right Half of Clay
40	150	3.5	0.9548 ± 0.0053 (c0/A35)	1.1187 ± 0.0052 (cs)2A7)
40	50	2.25	-	0.9670 ± 0.0038 (h0)D45)
40	50	2.5	-	0.9485 ± 0.0057 (h0)D5)
40	50	1.25	0.9344 ± 0.0041 (c0)D13)	1.0872 ± 0.0050 (h0)D25)
25	25	0.75	-	0.9475 ± 0.0043 (h0kE15)
25	25	0.25	0.9602 ± 0.0047 (c0kEp3)	1.1511 ± 0.0049 (h0kEp5)
10	65	0.875	-	0.9561 ± 0.0050 (h0)D18)
10	65	0.5	0.9194 ± 0.0041 (c0)Dp5)	1.0796 ± 0.0064 (h0)D1)

- - Used half-length WP model for this case rather than model with all Pu/U/Gd in half of the clay in a full-length WP, as was done for the other cases.

Table G-7. Effect on k_{eff} of Half Volume on One End of WP (Same Concentration)

Pu (kg)	U (kg)	Gd (kg)	Full Volume	Half Volume Right Half of Clay (Same Concentration)
21	14	0	0.9643 ± 0.0028 (ca)0j0)	0.9482 ± 0.0046 (ca.50)j0)
25	25	0.25	0.9602 ± 0.0047 (c0kEp3)	0.9424 ± 0.0055 (cskEp3)
50	75	2.0	0.9728 ± 0.0049 (cl0)b2)	0.9546 ± 0.0049 (c.50)b2)
140	30	8.0	0.9742 ± 0.0048 (cl0gb8)	0.9594 ± 0.0041 (c.50)gb8)

PREDECISIONAL DOCUMENT

Table G-8. Comparison of Gd and Sm in Degraded DHLW Glass/Pu Immobilization Glass

Case Description	Gd	Mole Equivalent Sm	No Absorber
25 kg ²³⁹ Pu, 25 kg ²³⁵ U, 0.25 kg Gd	0.9602 ± .0047 (c0kEp3)	1.0811 ± .0044 (cskE25)	1.1008 ± .0045 (c0kE0)
10 kg ²³⁹ Pu, 65 kg ²³⁵ U, 0.375 kg Gd	0.9734 ± .0043 (clDp4)	1.0945 ± .0052 (csDp4)	1.1810 ± .0042 (csDp0)
50 kg ²³⁹ Pu, 75 kg ²³⁵ U, 2 kg Gd	0.9728 ± .0049 (cl0ib2)	1.1868 ± .0058 (cs0ib2)	1.3954 ± .0048 (cx0ib2)
140 kg ²³⁹ Pu, 30 kg ²³⁵ U, 8 kg Gd	0.9742 ± .0048 (cl0gb8)	1.1313 ± .0052 (cs0gb8)	1.4950 ± .0047 (cx0gb8)

Additional cases were run to determine approximately the mass of Sm required to match k_{eff} values for the various combinations. The cases are as follow:

25 kg ²³⁹ Pu/ 25 kg ²³⁵ U/ 0.75 kg of Sm	0.9854 ± .0038 (cskE.75)
25 kg ²³⁹ Pu/ 25 kg ²³⁵ U/ 1 kg of Sm	0.9478 ± .0029 (cskE1)
25 kg ²³⁹ Pu/ 25 kg ²³⁵ U/ 2 kg of Sm	0.8330 ± .0040 (cskE2)
10 kg ²³⁹ Pu/ 65 kg ²³⁵ U/ 1 kg of Sm	1.0029 ± .0050 (csDp1)
10 kg ²³⁹ Pu/ 65 kg ²³⁵ U/ 1.5 kg of Sm	0.9396 ± .0043 (csDp1.5)
50 kg ²³⁹ Pu/ 75 kg ²³⁵ U/ 5 kg of Sm	0.9993 ± .0039 (cs0ib5)
50 kg ²³⁹ Pu/ 75 kg ²³⁵ U/ 6 kg of Sm	0.9501 ± .0041 (cs0ib6)
140 kg ²³⁹ Pu/ 30 kg ²³⁵ U/ 16 kg of Sm	0.9705 ± .0047 (cs0gb16)

Table G-9. Investigation of Dryout of Degraded Glass Configuration

Case Description	Base	No Reflector	80% H	50% H	25% H
21 kg ²³⁹ Pu / 14 kg ²³⁵ U/ 0.0 kg Gd	0.9843 ± 0.0028 (ca0j0)	0.9609 ± .0028 (cdw0j0)	0.9667 ± .0037 (cdx0j0)	0.9399 ± .0045 (cdy0j0)	0.8468 ± .0052 (cdz0j0)
25 kg ²³⁹ Pu / 25 kg ²³⁵ U/ 0.25 kg Gd	0.9602 ± .0047 (c0kEp3)		0.9571 ± .0053 (p8kEp3)	0.9320 ± .0044 (p5kEp3)	0.8842 ± .0058 (p3kEp3)
50 kg ²³⁹ Pu / 75 kg ²³⁵ U/ 2.0 kg Gd	0.9728 ± .0049 (cl0ib2)	0.9721 ± .0046 (cdwib2)	0.9756 ± .0048 (cdxib2)	0.9824 ± .0048 (cdyib2)	0.9447 ± .0076 (cdzib2)
140 kg ²³⁹ Pu / 60 kg ²³⁵ U/ 10.0 kg Gd	0.9738 ± .0030 (cl0ga10)	0.9677 ± .0042 (cdwga10)	0.9926 ± .0047 (cdxga10)	1.0193 ± .0050 (cdyga10)	0.9941 ± .0068 (cdzga10)

PREDECISIONAL DOCUMENT

Table G-10. Comparison of ²³⁸U in Degraded DHLW Glass/Pu Immobilization Glass

Pu/U/Gd Masses (kg)	0 kg ²³⁸ U	25 kg ²³⁸ U	50 kg ²³⁸ U	100 kg ²³⁸ U
40/50/1	0.9795 ± .0049 (cOjD1)	0.9766 ± .0052 (cjD1u1)	0.9618 ± .0031 (cjD1u2)	0.9535 ± .0055 (cjD1u3)
21/14/0	0.9643 ± .0028 (caI0j0)	0.9635 ± .0040 (caf0j0)	0.9487 ± .0039 (cad0j0)	0.9387 ± .0045 (cab0j0)
10/65/0.375	0.9734 ± .0043 (clDp4)	0.9587 ± .0043 (clDp4u1)	0.9537 ± .0037 (clDp4u2)	0.9395 ± .0044 (clDp4u3)

Table G-11. Variation of Hf Wt% in Zr for the Degraded Ceramic Waste Form

Pu/U/Gd Masses (kg)	0 wt% Hf	2 wt% Hf	4 wt% Hf	20 wt% Hf	100 wt% Hf
25/90/0.5	0.9841 ± .0038 (kC0Hf)	0.9724 ± .0037 (s1kCp5)	0.9612 ± .0040 (kC04Hf)	-	-
10/130/0.5	0.9976 ± .0044 (lB0Hf)	0.9915 ± .0042 (s1lBp5)	0.9827 ± .0054 (lB04Hf)	-	-
50/10/0	1.0080 ± .0035 (sz1le0)	0.9925 ± .0039 (sy1le0)	0.9862 ± .0044 (sx1le0)	0.9161 ± .0038 (sv1le0)	0.7164 ± .0039 (sw1le0)
50/75/1.2	-	0.9761 ± .0041 (sy1lc12)	-	0.9086 ± .0047 (sv1lc12)	-

Table G-12. Calculations to Determine Equivalent Hf Wt% in Zr to Replace 0.5 kg Gd for the Degraded Ceramic Waste Form

	25 kg ²³⁸ Pu / 90 kg ²³⁸ U / 0. kg Gd	10 kg ²³⁸ Pu / 130 kg ²³⁸ U / 0. kg Gd
4 wt% Hf	1.0806 ± .0035 (NkC04h)	1.1010 ± .0044 (NlB04h)
10 wt% Hf	1.0558 ± .0052 (NkC10h)	1.0719 ± .0062 (NlB10h)
20 wt% Hf	1.0110 ± .0042 (NkC20h)	1.0361 ± .0056 (NlB20h)
30 wt% Hf	0.9814 ± .0043 (NkC30h)	1.0041 ± .0038 (NlB30h)
35 wt% Hf	0.9559 ± .0046 (NkC35h)	0.9815 ± .0048 (NlB35h)
40 wt% Hf	0.9452 ± .0041 (NkC40h)	0.9644 ± .0040 (NlB40h)
45 wt% Hf	-	0.9520 ± .0046 (NlB45h)

PREDECISIONAL DOCUMENT

INTENTIONALLY LEFT BLANK

**APPENDIX H
ASSUMPTIONS**

Intentionally Left Blank

APPENDIX H ASSUMPTIONS

The range of parameters used (assumed) for input to the calculations of scenarios and resulting configurations is given in Table 7.3-1. The justification of these ranges is discussed in connection with the detailed tables: Table 4.1-1 for glass and ceramic dissolution rates, Table 4.1-2 for the internal fracturing factor, Table 4.1-3 for stainless steel dissolution (or corrosion) rate, Table 4.2-1 for solubility of neutronically active species, and Table 4.3-1 for environmental parameters.

The compositions of the clayey mass that contains the principal insoluble waste form degradation products, are given in Tables 5.4.5-1 and 5.5.2-1, for glass and ceramic, respectively. The bases for these compositions are the EQ 3/6 calculations described in the text (Section 5.4), so they are not, strictly speaking, assumptions. The values in these tables were used for the criticality calculations (MCNP) with the exception of the Pu and U compositions; the values for these parameters were determined from the dynamic mass balance equations.

It is assumed that the dissolution of the waste form is congruent. The basis for this assumption is that the components are homogeneously distributed (see Sections 2.1.1 and 2.2.1).

It is assumed that the individual ionic breakdown products (components) of the WF dissolution will go into solution as the WF is dissolved. However, those ions and uncharged species that are insoluble will immediately precipitate, generally near the point of dissolution. The basis for this assumption is that the fluid moves slowly (see Sections 2.1.1, 2.2.1, and 3.2.1).

It is assumed that water penetration of the WP barriers will occur at 3500 years. The basis for this assumption is the time to first pit penetration averaged over all WPs in the repository (TSPA 95, Ref. 3) using very conservative models of pit penetration for the corrosion-allowance material and the corrosion-resistant material. The results of this study are rather insensitive to the value of this parameter to within a factor of 3 (see Section 3.1.1).

It is assumed that the penetration time for the 1 cm thick stainless steel pour canister is 1100 years. The basis for this assumption is the time for 25% of the pits to penetrate the pour canister, using a stainless steel bulk corrosion rate of 0.1 μ /yr together with a pitting rate enhancement factor of 4, and an estimate of the standard deviation of the distribution of pitting rates of 50% of the mean rate. This estimate is somewhat arbitrary, but most of the cases considered in this study involve earliest time to criticality of more than 40,000 years, which will be fairly insensitive to uncertainty in start times of a few thousand years (see Sections 3.1.1 and 7.3.1).

It is assumed that the filler glass in the pour canister provides no protection against corrosion/dissolution of the WF. The basis for this assumption is the fact that the filler glass will be highly fractured (by at least a factor of 30). This assumption is also partly justified because it is conservative (favoring sooner waste form degradation and earlier opportunity for criticality) (see Section 3.1.1).

It is assumed that the geologic repository is in an unsaturated site, in an arid climate, exposed to an oxidizing atmosphere. The bases for these assumptions are the results of site characterization studies, which are summarized in Table 4.3-1 (see Section 3.3).

It is assumed that only the stainless steel of the pour canister makes a significant contribution to the potential acidification from the complete oxidation of Cr or Mo. The reasons for the neglect of the waste package inner barrier are twofold:

- The bulk corrosion rate of Alloy 825 or 625 is likely to be two orders of magnitude slower than for stainless steel.
- Insofar as there can be standing puddles on the outer surface of the inner barrier, the corrosion products dissolving into them will be carried off the surface of the WP, rather than going inside the WP to contribute to the acidification.

The reason for the neglect of the steel in the waste form containing can is also twofold:

- The container wall volume is only 25% of that of the pour canisters.
- The composition has not yet been finalized, and might even be some non-corrosion resistant material, for certain safeguard advantages (see Section 4.1).

It is assumed that in flow-through flushing the removal rate of a species is the product of the flow rate multiplied by the maximum concentration of the species in solution (solubility limit). This mechanism assumes that there is sufficient penetration in the lower portion of the waste package that the water flows through the package. It further assumes that all the water flowing through the WP is sufficiently mixed that it carries the maximum concentration of each species dissolved from the WF. The basis for this assumption is that it is physically possible and conservative (see Section 5.1).

It is assumed that exchange flushing of dissolved material occurs when the lower portion of the package is not penetrated, so that most of the package is filled with water, and a major fraction of the water incident on the WP will flow around the package only picking up dissolved species by physical mixing across the free surface boundary. In this situation, the removal rate of all the species is reduced (in comparison with the flow-through flushing) by an exchange factor representing this mixing. Generally, exchange flushing and flow-through flushing are mutually exclusive but it is possible for a given WP to have both (see Section 5.1).

It is assumed that there is no concentration, or focusing of groundwater onto the waste package; stated alternatively: the maximum rate volumetric flow through the WP is equal to the product of the infiltration rate multiplied by the WP cross-section area. This assumption is realistic for a WP partly filled with water, but it is very conservative for the much more rapid flushing by flow-through (see Section 5.1.3).

It is assumed that the collapsed WF configuration has the insoluble WF components collapsed to the bottom of the WP, in a clayey mass. In this configuration most of the completely altered (metamict if ceramic) WF loses its geometry and collapses as particulate onto a bed of clayey materials (silicates and other fine-grained solids). The exposed surface area is assumed to be enhanced by a factor up to 15,000 times (ceramic only). The neutron absorbers (Gd and iron) are assumed to be leached at rates dependent on the pH of the system which is controlled by the infiltration rate and the dissolution rate of the stainless steel container material. Criticality could occur earlier than from the initial geometry since sufficient Gd could have been flushed from the system. The basis for this assumption is that it is realistic (see Section 5.2).

It is assumed that the chemical processes can be organized into three time periods:

- EQ3/6 can be used to identify the pH trend and species present (qualitatively) when the alkali (DHLW) glass is degrading.
- Equilibrium calculations with EQ3/6 are used to determine the solubilities of U, Pu, and Gd at specific values of pH during the degradation period of the La-BS glass WF after the removal of the soluble products of the DHLW glass.
- While stainless steel is corroding, the pH can be determined from the quasi-steady state chromate concentration (determined by the balance between the stainless steel corrosion rate, which generates the presumably acidifying chromate ions, and the infiltration rate, which removes them).

When the latter time periods have a significant overlap, the separation of fissile from neutron absorber may be sufficient to permit criticality (see Section 5.3.1).

It is assumed that the solubility behavior of Gd for pH below 6.5 can be represented by:

$$\text{max Gd (ppm)} = 3 \times 10^{-3(\text{pH}-6.5)}, \text{ or } 95 \times 10^{-3(\text{pH}-6.0)}$$

The basis for this assumption is the thermodynamic equilibrium relations for these parameters.

The approach used for obtaining a representative composition for the degradation products consisted of:

- First, taking results from EQ6 runs at the time that the model predicted that all of the DHLW filler glass had reacted.
- Second, modifying that composition to a small extent on the basis of static mass balance considerations that would affect this composition under neutral to somewhat acidic conditions.

Because of the long time frames, the modeling assumed that the phases formed would be in equilibrium with the solution. Thus, quartz, rather than chalcedony, was assumed. The assumption

that quartz forms, which may occur in the time frames involved, means that the lower aqueous silica will result in a higher calculated soddyite solubility. Similarly, clay minerals, rather than a degraded leached glass ("gel"), were assumed. Some solids were, however, suppressed as being unlikely to form at low temperatures, even though the thermodynamics would predict their occurrence; garnet, biotite, and pyroxene, among others, were suppressed (see Section 5.3.5).

It is assumed that the corrosion of stainless steel can support chromate induced acidification, making the solution as acidic as pH=5. It is known that conditions as acidic as pH 4 to 5 develop in pits and crevices during corrosion of stainless steel. It remains unknown, however, whether such reactions will occur on a sufficiently broad scale, or rapidly enough, to lower the pH of an initially near neutral solution to such low pHs. For example, the mineral, eskolaite, Cr_2O_3 , is known to occur "as a major constituent of black pebbles in the bed of the Merume River, Guyana (Ref. 25, p. 197)," thus demonstrating that chromium oxide may survive for long times under oxidizing conditions. The assumption of chromate induced acidification is conservative with respect to criticality (based on the above reasoning that such conditions may arise within the waste package) because the result is removal of Gd while leaving fissile material behind (see Section 5.4.1).

It is assumed that the boron in borosilicate glass is removed from the WP upon glass dissolution and flushing by infiltrating water. The basis for this assumption is the high solubility of boron. This assumption is also conservative (see Section 5.4.5).

It is currently assumed that the absorption by zeolites, formed from concrete degradation or reaction, is the most likely mechanism for the concentration of fissile material in the invert. The reasoning leading to this assumption is given in the text (see Section 5.6).

It is assumed that the volume of clayey material at the bottom of the WP is equivalent to that displaced by the original four glass pour canisters within the waste package. The clayey material contains water in two forms: a fixed amount of hydrogen (bound as water of hydration of hydroxide) and a variable amount of free water (including adsorbed water). The H and O concentrations from bound water or OH are already represented in Tables 5.4.5-1 and 5.5.2-1 for the glass and ceramic WFs, respectively. The volume fraction of free water in the clayey material can be up to 45 vol% (maximum water fraction possible in the voidspace of the WP); the values actually used for the MCNP calculations varied between 0 and 20%, according to which gave the highest k_{eff} , in keeping with conservatism (see Sections 6.1.1 and 7.1.1).

It is assumed that the zeolite that might be present in the invert or near field may be represented by Chabazite, $\text{CaAl}_2\text{Si}_4\text{O}_{12}\cdot 6\text{H}_2\text{O}$. The justification for this assumption is given in Section 5.6. It is further assumed that a zeolite concentration in the invert would have a cylinder segment geometry similar to the clayey material configuration inside the WP, and the accumulation of ^{235}U would likely confirm to roughly this geometry. The justification for this assumption is that the invert itself has a cylinder segment geometry, and that effluent from the waste would likely be wicked horizontally and vertically throughout the invert (see Section 6.1.2).

It is assumed that the initial WF dissolution product factor is reduced with time so that it is proportional to the remaining waste form surface area, which is assumed to be proportional to the

two-thirds power of the remaining WF mass. The basis for this assumption is the further assumption that the WF fragments have all three dimensions of the same order of magnitude. This assumption is not applicable to the corrosion/dissolution of steel components because they are largely 2 dimensional (see Section 7.3).

It has been assumed that the short time period between the initial penetration of the pour canister (when dissolution can begin), and some significant bulk corrosion of the steel of the pour canister (which can support acidification), will not result in any loss of U or Pu from the WP. This may appear to conflict with the possibility that in the time between the breach of the WP and the onset of acid conditions following degradation of the filler glass, some of the WF could also be degraded and release some fissile material. If the pH is high enough (above 9) to make the U and Pu very soluble, a significant fraction of the U and Pu released from the WF could be removed from the WP during this short time. However, the assumption is justified for the following reasons:

- The filler glass dissolves much faster than the WF, so only a small fraction of total WF U and Pu will be released during the period of filler glass dissolution.
- It is not certain that the alkali from the dissolving filler glass will drive the pH sufficiently high to produce high solubility of U or Pu, largely because flushing will be removing the alkali simultaneously.
- The assumption is conservative.

It is further assumed that any Gd released during this interim time will be re-dissolved and removed from the WPs when the filler glass has fully degraded and the solution becomes acidic from the corroding stainless steel. The algorithms used do account for the loss of Cr that is released during this time, thereby reducing the period when the package solution can be acidic, which, in turn, reduces the potential for criticality (see Section 7.3).

It is assumed that the disposition of the undissolved WF during the degradation period can be represented by one of the following alternatives:

- All of the undissolved WF remains above or outside the clayey material at the bottom of the WP.
- The undissolved WF fragments and collapses into the clayey material where its components are assumed to be uniformly distributed for input to the MCNP calculations.

The first alternative represents the most conservative assumption with respect to the occurrence of criticality, while the second alternative represents the other extreme. Most of the calculations reported in Section 7 are based on the first alternative, but some results are also presented for the second alternative for comparison purposes and to demonstrate that the conclusions of the study are valid across the entire range of possibilities.

INTENTIONALLY LEFT BLANK

A0000000-01717-5705-00014 REV 01

H-6

PREDECISIONAL DOCUMENT

February 1997